

**FR900359, an inhibitor of guanine
nucleotide dissociation, effectively blunts
signaling of GTPase-deficient Gq
mechanism of action and relevance for
treating Gq-driven cancers**

Dissertation zur Erlangung des Doktorgrades
(Dr. rer. nat.)
der Mathematisch-Naturwissenschaftlichen Fakultät
der Rheinischen Friedrich-Wilhelms-Universität zu Bonn

vorgelegt von
Suvi Katariina Annala
aus Helsinki

Bonn 2019

Angefertigt mit Genehmigung der Mathematisch-
Naturwissenschaftlichen Fakultät der Rheinischen Friedrich-Wilhelms-
Universität Bonn.

1. Gutachter: Prof. Dr. Evi Kostenis
2. Gutachter: Priv.-Doz. Evelyn Gaffal

Tag der Promotion: 02.07.2019

Erscheinungsjahr: 2019

Meiner Mutter

Abstract

Uveal melanoma (UM), the most common cancer of the adult eye, is known to have poor prognosis. Over 50% of patients are likely to develop metastasis. In more than 80% of the cases UM is driven by an activating mutation in the Gq/11 protein. Thus, many attempts have been made to target downstream signaling of this oncogene. Unfortunately, none of these approaches have succeeded so far in clinical trials. Targeting only one or even two downstream effectors in combination, may not be sufficient to blunt the oncogenic dynamics of the Gq/11 protein. Direct inhibition of the oncogene itself was believed to be ineffective, since the mode of action of the only known inhibitors for Gq/11 proteins, FR900359 (FR) and YM-254890 (YM) respectively, was considered unsuitable for targeting the constitutively active oncogenes.

FR is a macrocyclic depsipeptide, produced by symbiotic bacteria. Recent studies have shown that by binding to G α -subunits of Gq/11 proteins FR inhibits the nucleotide exchange that is crucial for their activation. Because FR interferes with the rate-limiting step of G α activation, it was reasoned that this approach might be unsuitable to target a protein, which is already trapped in the active state.

Accidentally, however, Evelyn Gaffal, Thomas Tüting and coworkers found that FR inhibited diverse cancer hall marks in melanoma cells, harboring an activating mutation in the G11 protein. These surprising results prompted us to further investigate the inhibition properties of FR on the oncogenic Gq/11 protein. In the frame of this work, we demonstrate FRs' ability to suppress mitogenic pro-survival pathways over the canonical phospholipase C (PLC) effector cascade. Taking advantage of genome edited HEK293 cells lacking G α q and G α 11 proteins, we were furthermore able to show direct interaction of the molecule with its target protein. Results of FRET experiments together with molecular modeling gave first hints regarding the mechanism underlying the inability to target PLC-Gq^{mut} interaction. Whole cell label-free technology unveiled a possible mode of action of FR on the mutated protein. Most importantly, we were able to proof inhibition of the oncogene in a therapeutically relevant system. By using different uveal melanoma cell lines, we demonstrated in vitro and in vivo the inhibition of tumor progression by FR treatment. Further, direct comparison of FR with the other well described Gq-inhibitor YM, revealed the long-term superiority of FR, as we observed different drug vulnerability between the two molecules.

Kurzfassung

Krebs ist eine der häufigsten Todesursachen weltweit. Der Krebsentstehung liegt die ungebremste Zellteilung von Zellen mit abnormalem Wachstumsverhalten zugrunde. Das asoziale Verhalten bestimmter Zellen, sich unabhängig von den vorherrschenden Umgebungsbedingungen zu teilen, hängt mit der genetischen Veränderung des Erbgutes dieser Zellen zusammen. Aufgrund zahlreicher Kontrollmechanismen, die unkontrolliertes Wachstum und Replikation von defekter DNA in der Zelle verhindern, reicht oft eine Mutation im Genom nicht für die pathogenetische Transformation aus. Die Tumorgenese setzt ein Zusammenspiel von Mutationen, die zu Überaktivität wachstumsfördernder Onkogene, und Mutationen, die zu Aktivitätsverlust von Tumorsuppressoren führen, voraus. Doch hat sich die gezielte pharmakologische Suppression bestimmter Onkogene in klinischen Studien als effektive Strategie zur Bekämpfung der Tumorprogression bewiesen.

Aderhautmelanome gehören zu den häufigsten aber auch aggressivsten Melanomarten im adulten Auge. Über 50% der Patienten mit Primärtumoren entwickeln in den Folgejahren der Erstdiagnose Metastasen. Verglichen mit anderen Krebsarten ist die genetische Alteration relativ gering. Eines der bekanntesten Onkogene in diesem Zusammenhang ist das Gq/G11 Protein. Über 80% der Patienten, die an Aderhautmelanom erkrankt sind, tragen eine somatische Mutation in einer funktionellen Domäne des Proteins. Der Austausch einer einzigen Aminosäure an der betreffenden Domäne, führt zum Verlust der autokatalytischen Ausschaltregulation. Dies hat eine konstitutive Überaktivität des wachstumsfördernden Proteins zur Folge.

Im Rahmen dieser Arbeit befassten wir uns mit einem makrozyklischen Naturstoff, der kürzlich als selektiver Gq/11 Hemmstoff charakterisiert wurde. FR900359 ist ein Depsipeptid, das durch nicht ribosomale Synthese einer in Symbiose mit dem Immergrün-Gewächs *Ardisia Crenata* lebenden Bakterienart produziert wird. Das Depsipeptid verankert sich zwischen die Hauptdomänen des Gq/11-Proteins und verhindert dessen sterische Flexibilität. Durch die Einschränkung der Beweglichkeit innerhalb des Proteins kann der normale, rezeptorvermittelte Aktivierungsmechanismus nicht mehr stattfinden. Da aber das onkogene Gq/11 Protein durch die Mutation bereits im Grundzustand aktiviert vorliegt, hatte man dem Molekül zunächst die Fähigkeit abgesprochen, auch das onkogen mutierte Analogon des Proteins zu hemmen.

Durch einen Zufallsbefund an einer Melanom-Zelllinie mit mutierten G11 Protein wurde bewiesen, dass FR in der Lage war verschiedene krebstypische Merkmale zu unterbinden. Zellen, die mit FR behandelt wurden, zeigten vermindertes Wachstums- und Migrationsverhalten. Dafür schienen die Zellen in einen differenzierten Zustand überzugehen. Auf Grund dieser Beobachtungen entschieden wir uns das Phänomen der Hemmung des aktiven Gq/11-Onkogens durch FR näher untersuchen.

Anhand verschiedener Melanom Zellen sowie genomisch veränderter artifizierender HEK293 Zellen konnten wir zeigen, dass FR präferiert wichtige Gq/11 initiierte Überlebenssignalwege der Zelle gegenüber dem herkömmlichen Gq-Effektorprotein Phospholipase C- β (PLC β) hemmt. In diesem Zusammenhang gelang es uns darüber hinaus mit Hilfe von FRET-Experimenten, die Protein-Protein-Interaktionen

veranschaulichen, sowie mit molekularer Modellierung erste Hinweise für diese selektive nicht-Hemmung der PLC β zu sammeln.

Liganden-induzierte, dynamische Massenumverteilung in HEK Zellen mit onkogenem Gq, enthüllte eine Rezeptor-aktivierbare Fraktion des Gq Proteins und gab somit erste Aufschlüsse über die mechanistische Funktion des Hemmstoffs am aktiven Analogon. Die Existenz dieser Fraktion konnte dann mittels His-Pull-Down Assays sowie Dünnschichtchromatographie verifiziert werden. Die direkte Interaktion des Hemmstoffes am Protein belegten wir mit einer Mutagenese-loss-of-function-Studie.

Im Anschluss konnten wir die imposante Wirkung des Inhibitors in vitro aber auch in vivo im therapeutisch hoch relevanten Aderhautmelanom Kontext zeigen. Dabei führte die FR-Behandlung kultivierter Aderhautmelanomzellen mit Mutation am Gq/G11 Protein zu einer Hemmung diverser wachstumsfördernder Signalwege, dem Zellwachstum und auch der Tumorentstehung in einem xenographischen Mausmodell. Die Antwort der Zellen auf die Behandlung konnte auf die spezifische Hemmung des Gq/11-Onkogens zurückgeführt werden, da das Zellwachstum in den Kontrolllinien mit anderen onkogenen Treibermutationen unbeeinflusst blieb. Darüber hinaus zeigten wir die Überlegenheit von FR gegenüber einem strukturell verwandten und kommerziell erhältlichen Molekül YM hinsichtlich des Langzeitinhibitions potentials.

Somit diene diese Studie dem Nachweis, dass die direkte Adressierung des konstitutiv aktiven Gq/G11 Proteins in der Aderhautmelanom-Therapie durchaus ein attraktives Konzept darstellt. Die Moleküle FR und YM konnten dabei als erste strukturelle Basis für die Entwicklung therapeutisch relevanter Inhibitoren identifiziert werden. Zukünftig könnten diese Inhibitoren durch Modifikationen oder auch durch die Verbindung mit Transportmolekülen, die das mutierte Protein oder spezifisch das Gewebe mit der Mutation adressieren, realisierbare therapeutische Optionen darstellen.

Content

Introduction	1
1.1. Uveal melanoma	2
1.1.1 Chromosomal alterations and frequent mutations	2
1.1.2. Gq-signaling as oncogenic driver	3
1.2. Gq and G11 belong to the family of G proteins:.....	3
1.2.1. Mechanism of GDP release and GTP entry upon receptor activation	5
1.2.2. GTPase function as a switch off	6
1.3. GTPase-deficient mutants and cancer.....	6
1.3.1. GTPase-deficient GNAQ/GNA11 is often found in uveal melanoma	7
1.4. Diversity of Gq-signaling	7
1.4.1. Important effector proteins of the Gq-family.....	8
1.4.2. Gq signaling in uveal melanoma	11
1.5. Therapeutic options in uveal melanoma	15
1.6. GNAQ inhibitors	15
1.6.1. YM.....	16
1.6.2. FR	16
Goal of this study	19
Materials	21
2.1. Cell lines	21
2.2. Cell culture media and supplements.....	22
2.3. Plasmids, Bacteria, Primers.....	25
2.4. Mouse strains	26
2.5. Buffer and Solutions for Assays.....	27
2.6. Reagents	28
2.7. Assay and Microbiological Kits	30
2.8. Consumables	31
2.9. Labor Equipment	32

2.10. Software for Data Analysis	34
Methods.....	37
3.1 Cell culture protocols	37
3.2. Cell-based assays	39
3.4. Microbiological protocols	44
3.5. Data analysis	49
Results	51
4.1. FR inhibits canonical wild type $G\alpha_q$ but not GTPase-deficient $G\alpha_q^{Q209L}$ signaling in HEK cells	51
4.2. FR blunts mitogenic signaling in cutaneous melanoma cells with activated Gq/11	52
4.2.1. FR forces HCmel12 cells into differentiation and blunts pERK over PLC signaling	52
4.2.2. Mitogenic signaling and IP1 accumulation may not share the same upstream regulator	53
4.2.3. ERK phosphorylation is insensitive to FR in cutaneous melanoma cells with mutated B-Raf	55
4.2.4. Preferential inhibition of pERK over PLC by FR is a characteristic feature for cells harboring a GTPase-deficient mutant	56
4.3. FR directly interacts with mutated $G\alpha_q^{Q209L}$	57
4.3.1. FR blunts wild type but not GTPase-deficient activation of canonical PLC signaling	58
4.3.2. FR effects on Gq downstream signaling effectors AKT and YAP in endogenous Gq/11-clean background	59
4.3.3. FR triggers mass redistribution in cells expressing GTPase-deficient mutant	61
4.3.4 FR might act as a GDI on the GTPase-deficient $G\alpha_q^{Q209L}$ protein	64
.....	67
4.3.5 Addressing FR's inability towards canonical PLC signaling induced by GTPase-deficient $G\alpha_q$	68
4.4. Evaluation of FR capability to inhibit oncogenic Gq-signaling in uveal melanoma	72
4.4.1. Targeting canonical effector PLC β in uveal melanoma	72

4.4.2 FR inhibits pro-survival signaling in GNAQ ^{mut} but not GNAQ/11 ^{wt} cells	75
.....	87
4.4.3 Label-free whole cell response of UM cell lines upon FR application	87
4.4.4. FR inhibits tumor growth of in mice transplanted with UM harboring Gq ^{mut}	90
4.5. Comparison of mitogenic-signaling-inhibition potency of the two Gq inhibitors FR and YM	92
4.5.1. Drug vulnerability comparison between FR and YM in wash-out experiments	93
4.5.2. Evaluation of FR and YM binding addressed by site-directed mutagenesis ...	94
4.5.3 FR suppresses cancer hallmarks of uveal melanoma cells with mutated Gq protein with higher potency than YM.....	98
Discussion	103
5.1. FR as a tool to blunt mitogenic signaling in CM.....	104
5.2. Mechanistic insights into inhibition of the GTPase-deficient mutant	105
5.3. Hypothesis of FR pathway-selectivity	106
5.4. Targeting the oncogenic protein in a therapeutically relevant system	108
5.5. macrocyclic Gq-i FR and its analog YM in comparison	111
5.6. Limitation of this study and future perspectives	111
Summary	115
Reference	117
List of Figures	132
Abbreviations list.....	135
Publications	139
Acknowledgement	141

Introduction

Cancer is one of the major antecedents for death nowadays. It can be caused by external factors like tobacco, alcohol or chemicals leading to somatic mutations and gene fusions. However, internal factors like germline mutations, or immune conditions can also cause cancer (American Cancer Society). For cancer development it is more likely that multiple genes are altered than only one. In fact, often abnormal growth is initiated by a cooperative network of gain-of-function oncogenes and loss-of-function tumor-suppressors (Croce 2008). These oncogenic hits transform a normal cell into a tumor cell with stem cell properties supported by proto-oncogenes (Vicente-Dueñas et al. 2013).

Proto-oncogenes are proteins that are involved in cell growth, proliferation, differentiation and regulation of apoptosis. Due to mutational changes or chromosomal rearrangement these proteins lose their regulatory mechanisms and become overactive (Croce 2008). At that point in time the proto-oncogene transforms into a proper oncogene. Thereby, oncogenes do not only function as initiator for tumorigenesis but also play a role throughout cancer progression (Vicente-Dueñas et al. 2013). The cancer cell becomes dependent on its oncogenic drivers. In xenograft mouse models overexpression of certain proto-oncogenes have been reported to lead to tumorigenesis. But even though more than one gene alteration is believed to be needed for tumor development, this was not a one-way observation. Knockdown of a single cancer initiating gene was shown to arrest the cell's cell cycle, force the cells into differentiation or even induced programmed cell death (Weinstein 2002; Dancey 2006). Therefore, one therapeutic approach is to target one certain oncogene directly or indirectly by inhibiting downstream proteins that are activated by this oncogene (Dancey 2006).

Targeted therapy has become quite common in the treatment of cutaneous melanoma (CM). Activating mutations in certain genes responsible for expressing C-Kit, N-Ras or B-Raf are frequently found in this cancer type (Gray-Schopfer et al. 2005; Platz et al. 2008; The Cancer Genome Atlas Network 2015). They all belong to a group of proteins that promote the pro-proliferative mitogen activated protein kinase (MAPK) pathway (McArthur and Ribas 2013). Vemurafenib, which specifically targets the mutated version of B-Raf, has been shown to be more effective than dacarbazine, a chemotherapeutic agent that unselectively targets all rapidly dividing cells (McArthur and Ribas 2013; Knapen et al. 2018). Uveal melanoma (UM) is a subtype of ocular melanoma (Eagle 2013). On one hand these melanoma cells often show a lack of mutations in the MAPK pathway, but on the other hand they were detected with elevated tonus of this pathway. Instead another oncogene, the Gq/G11 protein has been found to be somatically activated in over 80% of the UM patients (van Raamsdonk et al. 2009). This work will focus on the GNAQ/GNA11 oncogene and its specific inhibition with a recently characterized molecule FR900359 (Schrage et al. 2015).

1.1. Uveal melanoma

Uveal melanoma is the most common cancer type in the adult eye with a high risk to form metastasis. Malignancy arises from melanocytes located anywhere in the uveal tract including the ciliary body, the iris and, most commonly, the choroid as shown in **figure 1** (Krantz et al. 2017; Carvajal et al. 2016; Eagle 2013). There are several risk factors counting into uveal melanoma incidence such as age, sex and race. Most cases of uveal melanoma are diagnosed between the age of 70 and 79 with a prevalence for light toned skin, blue eyes and male sex (Harbour 2012). Typical symptoms include the eyesight as diseased patients often suffer from visual field loss or blurry vision. However, around 30% of patients are without symptoms at the time of diagnosis. Early diagnosis is important as primary tumor size correlates with survival rates. Around 50% of the patients with primary tumors are likely to develop metastases that are disseminated by the blood stream and are prevalently found in the liver but also in lung or bone (Krantz et al. 2017).

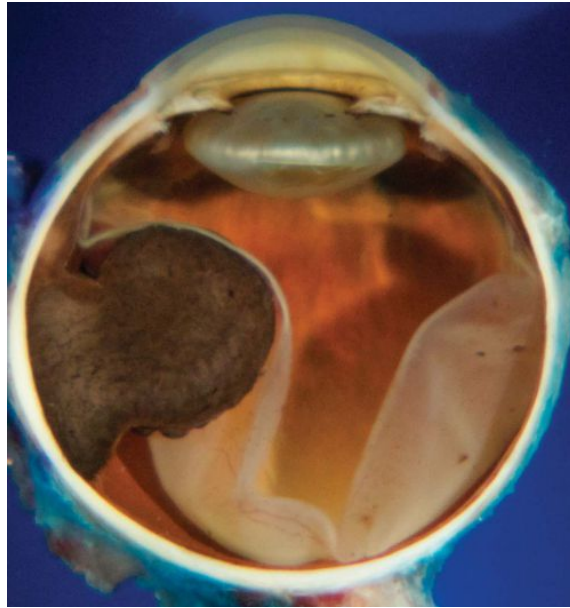


Figure 1: Uveal melanoma arising from the choroid; Borrowed from RC Eagle *Jr Eye* 2013

1.1.1 Chromosomal alterations and frequent mutations

Chromosomal alterations are relatively rare in uveal melanoma compared to other cancer types, but certain abnormalities were found to correlate with prognosis of the disease. Most common alterations occur in chromosomes 1, 3, 6, 8 and 9. Thereby, the loss of one copy of chromosome 3 is one of the most prominent markers. Monosomy 3 is detected in almost 50% of all UM samples and has been used to predict metastatic behavior. This chromosome 3 encodes a tumor-suppressor gene that is frequently mutated in UM. Higher risk to generate metastasis of these cells is suggested to be caused by downregulation of this suppressor, the BRCA1-associated protein 1 (BAP1) (Krantz et al. 2017; Harbour 2012). BAP1 is a deubiquitinating enzyme, which regulates important steps of the cell cycle like DNA repair or even differentiation (Masoomian et al. 2018).

In 2004 Onken et al. established a gene expression profile (GEP) system to categorize primary uveal melanomas into two classes based on their gene expression (Onken et al. 2004). The categorization correlated perfectly with metastasis behavior. In a later study by Monzon and co-workers the GEP-method could be evaluated as a reliable tool for prognostic use and is even recommended by the American Joint Committee on Cancer (AJCC) since 2017 (Plasseraud et al. 2017). Tumors of class 1 with a low risk to develop metastasis were detected with enhanced DNA copy numbers of genes on chromosome 6p and 8q and downregulated copy number on 6q. Significant alterations were not observed for this class on chromosome 3. In class 2 tumors, more likely to develop metastasis, upregulation of genes on 8q and downregulation of genes on 6q was

frequently detected. Thereby, no alterations were found in 6p. Additionally, gene clusters on chromosome 3 were affected. This observation was correlating with monosomy 3 as a risk factor for invasive behavior (Onken et al. 2004).

Another retrospective study with 81 patients revealed 5 genes that were mutated in the patients with high frequency: BAP1, SF3B1, EIF1AX and GNAQ/GNA11. Here mutations in BAP1, SF3B1 and EIF1AX were almost mutually exclusive. Same was observed for mutation of GNAQ and GNA11. BAP1 mutation was strongly correlated with class 2 GEP, whereas mutation in EIF1AX was associated with class 1 GEP. Mutation in SF3B1, GNAQ nor GNAQ11 did not show any significant higher occurrence in one of the classes compared to the other (Decatur et al. 2016). As mutations in GNAQ and GNA11 are commonly found in UM samples independent of the progression state of the tumor, it was suggested that this mutation occurs in early stage of tumor development and therefore does not correlate with prognosis of the disease. Furthermore, this led to speculation if mutation in GNAQ/GNA11 might be an initiator of oncogenic conduction (Onken et al. 2008).

1.1.2. Gq-signaling as oncogenic driver

The role of Gq signaling in uveal melanoma was further emphasized when two other mutations were discovered that affected proteins of the Gq-signaling-pathway (Moore et al. 2016; Johansson et al. 2015). Deep sequencing of UM samples identified a mutation in PLCB4 that was suggested to be of activating nature (Johansson et al. 2015). PLC β is the best known direct downstream effector of the Gq-family proteins (Harden et al. 2011). Occurrence of PLCB4 mutations was conformed in a later study by Yu Chen and co-workers. In this study another additional activating mutation was found on the Gq-coupled cysteinyl leukotriene receptor 2 (CysLTR2). Substitution of leucine with glutamine on position 129, a residue that normally stabilizes inactive G protein-coupled receptor (GPCR) conformation, was present in 4 of 9 UM samples, that did not carry mutations in either GNAQ/GNA11 or PLCB4. According to their prediction, these mutations were mutually exclusive (Moore et al. 2016). This observation is quite common for driver mutations affecting the same pathway (Cisowski and Bergo 2017). Transfection of the mutated receptor-induced cell growth in human melanocytes, demonstrating its proliferation driving function (Oldham and Hamm 2008).

1.2. Gq and G11 belong to the family of G proteins:

GNAQ/11 genes encode for proteins that belong to the family of guanine nucleotide-binding proteins (G proteins). These are heterotrimeric proteins consisting of a monomeric α -subunit encoded by 16 different genes and a $\beta\gamma$ -heterodimer, encoded by 5 and 14 genes for β and γ respectively, in mammals. Based on the homology of the α -subunit amino acid primary sequence, these proteins are categorized into 4 main classes: α_s , $\alpha_{i/o}$, $\alpha_{12/13}$ and the α_q family (Milligan and Kostenis 2006; Oldham and Hamm 2008).

The α_q family is divided into 4 subclasses $G\alpha_q$, $G\alpha_{11}$, $G\alpha_{14}$ and $G\alpha_{15/16}$ (mouse and human orthologs) based on their amino acid sequence and their common feature to activate phospholipase C dependent calcium and diacyl glycerin production (Hubbard and Hepler 2006). Whereas Gq and G11, which share 88 % sequence homology, can be found ubiquitously, G14 is primarily expressed in lung, liver, spleen and testis. G14 has less

similarity with Gq, as they share 81 % identical sequence. At least homology with Gq shows G16 with only 57 % match in protein sequence (**figure 2**).

G16 and its ortholog G15 are also rarely expressed, as they are exclusively found in hematopoietic cells (Wilkie et al. 1991; Offermanns and Simon 1995; Strathmann and Simon 1990).

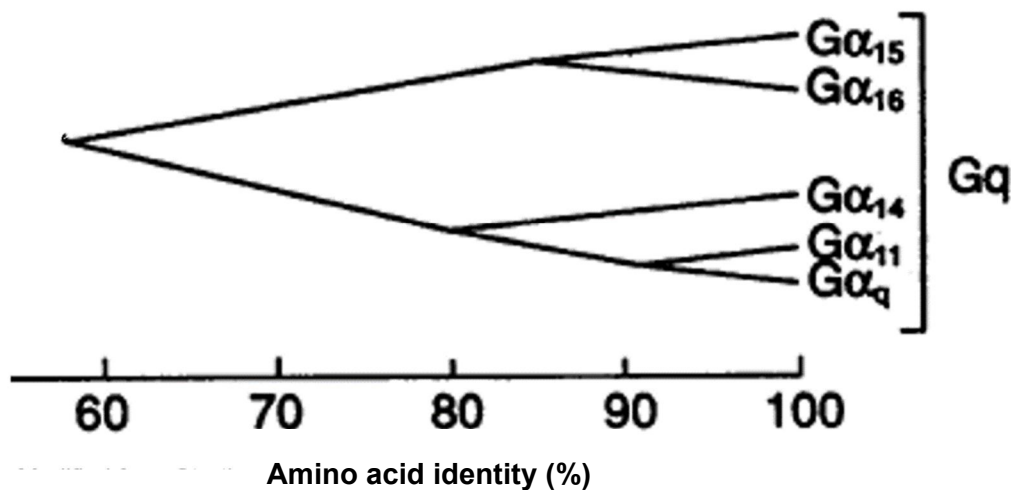


Figure 2: Homology between the Gq-family members. Shown are the sequence similarities between the proteins within the Gq family. Borrowed from Strathmann et al. *Science* 1991

Most structural diversity is found in the N terminus, where lipid modifications are attached post translationally (Sánchez-Fernández et al. 2014). These modifications affect the membrane localization of the protein as well as the effector and receptor interaction (Oldham and Hamm 2008). Whereas effector interaction among the family is considered to be the same, the range of receptor coupling differs a lot. G14, G15 and G16 have been found to couple to wide range of receptors in as much as G15 and G16 are even approached for agonist screening methods as universal adaptor G proteins (Milligan et al. 1996; Ho et al. 2001; Hubbard and Hepler 2006).

These proteins perform important tasks, as they transduce signaling initiated by extracellular ligands due to GPCR activation into the cell. In a sedentary state the heterotrimeric protein, is bound to guanine diphosphate (GDP) that is exchanged to guanine triphosphate (GTP) as a reaction on receptor coupling (Milligan and Kostenis 2006; Oldham and Hamm 2008). Activation causes dissociation of the $\beta\gamma$ -heterodimer from α , and both divisions can then interact with different effector proteins as illustrated in **figure 3**.

The alpha subunit has two domains, a Ras-like domain and a helical domain connected by two interdomain linkers. The helical domain is unique for each different alpha subunit, whereas the Ras-like domain is conserved throughout all families. This Ras-like domain provides the GTPase function and therefore operates as an autoregulated switch-off. Three flexible switches within this domain allow conformational rearrangements within the

α -subunit. The guanine nucleotide TCAT binding motive is located at the loop between the 6β -sheet and the 5α -helix at the end of the GTPase domain. Adapted to the TCAT sequence site GDP is trapped between the GTPase and helical domain in the inactive heterodimeric state of the protein (Oldham and Hamm 2008; van Eps et al. 2011; Wettschureck and Offermanns 2005).

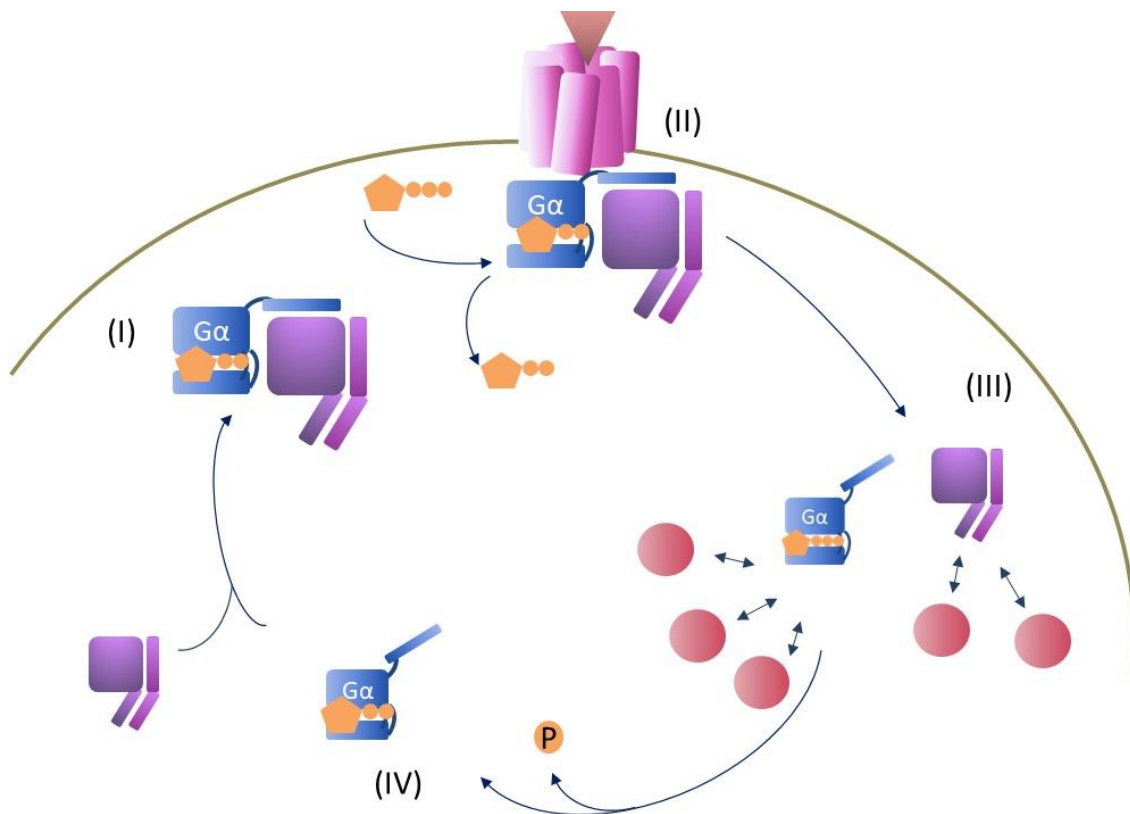


Figure 3: Receptor-mediated G protein activation. Schematic representation of the G protein-activation-cycle: The inactive GDP-carrying heterotrimer (I) can be activated by a ligand-bound receptor, that causes nucleotide exchange (II). The GTP-bound α -subunit loses affinity towards the $\beta\gamma$ -heterodimer. Consequently, both divisions separate from each other and can interact with different effectors (III). Using its intrinsic GTPase activity the α -subunit is able to transform the GTP to GDP (IV) and therefore regains its affinity towards the $\beta\gamma$ -heterodimer and they form a sedentary heterotrimer (I). Scheme adapted by Oldham & Hamm *Molecular Cell*

1.2.1. Mechanism of GDP release and GTP entry upon receptor activation

Upon ligand binding to the GPCR a conformational change occurs within its cytoplasmic domains, revealing a binding pocket for the C-tail of the α -subunit (Oldham et al. 2006; Mahoney and Sunahara 2016). Additional binding of $\beta\gamma$ -heterodimer is required to stabilize these contact points (Taylor et al. 1996; Kisselev et al. 1994). Paramagnetic resonance spectrometry revealed that receptor attachment to the C-tail of the alpha causes a shift within the subunit of its 5α -helix to the 6β -sheet (Oldham et al. 2006). Another consequence of receptor interaction is a rotating movement of $\beta\gamma$ -inter-subunit towards alpha that forces rearrangement of switch 1 and 2 within alpha. Both events together are suggested to initiate an outward directed movement of the two domains and

thereby simultaneously to increase the size of the interdomain space allowing GDP to be released from its binding site. The empty state of the G protein is a short transient one as the empty pocket is quickly occupied by the activating GTP (Oldham and Hamm 2008; van Eps et al. 2011).

1.2.2. GTPase function as a switch off

G α -proteins, as mentioned, exist in three different states: inactive binding GDP, transient no-G-binding and active binding GTP. To determine the active state the G protein uses its GTPase function to autocatalyze γ -P-hydrolysis and thereby converting GTP to GDP (**figure 4**). As a consequence the effector interaction is disrupted and the GDP-bound α -subunit can be re-associated with the $\beta\gamma$ -subunit to reset the inactive heterotrimer (Bourne et al. 1990).

In 1993 and 1994 two crystal structures of transducin, a light-responding receptor-coupled G protein, with GTP γ S and GDP-[AlF $_4$] $^-$ were published. These publications gave important insights into the geometrical configuration of the α -protein during the process of GTP- γ -phosphate hydrolysis. A H $_2$ O molecule performs a nucleophilic attack towards the γ -P of GTP. Noel et al. proposed arginine 174 and glutamic acid on position 203 to promote the γ -phosphate release by stabilizing the negatively charged transition state

(Noel et al. 1993). Shortly thereafter, the transducin-GDP-[AlF $_4$] $^-$ structure by Sondek et al. revealed Glutamine 200 as one major player in this process. As a requirement for the nucleophilic attack, the water molecule must be deprotonated. They suggest Q200 to be involved in the proton donation to the water molecule as well as in stabilization of the intermediate complex (Sondek et al. 1994). R174 and E203 are only present in the G α -family and are not found in the small G proteins (Noel et al. 1993). Therefore, it was suggested that these amino acids are responsible for more than 100-fold faster GTPase function compared to the small p21^{RAS} homologs (Mixon et al. 1995).

1.3. GTPase-deficient mutants and cancer

Before GTPase-deficient mutants were found in G proteins, they were reported in Ras genes. These Ras proteins belong to the class of small G proteins only consisting of the Ras-like domain. These mutations affected the GTPase activity and bestowed the protein with malignant transformation properties in NIH3T3 cells. Single point mutations on codon 12, 13, 61 and 63 in Ras were suggested to transform the protein into an oncogene (Barbacid 1987). Indeed, residue Q61 in Ras that corresponds to the Q200 in transducin

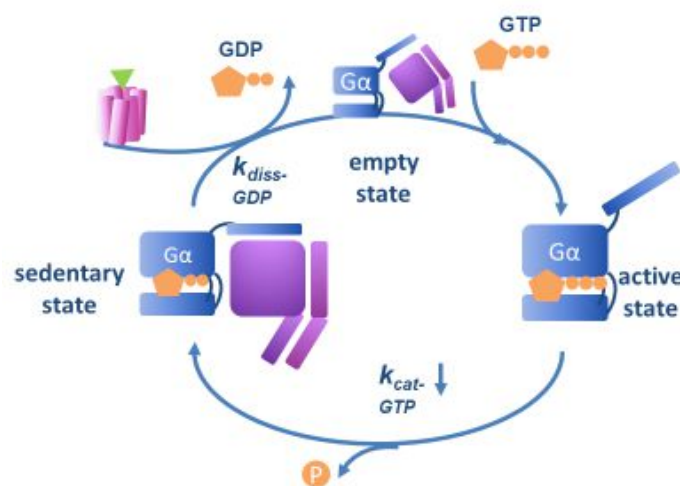


Figure 4: GTPase function as autocatalytic switch off. Upon receptor activation GDP can dissociate from the α -subunit. In this empty state the binding pocket can be re-occupied by GTP. The α -subunit uses its autocatalytic GTPase domain to enhance hydrolysis from the γ -phosphate of the GTP and thereby returns the protein to the inactive state. Scheme adapted and modified from Bourne et al. *Nature* 1990

(Mixon et al. 1995), has been found mutated in cancer from a wide spectrum of tissue e.g. skin, eye, pancreas, lung and many more. Activated Ras promotes pro-survival and inhibits anti-survival signaling regulated by an enzyme called mitogen-activated protein kinase (MAPK) (Pylayeva-Gupta et al. 2011).

Later, mutations of Gs proteins affecting the GTPase domain were first described in human pituitary tumors. These mutations affected Q277L (Ras corresponding Q61) and R201C/H of the GTPase domain of the $G\alpha_s$ protein, impairing its proper function. To determine GTPase activity the mutated constructs were transfected in α_s -deficient S49 cyc⁻ cells and the GTPase rate was measured in GTPase turn-off reaction ($k_{cat-GTP}$) on membranes. Both mutations reduced $k_{cat-GTP}$ approximately 30-fold compared to wild type. Elevated cAMP levels could be measured caused by the elongated active state of the Gs protein in those cells. These mutations led to overactivity of growth stimulating pathways, which is why they were also considered as oncogenes (Landis et al. 1989). Not much later, analogous activating mutations were also found in $G\alpha_{i2}$ (Lyons et al. 1990) and $G\alpha_q$ (Kalinec et al. 1992). Like the GTPase impaired p21Ras gene also the $G\alpha_q^{Q209L}$ was able to transform NIH3T3 cells and induce proliferation. Furthermore, in the same study Kalinec et al. showed enhanced tumor formation in nude mice injected with $G\alpha_q^{Q209L}$ expressing cells (Kalinec et al. 1992).

1.3.1. GTPase-deficient GNAQ/GNA11 is often found in uveal melanoma

In 2004 Van Raamsdonk and colleagues brought overactive Gq signaling and hyper-pigmentation into context for the very first time. A screening of over 30.000 mice revealed a dominant dark skin phenotypic sub-class (Dsk). Dsk1, Dsk7 and Dsk10 mice showed high pigmentation in the hair-bearing skin and some specific pigmentation patterns in non-hairy skin that delineated these mice from other Dsk with accumulating melanin in the epidermal skin layer. Hints as how hyper-pigmentation might occur was exposed as Dsk1, Dsk7 and Dsk10 were found to harbor activating mutations in either GNAQ or GNA11 (van Raamsdonk et al. 2004). Sensitized for GNAQ mutations in correlation with pigmentation Raamsdonk and colleagues performed sequencing for mutations in the GNAQ and GNA11 genes for a wide range of melanocytic neoplasms in a follow-up project. A total number of 236 samples was tested. The samples were categorized into naevi with 84, cutaneous and mucosal melanoma with 78 and uveal melanoma with 74 samples. Thereby, GNAQ mutations were detected in the highest frequency in blue naevi (83%) and uveal melanoma (46%) (van Raamsdonk et al. 2009). Similar results were obtained by Onken et al. in the same year. In this study he tested 49% of 67 primary and 54% of 58 posterior uveal melanoma samples to be positive for GNAQ mutation (Onken et al. 2004). The most extensive study followed in 2011. Van Raamsdonk et al. verified 713 melanocytic neoplasms of different types for mutations on position Q209 and 453 for mutations on position R183 of GNAQ and GNA11. Results were quite convincing as mutation in either of these genes was found in 83% of the uveal melanoma samples. By this means, codon Q209 was affected with higher frequency as only 6% of the samples had an amino acid replacement on position R183 (van Raamsdonk et al. 2010).

1.4. Diversity of Gq-signaling

For a better understanding of the complexity and diversity of Gq signaling, the most prominent effector proteins that are activated by Gq will be introduced first, before the description will move on to Gq signaling specifically in context of uveal melanoma.

1.4.1. Important effector proteins of the Gq-family

1.4.1.1. Phospholipase C

The best studied Gq-effector protein by far is the phospholipase C beta (PLC β). The mammalian phospholipase C is a membrane anchored enzyme that catalyzes the hydrolysis of phosphatidylinositol-4,5-phosphate (PIP₂), a membrane-bound phospholipid, into the second messengers diacyl-glycerin (DAG) and phosphorinositol-triphosphate (IP₃) as indicated in **figure 5** (Kadamur and Ross 2013; Thore et al. 2005). These second messengers regulate a broad range of cellular processes.

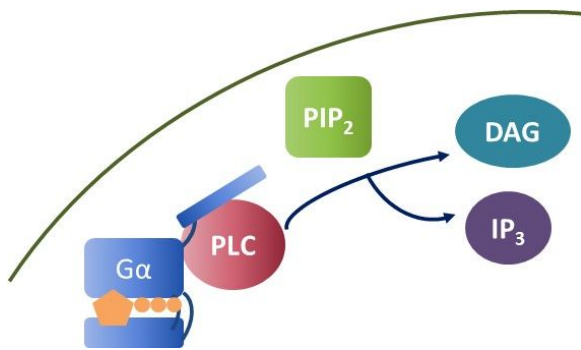


Figure 5: Gq activates PLC catalytic activity to hydrolyze PIP₂ into DAG and IP₃

Scheme adapted by Thore et al. *Journal of Cell Science* 2005

1.4.1.1.1. DAG-regulated effects

By binding to a conserved lipid binding cysteine rich domain (C1) that is found within a variety of kinases, DAG controls their activity. The most prominent kinase carrying the C1 domain is the protein kinase C (PKC). Two classes of PKCs are sensitive to DAG activation, the conventional PKCs (α , β , γ) and the novel class of PKCs (δ , ϵ , η , θ). They are distinguished by an additional C2 domain only found in the class of conventional PKCs. This additional domain is speculated to be involved in Ca²⁺-dependent membrane binding. PKC activation leads to a variety of physiological processes like constriction in smooth muscle cells, proliferation and even apoptosis (Harden et al. 2011; Webb et al. 2000).

1.4.1.1.2. IP₃-regulated effects

IP₃, the other second messenger generated by PLC β -induced hydrolysis process of PIP₂, binds to Ca²⁺ channels that are distributed on intracellular calcium stores. Binding of IP₃ on the tetrameric channel causes a conformational change within the protein and promotes the opening of the channel for calcium release. Additionally, autoregulation of these receptors prevents too high intracellular calcium levels, as elevated cytosolic levels spontaneously inhibit receptor function (Hanson et al. 2004). Receptor-regulated calcium release shows distinct temporal patterns on oscillating ion waves that affect different processes within the cell like proliferation, transformation, constriction and again even apoptosis, as it was shown that reduction of IP₃ receptors can inhibit apoptosis (Hanson et al. 2004; Berridge 2009).

1.4.1.1.3 Mechanistic insight into PLC β activation by Gq protein

Thirteen different isoforms of the mammalian PLC are known so far. They are divided by their properties into 6 different subclasses. Large structural patterns within the protein family are conserved as the catalytic X and Y domain, the triose phosphate isomerase (TIM), a C-terminal (CT) cysteine-rich C2 and a N-terminal pleckstrin homology (PH) region as well as the array with 4EF-hands (Harden et al. 2011; Yin and Janmey 2003). EF-hands are a specific helix-loop-helix motif within the protein that are discussed to bind calcium (Lewit-Bentley and Réty 2000). But only PLC β subclass has been shown to couple to Gq, as purified protein GPA-42, declared as Gq family member, was not able to activate isoforms γ and δ . Solely interaction with the beta class of PLC led to hydrolysis of phosphatidyl inositol 4,5-bisphosphate (Taylor et al. 1991). Some structural features are exclusive for this subclass, such as the long α -helix with 450 amino acids at the CT domain (Adjobo-Hermans et al. 2013).

The PLC β family includes 4 isoforms: β_1 , β_2 , β_3 and β_4 . The expression pattern between the subfamily is quite diverse. PLC β_1 is mostly found in the brain, PLC β_2 is expressed in cells of the hematopoietic system, PLC β_3 is found ubiquitously and interestingly PLC β_4 is exclusively expressed in brain and eye. It is noteworthy to mention, that this isoform was found to be mutated in several UM patients (Johansson et al. 2015). Even though all of the PLC β isoforms possess a long helical C-terminus, the sequence identity between those are quite low (Webb et al. 2000). These proteins are soluble and can be found in the cytosol, but a large fraction is also bound to the membrane under intrinsic conditions (Lee et al. 1987). Fluorescent-microscopy imaging of fluorescents-protein tagged PLC isoforms revealed cytoplasmic enrichment of isoforms 1 and 4 whereas 2 and 3 were constitutively bound to the membrane. By fractioning the protein and tagging the different sections the membrane binding effect could be associated to the C-terminus (Adjobo-Hermans et al. 2013).

The basal orientation of the protein at the plasma membrane is suboptimal for its catalytic activity as the active site is not facing its membrane-bound substrate phosphatidylinositol-4,5-bisphosphate. Disorientation of the active site could be associated to certain residues of the X/Y-linker. This linker is isolating the two catalytic TIM barrels and was found to be directed differently in active vs non-active protein. Activation of PLC β therefore requires a reorientation of the active site (Harden et al. 2011; Waldo et al. 2010).

Before Waldo et al. published the crystal structure of PLC β_3 together with the ALF4-activated G α_q , other groups have already shown the C-terminus of PLC to be one of the most important residues for protein-protein interaction. In this study it was shown that by truncation of the C-terminus from Gly934 or Ala867 activation by G α_q was severely impaired (Lee et al. 1993). Later the crystal structure of the active complex of PLC β_3 with G α_q did not only give insights to the binding sites but also promoted a special dynamic behavior of these two proteins described as a catch-and-release mechanism (Harden et al. 2011).

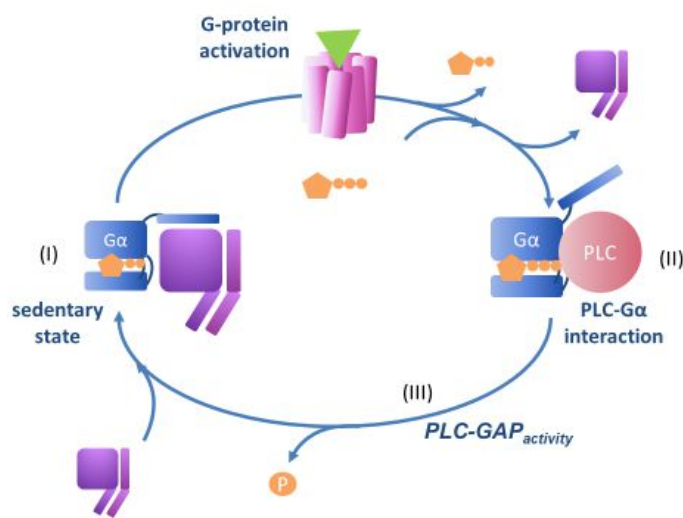
1.4.1.1.3.1. Catch and activation:

Three regions in G α_q are important for the interaction with this effector: a binding surface between switch 1 and 2 interacts with the connecting residue of the TIM barrel of PLC, secondly the canonical effector-binding surface formed by switch 2 and the α 3-helix of the

GTPase domain interact with a helix-turn-helix segment of PLC β_3 . And a third connecting point is the GTP-binding residue that directly interacts with a short amino acid sequence between EF3 and EF4 of the PLC β_3 . Upon Gq binding the orientation of the autoinhibiting X/Y-linker of PLC β_3 is sterically altered to unplug the catalytic site and therefore releasing intrinsic activity of the protein to hydrolyze phosphatidylinositol-4,5-phosphate and generate the second messengers IP3 and DAG (Waldo et al. 2010).

1.4.1.1.3.2. Release:

PLC does not only serve as a Gq effector but also acts as an GTPase-accelerating protein (GAP) as shown in **figure 6**. By using quench-flow kinetic methods Ross and coworkers have observed a 1000 fold increased GTPase activity in the presence of PLC β_1 (Mukhopadhyay and Ross 1999; Bernstein et al. 1992). GTPase activity of PLC β is related to the loop between EF3 and EF4. Here the crystal structure showed asparagine on position 260 to interact with Q209 and E212 of the GTPase domain of



Gq, thereby stabilizing a transition state important for the water molecule to perform hydrolysis of the γ -phosphate of GTP. GTP hydrolysis is proposed changing the conformation within Gq in a way that separates the binding sites and releases the effector. The functional asparagine is also found in other GAP proteins like RGS9 (Bernstein et al. 1992) and RGS2 (Nance et al. 2013).

Figure 6: PLC acts as a GAP for Gq proteins. In the presence of a ligand the inactive G protein (I) can be activated by the receptor. Activation leads to interaction of the α -subunit with PLC (II). This interaction has fast dynamics as PLC enhances the GTPase activity of α -subunit and therefore promotes the transformation of GTP to GDP.

1.4.1.2. Trio and other RhoGEFs:

The Rho-guanine nucleotide exchange factors regulate the activation of small GTPases of the Rho family. These proteins promote different cellular processes as dynamic changes of the cytoskeleton by inducing actin polymerization or expression of genes encoding proteins that are important for the cytoskeletal building e.g. actin (Jaffe and Hall 2005). In addition Rho activation has been recently connected to enhanced levels of Yes-associated protein (YAP) that upregulated the expression of pro-cell-growth genes as connective tissue growth factor (CTGF) and cysteine-rich angiogenic inducer 61 (CYR61) (Yu et al. 2012; Feng et al. 2014; Vaqué et al. 2012). RhoGEFs enhance the GDP release and thereby promote GTP entry to the guanine-nucleotide binding pocket of the small G proteins. Direct interaction of G α_q and the Trio family of RhoGEFs including Trio, Duet and RhoGEF61, has been reported multiple times (Vaqué et al. 2012; Feng et al. 2014; Rojas et al. 2007). These Dbl-RhoGEFs possess a conserved structural feature of a catalytic Dbl-domain altering with a PH domain. In the resting state, the PH domain

acts as a plug for the catalytic Dbl-domain and serves the protein as an autoinhibiting module (Lutz et al. 2007). By interacting with the C-terminal PH domain $G\alpha_q$ revokes the autoinhibiting function and restores the protein's guanine nucleotide exchanging activity (Rojas et al. 2007).

1.4.1.3. PKC ζ

PKC ζ belongs to the family of the atypical PKC isoforms that are insensitive towards DAG activation (Colón-González and Kazanietz 2006; Ananthanarayanan et al. 2003). Activation of PKC ζ by Gq is reported to induce phosphorylation of ERK5 involving direct interaction of MEK5, PKC ζ and Gq. Ribas and coworkers demonstrated ERK5 phosphorylation upon either ligand or mutational initiated Gq activation. ERK5 stimulation was independent of PLC β activation as same results were observed by using a constitutively active Gq construct lacking important sites for PLC β binding. Furthermore, they could demonstrate direct interaction in an immunoprecipitation assay as HA-tagged PKC ζ and Gq were found together while PKC ζ did not associate with Gs, Gi nor G12-isoforms (García-Hoz et al. 2010). In the follow-up study Ribas and co-workers exposed a new binding site for this effector in the Gq protein $\beta 4$ - $\alpha 3$ loop in $G\alpha_q$, as mutated $G\alpha_q$ lacking residues critical for PLC β and RhoGEF61 binding did not lower the amount of co-immunoprecipitated complex of Gq-PKC ζ (Sánchez-Fernández et al. 2016).

1.4.2. Gq signaling in uveal melanoma

Gq signaling is quite complex as it has regulating function in many crucial cellular processes like apoptosis, autophagy, cell differentiation, migration, cytoskeletal dynamics and much more. Furthermore signaling is dependent on the cellular background³⁸. Multiple reports were published in the last decades elucidating Gq as the perpetrator for the onset of different pro-survival pathways in uveal melanoma. In these reports Gq was shown to activate MEK, PI3K, or YAP dependent on its mutational status (van Raamsdonk et al. 2009; Zuidervaart et al. 2005; Chen et al. 2014; Ambrosini et al. 2013; Feng et al. 2014; Vaqué et al. 2012) (**figure 7**). These events will be introduced here in detail:

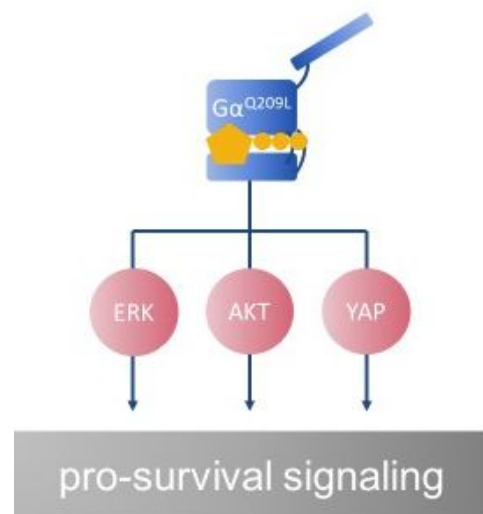


Figure 7: Overview of GNAQ/11 driven pro-survival pathways.

1.4.2.1. Activation of the MAPK-pathway:

MAPK is a serine-threonine kinase cascade typically known to be activated by growth factor binding to tyrosine kinase receptors (TKR). Onset of this kinase cascade leads to enhanced cell proliferation. This pro-proliferative pathway is found to be over-active in many malignant epithelial melanocytes. Over-activity is mostly associated with gain-of-function mutation in MAPK-upstream proteins as B-Raf or N-Ras (Dong et al. 2003) that are often detected in CM. UM cells lack mutations in these genes but also show high basal ERK activity (van Raamsdonk et al. 2009; Zuidervaart et al. 2005). Despite the absence of mutations in the classical ERK driver proteins, Zuidervaart et al. reported elevated ERK activity in 10 out of 19 established UM cell lines (Zuidervaart et al. 2005).

Beside of the TKRs also GPCRs have been found to activate this pathway (Gutkind 2000). Additionally it has been shown that in absence of the G proteins in the state of zero-G, GPCRs fail to signal to ERK (Grundmann et al. 2018). Whereas it is long known that mutated GNAQ is able to transform NIH3T3 cells since the early 90s (Kalinec et al. 1992) more in-depth investigations on GNAQ signaling in human melanocytes has been assessed only for the last 10 years.

2009 Bastian and coworkers could show for the very first time that transfection of GNAQ^{Q209L} into transformed primary melanocytes empowered the cells to grow unattached to substrate, which is a common nature of transformed cells. Furthermore, injection of melanocytes transfected with mutant GNAQ but not wildtype GNAQ initiated tumor growth in nude mice. To evaluate whether activation of the MAPK pathway by GNAQ contributes to the malignant behavior, they looked for ERK phosphorylation in these transfected melanocytes. GNAQ^{Q209L} transfected cells clearly showed elevated pERK levels. Further proof for the GTPase-deficient mutant to signal via ERK activation was done by using short interfering RNA to knockdown GNAQ in UM cells carrying this activating mutation (OMM1.3 and Mel202). ERK levels were significantly decreased in these cells compared to empty vector treatment (van Raamsdonk et al. 2009). Similar results were obtained in a later study where additional GNAQ involvement in PKC signaling was proven as knockdown of GNAQ not only depressed pERK but also PKC activity. Thus, they suggest PKC to be the missing link between GNAQ and ERK on-set, as PKCi could also depress pERK levels. But surprisingly they found synergistic effects on cell growth deceleration when combining PKC and MEK inhibitors (Chen et al. 2014).

1.4.2.2. Protein-kinase B (AKT) activation

The AKT/PI3K pathway is predominantly activated by growth factors and highly associated with cell cycle progression. Upregulation of this pathway has been observed in many cancer types. Cell cycle promotion by AKT activation occurs due to Cyclin D1 induction (Chang et al. 2003). Cyclin D1 binds to cyclin-dependent kinases (Cdk), which serve as cell cycle check-point regulators. The Cyclin D1-Cdk complex supports cell cycle steps and increases the expression of proliferation promoting genes such as E2F. Moreover, substantial evidence indicates Cyclin D1 upregulation to be a major requirement for metastasis (Casimiro et al. 2012).

Uveal melanoma cell line treatment with the PI3K inhibitor (PI3K-i) LY294002 (LY) inhibited cell proliferation and induced apoptosis. LY also blunted AKT phosphorylation of the cell samples demonstrated in western blot. An additional effect of the PI3K-i was the decreased expression of cyclin D1 (Babchia et al. 2010). The tested cell lines 92.1 and Mel270 both harbored a mutation in GNAQ (Griewank et al. 2012). By combining LY with the MEK inhibitor (MEK-i) UO126 synergistic effects were observed on cell proliferation and cyclin D1 expression (Babchia et al. 2010). Similar synergistic effects were observed by Woodman and co-workers. They could show that combination of the MEK-i and AKT-i was superior to single agent-treatment in cell proliferation as well as in apoptosis. The results were similar regardless of the mutational GNAQ/GNA11 state. But in cells with activating mutation in this gene basal levels of MAPK activation could be associated with GNAQ-signaling as GNAQ-siRNA inhibited MAPK phosphorylation. This correlation was not observed in GNAQ wildtype cells. GNAQ signaling in this study was only associated with ERK activation as GNAQ siRNA did not influence pAKT levels in any cell line.

Interestingly, Ambrosini et al. obtained different results by using the same cells. In this study, which was published only one year later, GNAQ siRNA inhibited both pERK and pAKT in GNAQ mutated cells (Ambrosini et al. 2012). But both studies indicate another driver for ERK and AKT in UM cells lacking mutation in GNAQ, as these cells had also high basal pERK and pAKT but were not sensitive to GNAQ knockdown. In all tested cell lines again, best results in depressing cell viability were achieved by the combination of MEKi and AKTi. In a xenograft experiment with injected 92.1 cells tumor growth was smallest in the cohort of mice, which were fed with both compounds (Ambrosini et al. 2012).

1.4.2.3. YAP

Most recently another pro-survival pathway has been demonstrated to be regulated by Gq signaling (Yu et al. 2014; Feng et al. 2014; Vaqué et al. 2012). YAP a transcriptional co-activator initiates the expression of proliferation activating proteins. Classically, YAP has been known to be a downstream target of the hippo-pathway. In this hippo pathway two major kinases MST1/2 and LATS1/2 function as core components that suppress YAP activation and therefore inhibit tissue growth and limit organ size (Zhao et al. 2011b). The hippo-pathway is activated under apoptotic stress e.g. high cell density in mammalian NIH-3T3 cells. Cell-cell contact in these cells decreased YAP activity, as YAP was excluded from the nucleus (Zhao et al. 2007). MST1/2 can be activated by caspase cleavage and in turn activate LATS1/2 that then will phosphorylate YAP. Phospho-tag at Ser127 is required for binding of a protein called 14-3-3. Adaptor protein 14-3-3 regulates the activity and localization of many proteins in numerous tissues (Schumacher et al. 2010). 14-3-3-YAP complex is unable to enter the nucleus and thereby, it is enriched in the cytoplasm. Further phosphorylation of the protein at Ser381 can lead to its ubiquitination. The recruitment of ubiquitin ligases to the phosphorylated YAP initiates the ubiquitination-dependent degradation (Zhao et al. 2010). Non-phosphorylated YAP is predominantly found in the nucleus and can bind to the transcription factor TEAD, a protein with TEA domain for DNA binding (Zhao et al. 2011b). Vassilev et al. could show that TEAD is mostly associated with YAP by using different mouse lineages. Furthermore, they could demonstrate that co-expressing YAP increased TEAD activity by 300x fold (Vassilev et al. 2001). TEAD-promoted activation of different genes e.g. Cyr61 and CTGF that are important for tissue development but that also has been linked to tumorigenesis in different cancer types (Zhou et al. 2016). Furthermore, elevated expression of Cyr61 in uveal melanoma compared to normal melanocytes was associated with the angiogenetic character of the tumor (Walker et al. 2002).

Introduction

In 2012 two independent groups published for the first time that serum initiated hippo-pathway deactivation could be contributed to an GPCR activation (Miller et al. 2012; Yu et al. 2012). Serum influence on YAP activity is well established in the field (Meng et al. 2015; Yu et al. 2014) but the knowledge about the mechanism was new when Yu et al. discovered that nuclear localization initiated by serum addition could not be mimicked by the addition of different growth factors. Instead they could identify phosphatidic acids as the activating compound. Further investigation revealed that activation of GPCRs by the lysophospholipids sphingosine 1-phosphate (S1P) or lysophosphatidic acid (LPA) causes deactivation of the LATS enzyme and thereby increases YAP activity. Knockdown of G12/13 abolished LPA effect on HEK cells as well as the Rho inhibitor C3. Further tests to clarify the role of other G proteins on YAP activity indicated a YAP promoting role for G12/13 and Gq/11-coupled GPCRs whereas Gs signaling seemed to antagonize the effects on YAP (Yu et al. 2012). Similar results were obtained by Miller et al. who also showed that activation of YAP can be induced by S1P. S1P effect was mediated by the S1P2 receptor as the effect could be prevented by using a specific antagonist of this receptor. They could also show that ligand-mediated activation via this GPCR was also Rho-dependent, as the results were converted by using the ROCK inhibitor Y-227632 (Miller et al. 2012).

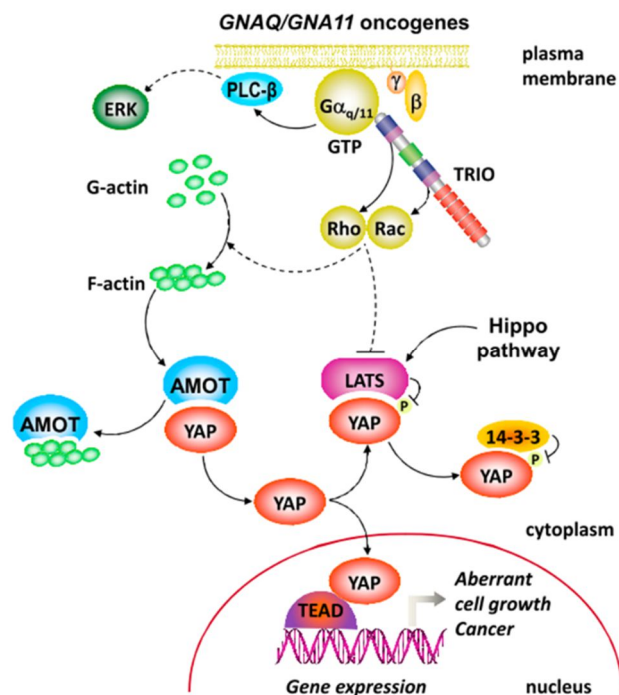


Figure 8: GNAQ signaling to induce YAP activity. Borrowed from Feng et al. *Cancer Cell* 2014.

Two years later in 2014 cell press released two articles back-to-back in *Cancer Cell*, that demonstrated YAP activity in uveal melanoma to be promoted by oncogenic GNAQ/GNA11 signaling. Both articles reported that increased fraction of nuclear YAP correlates with the mutational status of the Gq protein. Additionally, transfection of GNAQ^{Q209L} but not wild type GNAQ into HEK293 cells led to increased nuclear localization of YAP (Feng et al. 2014) or decreased fraction of phosphorylated protein¹⁰⁷. GNAQ signaling could be identified as perpetrator for YAP activation as knockdown of GNAQ by shRNA/siRNA in 92.1 (Yu et al. 2014) and in the metastatic-prone UM cell lines OMM1.3 (Feng et al. 2014) inverted YAP localization or phosphorylation state. Further knockdown approaches to elucidate GNAQ signaling pathway to YAP activation revealed a new pathway involving TRIO, Rho and Rac (**figure 8**). Thereby, it is suggested that RhoA and ROCK inhibit LATS activity and in addition the activation of RhoA decreases the fraction of angiominin (AMOT) associated YAP in favor for active YAP by inducing actin polymerization, as shown in figure 8. F-actin and YAP both then

compete for AMOT binding (Feng et al. 2014; Vaqué et al. 2012). Guan and coworkers have described YAP-AMOT interaction as a mechanism that regulates YAP localization and phosphorylation (Zhao et al. 2011a). TRIO is a RhoGEF that enhances the exchange of GDP to GTP in Rho proteins and therefore promotes its signaling. Trio is closely related to the p63-RhoGEF that has been co-crystallized with a $G\alpha_{i/q}$ chimera. In the same study, Lutz et al. could show that Gq was able to bind and activate Trio (Lutz et al. 2007).

1.5. Therapeutic options in uveal melanoma

Primary uveal melanoma is treated with either radiotherapy or surgery. Newer approaches e.g. with the ICON 1, a immunoconjugate of the tissue factor 7, is currently under clinical phase 1 study for primary UM (Yang et al. 2018). These are good options, but the problem is, that 50% of the UM develop metastasis. Once metastasis is detected survival rates drop. The median survival then decreases to less than 14 months as median (Krantz et al. 2017). Unfortunately, there is no successful standard therapy developed by now. Classic chemotherapeutics as Dacarbazine or Cisplatin were quite disappointing in their effects towards metastasizing UM (Carvajal et al. 2016). Checkpoint inhibitors as immunotherapy that have shown good results in the treatment of cutaneous melanoma did not show the desired effect in UM. Targeted therapy has become interesting since mutation in GNAQ/GNA11 have been revealed to be oncogenic driver for approximately 80% of all UM. Different approaches to target the downstream effectors as MAPK, PI3K, PKC or these in different combinations did not show great efficacy in clinical studies (Yang et al. 2018). At the beginning of our study direct targeting of the oncogene itself was not approached, very likely due to the lack of a chemical inhibitor to aim the oncogenic GNAQ. In the course of this project two other studies came out that considered this tactic to inhibit cell growth of uveal melanoma cells in vitro (Onken et al. 2018; Lapadula et al. 2018). These emerging studies together with our study underline the value and the essential need to investigate this field.

1.6. GNAQ inhibitors

Whereas modulation of G protein signaling on the receptor level with agonist or antagonist is widely in use, the direct inhibition of G proteins remains quite a challenge. Not many tools are available so far to modify the activity of this protein family. Pertussis toxin (PTX) is a well-established inhibitor of the G_i subfamily, but no inhibitors are known to reliably abolish G_s or $G_{12/13}$ signaling directly (Schrage et al. 2015).

In the past 10 years multiple reports about the two depsipeptides YM-254890 (YM) and FR900359 (FR) have progressively emerged in the GPCR community (**figure 9**).

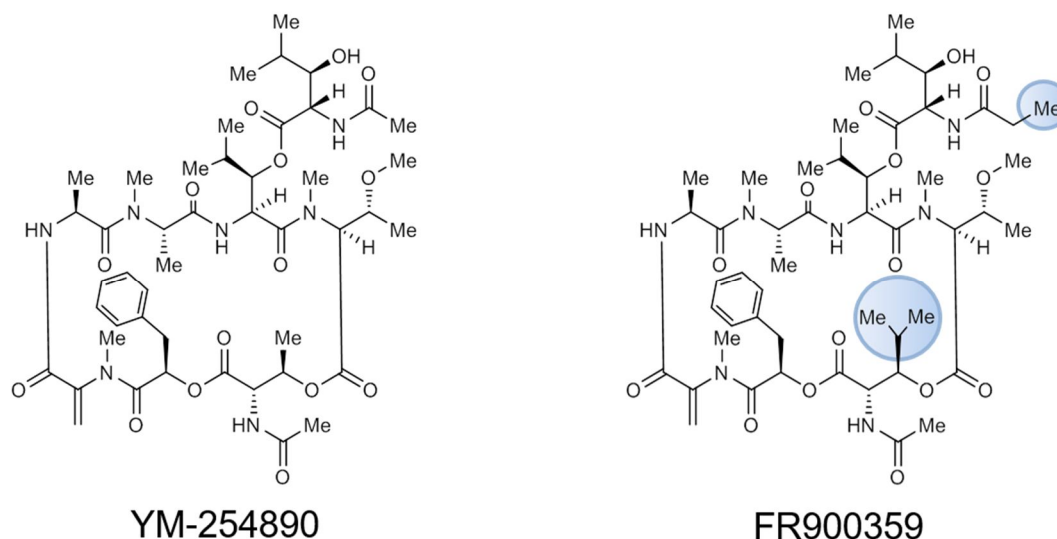


Figure 9: Comparison of YM-254890 and FR900359 structures. Borrowed from Schrage et al. *nature communication* 2015.

These two analogs have been validated regarding their biological behavior and mechanism of action and could be described as Gq/11 inhibitors (Schrage et al. 2015; Nishimura et al. 2010) (**figure 10**).

1.6.1. YM

YM, a depsipeptide isolated from the chromobacteria strain QS3666, was first described to inhibit ADP-induced platelet aggregation in human plasma (Taniguchi et al. 2004). Later on, Takasaki et al. could link the anti-thrombotic effects of YM to its ability to block Gq signaling. Inhibition of Gq was not receptor-dependent as signaling was abolished after activation of multiple Gq-coupled GPCRs. Additionally, activity of non-receptor dependent analog Gq^{R183C} could be blunted with the inhibitor. The mutation on R183C leads to elevated intrinsic activity without receptor involvement. But effects of YM were only observed for Gq/11/14 mediated signaling as it did not show any effect on the production of the second messenger cAMP upon Gi or Gs protein activation. Moreover, the mechanism of inhibition-activity could be accounted for the GTP-GDP exchange, as a mutation that completely lacks GTPase activity could not be addressed by YM application. This hypothesis was supported by a crystal-structure that showed the binding site of the depsipeptide in the inactive GDP-bound G $\alpha_{i/q}$ -chimera-G β_1 -G γ_2 heterotrimer. YM was shown to occupy two distinct regions that link the GTPase and helical domain on the alpha-subunit. Flexibility in these interdomain-linkers is important for the dissociation of the guanine-nucleotide and therefore for its activation (Nishimura et al. 2010). According to its function as a guanine-dissociation inhibitor (GDI) and in line with published data it is unable to inhibit the oncogenic GNAQ/11 protein (Takasaki et al. 2004; Kimple et al. 2011; Xiong et al. 2016).

1.6.2. FR

FR is a depsipeptide that is closely related to YM. Only 3 methyl-groups distinguish the two molecules structurally (Xiong et al. 2016). Originally FR is extracted from an evergreen plant called *Ardisa crenata* that is found in far eastern countries as Japan or

Korea. Its structure was first obtained by a Japanese working group in 1988 that also reported about the compounds ability to depress blood pressure and inhibit platelet aggregation (Miyamae et al. 1989).

It took more than a quarter of a century after structural clarification until the true nature of the FR compound was fully characterized in the course of a former study by our working group (Schrage et al. 2015). Here we identified FR as a specific inhibitor of Gq/11 and 14 proteins over all other G α isoforms. FR significantly reduced high affinity ligand binding, which occurs under guanine nucleotide-free ternary complex formation of ligand, receptor and G protein. Its mechanism of action was therefore identified as a guanine nucleotide dissociation inhibitor (GDI).

Shortly afterwards Kukkonen presented similar results on FR specificity in a relatively small study (Kukkonen 2016). In addition to the selectivity of FR we could demonstrate the lack of effects on cells in the absence of G α_q proteins, and therefore could proofed the pharmacological value of this depsipeptide (Schrage et al. 2015). As expected from its mechanism of action HEK293 cells transfected with the oncogenic GqQ209L protein could only be partly inhibited in IP1 accumulation assay. Here we will further investigate FR's capability to target the oncogenic GNAQ/GNA11 protein.

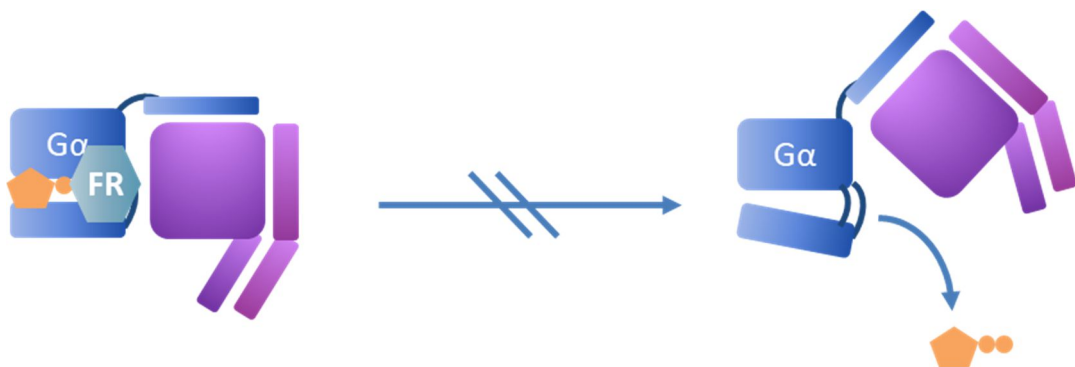


Figure 10 Scheme of FR function as a GDI. FR binds between the helical and the GTPase domain of the G α -subunit and prevents receptor-mediated interdomain rearrangement that normally allows the GDP to dissociate from its binding pocket.

Goal of this study

Activating mutations, disrupting GTPase function of Gq are present in 5.6% of human cancer (O'Hayre et al. 2013). Inhibition of this activated protein would therefore be highly desirable. FR900359 was recently described as selective inhibitor of the Gq/11/14 protein heterotrimer. Thereby FR significantly reduced high affinity ligand binding, which occurs under guanine nucleotide-free ternary complex formation of ligand, receptor and G protein. Thus, its mechanism of action could be identified as a guanine nucleotide dissociation inhibitor (GDI) (Schrage et al. 2015). One would assume that inhibition of GDP dissociation would not be the right strategic approach and therefore FR the wrong tool to silence signaling of those GTPase-deficient proteins. Here in this study we want to evaluate FR's capability to diminish mitogenic signaling in melanoma cell lines with high Gq tonus derived from either overactive wt or GTPase impaired Gq.

To verify the primary observation and to proof FR interaction with the GTPase-deficient mutant we further investigated FR's mechanism of action and want to unravel the reasons for selective pathway inhibition. HEK cells lacking Gq/G11 proteins offer an ideal genetic background for this endeavor because we can reintroduce the modified targets by transfection without confounding expression of endogenously expressed Gq/11 proteins with label-free dynamic mass redistribution technology, we were furthermore investigating the whole cell response upon the inhibition of a constitutively active protein. By examining the fractions of GTP-bound monomeric and receptor-activatable GDP-bound heterotrimeric state of the GTPase-malfunctioning Gq protein we want to rationalize our approach to target the oncogenic Gq with an inhibitor described as GDI.

Mutations on one of the hot spot residues Q209 or R183 are detected in over 80% of uveal melanoma samples from patients and are considered as oncogenic drivers. Many studies have focused on targeting Gq downstream effectors as therapeutically attempt towards uveal melanoma progression. So far, no effective therapy has been developed. In the course of this study we want to certify the direct inhibition of the oncoprotein itself as a feasible and effective strategy for UM tumor treatment.

YM another macrocycle, structurally close related to FR, has been described to have similar inhibition properties. In a head-to-head comparison we compared the drug vulnerability as well as the long-term inhibition capacity of these molecules regarding inhibition of proliferative behavior in a uveal melanoma cell system with mutated Gq. This comparison ideally helps to validate the best candidate for future translational medicine efforts and to develop a targeted therapy for stratified forms of uveal melanoma.

Materials

2.1. Cell lines

2.1.1. Melanoma Cells

Name	Biological source	GNAQ/GNA11	Producer
HCmel12	mouse	GNA11 ^{Q209L}	Professor Thomas Tüting University of Magdeburg
B16	mouse	wild type	from the American Type Culture Collection
BRIM4	human	GNAQ ^{Q209P}	Professor Richard Marais University of Manchester
Skmel28	human	wild type	Professor Dirk Schadendorf, University of Essen
MaMel119	human	wild type	Professor Dirk Schadendorf, University of Essen

2.1.2. Uveal Melanoma Cells

Name	Biological source	GNAQ/GNA11	Producer
Mel290	human	wild type	Professor Martine Jaeger University of Leiden
Mel285	human	wild type	Professor Martine Jaeger University of Leiden
Mel270	human	GNAQ ^{Q209P}	Professor Martine Jaeger University of Leiden
Mel202	human	GNAQ ^{Q209L}	Professor Martine Jaeger University of Leiden
92.1	human	GNAQ ^{Q209L}	Professor Martine Jaeger University of Leiden
OMM1.3	human	GNAQ ^{Q209P}	Professor Bruce R. Ksander Harvard Medical School

2.1.3. Human Embryonal Kidney 293 cells (HEK293)

Name	Genome edited	Producer
HEK293	non-edited	Professor Evi Kostenis University of Bonn
HEK293G $\alpha_{q/11}$ ^{-null}	Δ G $\alpha_{q/11}$ by CRISPR Cas9	Professor Asuka Inoue Tohoku University
HEK293 FFA2	Stably expressing FFA2 Flp-in	Professor Evi Kostenis University of Bonn

2.2. Cell culture media and supplements

2.2.1. media

Name	Manufacturer	Reference Number
RPMI 1640	Thermo Fischer Scientific	21875-034
DEMEM	Thermo Fischer Scientific	41965-039
MCDB 153	Sigma-Aldrich now MERCK	M7403-10X1L

2.2.2. Supplements and solutions for cell culture treatment

Name	Manufacturer	Reference Number
Penicillin/Streptomycin	Thermo Fischer Scientific	15140
Blasticidin	Thermo Fischer Scientific	A1113902
Hygromycin B	Sigma-Aldrich	H3274-50MG
Fetal calf serum	PANTM Biotech GmbH	P30-3702
Non-Essencial Amino	Thermo Fischer Scientific	11140068

Acids (NEAA 100X)

HEPES	Thermo Fischer Scientific	14025050
2-mercaptoethanol	Sigma-Aldrich	M6250-10ML
Trypsin-EDTA 0.05%	Thermo Fischer Scientific	25300054

2.2.3. Cell culture media and buffer**2.2.3.1. Washing buffer**Phospho-buffered saline solution (PBS)

Ingredients	Volume (ml)	Weight (g)	Final concentration
PBS tablets	-	-	10 mM
dH ₂ O	500		
KCL	-	0.1	2.68 mM
NaCl	-	4.0	140 mM

pH was adjusted to 7.45 with HCL

2.2.3.2. Cell culture media2.2.3.2.1. media for HEK293 and HEK293G $\alpha_{q/11}^{-null}$

Ingredients	Volume (ml)	Final concentration
DEMEM	500	10 mM
Penicillin/Streptomycin	5	1%
Fetal calf serum	50	10%

Materials

2.2.3.2.2. media for HEK293 FFA2

Ingredients	Volume (ml)	Final concentration
DEMEM	500	10 mM
Penicillin/Streptomycin	5	1%
Fetal calf serum	50	10%
Blasticidin	0.75 (of 10 mg/ml)	15 µg/ml
Hygromycin B	0.5 (of 10 mg/ml)	100 µg/ml

2.2.3.2.3. media for CM cells B16, HCmel12, Skmel28, MaMel119

Ingredients	Volume (ml)	Final concentration
RPMI 1640	500	10 mM
Penicillin/Streptomycin	5	1%
Fetal calf serum	50	10%
NEAA (100X)	5	1x
HEPES	0.5	1 mM
2-mercaptoethanol	0.18	20 µM

2.2.3.2.4. BRIM4

Ingredients	Volume (ml)	Final concentration
-------------	-------------	---------------------

MCDB 153	500	10 mM
Penicillin/Streptomycin	5	1%
Fetal calf serum	50	5%

2.2.3.2.5. media for UM cells Mel290, Mel285, Mel270, Mel202, 92.1, OMM1.3

Ingredients	Volume (ml)	Final concentration
RPMI 1640	500	10 mM
Penicillin/Streptomycin	5	1%
Fetal calf serum	50	10%

2.3. Plasmids, Bacteria, Primers

2.3.1. generated pcDNA3.1+ plasmids with ampicillin resistance;

Insert gene	template	Primer forward	Primer reverse
GNAQ-HA	Was obtained by internal source from Professor Evi Kostenis; Served as template to generate all following constructs:		
GNAQ ^{Q209L} -HA	GNAQ-HA	5'-GAT GTA GGG GGC CTA AGG TCA GAG AG-3'	5'-CTC TCT GAC CTT AGG CCC CCT ACA TC-3'
GNAQ ^{R183C} -HA	GNAQ-HA	5'-CAA CAA GAT GTG CTT AGA GTT TGT GTC CCC ACC ACA GGG ATC ATC-3'	5'-GAT GAT CCC TGT GGT GGG GAC ACA AAC TCT AAG CAC ATC TTG TTG-3'
GNAQ ^{F75K} -HA	GNAQ-HA	5'-GCG CGG CAA AAC CAA GCT GGT GTA TCAG-3'	5'-CTG ATA CAC CAG CTT GGT TTT GCC GCG C-3'
GNAQ ^{F75KQ209L} -HA	GNAQ ^{Q209L} -HA	5'-GCG CGG CAA AAC CAA GCT GGT GTA TCAG-3'	5'-CTG ATA CAC CAG CTT GGT TTT GCC GCG C-3'
GNAQ ^{I190W} -HA	GNAQ-HA	5'-CAG GGA TCT GGG AAT ACC	5'-GTA AGT CAA AGG GGT ATT CCC AGA

Materials

		CCT TTG ACT TAC-3'	TCC CTG-3'
GNAQ ^{I190WQ209L} -HA	GNAQ ^{Q209L} -HA	5'-CAG GGA TCT GGG AAT ACC CCT TTG ACT TAC-3',	5'-GTA AGT CAA AGG GGT ATT CCC AGA TCC CTG-3'
GNAQ ^{I190N} -HA	GNAQ-HA	5'-CAG GAT CAA CGA ATA CCC CTT TGA CTT ACA AAG-3'	5'-CAA AGG GGT ATT CGT TGA TCC CTG TAG TGG G-3'
GNAQ ^{I190F} -HA	GNAQ-HA	5'-CAG GGA TCT TCG AAT ACC CCT TTG ACT TAC-3'	5'-GTA AGT CAA AGG GGT ATT CGA AGAT CCC TG-3'
GNAQ ^{F75A} -HA	GNAQ-HA	5'-GCG CGG CGC CAC CAA GCT GGT GTA TCA G-3'	5'-CTG ATA CAC CAG CTT GGT GGC GCC GCG C-3'
GNAQ ^{R60K} -HA	GNAQ-HA	5'-CAA GCA GAT GAA GAT CAT CCA CGG GTC GGG-3'	5'-GTG GAT GAT CTT CAT CTG CTT GAT GAA GGT GCT C-3'
GNAQ ^{V184M} -HA	GNAQ-HA	5'-GCT TAG AGT TCG AAT GCC CAC TAC AGG GAT C-3'	5'-GTA GTG GGC ATT CGA ACT CTA AGC ACG TCT TGT TG-3'

2.3.2. Bacterial strain

DH5 α TM competent cells purchased from Invitrogen (ref. number: 18265017) were used for amplification of recombinant plasmids.

2.4. Mouse strains

NOD scid gamma is an immune deficient laboratory mouse line lacking NK-cells and lymphocytes.

Athymic Nude Mouse NU(NCr)-Foxn1nu mice is another immune deficient nude laboratory mouse line. These mice have a deletion in the FOXN1 gene and are athymic. Therefore, they are unable to produce T-cells.

Lack of immunity enables the mice to host a wide range of human cells and is therefore suitable for xenograft experiments. Here we used mice at the age of 7 to 8 weeks with female sex.

2.5. Buffer and Solutions for Assays

2.5.1. Aluminum fluoride for G protein activation used in IP1 assay

AlCl_3 and NaF were dissolved in IP1 assay buffer to the concentration of 2.4 AlCl_3 and 80 mM NaCl. Due to poor stability of $[\text{AlF}_4]^-$, AlCl_3 2.4 mM and NaF 80 mM were freshly combined directly before use in a ratio of 1:1:2 (AlCl_3 : NaF: IP1-buffer) to a final concentration of 300 μM .

2.5.2 HBSS Buffer for DMR assay

HBSS buffer from Invitrogen (ref. number: 14025-050) was supplemented with HEPES to a final concentration of 20 mM.

2.5.2. Poly-D-Lysin (PDL) plate-coating solution

Aliquots of 50 ml 1x solutions were prepared by dissolving 5 mg of PDL in 50 ml dH_2O . Afterwards solution was sterile filtered.

2.5.3. Polyethyleneimine transfection solutions

Polyethylenimine from PolyScience (ref. number: 23966) was dissolved in PBS 1x to a final concentration of 1mg/ml.

2.5.4. LB (Luria Bertani) Medium for bacterial growth

In 1000 ml distilled water 10g Tryptone, 5 g yeast extract and 5 g sodium chloride are dissolved. Medium was autoclaved before use.

2.5.5. Agar plate coating for bacterial colony growth

1.2 g of agar was dissolved in 80 mL of warm LB medium to a final concentration of approximately 1.5%. Ampicillin was added for colony selection. Medium was 8 mL of dissolved agar solution, which was poured on 56 cm^2 bacterial culture plates.

2.5.5. EtOH 70% for DNA extraction

730 mL of absolute EtOH were mixed together with 270 mL of distilled water.

2.5.6. Tris 1 M buffer

129.1 g of Tris was dissolved in 1000 mL distilled water. Afterwards HCL was used to adjust the pH to 6.8.

2.5.7. Lysis buffer for western Blot

56640 µl distilled water was mixed together with 1500 µl 1 M Tris buffer and 1800 µl of 5 M NaCl. Triton and IGEPAL were both added to a final concentration of 1%.

2.5.8. Washing buffer for western Blot

1 mL Tween was added to 999 mL of PBS solution.

2.6. Reagents

2.6.1. Compounds and Assay Reagents

Name	Manufacturer	Reference Number
Agarose	Invitrogen	05040
Aluminium Fluoride	ZVE Bonn	125098
Antioxidant NuPage	Life Technology	NP0005
Ampicillin	Roth	K.029.1
Atropin	Sigma-Aldrich	A0132
Bis-Tris 10%	Life Technology	NP0315Box
BSA Bovine serum albumin	Sigma-Aldrich	A6003
C3	Sigma-Aldrich	402907
Carbachol	Sigma-Aldrich	C4382
DNA 1kb ladder	New England Biolabs	N3272
DMSO	Roth	A994.2
EDTA		
EGF	Sigma-Aldrich	E 9644
Ethidiumbromide	Roth	2218.1

Fasudil	Tocris	541
FR900359	University of Bonn in house production (AG König)	
Fsk	Tocris	1099
Glycerin 99%	Grüssim	11052
Gö 6976	Calbiochem	365250
Gö 6983	Tocris	2285
IGEPAL		
Kaleidoscope standard	Bio-Rad	161-0324
LDS SB	Life Technology	NP0007
LY294002	Sigma-Aldrich	L9908
Methanol	Sigma-Aldrich	125678
MOPS SDS RB	Life Technology	NP0001
Natrium Chloride	Fischer Bioreagenz	BP358-212
Pfu-DNA-Polymerase	Promega	M774A
Poly-D-lysine hydrobromide (PDL)	Sigma-Aldrich	P6407
Protease Inhibitor Cocktail	Sigma-Aldrich	P8340
Roti-Block	Roth	A151.2
Sample Reduction Agent	Life Technology	NP0009
Temed	Roth	2367.3
Trametinib	selleckchem	S2673
Transfer Buffer	Life Technology	NP000P-6
Tris	AppliChem	A2264
Triton X	Fluka	93420
Tryptone	Roth	8952.1
Tween	Sigma-Aldrich	P1379
U73122	Tocris	1268
U73343	Tocris	4133
vemurafinib	selleckchem	S1267
Yeast extract	Merck	1.03753.0500
YM254890	wako	253-00633

2.6.1. Antibodies for Western blot

Name	AB classification	Manufacturer	Reference Number
------	-------------------	--------------	------------------

Materials

actin AB	primary	Santa Cruz	sc-47778
gp100AB	primary	abcam	ab137078
anti-rabbit	secondary	antibodies-online	ABIN102010

2.7. Assay and Microbiological Kits

Name	Manufacturer	Reference Number
Pierce™ BCA Protein Assay Kit	Thermo Scientific	23225
Amersham ECL prime Western Blotting	GE Healthcare	RPN2236
innuPREP DNA Mini Kit	Analytik jena	845-KS-1040250
innuPREP Gel Extraction Kit	Analytik jena	845-KS-5030050
IP -One HTRF® assay kit	Cisbio bioassays	62IPAPEJ
NucleoBond Xtra Midi	Macherey-Nagel	740414.10
Phospho-AKT -Ser473 HTRF® assay kit	Cisbio bioassays	64NKPPEG
Phospho-ERK - Thr202/Tyr204 HTRF® assay kit	Cisbio bioassays	64ERKPEI
Phospho-YAP-Ser127 HTRF® assay kit	Cisbio bioassays	64YAPPEG
total-AKT HTRF® assay kit	Cisbio bioassays	64NKTPEG
total-ERK HTRF® assay kit	Cisbio bioassays	64NRKPEH
total-YAP HTRF® assay kit	Cisbio bioassays	64YATPEG

2.8. Consumables

Consumables	Company	Model
12-well plate Costar	Corning	3512
6-well plate Costar	Corning	3506
96-well plate Costar	Corning	9017
Blotting sponge	Thermo Fischer Scientific	EI9052
cell culture dish 21 cm ²	Corning	430161
cell culture dish 55 cm ²	Corning	430167
cell culture flask 175 cm ²	Corning	431079
cell culture flask 25 cm ²	Corning	430168
cell culture flask 75 cm ²	Corning	430729
cyrogenic vials 1.5 ml	Thermo Fischer Scientific	5012
Falcon 15 ml	Corning	430791
Falcon 50 ml	Corning	430829
Gel cassette	Thermo Fischer Scientific	NC20.15
Gel loading tips	Bioplastics	B71932
Hydrobond TM-C membranes	GE Healthcare	RPN203E
ibidi microscopy plates	ibidi	89626
micro tubes 1.5 ml	labomedic	115105
micro tubes 2 ml	Eppendorf	30119401
micro tubes 5 ml	labomedic	115106

Materials

microplate 384-well Epic plate	Corning	5042
microplate 384-well Greiner plate	Greiner	784080
Parafilm	labomedic	1447011
Pipette tips 10 µl	labomedic	110.727
Pipette tips 1000 µl	Greiner	686290
Pipette tips 200 µl	labomedic	70.760.002
Pipetting tip 10 ml	Eppendorf	0030069463
Pipetting tip 2.5 ml	Eppendorf	0030069447
Pipetting tip 25 ml	Eppendorf	0030069390

2.9. Labor Equipment

Apparates	Company	Model
Autoclave	Systeme Brunswick Scientific	3850 ELV
Bacterial Incubator	Buch+Holm	HT-INFORS
Cell Culture Bench	Thermo Fischer Scientific	Herasafe
Cell Incubator CO2	Thermo Fischer Scientific	HERAcell 240
Centrifuge adjustable temperature	Sigma-Aldrich	6K10
Centrifuges for Eppis	Eppendorf	Mini spin
Centrifuges for Falcons	Eppendorf	5810
Chamber for Cell counting	Brand	Neubauer
Fluorescence microscope (FM)	Leica	DM IL LED Fluo

FM Camera	Leica	DFC 360 FX
Freezer max. -20°C	Liebherr comfort	Liebherr
Freezer max. -80°C	Heraeus	Herafreeze
Heater for Eppis	Grant Instruments	QBT2
Liquid nitrogen cell tank	GermanCryo	MVE-Tec 3000
Microplate Reader for Bredford	Tecan	Sunrise-Basic
Microplate Reader for HTRF®	Berthold Technologies	Mithras LB940
Microwave	LG	Intello Wave
pH meter	Mettler Toledo	Seven Easy
Pipette Assistent	Accu-jet pro	Brand
Pipette automatic medium	Rainin	E4 XLS 20-200 µL
Pipette automatic small	Rainin	E4 XLS 2-20 µL
Pipette large	Eppendorf	100 - 1000 µl
Pipette medium	Eppendorf	0.5 - 10 µl
Pipette multi-channel	Brand	Transferpette-12
Pipette small	Eppendorf	10 - 100 µl
Pipette stepper	Eppendorf	Multipette plus
Precision Scale	Sartorius	TE6101
Refrigerator 4-8°C	Thermo Fischer Scientific	Laboratory refrigerator
Scale	Sartorius	TE64

Materials

Vacuum pump system	HLC BioTech	AP 15 Membrane Pump
Vortexer	Heidolph	Reax Top
Water purifier	Millipore	Milli Q Water system
XCell II Blot Module	Thermo Fischer Scientific	EI0002
XCell SureLock	Thermo Fischer Scientific	EI0002

2.10. Software for Data Analysis

Name	Company	Usage
Adobe Acrobat Reader	DC Adobe Systems Inc.	Data Research
Epic Transform table to column macro	Corning® Inc.	data Configuration
Citavi	Swiss academic software	Citation
DeVision® G v1.0	Decon Science Tec GmbH	Imaging
Epic Autoalign	Corning® Inc.	Plate Alignment
Epic Imager	Corning® Inc.	Trace Visualization
GATC Viewer 1.0	GATC Biotech AG	Sequencing
Gel-Pro Analyzer	Media Cybernetics, L.P.	Blot Quantification
Gelscan software V6.0	Bioscitech	Gel Analysis
GraphPad Prism6&7	GraphPad Software Inc	Data Analysis
Leica Application Suite 3.3.1	Leica Microsystems	Imaging

Mendeley	Mendeley Ltd.	Literature
MikroWin® 2000 AdvII v4.41	Mikrotek Laborsysteme GmbH	Plate Reading
Office Excel® 2010	Microsoft Corporation	Data Analysis
Office PowerPoint® 2010	Microsoft Corporation	Scheme Configuration
Office Word® 2010	Microsoft Corporation	Text Configuration
X-Flour4	Microsoft Tecan sunrise	Plate Reading

Methods

3.1 Cell culture protocols

For all cell culture procedures whereupon the cells were kept in culture or were meant to be stored, working steps were performed under aseptic conditions using a sterile bench with integrated laminar air flow system. Benches were cleaned with 70% EtOH before use and additionally, the benches were irradiated with UV-light for 30 minutes on every working day.

3.1.1. Freezing and Unfreezing Cells for Culturing or Storage

Not all cell lines were used at the same time. To assure the durability of cells, the storage took place in liquid nitrogen tanks with -196°C . To revitalize frozen cell lines in purpose to in-cooperate them to the culturing procedure, medium was preheated in the water bath to 37°C . Cryogenic vials containing cells from the nitrogen tank were quickly thawed and resuspended in warm medium. Cell suspension was centrifuged for 3 min. Afterwards, medium was resorbed carefully, and cells were provided with new medium. Medium exchange after thawing is important, as the medium for freezing contains 10% DMSO. DMSO addition serves to prevent the formation of larger crystals in the medium, that would harm the intact cells. For cells under culture conditions DMSO in high concentrations is toxic and must be removed quickly. Thereafter cells were seeded into cell culture flasks.

To utilize cells later, they were frozen in cryo-medium consisting of pure FCS supplemented, as already stated, with 10% DMSO. Therefore, cells were detached with trypsin and resuspended in growth medium. A centrifuging step followed for 3 minutes with 800 g. Afterwards the medium was removed, and the pellet was dissolved in approximately 3 ml cryo-medium for a 75 cm^2 culture flask with a confluency of approximately 80% to 90%. Next, 1 ml of the cell suspension was respectively transferred into 3 cryogenic vials, and immediately transferred in styrofoam boxes in the -80 freezer for 24 hrs before placing them into the liquid nitrogen tank. Direct freezing in the nitrogen tank would harm the cells, as the freezing rate is an important factor for crystal growth. Large crystals possibly could punctuate the cell membrane and destroy the cells.

3.1.2. Cell Culture Conditions

Cell lines were cultivated at 37°C in a moisture atmosphere with 5% CO_2 . All media were supplemented with penicillin (100U/ml) and streptomycin (100 mg/ml). 5% FCS was added to MCDB 153 medium designed for low-serum growth while all other media were enriched with 10% FCS.

3.1.3. Passaging and Harvesting Cells

To prevent over-growth and to ensure a good cell viability cells were splitted one to two times a week depending on cell proliferation activity. And a new cell flask was used after at least 10 passages.

First, old medium was aspirated, and cell ground was washed with 5 ml 1x PBS for 75 cm^2 cell culture flasks. Then 2-3 ml trypsin-EDTA (0,05%) was added to detach the cells. Depending on the cell's adhesion to the surface, the cells were incubated with trypsin for

Methods

2 min at room temperature or for stickier cells 2 min at 37°C. To stop trypsin reaction 8 ml of FCS supplemented medium were added to the detached cells. Cells then were either used for cell counting and were prepared for assays or simply passaged. For passaging cells were divided in a ratio of 1:2 up to 1:10 for fast dividing cells. After passage-procedure was repeated over 80 times, new cells were thawed to ensure reproducible results.

3.1.4. Cell counting

The hemocytometer (Neubauer) was used for cell counting purpose. This hemocytometer possesses two counting chambers with a grid of 9 subdivisions. A glass cover was placed over the grid area. The distance between glass cover and chamber is 0.1 mm and created a defined volume space for 10 µl cell suspension. For the cell counting procedure cells were first detached and afterwards the suspension was diluted to a concentration between 250.000 and 2.500.000 cells/ml. Finally, 10 µl of the cell suspension was loaded with a micro-pipette to the chamber and at least three squares were counted. The number of cells were averaged. To calculate the amount for 1 ml cell suspension, the cell number was multiplied by 10^4 and corrected by the dilution factor.

3.1.5. Transfection of HEK293 cells with PEI

All DNA-constructs used in the study were transfected transiently with plasmids into the host cells. All assays with these cells were performed 48 hrs post transfection.

In a 6-well plate with a growing area of 9 cm² the following procedure was used:

Cells were seeded 24 hrs before transfection to grow adherent.

Preparation of 2 tubes:

Tube 1: 1 µg DNA was added to 100µl PBS

Tube 2: 3 µl PEI solution was added to 100µl PBS

Both tubes were vortexed and tube 2 was added slowly to tube 1. Afterwards the tube-mix was again vortexed and incubated at room temperature for 15 minutes. Transfection solution was dropwise added to the adherent growing cells at a density of approximately 80%.

In case, larger number of transfected cells were needed for the assays, cells were seeded either in 21 cm² or 55 cm² cell culture plates. The amount of ingredients then was extrapolated proportionally to the increased growing area.

3.1.6. Poly-D-lysine coating

For assays that require performance under adherent conditions, and that were carried out in a 96-well plate format, the plate was coated with PDL to enhance cell adhesion on the ground. Each well was coated with at least 50 µl of PDL solution under the sterile bench. Next, the plates were incubated for 1 hr at 37°C in the cell culture incubator. Afterwards,

the plates were washed with 1x PBS for two times and the liquid was removed by centrifuging the plates upside down. Before use, the plates were sterilized under UV light for 1 hr or stored at 4°C for a maximum of two weeks.

3.2. Cell-based assays

3.2.1 Homogenous time resolved fluorescence (HTRF®) cell-based assays

HTRF®-technology is based on fluorescence resonance energy transfer technology (FRET). A FRET signal is generated when an energy donor is activated by excitation light and is in close proximity to its acceptor molecule. The special feature for this technique lies in the combination of FRET with a time resolved measurement. Therefore, lanthanides with a long half live emission are used as FRET donors. This method provides much higher sensitivity of the assay, as short life background noise of scattered excitation light or other disturbing fluorescent material in the sample, can be ignored. The FRET measurement is performed with a delay of 50 to 150 micro-seconds after excitation at two wave lengths, 620 nm (donor) and 665 nm (acceptor). A ratio between both measurements helps to correct well-to-well variability, as quenching trough disturbing compounds would occur at both weave lengths, and therefore should not affect the ratio. Thereby the donor emission serves as an internal reference signal and the acceptor signal provides information about the proximity of both molecules (Degorce et al. 2009).

3.2.1.1. IP1 accumulation assay

The HTRF® IP1 assay takes advantage of LiCl addition, that prevents the last step in IP3 degradation, as it blocks dephosphorylation of IP1 and therefore leads to an accumulation of this second messenger (Zhang and Xie 2012). In this Cisbio designed competitive immuno assay, endogenously expressed IP1 and artificial D2-labeled IP1 compete for the Tb³⁺-cryptate labeled IP1-antibody. The more IP1 is produced by the cell, the lower are the detectable FRET signals.

IP1 accumulation was measured by using the above described HTRF® technology by Cisbio® by following the suspension cell-based assay protocol in 384-well greiner plates. First, cells were harvested and washed in 1x PBS. Then cells were centrifuged for 3 minutes with 800 g and PBS was removed. Afterwards, cells were resuspended in IP1 stimulation assay buffer containing the LiCl. Next, 7 µl of the cell suspension was pipetted in each well followed by compound addition to a total volume of 14 µl. For basal IP1 detection cells were incubated with 7µl FR 2x concentrated for 1 hr at 37°C. To expose inhibition of ligand-induced IP1 accumulation, FR was added in a 3.5 µl volume 3x and incubated for 1 hr, followed by an additional 30 minutes incubation step with desired ligand in 3.5 µl in a 4x concentration. Afterwards, 3 µl of IP1 d2 conjugate and 3 µl of anti-IP1 Eu cryptate, dissolved in lysis buffer, were added. The plate was measured after 1 hr at room temperature with Mithras LB 940 Multimode Microplate Reader (BERTHOLD TECHNOLOGIES). The ratios were either normalized to an internal control or converted to IP1 in nM by using the kit's standard curve and non-linear regression. Cell numbers were adjusted to the linear range of the assay kit as follows: Hcmel12 10kc/w; B16 50kc/w; BRIM4 25kc/w; HEK293: 60kc/w; all UM cell lines: 10kc/w. In cases when assays were performed with multiple cell numbers, these are indicated in the respective figures.

Methods

3.2.1.1.2. IP1 accumulation assay wash-out experiment:

To analyse drug vulnerability of the Gq-i FR and YM cells were incubated with 1 μ M of the inhibitors for 1 hr in PBS solution. Afterwards cells were spun down for 3 min at 8,000 g and the buffer was separated from the cell pellet. Next, the cell pellet was resuspended in fresh buffer and incubated for 5 min at room temperature. The procedure was repeated for 6 times. In the last step, cells were resuspended in IP1 stimulation buffer and 7 μ l of the cell suspension was transferred into 384-well greiner plates. Subsequently the cells were treated with carbachol for 30 min before they were lysed and treated with antibodies as described in 3.2.1.1.

3.2.1.2. HTRF®-based phospho-kinase ERK, YAP and AKT assays

Compound-induced changes in phosphorylated fractions of proliferation activating proteins were quantified by using HTRF® technology (Cisbio) following the two-plate assay protocol for adherent cells in PDL-coated 96-well plates. This assay utilizes two antibody-binding sites on the protein surface at a short distance. These anti-bodies are labeled with d2 or Eu³⁺ cryptate to create FRET signaling.

Total and phosphorylated protein amounts were measured from the same lysates.

For optimizing the assay window cell density and starvation conditions were modified as follows:

Total/pERK: HEK 40,000 cells/well, HcMel12 25,000 cells per well, B16 50,000 cells/well; Uveal melanoma cells 25,000 cells/well. Inhibition of basal ERK phosphorylation was detected without prior starving while cells were starved at least 4 hrs before stimulation with a receptor agonist.

Total/pYAP: To ensure activation of the Hippo-pathway cells were starved over-night and were seeded in a high cell density (100,000 cells/well of HEK and 75,000 cells/well of UM cells)

Total/pAKT: All cell lines were seeded to a density of 75,000 cells per well. Cells were not starved, and medium was changed 1 hr before compound addition to promote basal proliferation and cell survival pathway.

Procedure for ERK and AKT assay:

Cells were harvested and counted, and cell suspension was adjusted to the final concentration of required cells per 100 μ l growth medium. Next 100 μ l were seeded into 96-well PDL coated assay plates 18 hrs before the assays were performed. On the next day the medium was exchanged for 40 μ l of fresh medium, to create a growth friendly atmosphere. FR was added in 20 μ l (3x) medium and incubated for 1 hr or in case of kinetic measurement for 15 min, 30 min, 1 hr and 2 hrs Afterwards, cells were either directly lysed or, for ligand-induced ERK or AKT phosphorylation, stimulated for another 3 minutes with 20 μ l of carbachol or with propionic acid dilution (4x). All incubation steps

were performed under cell culture conditions at 37°C. Thereafter, the adherent cells were lysed with 50 µl lysis buffer per well and the plate was incubated at room temperature while shaking for at least 1 hr. Next, 16 µl of the lysates were transferred for detection of phosphorylated and another 16 µl for total protein amounts into 384-greiner plates. To avoid an overflow of the anti-bodies in the following step, the plate was centrifuged shortly before 4 µl freshly mixed D2 and Cryptate anti-body-mix was added to the wells. To protect the probes from light exposure, the plates were covered in aluminum foil overnight before the homogenous time resolved FRET signal was detected by using Mithras LB 940 multiplate reader according to manufacturer's instruction. HTRF® ratios were either normalized to internal assay control or shown as raw data.

Procedure for YAP assay:

Four hours after cells were seeded in 50 µl into the 96-well plates and the cells were attached to the PDL-coated ground the growth medium was exchanged for 50 µl medium lacking FCS. The cells were starved overnight and on the next day compounds were added in 25 µl (3x) and FR and forskolin were incubated for 1 hr, or in case of kinetic measurement for 15 min, 30 min, 1 hr and 2 hrs. Next cells were lysed, and lysates were handled analog to the ERK and AKT assay.

3.2.2. Cell Imaging

A portrayal of cell morphological changes or cell density under different treatment conditions on adherent cells were taken by Leica DFC 360FX microscopy.

3.2.2.1. Imaging of HcMel12 cells after 72 hrs of FR treatment

HcMel12 cells were seeded in a density of 30,000 cells per well in a PDL-coated 6-well cell culture plate in 2 ml growth medium. FR and vehicle control were added three hours later in 1 ml medium solution (3x), and cells were incubated for three days under cell culture conditions.

3.2.2.2. Imaging of UM cell density after 72 hrs of FR, LY or trametinib treatment

To capture antiproliferative effects of vehicle control, FR, PI3K-i LY and trametinib on uveal melanoma cells, the cells were seeded at the density of 15,000 cells per well for 92.1 and Mel285 and at the density of 30,000 cells per well for Mel270, Mel290, Mel202 and OMM1.3, in 100 µl RPMI medium on 96-well ibidi® plates for high resolution microscopy coated with PDL. Three hrs after seeding the cells the compounds were added in 100 µl medium and the plates were placed for another 72 hrs into the incubator under cell culture conditions. Afterwards, cells were fixed with 4% PFA for 20 min at room temperature and washed twice with PBS. Images were taken by Leica DFC 360FX microscopy.

3.2.2.3. Imaging of anti-proliferative effects of the Gq-i FR and YM in a head-to-head experiment

Mel270 UM cells were seeded in 2 ml growth medium at a density of 200,000 cells per well in a PDL-coated 6-well plate. 500 µl FR, YM or vehicle, in a final concentration of 10 µM, were added and incubated for 1 hr. Afterwards the medium was removed, and the

Methods

cell ground was washed with 1x PBS. Next, new medium was applied to the cells and microscopic pictures were taken after 4 and 6 days.

3.2.3. gp100 protein detection via western blot

3.2.3.1. Cell treatment:

HCmel12 cells were seeded in 6 cm petri dishes to reach 80% confluence on day 3. Five hours after seeding, cells were treated with FR in 10 nM, trametinib in 1 μ M or vehicle control (DMSO). Cells were then lysed to perform Western Blot analysis for gp100 expression.

3.2.3.2. Cell lysates:

To analyze gp100 protein expression in HCmel12 cells, the medium was aspirated, and the cell layer was washed with cold 1x PBS. Ice cold lysis buffer supplemented with protease cocktail inhibitor was added in the following step. Thereafter, the cell suspension in lysis buffer was transferred into 1.5 ml tubes that were directly placed on a shaker at 4°C. Finally, the tubes were centrifuged at 15,000 g at 4 °C for 10 min and the supernatant was used to determine the protein concentration.

3.2.3.3. Determination of the protein content of lysates

To ensure that equal amounts of protein lysates were used for each sample in the western blot analysis the concentration of the protein lysates was determined with the Pierce BCA Assays Kit using a BSA standard curve from 0 μ g/ μ l to 10 μ g/ μ l. Thereby, 200 μ l of protein detection reagent was added to each sample and incubated for at least 30 min at 37°C. Afterwards, the absorbance was measured at 560 nm and the concentration was determined by using the standard curve.

3.2.3.4. SDS-Gel electrophoresis and blotting

The protein amount of the samples was detected by 10% SDS gel electrophoresis. 10 μ g total protein was mixed together with NuPage reducing agent and sample buffer to a 1-fold end concentration. Next, 500 μ l of NuPage antioxidant was added to the chamber filled with running buffer. The samples were pipetted to the gel wells. To define protein size 2.5 μ l Magic Marker and 5 μ l Kaleidoscope Standard were used. The probes were separated over 3 hrs at 60 V. Thereafter, the gel was blotted on a nitrocellulose membrane for 2 hrs at 25 V in NuPage transfer buffer. Blotted membranes then were rinsed in PBS supplemented with 0.1% Tween-20. To minimize unspecific binding of the antibodies, membranes were treated with Roti-Block for 1 hr at room temperature before primary antibodies were incubated overnight in Roti-Block. Thereby gp100 was diluted in a ratio of 1:5,000 and actin was diluted in a ratio of 1:2,500. On the next day the membranes were washed and incubated for 1 hr with anti-mouse secondary antibody diluted 1:10,000 in Roti-Block. Finally, the separated protein fractions were visualized by using the chemiluminescence-based blotting detection reagent Amersham ECL Prime Western. Pictures of the blots were used to quantify the amounts using the Gelscan software. Actin served as the internal standard to normalize the amount of gp100 in the different treated samples.

3.2.4. Dynamic mass redistribution

Whole cell response upon Gq-inhibition was monitored by using the label-free measurement of real time mass redistribution taking advantage of the Epic® System developed by Corning®. This highly sensitive method allows visualizing a whole cell response upon ligand stimulation of certain proteins in or on the cells. Thereby, the activation or inhibition of proteins cause changes in the cellular signaling that triggers re-localization of cellular compartments (Schröder et al. 2010). To detect these dynamic redistribution processes within the cell, the cells are grown in an mono-layer on a transparent cell culture plate with integrated biosensor at the bottom (Lee et al. 2008). Here the bottom is exposed to polarized brightfield light. The reflection of these light rays is dependent on the optical density of the cells within the first 150 nm from the biosensor. Compounds that causes rearrangement of mass in the cell, affect the density. Thereby shifts of the reflecting light in pm are translated into optical traces (Schröder et al. 2010).

3.2.4.1. DMR procedure

Transfected CRISPR-Cas9 $G\alpha_{q/11}$ ko cells and non-transfected UM cell lines were harvested and seeded in 30 μ l growth medium at in the density of 15,000 cells per well 24 hrs before detection into fibronectin coated 384-well sensor microplates. The cell suspension was spun down shortly, and the plate was placed over night in the cell culture incubator. On the next day the medium was removed, and the cells were washed with HBSS buffer supplemented with 20 mM HEPES and adjusted with the respective DMSO concentration that is used at the application-step during the assay. This DMSO-adjustment is important as many compounds are dissolved in DMSO, but DMSO itself can cause huge traces. In the final washing-step 30 μ l were left in the wells and the plate was positioned on the reader for 1 hr This resting time is implemented before starting the experiment to let the cells equilibrate as mechanical stress during washing can negatively impact the results. All steps, except washing, were performed under 37°C, as the reader itself is also placed in an incubator.

During the resting time compounds are prepared and 25 μ l were transferred into compound plates. Then the liquids were spun down. As DMR is very sensitive to temperature the compound plate with a lid was placed in the incubator for at least 15 minutes before 10 μ l were mechanically added to the plate by using the automatic pipetting system Selma (CyBi).

Before the measurement was started, the cell layer within the plates was aligned with the Epic aligner tool. Then the optical traces were recorded with the Epic Imager tool. Shifts of the reflected light upon compound addition were measured over 3600 sec, thereby every 30 sec new data were collected. After the measurement the data were transformed into Excel sheets by using the option 'Transform table to column' of the software.

To subtract the mechanical impact on cells due to compound addition, all traces were baseline-corrected by the traces caused by buffer addition.

Methods

To quantify basal FR effects the AUC of negative DMR traces were calculated for 1 hr and normalized on the maximal response. For FR effects on ligand-induced traces the AUC was evaluated for positive DMR for the same time frame.

3.4. Microbiological protocols

3.4.1. LB plates for bacterial growth

To prepare plates for bacterial growth, Luria Bertani agar was heated in the microwave till it was completely liquified. Ampicillin was added in 100 µg/ml for colony selection. To avoid degradation of the antibiotics the LB Medium was prior cooled down to 60°C. Afterwards, approximately 8 ml were added in 55 cm² plates and stored upside down at 4°C until used.

3.4.2. Transformation of plasmid DNA

DH5-α E. coli cells were used for plasmid amplification. Therefore, tubes containing 100 µl of competent cells were taken from the -80°C freezer and were thawed on ice before approximately 20 to 50 ng plasmid DNA was added to the tubes. To ensure that the bacterial cells were permeable for transformation, the cells were heat shocked. After 30 min of incubation on ice with the DNA the tubes were placed on a heat block, that was set to 42°C, for 90 seconds and placed immediately afterwards back on ice. Subsequently 500 µl of LB medium were applied to the bacterial cell solution and incubated while shaking at 37°C for 1 hr 100µl of bacterial suspension was plated on the LB covered dishes with selective antibiotic. The plates were placed up-side down into the incubator overnight and on the next day a colony was picked.

3.4.2. Plasmid DNA extraction

After transformation a colony was picked and grown in 5 mL LB medium overnight on a shaker at 37°C. On the next day the LB medium was removed by using a centrifuge and the amplified plasmid DNA from competent cells was isolated with the innuPREP Plasmid DNA Midi kit following the protocol for high copy plasmids. Thereby, the cells were lysed, and the plasmid were isolated by column chromatography. The column was washed to purify the DNA with washing buffer and finally the DNA was eluted by using elution buffer. The DNA was precipitated with pure isopropanol and the pellet was spun down. Next the DNA was washed with small amount of 70% EtOH and afterwards air dried under the bacterial bench. When the DNA was completely dried, the pellet was resuspended in DNase-free pure water and stored at -20°C.

3.4.3. Determination of DNA concentration

DNA concentration and purity were detected by using a UV-spectrometer. The concentration of the DNA sample diluted in water was determined at 260 nm by using the following formula:

$$C [\mu\text{g/ml}]: \text{OD}_{260\text{nm}} \times D \times 50$$

OD: optical density; D: dilution factor

Additionally, the purity was determined by measuring the absorbance at 280 nm. The ratio of the optical density at 280 nm to 260 nm should be between 1.6 and 2 for good quality.

3.4.4. Site directed mutagenesis

Amino acid substitutions to create GTPase-deficient $G\alpha_q$ versions $G\alpha_q^{Q209L}$ and $G\alpha_q^{R183C}$ (Kalinec et al. 1992) or loss of $G\alpha_q$ inhibitor-function (Nishimura et al. 2010) were introduced by site-directed mutagenesis (Zheng et al. 2004). This method requires single stranded DNA as template. Optimally, the plasmid DNA was obtained from an E.coli source, that produce Dam-methylated DNA, that can be used to digest the template after the product is produced by PCR (Mierzejewska et al. 2014). We used pcDNA3.1+ that was amplified in E. coli strain DH5 α . The target mutation was introduced by the primers that include the desired modification in the nucleotide sequence. Primers were either designed using the bioinformatic primer design tool PrimerX or manually by following a non-overlapping primer design protocol (Zheng et al. 2004). The polymerase chain reaction was performed using the Pfu-polymerase for higher precision in a thermo-cycler. Proof-reading ability of Pfu allowed very small amounts of starting DNA, due to high efficiency and low incidences of random mutations.

Used primer sequences can be found in the material section

3.4.4.1. Mutagenesis PCR

A master mixed was prepared on ice and a negative no-template (nT) control was implemented to each reaction performance as follows:

Components	Volume (μ l)
Template (water for nT control)	1
Primer mix	2
DMSO	2.5
dNTP	1 of 10 mM
DNase free-water	37.5

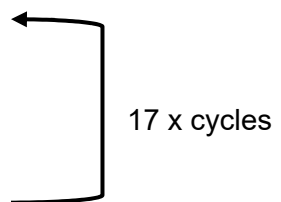
Methods

Reaction buffer	5
Pfu-polymerase	1

The Pfu-polymerase was added directly before placing the samples in the thermo-cycler.

The thermo-cycler was programmed as follows:

Steps	Temperature (°C)	Time (s)
Initial denaturation	95	120
Denaturation	95	50
Annealing	60	50
Elongation	72	480
Storage	4	Until use



3.4.4.2. Digestion of template DNA

To digest the template 1 μ l of digestion enzyme DpnI was added to each reaction tube. The mixture was vortexed shortly and centrifuged afterwards. Subsequently, the tubes were incubated for at least 1 hr at 37°C. Finally, the DNA was either stored at -20°C or amplified by transformation.

3.4.5. Sequencing for mutation c. G1888T (p. D630Y) in PLC β 4 in Mel290 cells

To verify the presence or absence of the hot-spot activation mutation G→T in PLC β 4 gene at G1888 in the uveal melanoma cell line 290 we amplified a 240 bp long segment of the DNA including the region. Therefore, we extracted the DNA and amplifies the region of interest by PCR. Afterwards, we send the extracted DNA for sequencing.

3.4.5.1. DNA extraction

The DNA was extracted using innuPREP DNA Mini Kit (Analytik Jena) following protocol #4 for DNA extraction form cell culture. Therefore, we harvested 3×10^6 cells of Mel290. The cells were spun down, and the cell pellet was washed with PBS. Then, the cells were centrifuged at 5,000 g for 10 min and the supernatant was discharged. Next, the cells were lysed, and the DNA was separated chromatographically. To purify the DNA the column was washed and finally the DNA was.

3.4.5.2. Amplification of DNA fragment

Forward and reverse primers were designed to frame the region of interest. Shown is the exon that encodes pD630. The exon is marked in red embedded in non-marked intron sequence (**figure M1**). Region in Sequence with Introns (Exons red) source Ensembl!

```
CCATGGCAGCTGTGACAATCTGCCCAAATGAAAATTGTTTTATAATCCACACAGTGAAC
TGTGATCTTAAGCATCATTTGTAAATGTGAAATCTGCTCTGTGCTGTCTACTTGTGGTC
ATTGTTGGCCTAGACCTTTGTTGTTTTAGCTCTTTGTTGTTATTTTTCTCTGCTGTAGG
ACTCTTTTTTCTGTTTTCTTAATAAGTTACAGTTATAACAAACGGCAAATGAGTCGCA
TTTACCCCAAGGGAGGCCGAGTCGATTCCAGTAATTACATGCCTCAGATTTTCTGGAACG
CTGGCTGCCAGATGGTTTCACTGAACTATCAAACCCAGGTAGGAGCTGATGTCCAGTGA
CCCCAAATTCCATGAGAACACTTTGACAGGATGGTGCCAGCACTTCCCATCAGTTGGCTG
TGGGCATTTTTTAAAGGAAGCAGACATATGGCAAAGCAATGTGTTATTGGATTTATATAA
TGGTGAGAAATAAAAAAAAAAAAAACCAAATAGAGCAAACAATGGTAGAAGATAATGTGT
TGTGATTGGAATTTAATTCCTTTCATAAATGCCATGACTATTCCTGCTAACCATTATCCC
ATATTCCAAAATATTTCTCATTTTTCTTCTTTTGGATCAAAGTTGTTATCTTTGTTTCC
```

Figure M1: Sequence of PLB4

Primers are marked in grey, marked thereby reverse primer was reversed and complemented to perform PCR; amino acid of interest is marked in blue G1888.

The polymerase reaction was performed by using GoTaq polymerase enzyme and reaction buffer.

Components	Amounts
Template	0.5 µg
primer sense	0.5 µM
primer antisense	0.5 µM
dNTP	1 µl of 10 mM
GoTaq G2 Polymerase	0.25 µl
Reaction buffer	10 µl
DNase free-water	Ad 50 µl

The thermo-cycler was programmed as follows:

Methods

Steps	Temperature (°C)	Time (s)
Initial denaturation	95	120
Denaturation	95	30
Annealing	52	30
Elongation	68	15
Final extension	68	300

← 40 x cycles

3.4.5.3. DNA separation by agarose gel-electrophoresis

To separate the PCR product from the genomic DNA, the sample was separated by agarose gel electrophoresis. Here the negatively charged backbone moves towards a positive charged anode in an electric field. Thereby the size of the DNA fragments is crucial for the velocity.

To prepare the gel agarose was dissolved under heat exposure in 1x TAE buffer to a final concentration of 5 %. Next, 2.5 mg/ml ethidium bromide to visualize the DNA fragments under UV light were added. The solution was poured into the chamber form and a comb to form wells was inserted. After the gel stiffened it was placed into an electrophoresis chamber and the wells were loaded with the sample a no-template control and a 100 bp ladder to determine the band sizes. Finally, the gel was run for 20 minutes at 100 V.

3.4.5.4. DNA Gelextraction

The expected DNA length was 264 bp and could be detected under UV light.

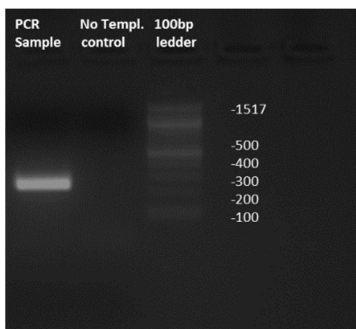


Figure M2: PLCB4 PCR product.

Band size 264bp

The innuPREP Gel Extraction Kit was used to extract the DNA product from the gel for sequencing purpose. Therefore, the band was cut out of the gel under UV light and 300 mg of the gel was solubilized with the kit's lysis buffer. The DNA was extracted from the solution by a chromatographic column and after separation, the prob was send to GATC-sequencing.

3.5. Data analysis

To analyze the obtained data we made use of the Prism 7 and Excel software. Dots and bars, if not states otherwise, represent the mean of n indicated experiments with s.e.m. Concentration-response or -inhibition curves were obtained by non-linear regression with 4 parameters. Quantification of DMR traces was succeeded by calculating the area under the curve for restricted areas and defined duration. For statistical analysis unpaired t-test or, in case that the values were compared to a 100 % reference, a one-sample t-test was used. IC_{50} values were attained by non-linear regression. Significance levels were set as follows: * $P < 0.05$ was considered significant, ** $P < 0.01$ very significant, and *** $P < 0.001$ extremely significant.

Results

4.1. FR inhibits canonical wild type $G\alpha_q$ but not GTPase-deficient $G\alpha_q^{Q209L}$ signaling in HEK cells

FR has been characterized as a specific Gq/11/14 inhibitor with high potency. The molecule binds to the alpha subunit of the heterotrimer to prevent receptor initiated interdomain movement (Schrage et al. 2015). If this movement is impaired, GDP release and, as a consequence, GTP entry cannot take place (Nishimura et al. 2010). Activation of further signaling cascades is inhibited as GTP is unable to cause structural rearrangements within the G alpha subunit to cause dissociation of the $\beta\gamma$ -heterodimer from the α -subunit (Oldham and Hamm 2008). Ostensibly clear, targeting a GTPase-deficient $G\alpha$ subunit with an inhibitor that prevents GDP dissociation was thought to be ineffective (Nishimura et al. 2010; Takasaki et al. 2004; Kimple et al. 2011). This assumption was made, as the GTPase-deficiency within the $G\alpha$ -subunit has been reported to trap the protein in the activated GTP-bound state (Kleuss et al. 1994) and therefore, inhibition of GDP dissociation consequently would be pointless. In line with this hypothesis, FR did not blunt basal IP1 accumulation in immortalized HEK293 cells transfected with $G\alpha_q^{Q209L}$ fully, while inhibition was easily achieved in cells transfected with even higher amounts of the $G\alpha_q^{wt}$ (**figure 11**). As a caveat, inhibitor effects are potentially confounded in the HEK cell system by the activity levels of Gq and G11 proteins which are endogenously expressed in the cells.

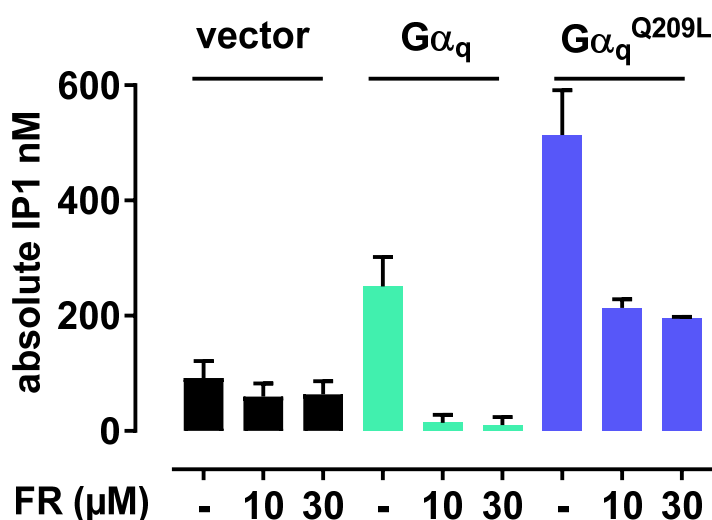


Figure 11: Gq inhibitor FR lacks capability for complete inhibition of $G\alpha_q^{Q209L}$ -induced IP1 accumulation.

HEK293 cells transiently transfected with 1.5 $\mu\text{g}/21 \text{ cm}^2$ wild type or 0.2 $\mu\text{g}/21 \text{ cm}^2$ $G\alpha_q^{Q209L}$ or vector. 30 kc/w were incubated with stated concentration of FR for 2 hrs. Bars represent the means with error bars indicating s.e.m. of 3 independent experiments.

4.2. FR blunts mitogenic signaling in cutaneous melanoma cells with activated Gq/11

Astonishing results were reported by Tanja Slodczyk in her doctoral thesis. She found that FR was able to blunt typical oncogenic markers in HCmel12 mouse melanoma cells harboring the G α_{11} protein with a point mutation on this activating hot spot residue Q209. In her thesis she could show that cell growth as well as metabolic activity was highly reduced when the cells were treated with the Gq inhibitor FR. While most other antitumoral agents reduce cell growth in a cytotoxic manner, FR did not trigger the number of apoptotic cells compared to control. Instead, inhibition of cell growth was linked to enhanced cell number in the G1 phase of the cell cycle and therefore, reduced number in the other cell cycle phases. Higher fractions of the cells in the G1 phase, indicates differentiation (Tanja Alten 2017).

4.2.1. FR forces HCmel12 cells into differentiation and blunts pERK over PLC signaling

Differentiation in cutaneous melanoma cells is associated with higher pigmentation and enlarged cell shape. Thus, we could confirm these phenotypic changes using light microscopy images (**figure 12A**). The cells seemed flatter and darker in the FR treated group versus cells treated with vehicle control only.

Gp100 belongs to the group of melanocyte differentiation antigens (MDA) that are upregulated at the stage of differentiation. This MDA plays an important role in the polymerization of melanin and the genesis of melanocytes (Pitcovski et al. 2017). Treatment of the HCmel12 cells with FR or the MEK inhibitor trametinib resulted in a significant increase of gp100 expression (**figure 12Bi, Bii**). Subsequent to these findings, we took a closer look into Gq related signaling cascades in these cells. Initially, we verified activated G α_{11} tonus by measuring IP1 accumulation. G α_{11} was found to be intrinsically active, as we detected approximately proportionally increased IP1 production by elevating cell numbers without any agonist stimulation (**figure 12C**).

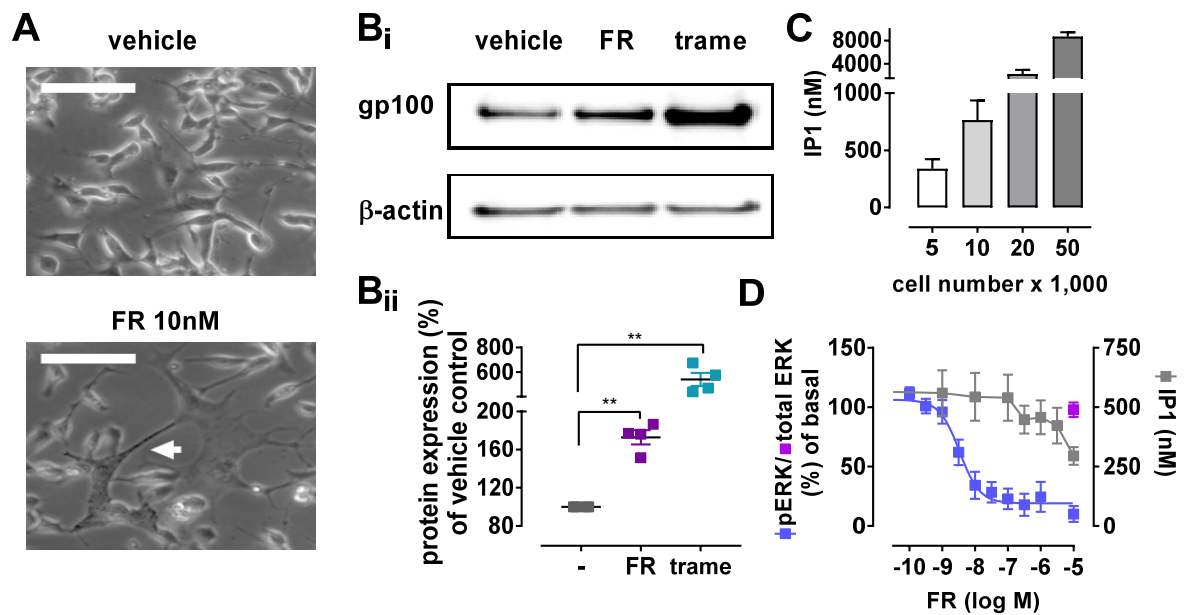


Figure 12: FR suppresses downstream pro-survival but not canonical PLC signaling pathway of oncogenic $G\alpha_{11}^{Q209L}$ in the mouse melanoma cell line HcMel12.

Cell morphological changes captured by brightfield microscopy imaging after 72 hrs incubation with either FR 10 nM or vehicle control. Scale bar represents the length of 5 μ m (**A**). Images were kindly provided by Julian Patt (AG Kostenis, University of Bonn). (**B**) Representative western blot detection (**Bi**) and quantification ($n=4$) using β -actin as standard (**Bii**) of cells preincubated with FR 10 nM, MEK-i trametinib 1 μ M or vehicle control for 72 hrs before lysis. Western blots were done by Eva Pfeil University of Bonn (lab of Evi Kostenis). Basal IP1 tonus measured after 1 hr incubation in buffer containing LiCl to prevent degradation and to initiate accumulation for increasing cell numbers as stated (5 kc/w $n=4$; 10 & 20 kc/w $n=6$; 50 kc/w $n=2$) (**C**). Inhibition potency of FR measured after 1 hr incubation for adherent cells in medium (ERK) or for cells in LiCl assay-buffer suspension (IP1). Protein levels were detected with HTRF anti-bodies for either phospho-ERK ($n=7$), total-ERK ($n=3$) or IP1 ($n=7$) (**D**). (**Bii-D**) bars or dots represent the means with s.e.m. of n independent experiments. **Bii**) Significant effect to buffer was calculated by one-sample t-test.

In accordance to so far published data (Xiong et al. 2016) and our own data (**figure 11**) in HEK293 cells, IP1 accumulation triggered by the oncogenic G11 protein was affected only at very high FR concentrations. In contrast, inhibition of phosphorylation of the proliferation promoting protein ERK was completely blunted by FR at low nanomolar concentrations. Simultaneously, FR did not affect the amount of total ERK proteins (**figure 12D**).

4.2.2. Mitogenic signaling and IP1 accumulation may not share the same upstream regulator

Both, pERK and IP1 production are reported to share the same Gq-dependent upstream signaling regulator PLC β (Gutkind 2000). Interestingly, only ERK signaling was FR sensitive. Whereas, IP1 accumulation was only inhibited to a very small degree in

Results

HCmel12 cells with even much higher inhibitor concentrations. Provided that ERK phosphorylation occurs as downstream event of PLC β activation in this cell line, theoretically, IP1 accumulation should be blunted in a similar concentration range as ERK phosphorylation. To further investigate this discrepancy, we tried to prevent ERK signaling by blocking PLC signaling. For this purpose, we used the widely known PLC inhibitor U73122 (Bleasdale et al. 1990). Specificity of U73122 has been questioned, as the molecule was additionally shown to inhibit calcium channels (Macmillan and McCarron 2010) and was even reported to function as an activator on purified PLCs (Klein et al. 2011). Hence, we included the non-functional but structurally very closely related molecule U73343 (Bleasdale et al. 1990) to distinguish between specific and unspecific effects.

As predicted by literature (Vaqué et al. 2012), U73122 inhibited ERK phosphorylation in a concentration-dependent manner. But, biological relevance of these results remained uncertain, as the non-active analog also depressed activation of the protein (**figure 13A**).

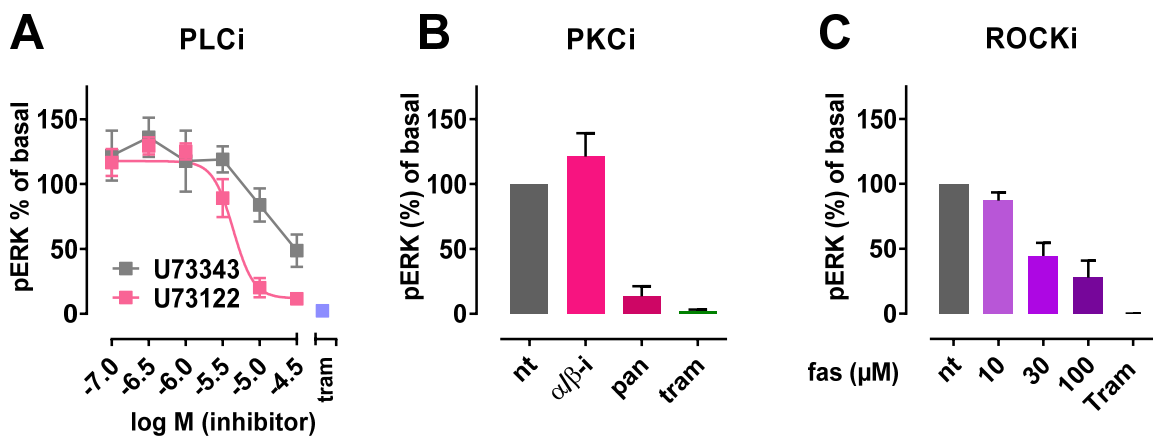


Figure 13: Inhibition of basal ERK phosphorylation in HCmel12 cells by targeting various Gq-downstream effectors.

Intrinsic HCmel12 pERK levels after 2 hrs incubation with U73122 or U73343 ($n=4-6$) in the indicated concentrations (**A**) or with selective α/β PKC-i Gö 6976 1 μ M ($n=6$) and pan-PKC-i 10 μ M ($n=3$) (**B**) or fasudil in the indicated concentrations ($n=3-5$) (**C**). MEK-i trametinib was used as control in 1 μ M (**A-C**). Dots and bars represent mean with s.e.m. of n independent experiment days. All experiments were performed with adherent cells using a density of 25 kc/w in PDL-coated 96-well plates.

Thus, we chose to focus on PKC as a chain link between PLC β and ERK activation (Gutkind 2000). Pan PKC inhibitor Gö 6983 (Gschwendt et al. 1998) was able to abolish ERK phosphorylation completely. Interestingly, the same effect was not observed with the selective PKC inhibitor Gö 6976, which targets the Ca²⁺-dependent PKC isoforms α and β , that are often related as downstream effectors of PLC (Martiny-Baron et al. 1993), retaining the possibility of PLC-independent PKCs to be additionally involved in the Gq/11 mediated ERK1/2 phosphorylation in HCmel12 cells (**figure 13B**).

Another hint for the involvement of multiple Gq/11 effectors in ERK phosphorylation was achieved with the Rho-kinase inhibitor fasudil (Ying et al. 2006). RhoA was reported to be activated by the direct Gq effector family of the RhoGEFs (Rojas et al. 2007; Vaqué et al. 2012). Fasudil reduced the fraction of phosphorylated ERK protein by approx. 60-70% (**figure 13C**). This is not a surprise, as RhoA was demonstrated to enhance cell cycle progression and increasing cyclin D1 expression by constant activation of ERK (Etienne-Manneville and Hall 2002). However, high concentrations were needed for detectable effects and therefore specificity of these effects can be questioned.

These findings further underline the hypothesis that mechanism of Gq-regulated MAPK-signaling activation is quite complex and may not be as straight forward like the often described Gq-PLC-PKC-RAF-MEK-ERK (Gutkind 2000) pathway.

4.2.3. ERK phosphorylation is insensitive to FR in cutaneous melanoma cells with mutated B-Raf

Next, we looked for another cutaneous melanoma cell line, the BRIM4 with a mutated $G\alpha_q^{Q209P}$ protein. In addition to the mutation on this hot spot residue of the Gq protein, these cells harbor a mutation in B-Raf^{V600E}. B-Raf is a common proto-oncogene known to drive proliferation by permanent ERK activation. Mutations in B-Raf or N-Ras are typically found in this type of cancer (Gray-Schopfer et al. 2005). Substitution of valine on position 600 in the amino acid sequence to glutamic acid is the most common mutation in the B-Raf protein. This amino acid substitution enhances the enzyme's catalytic properties and thereby increases mitogenic signaling by MEK-ERK activation (Rubinstein et al. 2010). This cell line was very interesting to investigate FR's potential to diminish mitogenic ERK signaling in a system, where ERK phosphorylation is not exclusively driven by the constitutive activity of the Gq protein.

Again, we first confirmed constitutive activity of the Gq protein by measuring PLC activity by IP1 accumulation assays, as the canonical effector protein of Gq. Massive IP1 accumulation was observed even by low cell numbers. Furthermore, IP1 production correlated with increased cell numbers (**figure 14A**). Consistent with the results obtained by the HcMel12 cells, treatment of BRIM4 cells with FR led only to moderate inhibition of IP1 accumulation, as 1 μ M FR could only depress 50% of the elevated basal IP1 production. But in these cells ERK phosphorylation was only impaired to a small degree (**figure 14B**) suggesting that Gq/11 is unlikely to be the main ERK driver in these cells. Rather the mutated B-Raf protein is suspected for MAPK-pathway initiation. This hypothesis is supported by the fact that ERK signaling was highly sensitive to the selective mutant B-Raf^{V600E} inhibitor vemurafenib (Kim and Cohen 2016) (**figure 14C**).

Results

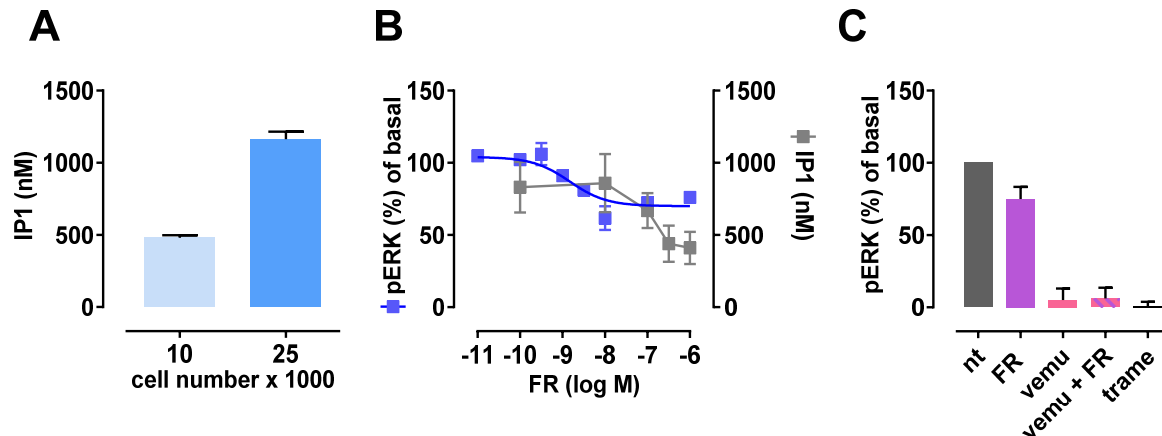


Figure 14: FR partly attenuates pERK in melanoma cells with additional B-Raf mutation.

Basal IP1 tonus measured after 1 hr incubation in stimulation buffer containing LiCl using 10 and 25 kc/w (n=3) (**A**). 10 & 20 kc/w n=6; 50 kc/w n=2). FR inhibition curve measured after 1 hr incubation for adherent cells in medium (ERK) or for cells in LiCl assay-buffer suspension (IP1). pERK or IP1 levels were detected with HTRF anti-bodies for either phospho-ERK (n=3) or IP1 (n=4) (**B**). ERK phosphorylation after pretreatment with FR in 100 nM, or vemurafenib in 1 μ M or the combination of both, or trametinib 1 μ M (n=3) (**C**). Dots and bars represent mean with s.e.m. of n independent biological replicates. All experiments were performed using 25 kc/w in PDL-coated 96-well plates for ERK and 384-well format for IP1.

4.2.4. Preferential inhibition of pERK over PLC by FR is a characteristic feature for cells harboring a GTPase-deficient mutant

To test, whether preferential inhibition of the ERK signaling cascade over canonical PLC is a general occurrence, or if it is strictly related to GTPase-deficient mutants, we examined these pathways in the mouse cutaneous melanoma cell line B16 that is wild type for Gq-family proteins (Schrage et al. 2015).

B16 cells showed high basal IP1 levels compared to other cutaneous melanoma cell lines such as Skmel28 and Mamel19 with wild type Gq/11 proteins, indicating intrinsic Gq activity (**figure 15A**). Elevated Gq activity can arise for many more reasons than malfunction of the GTPase domain. High Gq tonus might be explained e.g. by constitutively active receptors (Moore et al. 2016) or a receptor cross talk of autocrine-activatable tyrosine receptor kinases that transactivate GPCRs (Garcia-Recio et al. 2013).

In accordance to FR's mode of action as a GDI that prevents the initial activation of the protein and therefore should preclude signaling of all downstream cascades, FR inhibited pERK as well as IP1 accumulation in a very sensitive manner. Direct comparison between the inhibition of these pathways exposed ERK phosphorylation to be slightly more sensitive (**figure 15B**). Additionally, we confirmed that FR did not impact total amount of ERK proteins (**figure 15C**). However, the difference between pathway sensitivity was by far less pronounced as compared with the Hcmel12 cell line.

These results only reflected the inhibition behavior of permanent intrinsic Gq activity. To further confirm, whether ligand-induced signaling could be blocked in the same manner, we stimulated either HEK293 cells, which endogenously express the muscarinic receptor

M3 with carbachol (**figure 15D**) or HEK293 cells stably expressing the FFA2 receptor with the receptor ligand propionic acid (**figure 15E**). As expected, in both cases Gq-PCR stimulated IP1 and ERK phosphorylation were perfectly inhibited. Again, FR did neither enhance nor degrade the total amount of ERK proteins (**figure 15F**). The huge discrepancy between PLC β and ERK inhibition potency of FR seemed to be an exclusive hallmark for the GTPase-deficient mutant.

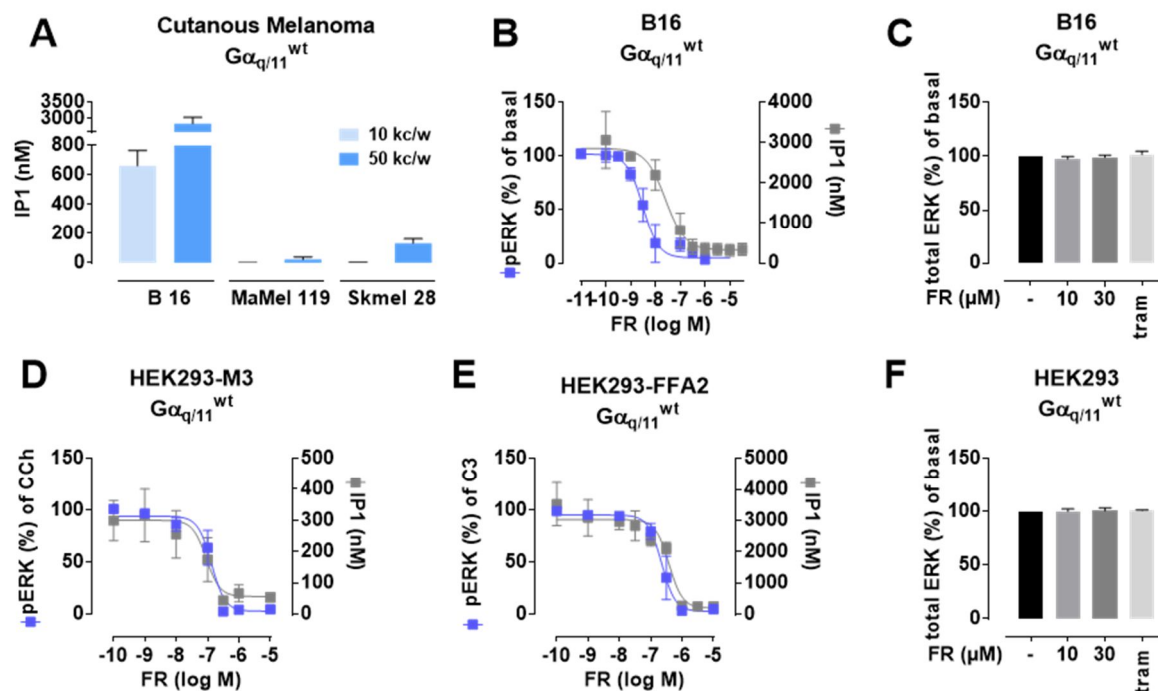


Figure 15: FR inhibits canonical and mutagenic signaling driven by wild type Gq/11.

Basal IP1 tonus of different cutaneous melanoma cell lines measured after 1 hr incubation in stimulation buffer containing LiCl using 10 and 50 kc/w (n=3) (**A**). Inhibition potency of FR on B16 mouse melanoma cells measured after 1 hr incubation for adherent cells in medium (ERK; n=4) or for cells suspended in LiCl assay-buffer (IP1; n=3) (**B**). Total ERK levels of B16 cells after 1 hr FR incubation in concentration as indicated and trametinib 1 μ M (n=3) (**C**). Ligand-induced inhibition of pERK (n=6) and IP1 (n=4) accumulation in HEK cells endogenously expressing M3-muscarinic receptor (**D**) or stably transfected with FFA2 receptor (**E**). Cells were preincubated for 1 hr with FR. Receptor agonists were incubated for 3 min for pERK and 30 min for IP1 in following concentrations: 30 μ M CCh (**D**) or 1 mM C3 (**E**). FR effect on total ERK protein in HEK293 cells after 1 hr incubation of FR as indicated in the figure and trametinib 1 μ M (**F**). Dots and bars represent mean with s.e.m. of n independent experiments (**A-F**).

4.3. FR directly interacts with mutated G α_q ^{Q209L}

To further proof FR interaction with the GTPase-deficient analog of the G α_q protein we took advantage of HEK cells lacking G α_q and G α_{11} proteins engineered by CRISPR Cas9 technologies. These cells offer the possibility to truly discriminate between the different constructs in a perfectly clean background, whereas in the melanoma cell-background one of these proteins would always be un-mutated as GNAQ/GNA11 are mutually exclusive (van Raamsdonk et al. 2009). Transfection to non-genome edited HEK293 cells

Results

would as well not be the perfect option, as HEK293 cells endogenously express $G\alpha_q$ and $G\alpha_{11}$ proteins (Atwood et al. 2011).

4.3.1. FR blunts wild type but not GTPase-deficient activation of canonical PLC signaling

Upon transfection of the plasmids into the HEK293 $G\alpha_{q/11}$ -null cell system, the expression of both constructs was verified by measuring IP1 generation as readout of the canonical Gq-effector PLC β . Cells expressing either wild type or QL-mutant variation of the $G\alpha_q$ showed elevated basal IP1 levels compared to cells treated with vector control (**figure 16A**). While non-genome edited HEK293 cells showed much higher IP1 levels with the GTPase-deficient mutant (**figure 16B**), the difference between wild type and QL was not significant in the HEK293 $G\alpha_{q/11}$ -null cells (**figure 16A**).

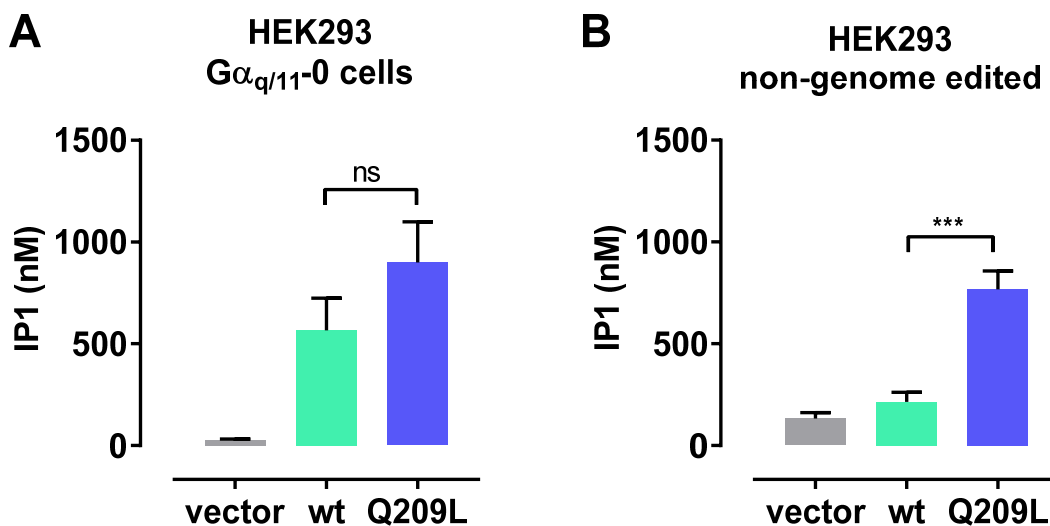


Figure 16: Transiently expressed $G\alpha_q$ wt and mutated $G\alpha_q^{Q209L}$ increase PLC activity in HEK293 cells.

Basal IP1 tonus of HEK293 lacking Gq/11 (A) proteins or non-genome edited HEK293 cells (B) after 1 hr incubation in IP1 stimulation buffer. Cells were tested 48 hrs post transfection with equal amounts of plasmid DNA without or with inserted sequence for either wild type Gq or GqQ209L (1,2 μ g/21 cm^2). Significance was calculated by using the unpaired t-test.

Yet again, in the Gq/11 null background PLC β - $G\alpha_q^{Q209L}$ -interaction could not be blunted by FR up to very high concentrations, indicating the impossibility to target the GTPase-deficient protein with an inhibitor that acts as GDI. Consistent with the data obtained in B16 Gq/11 wild type cells and the data generated in ligand-induced IP1 accumulation in non-Gq-transfected HEK293 cells (**figure 15B,D,E**), FR perfectly counteracted the activation of PLC by the transfected wild type $G\alpha_q$ construct fully (**figure 17A**).

Subsequently, we wanted to re-evaluate inhibition of mitogenic ERK signaling driven by the GTPase-deficient mutant, as seen in Hcme12 cells. By measuring total ERK, we could show that expression of the Gq proteins itself depressed the total amount of ERK

proteins (**figure 17B**). Thus, we calculated the attained phosphorylated protein levels by accounting the phosphorylated fraction in relation to the total protein amount (**figure 17C**).

Tendency in inhibition could be observed for the Q209L construct and could be confirmed for wild type Gq but diverging amounts of the phosphorylated fraction and a relatively small assay window for the oncogenic protein forced us to look for other pro-survival pathways to really quantify effects. The results were not completely surprising as reports about elevated ERK levels upon Q209L transfection are quite diverse (Gutkind 2000; Thomas et al. 2016). Thus, we concluded that HEK cells might not be the right system to investigate basal ERK activity driven by oncogenic G proteins.

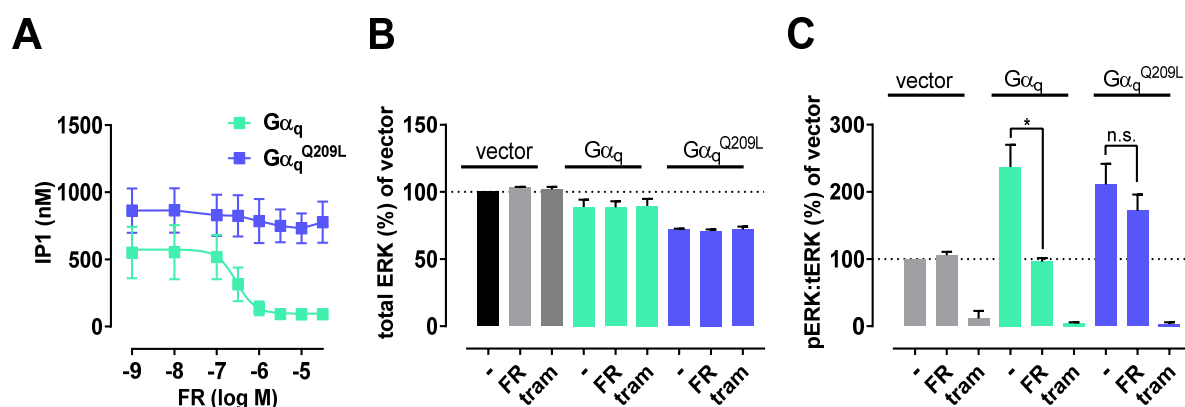


Figure 17: FR effect on canonical PLC activation versus mitogenic ERK phosphorylation in HEK cells expressing wild type and Q209L construct.

Inhibition of intrinsic IP1 tonus after 1 hr incubation with FR in stated concentrations $n=3$ (A). Total ERK protein $n=4$ (B) or pERK to totalERK in $n=4$ (C) after 1 hr incubation of vehicle, FR in 10 μM or trametinib in 1 μM in HEK293G $\alpha_{q/11}$ ^{-null} cells 48 hrs post transfection with the indicated constructs. Dots and bars represent means of n independent experiments. Significance was calculated by using the unpaired t-test.

4.3.2. FR effects on Gq downstream signaling effectors AKT and YAP in endogenous Gq/11-clean background

As ERK signaling in HEK cells was not found to be suitable to appraise FR effects on the GTPase-deficient mutant, we looked for other Gq downstream effectors with similar function in proliferation. Like ERK, AKT is a critical factor for tumorigenesis in cutaneous melanoma or uveal melanoma. The activation PI3K-AKT/Protein-kinase B pathway leads to cyclin D1 overexpression and appropriately enhances cell cycle progression (Porta et al. 2014; Kanzler and Swetter 2003). Therefore, we wanted to test, whether we could use AKT phosphorylation as an appropriate tool to evaluate FR effects on more pro-survival pathways by using the Gq/11 null background.

In uveal melanoma with Gq-mutations, AKT phosphorylation has been associated with constitutive Gq-signaling, as silencing of the protein by siRNA reduced the phosphorylated fraction of AKT (Ambrosini et al. 2013). In contrast Gq has been reported to play an opposite role in AKT activation in HEK-cell context. Wong and his co-workers could show inhibition of the AKT signaling pathway that was initiated by the transfection of the oncogenic G α_q^{Q209L} protein into the HEK293 cell system (Chen et al. 2014).

Results

For these reasons we expected to see enhancement of AKT phosphorylation by FR application to HEK cells transiently expressing $G\alpha_q$ proteins. However, in contrast to the published data, we were not able to sense any phosphorylation-stimulus of $G\alpha_q$ signaling by transfection of these constructs into our HEK cells lacking endogenous $G\alpha_q$ -family proteins. These observations accounted for both proteins, wild type and the Q209L-mutant. AKT phosphorylation at basal level was comparable to vector transfected cells and FR did neither significantly enhance nor reduce these fractions (**figure 18A**). Apparently, the transient expression of these constructs does not account in AKT signaling.

To verify the accuracy of our assay, we tried to reconstruct published data and detect Gq-receptor ligand carbachol-induced depression of phosphorylated AKT (Bommakanti et al. 2000). Therefore, we tested HEK293 cells with endogenous Gq/11 expression-levels. We found Gq involvement in AKT signaling in these non-genome edited HEK cells. Activation of the muscarinic M3 Gq-coupled receptor by carbachol decreased basal AKT phosphorylation as published. Additionally, we were able to regain basal level by using the Gq inhibitor FR (**figure 18B**). The FR effect on carbachol signaling was concentration-dependent and was maximal at 10 μ M (**figure 18C**).

This might hint that signaling modulation of AKT through Gq can differ between permanent and acute activation of Gq proteins. High basal Gq tonus that is also observed for Gq wt transfected HEK293 $G\alpha_{q/11}^{-null}$ cells might initiate a compensation mechanism. However, as results were not inherently conclusive, we moved on to test FR-Gq^{mut} interaction on other Gq-cancer related pathways.

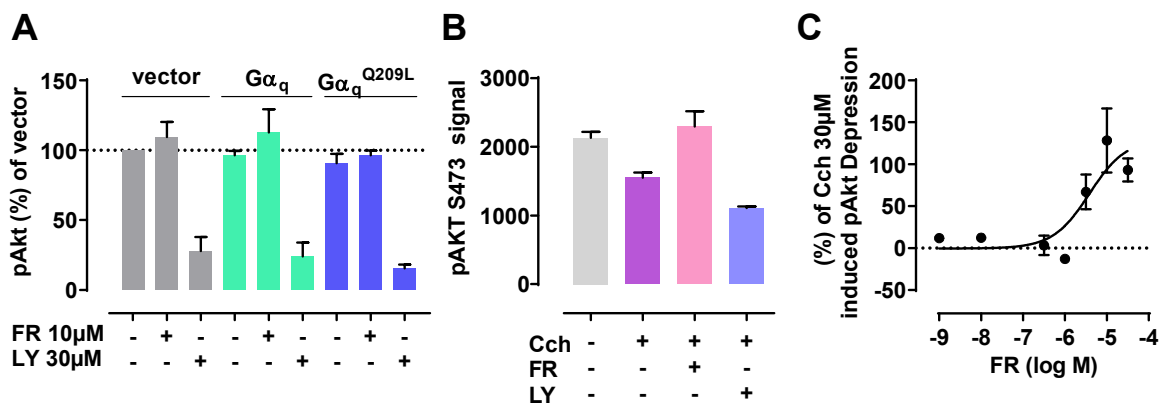


Figure 18: AKT phosphorylation regulated by Gq signaling in HEK293 cells.

Phosphorylation of AKT proteins after 1 hr incubation with either FR in 10 μ M or PI3Ki LY294002 in 30 μ M in either wild type or GTPase-deficient Gq transfected HEK293 $G\alpha_{q/11}^{-null}$ cells (n=3) (**A**). Ligand-induced CCh depression with or without preincubation of 10 μ M FR or LY294002 30 μ M in non-genome edited HEK293 cells (n=2) (**B**). Quantification of FR effects on ligand-induced AKT dephosphorylation (n=2) (**C**).

Yes-associated-protein (YAP), a transcriptional coactivator regulated by the hippo pathway, was recently linked to oncogenic $G\alpha_q$ signaling. This signaling is reported to be mediated by a complex machinery involving Trio-Rho/Rac-promoted LATS inhibition and actin polymerization (Feng et al. 2014; Vaqu e et al. 2012; Yu et al. 2014). In the presence

of Gq signaling LATS is impaired to phosphorylate YAP. Phospho-untagged YAP is able to penetrate through the nucleus and form an active complex with the transcription factor TEAD followed by expression of diverse growth promoting genes.

By blocking Gq signal with FR we could induce increased phosphorylated YAP levels in both mutant and wild type transfected cells while vector transfected HEK293G $\alpha_{q/11}^{-null}$ cells remained unaffected (**figure 19A**). FCS was used as an internal control. Consistent with published data FCS decreased the amount of phosphorylated YAP as expected. Guan and co-workers identified LPA and S1P, two GPCR-ligands, as the YAP activating components in serum. Both compounds are suggested to initiate G12/13 and Gq-mediated RhoA signaling (Yu et al. 2012). The total YAP protein amount was not affected either by 1 hr of FR or FCS incubation (**figure 19B**). Quantification of the effects revealed that inhibition of G α_q^{Q209L} was slightly less sensitive towards FR (**figure 19C**). These data strongly indicate, that inhibition of oncogenic Gq signaling by FR is not restricted to wild type Gq but can be extended to the GTPase-deficient mutant as well.

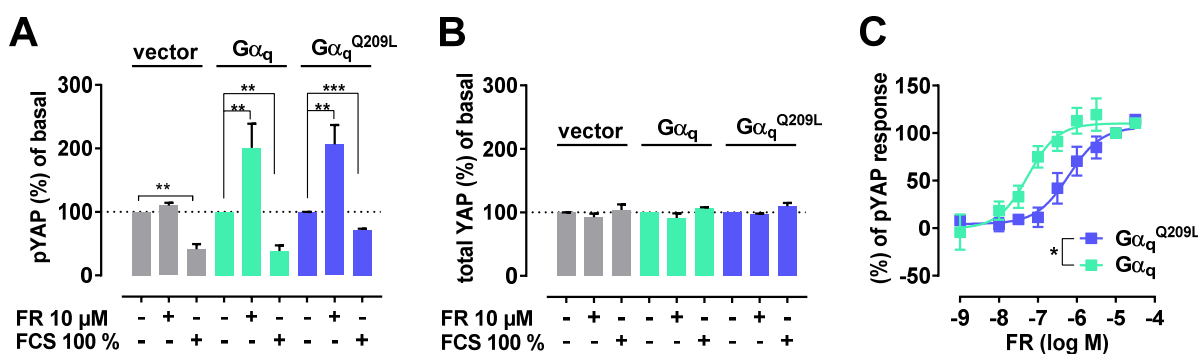


Figure 19: YAP phosphorylation regulated by Gq signaling in HEK293 cells.

Phosphorylation of YAP protein (**A**) ($n=5$) or total amount of YAP proteins (**B**) ($n=3$) after 1 hr incubation with either FR in 10 μ M, 100% FCS or vehicle in HEK293G $\alpha_{q/11}^{-null}$ cells transfected with vector, wild type or GTPase-deficient Gq. Quantification of FR potency on wild type vs QL transfected cells ($n=5$) (**C**). Dots and bars represent the mean with s.e.m. of n independent experiments. Significance was calculated by using the one-sample t-test (**A**) or Wilcoxon test (**B**).

4.3.3. FR triggers mass redistribution in cells expressing GTPase-deficient mutant

A broad-range of G protein-mediated signaling is related to morphological changes of cells (Schröder et al. 2010; Schröder et al. 2011). Gq and G12/13-proteins are known to activate small RhoGEFs that are involved in dynamic processes of the cytoskeleton (Rojas et al. 2007). Compound-induced dynamic mass redistribution can be measured in real-time by using Coring Epic technology (Schröder et al. 2010; Schröder et al. 2011). DMR is not only able to detect agonist-provoked GPCR-signaling but is also able to uncover constitutive receptor activity. Thereby, inverse agonists have been shown to form opposite directing DMR traces to agonists (Lee et al. 2014) indicating reversed movements of the mass within the cell. However, label-free detection of receptor independent constitutively active G protein inhibition has not been addressed so far.

Results

Thus, we were positively surprised, as we could indeed evaluate FR effects on the GTPase-deficient mutant $G\alpha_q^{Q209L}$ by taking advantage of this label-free method.

Cells perfectly responded to endothelin growth factor (EGF) and forskolin (Fsk), independent of the transiently expressed protein (**figure 20A**). Cell response to these compounds does not rely on G protein activation and therefore, they were used as general cell viability controls. Carbachol served as a transfection control. In HEK cells CCh binds to the muscarinic Gq-coupled receptor M3, whose activation triggers upwards directed traces in this cell system (Schröder et al. 2010).

Cells lacking Gq/11 proteins consequently did not respond to carbachol, as these cells miss the proteins to transfer the signal of the M3 receptor into the cell. Cells expressing the Gq protein constructs responded to carbachol addition (**figure 20A**) indicating the presence of the signaling adaptor for the receptor.

FR exposition on HEK cells transfected with vector or wild type $G\alpha_q$ did not elicit shifts in the DMR traces compared to buffer injection. In contrast, FR application on HEK cells expressing constitutively active $G\alpha_q^{Q209L}$ triggered upwards movement of cellular mass from the sensor within the detectable area of the cell mono-layer (**figure 20B**). Upwards movement of mass then was translated to negative optical DMR traces.

Likewise, inverse agonists of constitutively active receptors that reverse the signal direction of agonists, Gq inhibition by FR led to opposite directed optical traces compared to ligand evoked Gq activation. By this means we can conclude, that inhibition and activation of Gq induces adverse cell reactions regarding the cell's mass redistribution. In contrast to the negative FR triggered traces, CCh induced pm shifts of the reflected light that revealed cellular mass movement towards the sensor. This movement was converted into positive traces.

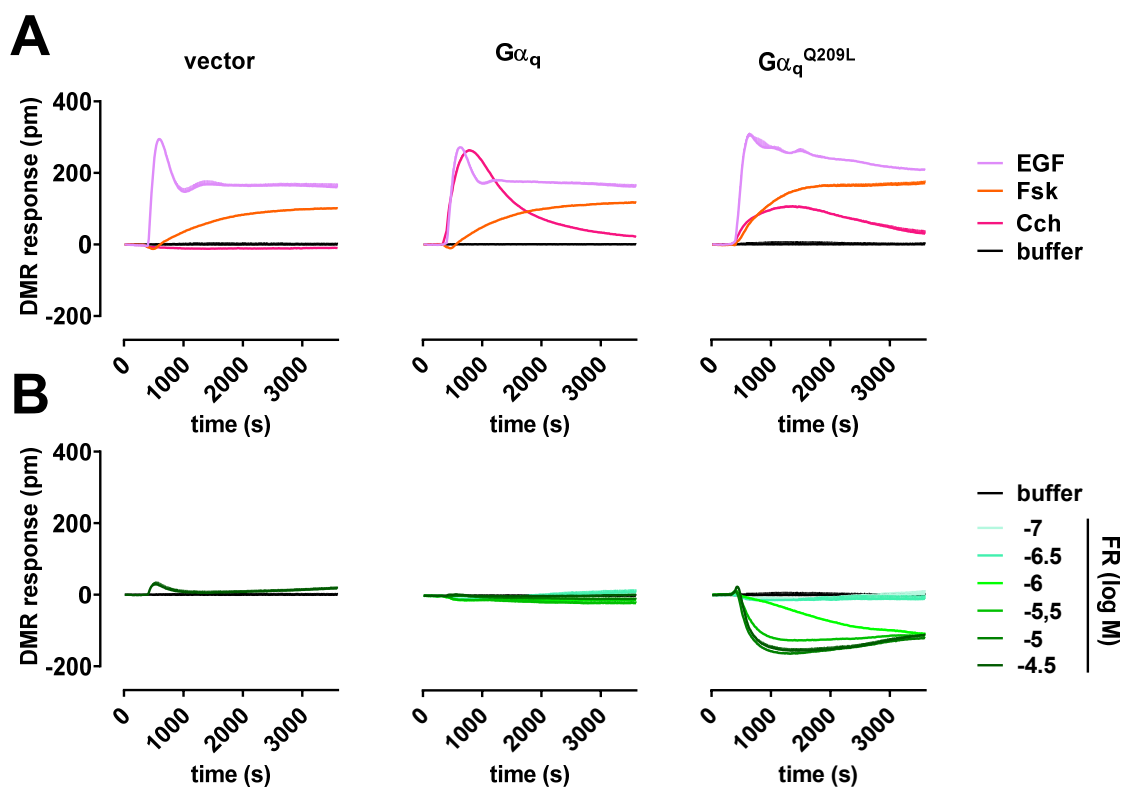


Figure 20: DMR bio-sensing of intrinsic Gq inhibition by FR

DMR profiles of cell viability controls EGF in 50 μM , Fsk in 30 μM and transfection control CCh in 30 μM (A). DMR traces induced by FR application in indicated concentrations (B) in HEK293 $G\alpha_{q/11}^{\text{null}}$ cells transfected with 1.3 $\mu\text{g}/9 \text{ cm}^2$ plasmid with or without insert encoding wild type or Q209L $G\alpha_q$. Shown are representative traces of $n=3$ independent experiments.

Signaling amplitude of the negative FR traces was concentration-dependent and could be converted to a concentration-response curve by calculating the negative area under the curve of FR initiated traces within the first hour of measurement (figure 21). Even though, basal wild type Gq tonus was detectable in the IP1 assay of transfected genome edited HEK293 $G\alpha_{q/11}^{\text{null}}$ -cells, this tonus apparently was insufficient to instigate notifying changes within the cell after FR application by DMR. Negative traces seem to appear only as an inversion of permanently elevated Gq signaling.

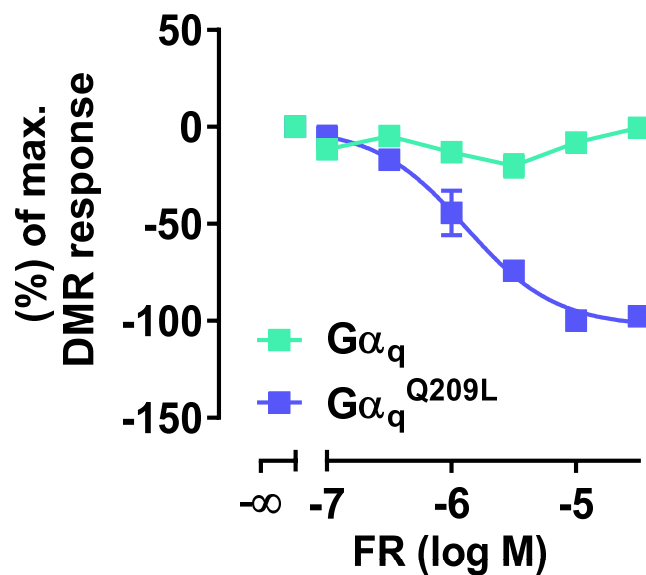


Figure 21: Quantification of DMR bio-sensing of intrinsic Gq inhibition by FR

FR concentration-inhibition-curve of negative DMR traces upon FR application in either wild type or GTPase-deficient Gq transfected HEK293Gα_{q/11}^{-null} cells. Dots represent means of 3 independent experiments with s.e.m.

4.3.4 FR might act as a GDI on the GTPase-deficient Gα_q^{Q209L} protein

The inhibition of the GTPase-deficient Gα_q^{Q209L} by the macrocyclic FR, was unpredicted, as this mutant is reported to be completely receptor independent and therefore, constitutively GTP-bound (Kleuss et al. 1994). According to this concept FR as a GDI was thought to miss its target, the Gα_q^{Q209L} protein (Kimple et al. 2011). Thus, against this concept, we were able to proof FR to interfere with this mutated version of the Gq protein. In the following step, we wanted to enlighten the mechanism behind FR's mode of action on this GTPase-deficient mutant.

4.3.4.1 DMR reveals receptor-activatable fraction of Gα_q^{Q209L}

The first possible hint was buried in the DMR whole cell experiments. Initially thought as a control for wild type Gα_q transfection, CCh surprisingly evoked a response in mutant Gα_q^{Q209L} expressing cells. This signal was compromised but still detectable. CCh mediated signal in wild type as well as in Q209L transfected cells was clearly receptor mediated, as the signal was sensitive to atropine (**figure 22A**), a competitive antagonist on the muscarinic receptor subtypes M1-M5 (Wall et al. 1992). GPCRs are known to activate heterotrimeric G proteins (Oldham and Hamm 2008). Most likely Gα_q^{Q209L} exists also in the GDP-bound-heterotrimeric version.

Compromised CCh signals could not be related to poor cell viability of these cells, as Fsk and EGF, the non-G protein dependent controls, showed signals that were similar in the pm-shift range compared to wild type Gq transfected cells (**figure 22B**). This carbachol-promoted traces could be abolished by FR in a concentration-dependent

manner unaffected by the mutational state of the protein. Notable FR-induced negative traces could also be observed in the presence of the receptor agonist, but again these traces were unnoticeable in wild type $G\alpha_q$ transfected cells. These results again suggest that negative traces reveal only high permanent intrinsic activity, and further, that this behavior cannot be mimicked by receptor activation (**figure 22C**). Quantification of CCh signal inhibition by FR exposed no difference in sensitivity between both versions of the protein calculated by the positive AUC within one hour of measurement (**figure 22D**).

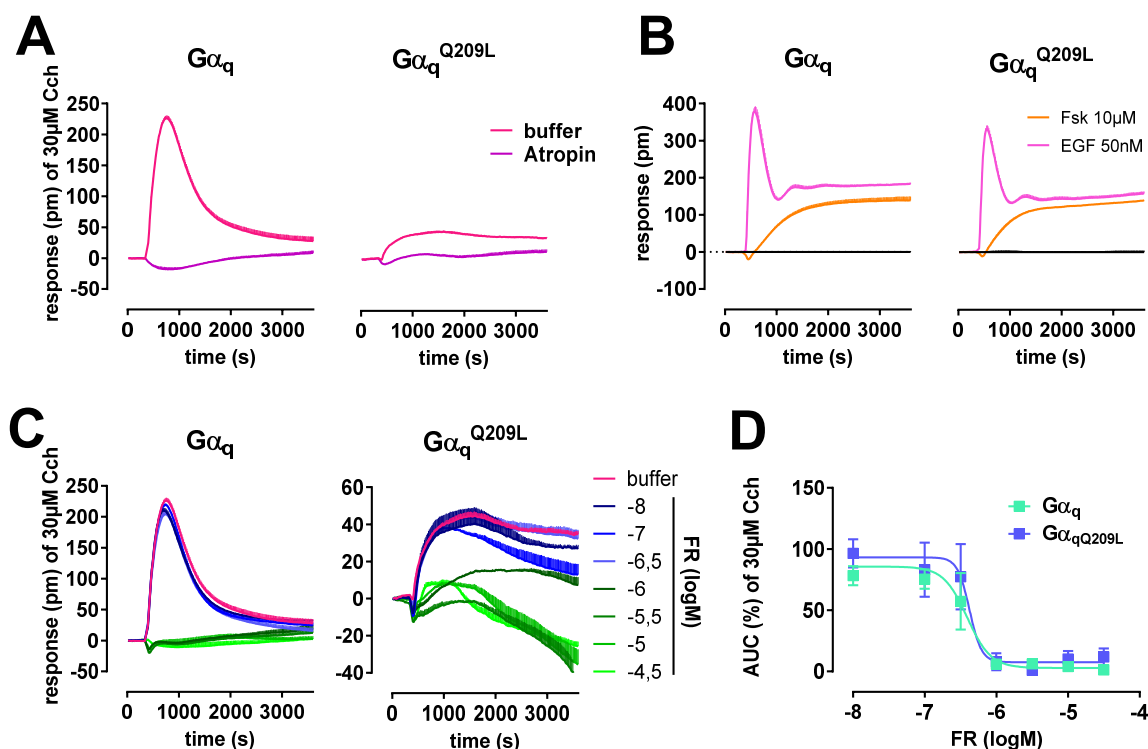


Figure 22: DMR bio-sensing of intrinsic Gq inhibition by FR

DMR profiles of carbachol 30 μM pretreated with buffer or atropine in 100 μM for 1 hr (A) or of cell viability controls EGF in 50 μM, Fsk in 30 μM (B) or of carbachol 30 μM pretreated with buffer or FR in indicated concentrations (C) in HEK293Gα_{q/11}^{-null} cells transfected with 1.3 μg/ 9 cm² plasmid with or without insert encoding wild type or Q209L Gα_q. (D) Quantification of the FR effect on CCh calculated by the positive area under the curve of 1 hr normalized on the buffer control. Shown are representative traces of n=3 independent experiments (A-C). (D) Dots represent the mean with s.e.m. of three independent experiments.

As FR functions as GDI on GDP-bound Gq and as we obtained first hints, that Gα_q^{Q209L} exists at least fractionally in the GDP-bound state, this might be an explanation for FR to interact with the GTPase-deficient mutant.

4.3.4.2 Immunoprecipitation confirmed GDP-bound Gα_q^{Q209L}

To further confirm the nucleotide binding state of constitutively active Gα_q^{Q209L} we decided to perform immunoprecipitation with [³²P]orthophosphate-labeled GTP and GDP in transfected HEK293 cells. Hence, wild type Gα_q was exclusively extracted with GDP whereas Gα_q^{Q209L} was found to be attached to both versions of the nucleotide (**figure**

23A). The next question to assess was to test our hypothesis, where the GDP-bound $G\alpha_q^{Q209L}$ subunit would exist as monomer, or if it largely exists in a sedentary state committed to the $\beta\gamma$ -heterodimer. His-pull-down assay demonstrated that $\beta\gamma$ -heterodimer was indeed attached to a large amount of $G\alpha_q^{Q209L}$, thereby binding was exclusive for the fraction of GDP (**figure 23B**).

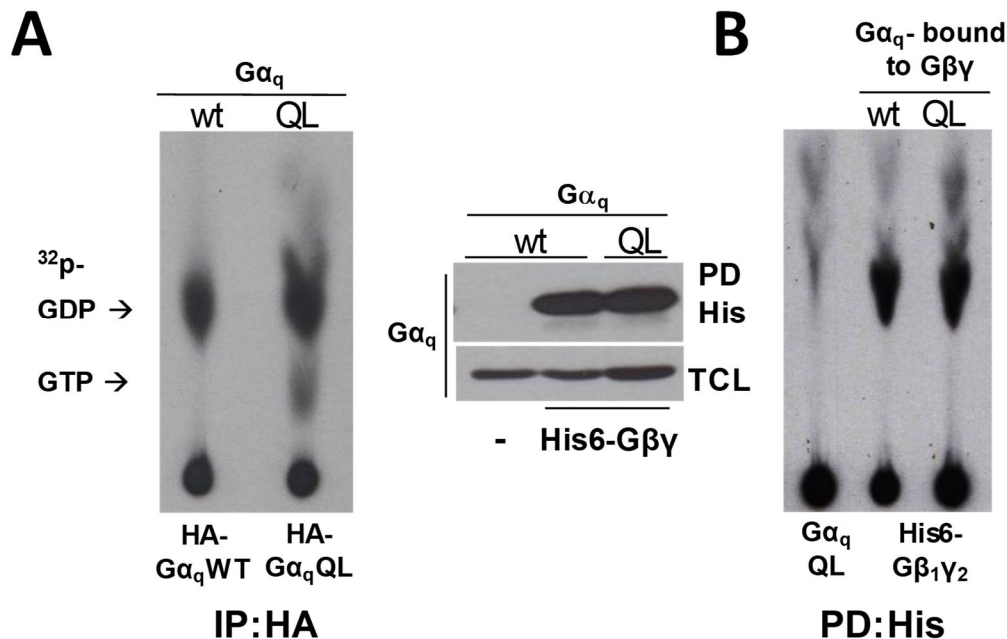


Figure 23: Detection of GDP and GTP-bound $G\alpha_q$

A) Thin layer chromatography of lysates of $[^{32}P]$ orthophosphate-labeled HEK293T cells transfected HA-tagged $G\alpha$ subunits. Subunits were isolated either by immunoprecipitation (IP:HA, left panel) or by their interaction with His6- $G\beta\gamma$ isolated by pull-down with talon resin (PD:His, right panel) Data was kindly provided by Daniel Cervantes-Villagrana from the working group of Prof. José Vázquez-Prado (from the Cinvestav-IPN, Mexico).

4.3.4.3. Binding site comparison of FR on wild type and GTPase-deficient $G\alpha_q$ indicate FR to act as GDI on both proteins

Signaling conducted by either wild type Gq or GTPase-deficient mutant was in both cases sensitive to FR in the phospho-YAP assay. Thus, we made use of this readout to investigate, whether binding surface of the molecule differ between the both proteins. In 2010 Nishimura et al. published the co-crystallization of the $G\alpha_{i/q}\beta\gamma$ -heterotrimer with YM, the structurally closely related macrocycle. They identified thirteen residues mainly on the interdomain linkers that created a hydrophilic gap for YM (Nishimura et al. 2010). Binding into this gap, the molecule was shown to act like a wedge in the cleft of these linkers. Thereby, YM compromised the flexibility of switch 1 (linker 2). Flexibility within this region has been reported to be a major requirement for GDP release (Oldham and Hamm 2008). By preventing GDP-GTP-exchange, YM enabled the alpha subunit to be activated by the receptor (Nishimura et al. 2010). To address the question, whether FR binding on

wild type or GTPase-deficient Gq protein would be the same, we mutated residues in both linkers between the GTPase and helical domain. Thus, we assumed FR and YM to share the same interface on the protein as suggested in the structure relationship study of Strømgaard and co-workers (Zhang et al. 2018).

Mutation of the non-polar amino acid phenylalanine on position 75 in linker 1 to lysine led in both proteins to a slight shift in FR inhibition curve. More severe was the reduction of activity when isoleucine on position 190 was exchanged to the sterically much bigger tryptophan. As mutation mediated loss of function behavior of FR was the same for wild type and the Gq^{Q209L} protein, we postulate direct interaction and similar binding mode of FR for both proteins (**figure 24A**). The mutation Q209L that drives the GTPase-deficiency and consequently leads to the constitutive activity, is located in the Ras like domain, but it is not directly affecting FR binding site as illustrated (**figure 24B**).

Crystal structure comparison between transducin, a G α -subunit that is activated by a light-inducible receptor, in the GTP-bound and the GDP-bound state, both published by Paul Sigler and co-workers (Lambright et al. 1994), showed that nucleotide variation only has minor impact on the overall structure of the G α protein. However, the key regions, where these structural differences occurred, were the three flexible switches. As switch 1 is part of the YM and apparently also of the FR binding pocket and is shifted about 2 Å, Nishimura et al. predicted YM not to bind on the GTP-bound G α (Nishimura et al. 2010). Therefore, it is likely that FR also binds to G α _q^{Q209L} in the GDP-bound state also acting as a GDI.

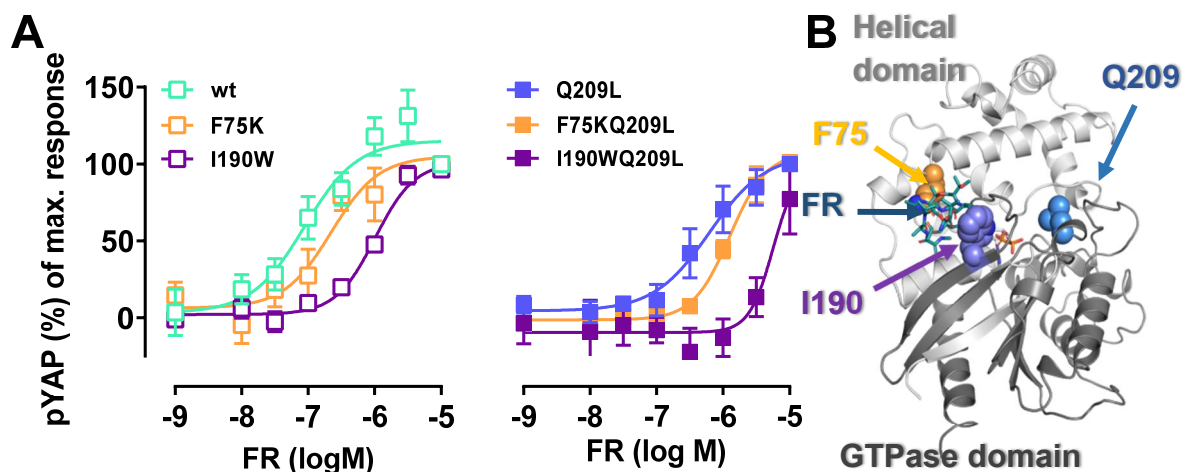


Figure 24: FR binding on wild type and GTPase-deficient G α _q

(A) Quantification of FR potency in YAP phosphorylation assay initiated by G α _q^{wt} or G α _q^{Q209L} and modification of these proteins by side directed mutagenesis in HEK293G α _{q/11}^{-null} cells transfected with 1.3 μ g/ 9 cm² of indicated constructs. (B) Cartoon illustrating FR binding site on G α _q highlighting modified residues. Illustration was kindly provided by Stefania Monteleone from the working group of Peter Kolb, Philipps-University Marburg. (Pdb 3AH8)

4.3.5 Addressing FR's inability towards canonical PLC signaling induced by GTPase-deficient $G\alpha_q$

4.3.5.1. FR inhibits PLC-interaction of a GTPase impaired $G\alpha_q$, that is still substrate for GAP

If FR functions as GDI on mutational $G\alpha_q^{Q209L}$, signaling of all effector proteins should be affected. The answer to the question, why FR is unable to inhibit canonical PLC signaling may lay in the properties of the effector itself. Interaction between $PLC\beta$ and $G\alpha_q$ is quite fast, and is described to have a kiss-and-run like dynamic (Adjobo-Hermans et al. 2013). PLC catches activated $G\alpha_q$ that is deactivated shortly afterwards by the GAP-activity of the effector. In the presence of Gq-coupled receptor ligands that bind to the receptor, the PLC -inactivated Gq protein can be reused for PLC interaction post reactivation by the ligand-induced receptor (Harden et al. 2011). In this state the G protein cycles between activated and inactivated state (Oldham and Hamm 2008) as illustrated in **figure 25**.

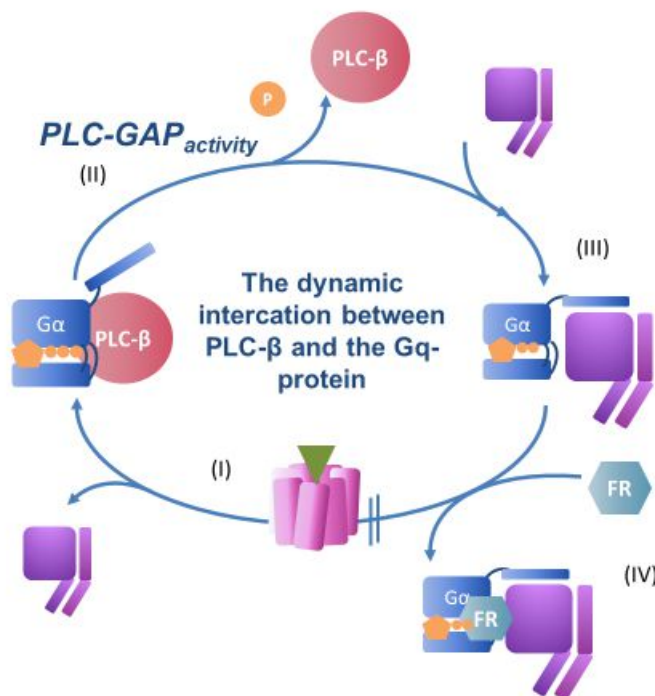


Figure 25: Schematic description of PLC-Gq interaction and GAP activity.

Ligand-activated GPCRs provoke the exchange of GDP versus GTP in the α -subunit of the Gq protein (I). This nucleotide-exchange releases the α -subunit from the $\beta\gamma$ -heterodimer. In the monomeric state the α -subunit can interact with its canonical effector $PLC\beta$. This interaction is fast, as GAP activity of $PLC\beta$ accelerates the GTPase function and therefore promotes the autocatalytic switch-off function of the α -subunit (II). This favors the formation of the inactive heterotrimer (III). By applying FR to the system, an accumulation of the protein is achieved. In the complex with the inhibitor the Protein is no longer available to the activation circle (IV).

Substitution of glutamate on position Q209 to leucine lead to a dramatic loss of GTPase function and was reported to lose sensitivity towards GAP activity by $PLC\beta 1$ or $RGS4$ (Berman et al. 1996). R183 is another hot spot residue known to impair GTP hydrolysis. Proteins with substitution of the arginine by cysteine on this position are also known as

oncogenes in certain cancer types. In contrast to the Q209 residue, where GTPase activity is reported to be majorly impaired, mutation on R183 decelerates the enzymatic function less. Additionally, R183C mutation has been shown to be a substrate for GAP proteins, as it did not to interfere Gq-affinity towards RGS2 (Nance et al. 2013; O'Hayre et al. 2013).

To investigate inhibition properties of FR for this GTPase-deficient but still GAP sensitive mutant, we transfected HEK293 cells with this R183C analog of $G\alpha_q$. Specifically, we wanted to know whether FR would succeed to blunt PLC mediated effects conducted by $G\alpha_q^{R183C}$. Therefore, we used IP1 accumulation as a direct PLC readout.

As expected from the slower hydrolysis rate and by this means from the bigger fraction of GTP-bound protein, the transfection of the construct led to elevated IP1 levels compared to cells transfected with wild type Gq. In contrast to the GTPase-deficient Q209L the R183C construct was FR sensitive with a similar IC50 value (**figure 26A**). As R183 is much closer to the FR binding region compared to Q209 (**figure 26B**), it is unlikely that the amino substitution on position Q209 itself modifies the FR binding pocket and thereby causes the inability of FR to inhibit PLC- $G\alpha_q^{Q209L}$ interaction.

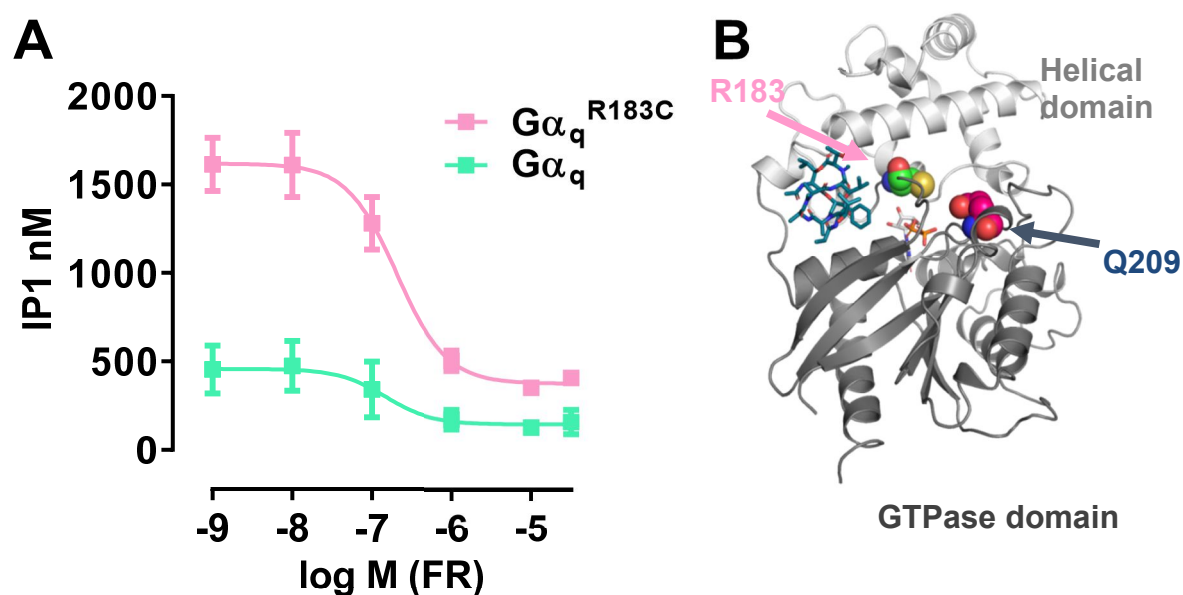


Figure 26: FR inhibition of PLC- β downstream signaling initiated by GTPase impaired Gq R183C

(A) Inhibition of cell-intrinsic IP1 tonus of HEK293 $G\alpha_{q/11}^{-null}$ cells 48 hrs. post transfection with the indicated constructs after 1 hr incubation with FR in stated concentrations $n=5$ in stimulation buffer. Dots represent the means of n independent experiments with error bars representing s.e.m. (B). Cartoon illustrating FR binding site on $G\alpha_q$, highlighted are the two hot-spot mutations R183C and Q209L. Illustration was kindly provided by Stefania Monteleone from the working group of Peter Kolb, Philipps-University Marburg. (Pdb 3AH8)

Results

Another possibility for different inhibition effects on IP1 accumulation by FR could be different kinetics between PLC-G α_q and PLC-G α_q^{Q209L} . While activated wild type Gq cycles between PLC-bound G α -GTP and PLC-unbound heterotrimer, the GTP-bound fraction of the GTPase-deficient G α is darn to stay permanently PLC-bound. By losing the ability to perform proper GTPase activity, PLC might be unable to release the G α_q^{Q209L} from the complex. In this model FR would be impaired to prevent PLC-G α_q^{Q209L} interaction, as they stick together from the beginning. This hypothesis will be investigated next.

4.3.5.2. FR decreased kinetic on-rate for PLC- G α_q but not PLC- G α_q^{Q209L}

To enlighten the FR inhibition properties on the direct interaction of G α_q^{Q209L} and PLC β we made use of FRET tagged constructs. FRET assays helped us to measure the interaction of the proteins on HEK cell membranes that were prior transfected with tagged PLC together with either tagged G α_q^{wt} or G α_q^{Q209L} and the non-tagged M3 muscarinic receptor.

Stimulation of membrane preparation from cells transfected with wild type Gq with carbachol initiated interaction between PLC and G α_q that was translated to elevated fluorescence resonance energy transfer. Basal FRET signal of membranes transfected with the GTPase-deficient analog were elevated compared to wild type protein. These results suggest that PLC and G α_q^{Q209L} are already interacting without ligand stimulus. This interaction could not be further enhanced by Gq-receptor ligand carbachol application (**figure 27A**).

The adjoining step was to look for FR provoked changes on PLC β and G α_q interaction in real time. As expected, the addition of CCh to membranes with wild type G α_q -induced the interaction between the proteins. The interaction reached a signaling-plateau, describing a steady-state between the PLC-bound-G α_q -GTP and non-PLC-bound G $\alpha\beta\gamma$ -heterotrimer. The PLC-G α interaction was reversible and could be abolished quickly after carbachol removal, as detected by decreased FRET-signal. When Gq-inhibitor FR was applied during the phase of ligand-induced steady-state, FR reduced the on-rate of PLC and G α_q , as FRET signal was significantly depressed over time compared to just carbachol eluted membranes. After a wash-out period CCh was only able to re-evoked signaling in non-FR treated cells (**figure 27B**).

This result implements that steady-state under FR treatment was no longer sustainable, and therefore signal amplitude started to decline. PLC releases G α by its GAP activity and therefore favors the re-association of α -subunit with $\beta\gamma$ -heterodimer to form a heterotrimer. This heterotrimer then again is available for receptor activation. In the view of the fact, that FR inhibits Gq in the GDP-bound heterotrimeric state, it is likely that, FR catches the G $\alpha\beta\gamma$ -complex by preventing the guanine dissociation and thereby withdraws the protein from receptor activation. Furthermore, withdrawal of the protein from this activation cycle by FR is irreversible, since washing out FR did not re-provide the protein to the activatable system, as observed by carbachol addition.

A completely different picture occurred when we looked for membranes provided with G α_q^{Q209L} . As already stated, the basal interaction of PLC β - G α_q^{Q209L} -FRET levels were already elevated and could not be further enhanced by receptor activation. But we could

also observe that this elevated basal FRET level could not be lowered by FR addition. Remarkably, PLC- $G\alpha_q^{Q209L}$ seem to be stacked together (**figure 27B**).

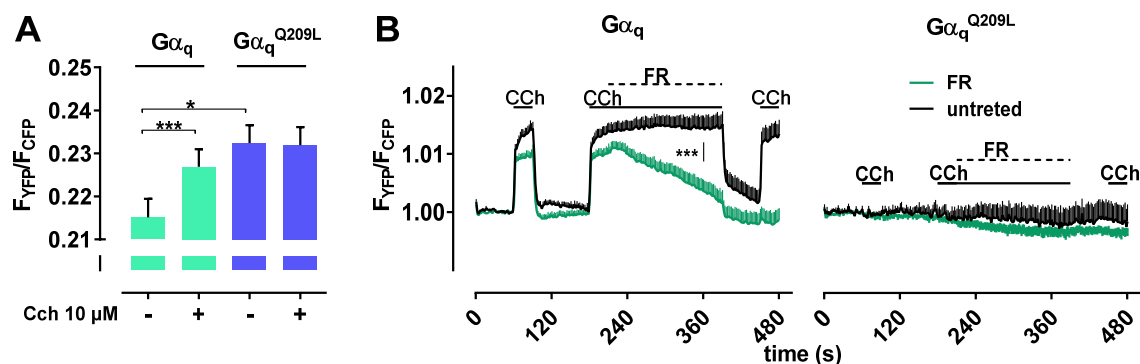


Figure 27: PLC β 3 interaction with wild type $G\alpha_q$ and GTPase-deficient $G\alpha_q^{Q209L}$ interaction in presents and absents of FR.

(**A,B**) Single cell FRET imaging in HEK293T cells expressing M_3 -R, $G\beta_1\gamma_2$, YFP-PLC β 3 and CFP-Gaq-wt shown in absolute F_{YFP}/F_{CFP} ratio of experiments (wt n=35; QL n=40) **A**). And single cell FRET imaging of cells super-fused with buffer and buffer with 10 μ M CCh consecutively as indicated. Cells were or were not additionally exposed to 1 μ M FR900359 during the long period of CCh exposure. (wt n= 17; QL n=24) **B**). Significance was calculated by using unpaired t-test (**A**, and **B** at 360 s). FRET images were kindly provided by the lab of Professor Buenemann from the University of Marburg.

4.3.5.3. FR does not interfere with PLC- $G\alpha_q$ protein-protein interaction

Taking advantage of the available crystal structure of YM with the $G\alpha_{i/q}$ chimera and our knowledge that FR and YM share similar binding sites, we modeled the $G\alpha_q$ -PLC β -FR complex. Here we were able to demonstrate that FR does not interfere the binding of the $G\alpha$ -subunit with PLC β , as there is enough space for FR to fit in (**figure 28**).

So far, no crystal structures of $G\alpha_q$ in complex with Trio are available, but structure of p63RhoGEF that is closely related to TRIO was published in 2007 (Lutz et al. 2007). The specific binding site of p63RhoGEF is also found in the other protein family members TRIO and DUET. Superimposition of those crystal structures could show, that the two effectors PLC and p63RhoGEF are engaged to the $G\alpha$ subunit in a strikingly similar manner. In both cases the α 3 helix and switch II of the $G\alpha_q$ interacts with a helix-turn-helix structure of the effectors (Charpentier et al. 2016). Thus, differences in inhibition of TRIO (YAP) and PLC (IP1) activation most likely cannot be explained by inhibition of special protein-protein-interaction. These findings support the theory that lack of PLC inhibition by FR must be due to PLC-specific feature.

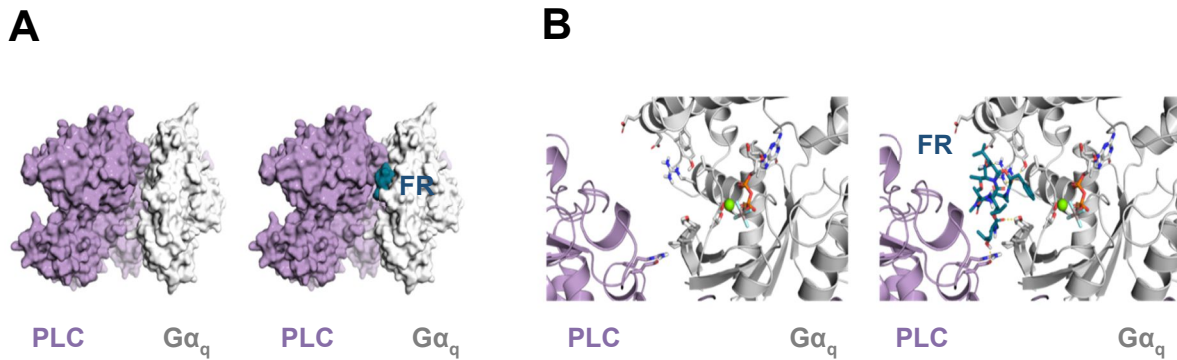


Figure 28: PLC-β3 interaction with wild type Gα_q and GTPase deficient Gα_q^{Q209L} interaction in presence and absence of FR.

Cartoon illustrating the overall surface structure (A) and zoom-in view of the binding site (B) of an AlF₄⁻-dependent complex of Gα_q and PLCβ3 (PDB: 3ohm). FR (dark green) fits easily between the domain interfaces of the active Gα_q-PLCβ3 complex. Cartoon was modelled by Stefania Monteleone from Professor Peter Kolb's lab, Philipps-University Marburg. (PDB 3ohm)

4.4. Evaluation of FR capability to inhibit oncogenic Gq-signaling in uveal melanoma

As already stated, activating mutations of GNAQ and GNA11 are oncogenic drivers in specific types of cancer. They have been detected in 5.6% of human tumor with approx. 66% occurrence in the eye and ~6% in the skin melanoma. The most prominent ocular cancer with constitutively active Gq/11 is the uveal melanoma (O'Hayre et al. 2013). About 83% of the patients harbor a genetic alteration in one of the hot spot residues Q209 or R183 of either GNAQ or GNA11 (van Raamsdonk et al. 2009). Consequently, we wanted to evaluate effects upon Gq inhibition by FR in this therapeutically relevant system.

4.4.1. Targeting canonical effector PLCβ in uveal melanoma

We tested 5 non-metastatic UM cell lines. Of these two cell lines had no mutations in GNAQ or GNA11: Mel290, Mel285 and three carried a mutation in the GNAQ gene: Mel270 (Q209P), Mel202 (Q209L) and 92.1(Q209L). Additionally, we tested the metastatic cell line OMM1.3 with a mutation in GNAQ (Q209P) (Griewank et al. 2012).

Initially, we verified the absence or presence of intrinsic Gq activity by examining elevated IP1 levels under non-stimulating conditions. In all cell lines increment of cell number enhanced detectable the absolute amount of IP1 accumulation in a proportional manner (**figure 29A**). Surprisingly, also the GNAQ wt cell line Mel290 showed quite high IP1 tonus. But further activation of G proteins by [AlF₄]⁻ only enhanced IP1 levels of GNAQ wt cell lines Mel285 and Mel290 (**figure 29B**). [AlF₄]⁻ mimics the γ-phosphate of the GTP and therefore serves to activate the G proteins (Lyon and Tesmer 2013). Lack of response of the cell lines with constitutively activated Gα_q to [AlF₄]⁻ implicates that PLC-Gα_q-interaction is already at the maximum. These findings corresponded to the observations we made in the FRET-PLC- Gα_q experiments in transfected HEK cell membranes. Receptor agonist carbachol could only enhance the interaction between the

wild type $G\alpha_q$ and PLC, whereas ligand-induced receptor activation did not increase FRET signal in membranes when GTPase-deficient $G\alpha_q^{Q209L}$ was transfected.

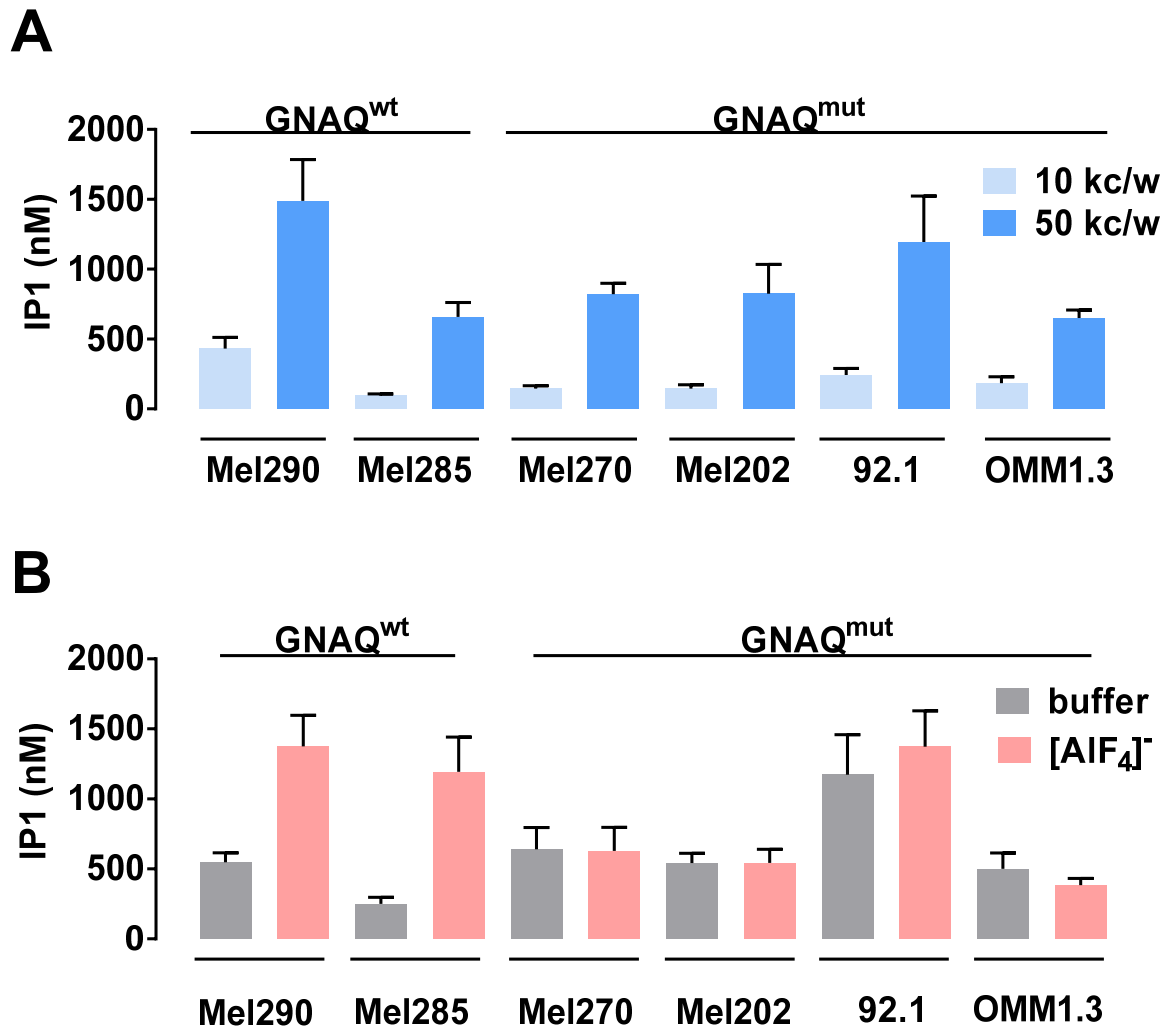


Figure 29: Intrinsic Gq activity in uveal melanoma cells expressing either wild type Gq or GTPase-deficient mutant.

(A) Quantification of cell-intrinsic IP1 production in UM lines of 10 and 50 kc/w after 1 hr incubation in stimulation buffer. (B) Inositol-monophosphates (IP1) from AlF_4^- (300 μM) stimulated cells accumulated over 1 hr using 30 kc/w. Data for Mel280, Mel290, 92.1, and OMM1.3 ($n=4$); data for Mel270 and Mel202 ($n=3$). All biological replicates are independent experiments with at least two technical replicates. Bars represent means with error bars denoting s.e.m.

Next, we tested PLC activity towards FR sensitivity. Results here were quite unexpected as they apparently not only vary by mutational state of Gq protein but also within the different cell lines. Whereas FR uncovers Gq as the perpetrator for basal IP1 tonus in Mel285 cell line, the same was not observed within the other wild type GNAQ/GNA11 cell line Mel290, where PLC activity was elevated. The IP1 tonus in these Mel290 cells was

Results

even higher compared to the mutated GNAQ cell lines Mel202, Mel270 and OMM1.3. Surprisingly, in this case FR was unable to depress the quite high basal activity.

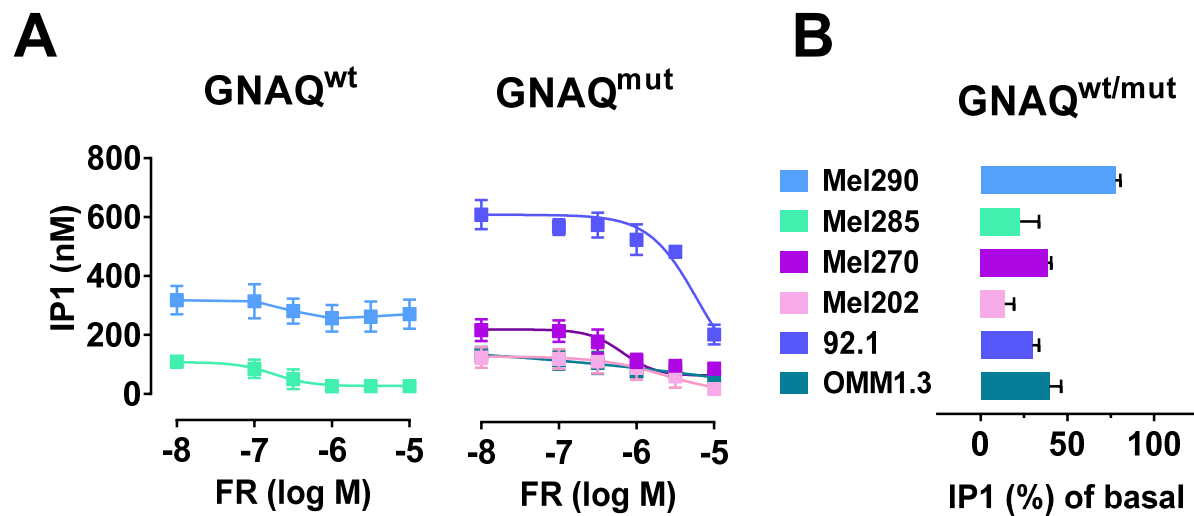


Figure 30: Intrinsic Gq activity in uveal melanoma cells expressing either wild type Gq or GTPase-deficient mutant.

(A) FR sensitivity of basal IP1 accumulation of indicated uveal melanoma cell lines in 30 kc/w and (B) sensitivity towards inhibition by Gq inhibitor FR (concentration effect mode and maximal inhibition @ 10 μ M FR. Dots and bars represent means and s.e.m. of n=4 biological replicates.

To our astonishment, all cell lines harboring the GNAQ^{mut} gene were at least to some extent sensitive towards FR. Inhibition curves of IP1 accumulation were only slightly shifted to the right compared with GNAQ/GNA11 wild type cell line Mel285. Only in 92.1 cell line IP1 levels remained mostly unaffected up to 3 μ M (**figure 30A**). But clearly most of the IP1 tonus in this cell line was Gq mediated, as we were able to depress accumulation to less than 30% of basal level by using very high concentrations up to 10 μ M of FR (**figure 30B**).

Conspicuously, the IP1 tonus in the other mutated cell lines Mel270, Mel202 and OMM1.3 was quite low and therefore did not indicate excessive PLC activity. Cellular background with its protein composition in quantity but also in its facility of different protein isoforms might be a crucial factor when it comes to PLC inhibition. Whereas HEK cells harbor the PLC β isoforms 1 & 2 (Atwood et al. 2011) which both are known to accelerate GTP-hydrolysis, UM cells also express the PLC β_4 that is generally highly present in retina and cerebellum. Little is reported so far about GAP activity of the β_4 isoform and its GAP function (Lyon and Tesmer 2013; Johansson et al. 2015). Furthermore, other components within the cell might vary, like the GDP/GTP content as well as the expression pattern of GAP proteins like RGS.

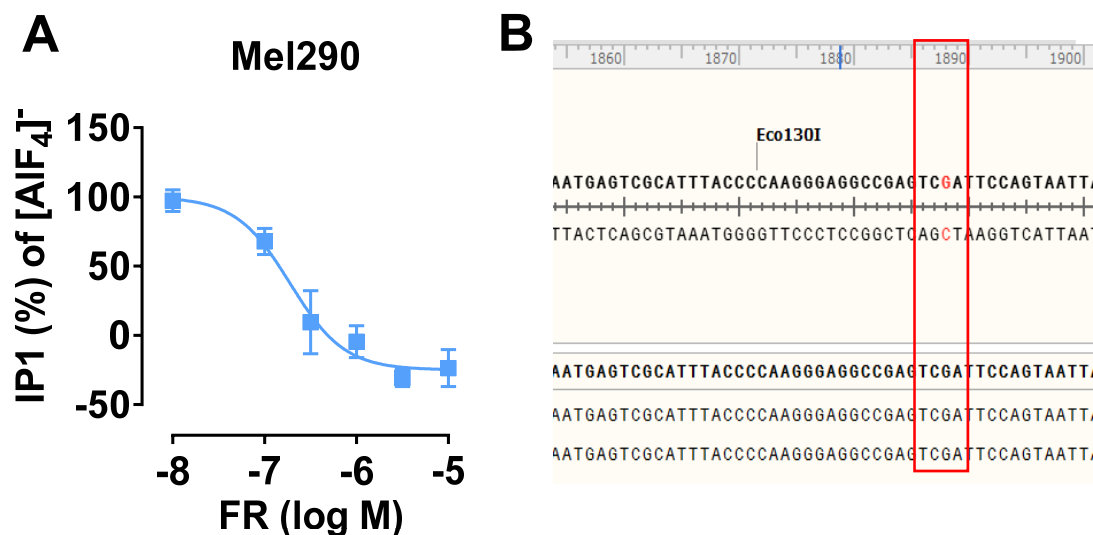


Figure 31: FR blunts [AIF₄]⁻-mediated IP1 accumulation in Mel 290 cells.

Inhibition of IP1 production after 30 min stimulation with 300 μ M [AIF₄]⁻ in Mel290 cells pre-treated with FR or vehicle for 1 hr (n=4) with 30 kc/w. Values were normalized to the [AIF₄]⁻ stimulated vehicle control. Sequencing of *PLCB4* for mutation at residue c.G1888T (p.D630Y) confirms absence of hotspot mutation.

While FR only had minor impact on basal IP1 levels in Mel290 cells, G protein-stimulated IP1 accumulation by [AIF₄]⁻ was completely blunted with the inhibitor. By this means, we were able to exclude the probability of FR to be incapable to penetrate through the membrane of Mel290 cells (**figure 31A**). These findings also assume an additional driver for basal IP1 enrichment than the Gq protein.

Johansson et al. identified in 2015 an activating mutation in the *PLCB4* gene encoding for the PLC β_4 isoform. This mutation affected position D630 (c.G1888T) and was thought to bestow the protein with elevated enzymatic activity. As PLC is a Gq downstream effector the mutation was suspected to be an alternative oncogenic operator in uveal melanoma cells (Johansson et al. 2015). As this would be the perfect explanation for high basal IP1 production we sequenced Mel290 for this mutation but could only show absence of *PLCB4* mutation in this residue (**figure 31B**).

4.4.2 FR inhibits pro-survival signaling in GNAQ^{mut} but not GNAQ/11^{wt} cells

Since the discovery of GTPase-deficient mutations of the Gq/11 protein in uveal melanoma as one of the major oncogenes in 2008/2009 (Onken et al. 2008; van Raamsdonk et al. 2009) many different Gq downstream effectors have been targeted to prevent cell proliferation (Chen et al. 2014; Ambrosini et al. 2013). Here we will evaluate the inhibition capacity of ERK, AKT and YAP signaling by direct targeting of the oncogene with FR.

4.4.2.1. FR blunts ERK signaling in GNAQ^{mut} but not GNA^{wt} cells

Activation of the MAPK pathway upon Gq activation is linked to signaling conduction by PLC β (Gutkind 2000). This paradigm could not be observed in Hcmel12 cells, as ERK inhibition was reached within very low FR concentrations but IP1 accumulation was

Results

insensitive to treatment with the inhibitor (**figure 12**). In this context we wanted to evaluate any correlations between elevated basal ERK phosphorylation and IP1 accumulation in the uveal melanoma cell by using HTRF® technology by Cisbio. All cell lines showed elevated pERK significantly over background. Thereby, ERK phosphorylation in all cases was sensitive towards trametinib (**figure 32A**). Trametinib is a potent MEKi that has shown impressive response rates of over 20% in melanoma patients in phase III study (McArthur and Ribas 2013) with mutated B-Raf but was mainly unresponsive in uveal melanoma patients in a phase I study (Carvajal et al. 2016).

Interestingly, high IP1 values could not always be associated with high basal ERK phosphorylation or vice versa. Highest tonus of mitogen-activated protein kinase signaling was detected for Mel290 and Mel285 even though IP1 levels of Mel285 were quite low. In addition, no correlation between these two signaling pathway readouts could be drawn in the cell lines with $G\alpha_q^{mut}$. Despite 92.1 had quite high IP1 tonus its extent of phosphorylated ERK was comparatively weak to the other cell lines as Mel270, Mel202 and OMM1.3 that showed moderate basal ERK activation. MAPK-pathway in wild type GNAQ/GNA11 UM cells seem to be under promotion of another origin than Gq as ERK phosphorylation was not sensitive towards Gq inhibitor FR. In contrast, all cell lines with mutated GNAQ gene responded to Gq inhibition with depressed fraction of phosphorylated ERK1/2 protein (**figure 32B**). Further effects of FR on the total amount of ERK proteins were not detected (**figure 32C**).

These observations were in perfect line with the results obtained by a study made by Woodman and co-worker. By knocking down GNAQ with siRNA they were able to block activation of MAPK in cells with GNAQ^{mut} Mel202 and 92.1 whereas MAPK activity the GNAQ^{wt} cell lines Mel290 and Mel285 remained unaffected (Khalili et al. 2012).

Taken both observations together, we can conclude that FR truly inhibits ERK signaling only in cell lines when ERK signaling is under promotion of GNAQ that functions as an oncogene.

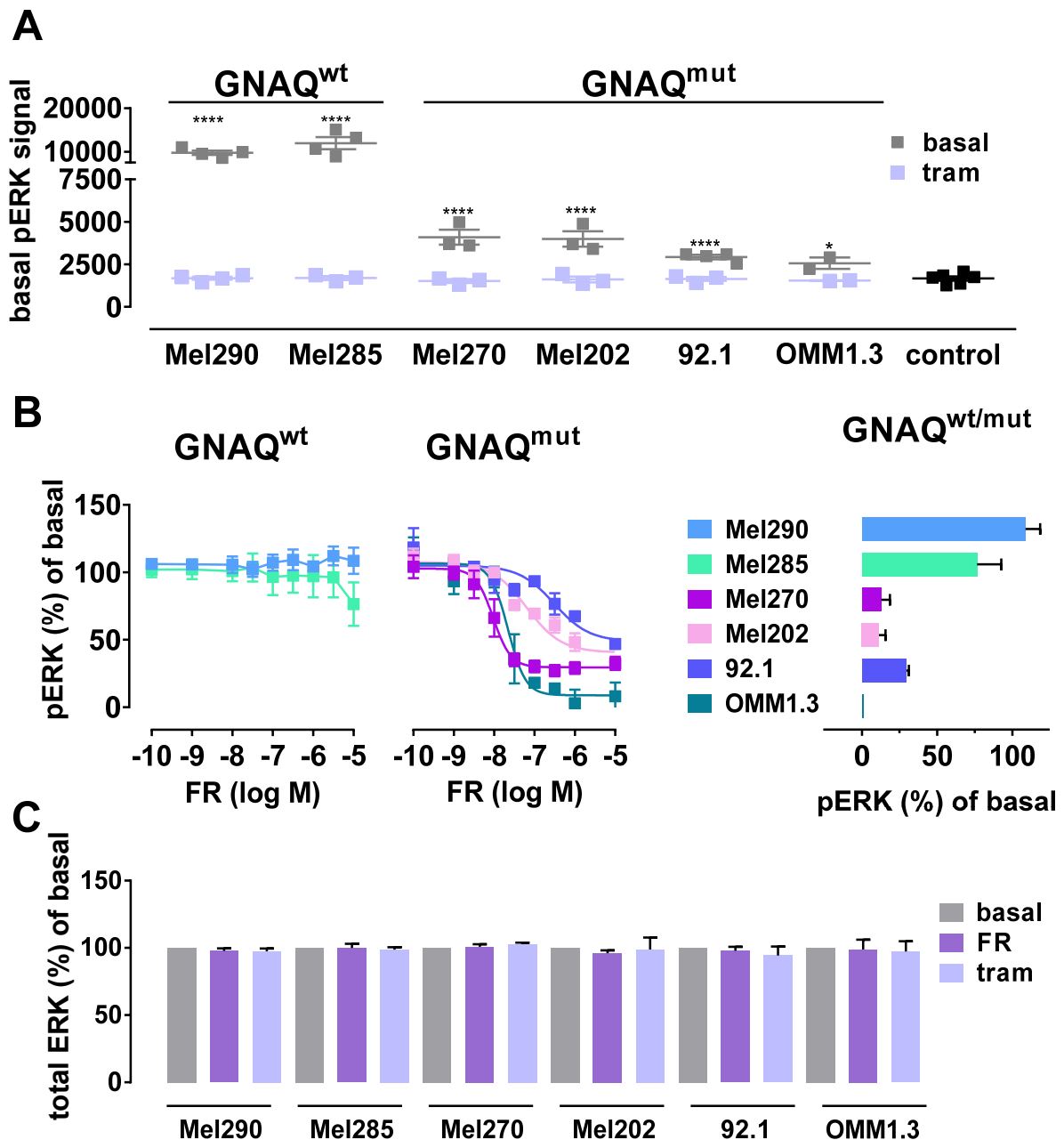


Figure 32: FR inhibits ERK signaling in uveal melanoma cells carrying GTPase-deficient Gq mutant.

(A) Comparison of basal phosphorylated ERK1/2 amounts in the absence and presence of MEK inhibitor trametinib in 1 μ M (tram) (Mel290, Mel285, 92.1 n=4; Mel270, Mel202, OMM1.3 n=3). (B) FR modulation of pERK1/2 levels in wild type and mutant UM lines (concentration effect mode and maximal inhibition @ 10 μ M FR, n=3 for all cell lines). (C) Impact of FR and trametinib on total ERK amount in indicated cell lines. (A-C) Incubation time 1 hr in medium. Bars and dots represent the mean of indicated n number with s.e.m. Significant effects to neg. control were calculated by using the one-sample t-test (A).

Results

Another interesting information we gained from this data, was that inhibition of the MAPK-pathway again was more sensitive in GTPase-deficient cell lines than PLC activation, even though it was clearly detected that both pathways were driven by Gq. Likewise, unexpected was the observation that FR potency regarding ERK phosphorylation varies between the amino acid substitution on position Q209.

While in the cell lines OMM1.3 and Mel270 glutamine is substituted for proline, in Mel202 and 92.1 cells leucine replaces the original amino acid and disturbs GTPase activity. Dephosphorylation of ERK was slightly easier achieved in OMM1.3 and Mel270 compared to the other two mutated cell lines. But if we also consider the results of the cutaneous melanoma cell lines BRIM4 (GNAQ^{Q209P}) and HCmel12 (GNA11^{Q209L}) (**table 1**) it is more likely that variations regarding pathway sensitivity may lay in the different cellular background with different protein features, as HCmel12 cells that carry a leucine on this hot spot position was extremely sensitive towards FR in this assay. Another possibility could be that amino acid variations in Gq and its consequence towards FR sensitivity might not be transferrable one-to-one on the G11 protein.

	Mel270	OMM1.3	Mel202	92.1	BRIM4	HCmel12
GNAQ/ GNA11	GNAQ Q209P	GNAQ Q209P	GNAQ Q209L	GNAQ Q209L	GNAQ Q209P	GNA11 Q209L
pIC ₅₀ ±s.e.m.	8.02 ± 0.42	7.71 ± 0.08	7.20 ± 0.13	6.51 ± 0.23	8.83 ± 0.23	8.47 ± 0.11

Table 1: FR inhibition potency in correlation to amino acid substitution at position Q209

4.4.2.2. FR and MEK-i trametinib inhibit proliferation GNAQ^{mut} UM cell lines

Proliferation activity is known to be upregulated as neoplastic promotion in uveal melanoma (Krantz et al. 2017). Hence, we looked for ramification of FR treatment on cell growth after 72 hrs. on the uveal melanoma cell lines. Again, Mel290 and Mel285, both provided with the wild type GNAQ/GNA11 genes, were insensitive towards Gq inhibition. Conclusively with the fact that ERK was not under Gq promotion, trametinib showed better effects on proliferation in these cell lines. But still ERK inhibition did not stop the cells completely from proliferation. Most likely, these two cell lines have another oncogenic driver and may use an additional proliferation pathway than just MAPK.

A completely different picture occurred in all cell lines with mutated Gq protein. Proliferation was inhibited by targeting the oncogenic Gq protein with FR in a nanomolar concentration range. Despite of OMM1.3 all other cell lines showed impressive responded to the MEK-i trametinib. Thereby, results were very similar to Gq inhibition (**Figure 33A/B**).

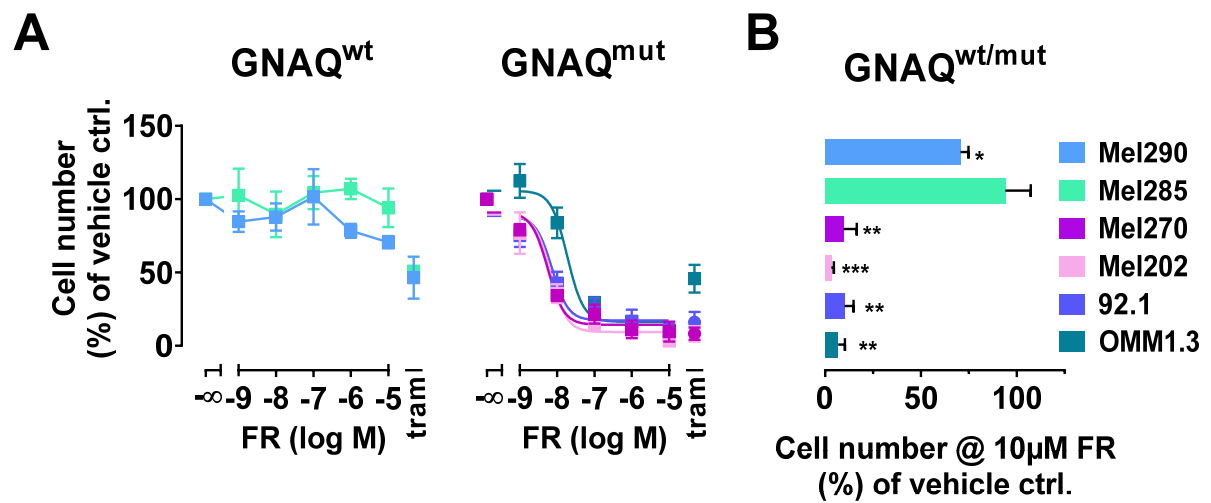


Figure 33: FR inhibits proliferation in GTPase but not wild type Gq uveal melanoma cell lines.

(A) Effect of FR on cell growth of Gq wildtype and mutant UM lines in culture after 72 hrs. of FR or trametinib exposure. For the quantification, the effects were normalized to vehicle-treated controls. (B) FR modulation of proliferation in wildtype and mutant UM lines (concentration effect mode and maximal inhibition @ 10 μ M FR, n=3 for all cell lines). All bars and dots represent the means of n indicated experiments with s.e.m. Significant effect to vehicle control was calculated by using the one-sample t-test.

Results from proliferation assays could be confirmed by bright field microscopy imaging. Not only cell density but also cell adhesion to the PDL-coated surface of the wells and cell shape appeared to be impaired in the FR- and trametinib-treated plate-wells cultured with mutated uveal melanoma cell lines in a concentration-dependent manner after 72 hrs. of drug application. Cells were significantly reduced, and the remaining cells were either rounded or looked stressed. Treatment with either of the substances seems to provoke cell death. The imaging pictures of GNAQ/GNA11 wild type cells again reconfirmed the observations from the proliferation assays. Cell density and cell shape of Mel290 and Mel285 did not differ in the vehicle treated versus FR treated wells. Additionally, in the MEK inhibitor trametinib was superior to Gq inhibition, as the cell density seemed to be slightly lower. But none of the two inhibitors could show satisfying results in the wild type cells (**figure 34**).

From these results we can conclude, that ERK activation in uveal melanoma most likely is then driven by Gq when this protooncogene has gained proper function as oncogene. Further we were able to show that ERK activation does not correlate in all cases with proliferation activity as shown in GNAQ/GNA11 wild type cells. But even MEKi was quite promising for cell lines with mutated Gq protein, targeting only this pathway could not proof itself in clinical trials.

Results

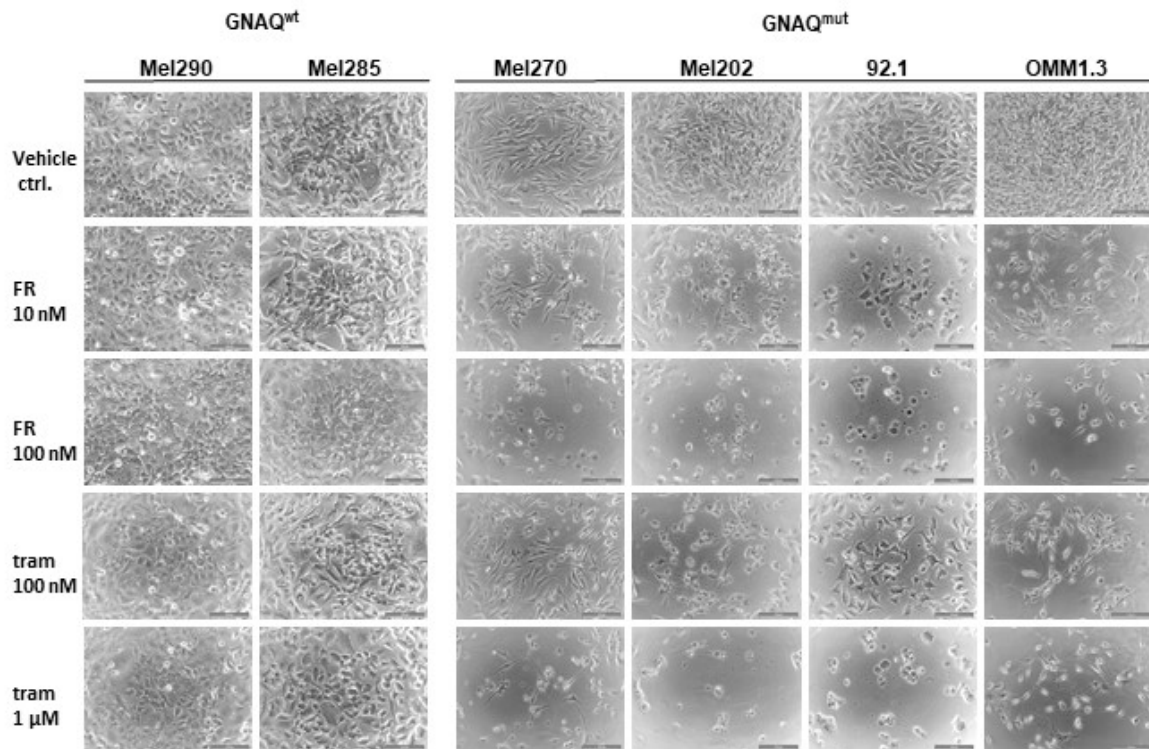


Figure 34: Inhibition of ERK signaling prevents cell growth in GNAQ^{mut} UM cell lines

(A) Bright field imaging of cells after 72 hrs. of treatment with FR in 10 and 100 nM and trametinib in 100 nM and 1 μ M at cell culture conditions. Shown are representative images from n=3 independent experiments. Images were kindly provided by Julian Patt, working group of Professor Evi Kostenis, University of Bonn.

In a Phase I dose-escalation trail published in 2012 Fecher and co-workers could not detect any significant response of 16 UM patients with this specific MEKi. In vitro and in vivo does not always seem to have a good correlation (Falchook et al. 2012). Therefore, we went along to investigate other Gq downstream signaling pathways that are known to promote tumorigenesis and progression.

4.4.2.3 AKT signaling is partially under G α_q promotion in G α_q ^{mut} UM cell lines

The phosphatidylinositol-3-kinase (PI3K)/AKT/mTor signaling pathway regulates numerous events in cell growth, cell survival, cell cycle and cell division. It is known to be upregulated in cells under pathological conditions and therefore, seems to be crucial in cancer. Phosphorylated AKT is upregulated in over 50% of uveal melanoma samples (Carvajal et al. 2016). Babchia et al. could demonstrate that targeting ERK and AKT in combination inhibited cell proliferation also in UM cells with mutated GNAQ with a synergistical effect. PI3K activation of AKT positively regulated cell cycle processes by increasing Cyclin D1 expression and promoted tumorigenesis in this manner (Babchia et al. 2010). Furthermore, elevated pAKT levels have been connected to metastatic diseases (Harlé et al. 2015).

Thus, it was no surprise that we measured valid amounts of phosphor tagged protein within all UM cells using FRET-based HTRF® technology (**figure 35A**). Extreme high values were detected for the Mel290 cell line. For this GNAQ/GNA11 wild type cell line we could correlate the elevated tonus of this pathway with proliferation activity, as light microscopy revealed that by inhibiting the AKT activating kinase PI3K with a molecule called LY294002 (LY), we were able to visibly decrease the cell number compared to vehicle treated cells after 72 hrs. This not was observed for the other GNAQ/GNA11 wild type line, Mel285. While phosphorylated protein amount was comparably high, in Mel285, inhibition of this pathway only slightly affected the cell density after three days of LY incubation.

In the GNAQ^{mut} cell lines with moderate pAKT tonus, PI3K-AKT signaling seems to be involved in cell cycle progression. Most severe was this observation for the metastatic OMM1.3 cell line, since even 3 μ M LY compound was enough to reach maximal effect of growth inhibition, whereas the effect on visible proliferation in all other cell lines could benefit from 10-fold increase of the substance (**figure 35B**).

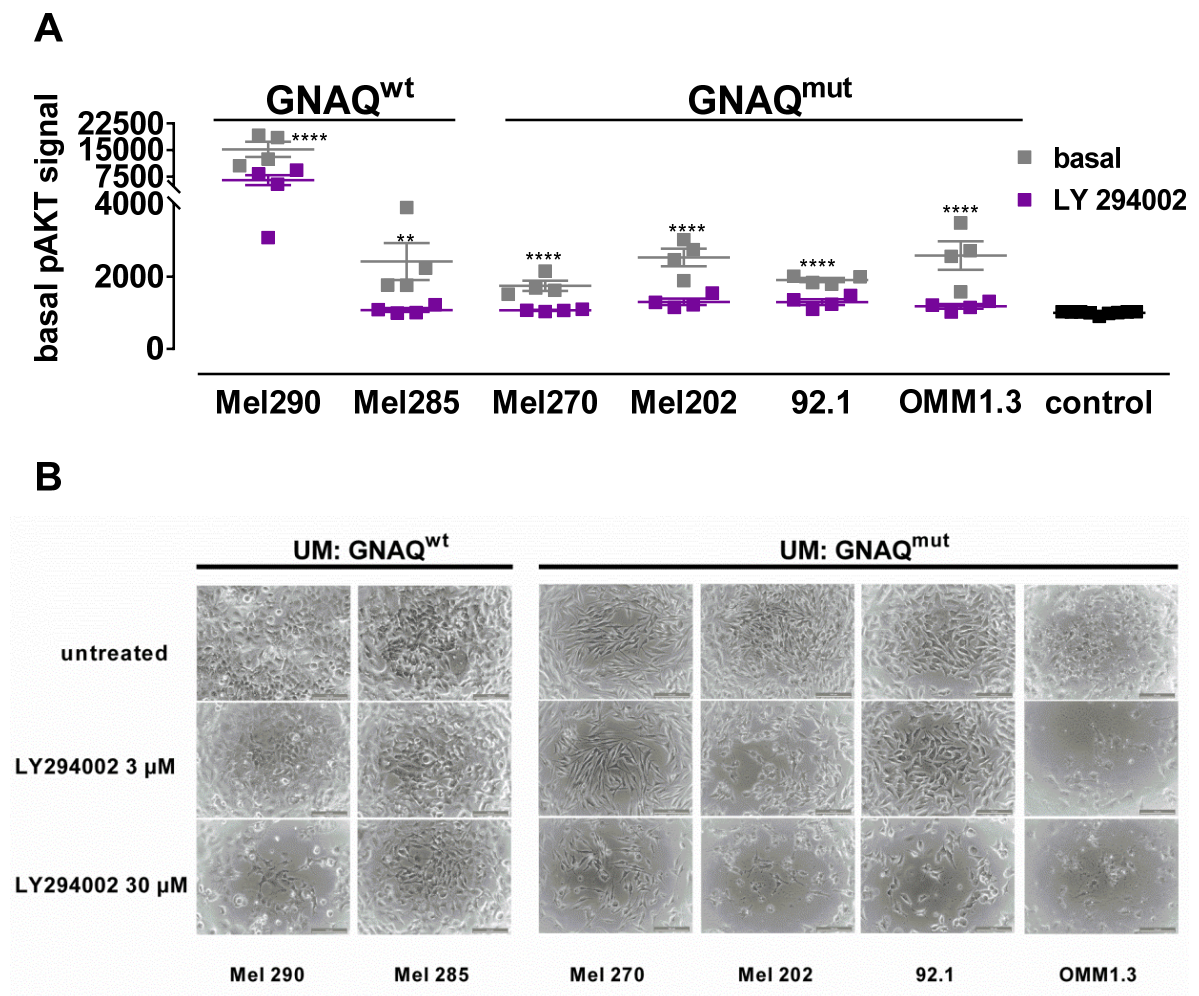


Figure 35: AKT pathway activity in uveal melanoma cells

(A) Intrinsic ATK phosphorylation on Ser473 and after 1 hr incubation of PI3K I LY294002 in 30 μ M or vehicle. Each dot represents the mean of an individual experiment day. The means of n experiments are represented by the horizontal line and the vertical line indicate s.e.m. (B) Bright

Results

field imaging of cells after 72 hrs. of treatment with LY in 3 and 30 μM at cell culture conditions. Cell Images provided by Julian Patt, University of Bonn, lab of Evi Kostenis. Significant effect to neg. control was calculated by using the one-sample t-test.

In the following step, we wanted to investigate Gq involvement in AKT phosphorylation in the different UM cell lines. PI3K inhibitor LY thereby served as a control. LY inhibited the activation of the protein in all UM cell lines within the first 15 min to its fullest extent (**figure 36A**). Thereby, the total protein amount was not decreased (**figure 36B**). Kinetic measurement of AKT dephosphorylation with the Gq Inhibitor showed a depression-maximum after 1 hr incubation in GNAQ mutant cells while wild type GNAQ/GNA11 cells remained completely unaffected over 2 hrs. During the time of kinetic measurement FR did not trigger AKT total protein degradation (**figure 36C/D**). From these observations we concluded that wild type Gq signaling is not involved in this pro-survival pathway in either Mel290 nor in Mel285. The need of longer incubation time for FR in comparison to LY may occur due to the fact, that LY targets the enzyme responsible for AKT phosphorylation directly whereas FR interferes more upstream in the signaling cascade.

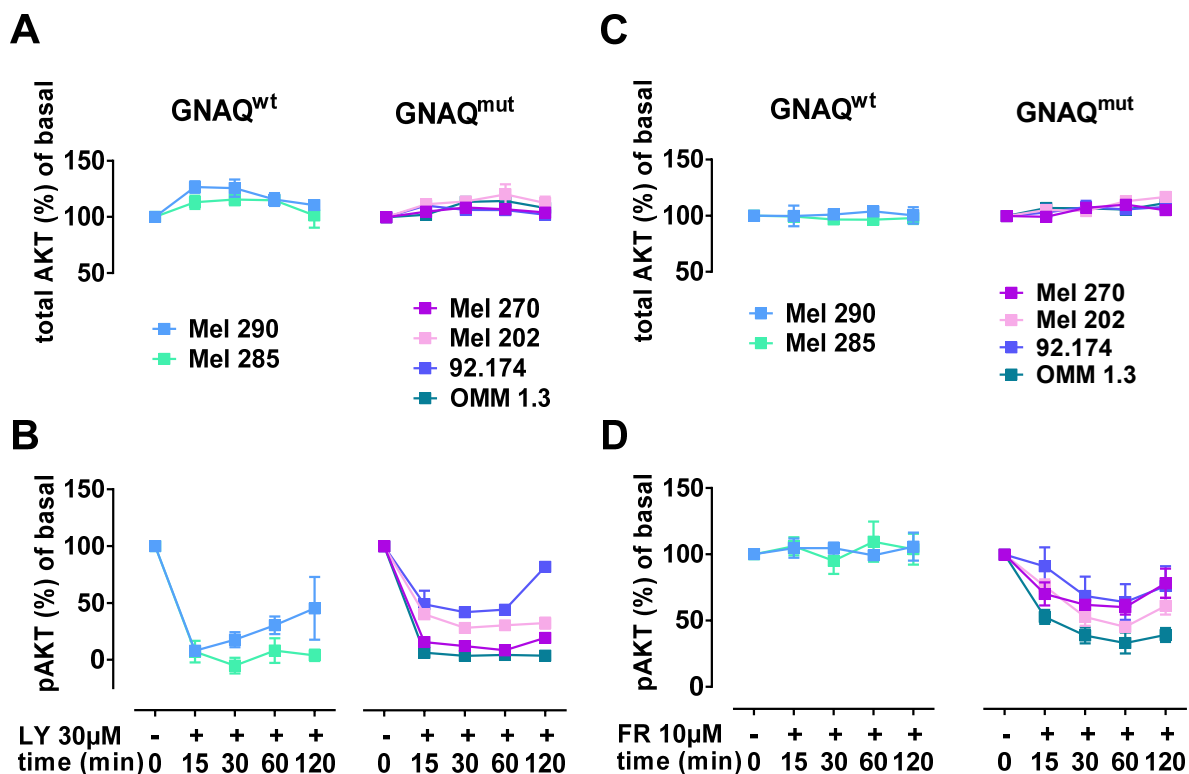


Figure 36: Time dependent inhibition of AKT phosphorylation in UM cells

(A,C) Kinetic measurements of total and (B,D) phosphorylated amount of AKT protein in UM lines in absence and presence of AKT inhibitor LY294002 in 30 μM (A,B) or Gq inhibitor FR (C,D) in 10 μM ($n=4$ pAkt and total $n=3$ AKT). The data was generated with the totalAKT or the pAKT HTRF[®] assay kit from Cisbio. Each dot represents the mean of n experiments with s.e.m..

After determination of the ideal time point, we quantified FR effects on all cell lines. In none of them AKT phosphorylation was exclusively triggered by Gq, as we could detect

pAKT signaling over background after application of high FR concentrations in all cell lines.

Whereas 83% of all UM samples carry an activating mutation in GNAQ/GNA11 metastatic UM samples have even 13% higher statistics for one of these mutations (Krantz et al. 2017). AKT signaling-pathway is associated with higher risk of metastatic diseases. This might hint that oncogenic GNAQ signaling through AKT activation in GNAQ^{mut} cells is most essential for cells with metastatic properties. Notable is, that inhibition of this pathway had the biggest impact on cell proliferation in this cell line. This could be an explanation why the metastatic cell line OMM1.3 responded to Gq inhibition stronger than the primary tumor cell lines.

Interestingly again, sensitivity of inhibition curves were quite similar between those cell lines with the same amino acid substitute Q209P and for those with Q209L, as a plateau is reached approximately between -7.5 and -7 logM for Mel270 and OMM1.3 (both P209) and no plateau was reached for Mel202 and 92.1 (both with L209) up to 10 μ M FR. Variation in amino acid might have an impact on FR inhibition of the AKT pathway (**figure 37A/B**).

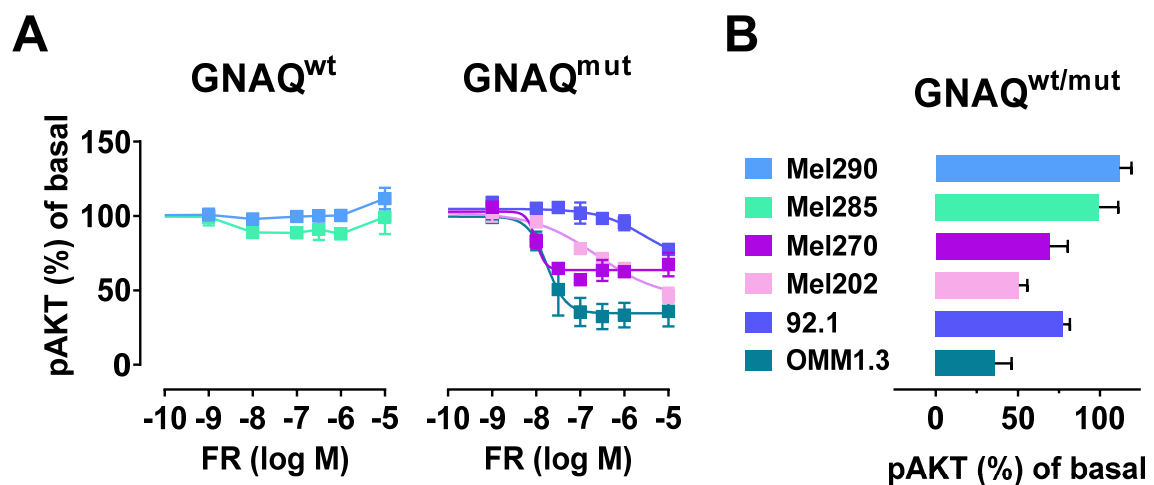


Figure 37: FR inhibits partially AKT phosphorylation in UM cells with mutated GNAQ

(A) FR inhibition potency on AKT phosphorylation after 1 hr of incubation (Mel290, Mel285, Mel202 n=3) (Mel270, OMM1.3 n=4). (B) pAKT inhibition @ 10 μ M FR. Dots and Bars represent the means of n independent experiments, Error bars indicate s.e.m..

4.4.2.4. FR reveals diverse picture of oncogenic Gq involvement in YAP phosphorylation

Nuclear enrichment of the gene expression regulator YAP has been claimed to correlate with mutational status of the Gq protein in human UM tissue samples. Yu et al. could show that YAP is primarily located in the nucleus in UM cell lines with mutated GNAQ genes, while cells with mutated B-Raf were detected with high cytoplasmic protein levels. In line with these findings, they were able to correlate Gq activity with the fraction of non-phosphorylated YAP protein in GNAQ mutated cell lines. By using short hairpin RNA to knockdown Gq they could enhance phosphorylated fraction of YAP in Mel270 and 92.1. Furthermore, knockdown of YAP restricted tumor size in a xenograft model with 92.1 cells injected to nude mice emphasizing the role of YAP in tumor formation (Yu et al. 2014). In parallel Feng et al. obtained similar results. By using OMM1.3 cells in an analog xenograft experiment with shYAP they were able to prove YAP involvement in tumor growth in a similar way, as vehicle treated tumors were significantly larger. In vitro knockdown of either Gq or its downstream effectors Trio, RhoA or ROCK decreased the mRNA expression of the YAP-regulated genes CYR61 and CTGF in OMM1.3 cells massively. Again, these results were pointing out the role of oncogenic Gq as regulator for YAP activity in these cells (Feng et al. 2014).

In agreement with both back-to-back published articles we measured tendency of higher phosphorylated basal YAP in Gq wt cell lines while pYAP was lower in cells with mutated Gq (figure 38).

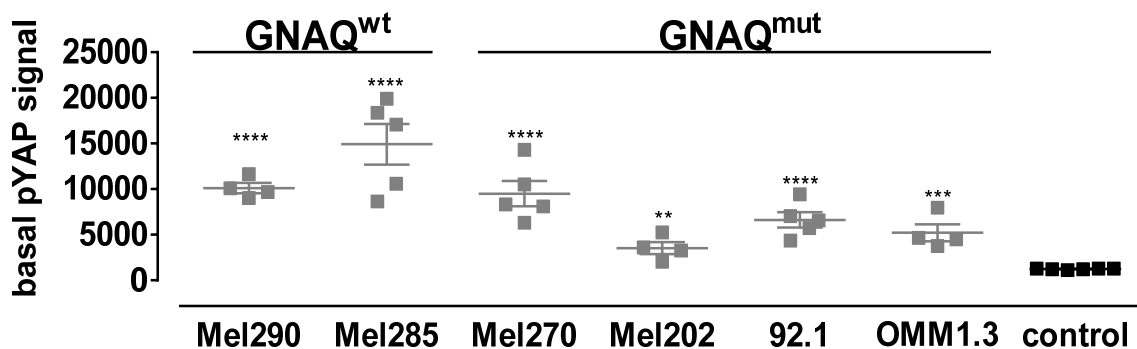


Figure 38: FR inhibits partially AKT phosphorylation in UM cells with mutated GNAQ

Non-stimulated, basal YAP phosphorylation after overnight starvation. Each dot represents an individual sample. Horizontal line indicated the average of n experiment days and vertical line shows s.e.m.. Mel290, Mel202 and OMM1.3 n=4; Mel285, Mel270 and 92.1 n=5. Significant effect to neg. control was calculated by using the one-sample t-test.

Next, we wanted to ascertain if Gq inhibition by FR could elevate the phosphorylated amount of YAP protein and thereby inactivate the protein in the different uveal melanoma cell lines. The first step was to monitor time dependent effects after 15-, 30-, 60- and 120-min incubation with 10 μ M FR under cell culture conditions. Results were only very

moderate but most promising after 1 hr incubation as small increase of pYAP could be noted for 92.1 and OMM1.3. But cell lines Mel290, Mel270 and Mel202 remained completely unaffected (**figure 39**).

Ligand-induced Gs activation has been reported to antagonize Gq effects on YAP activity (Yu et al. 2012). By using forskolin to directly activate the Gs downstream effector adenylyl cyclase Yu et al. could enhance phosphorylated fraction of YAP in the 92.1 cell line. These cells harbor $G\alpha_q^{Q209L}$ version of the $G\alpha_q$ protein. Therefore, we added forskolin as an additional control and repeated the experiment after 1 hr incubation.

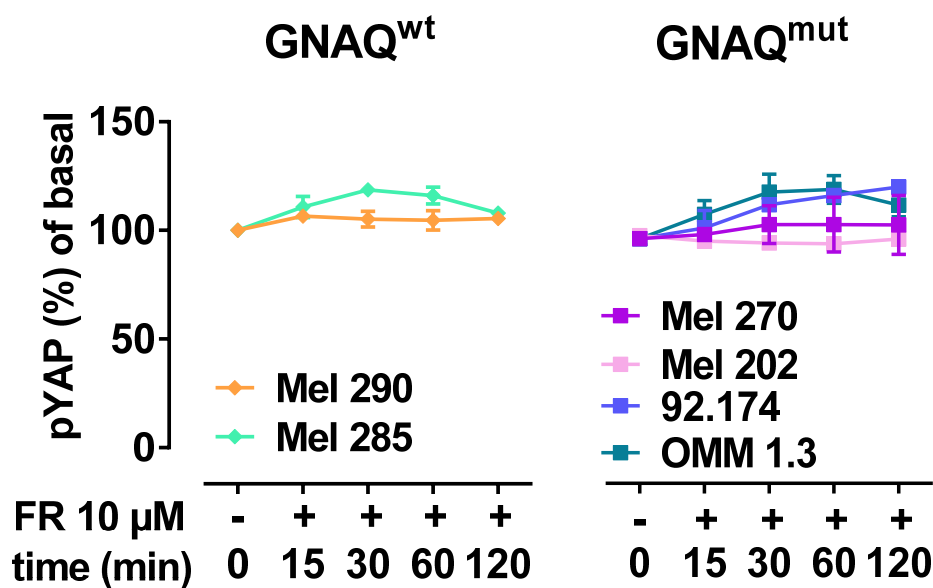


Figure 39: Time dependent FR effect on YAP phosphorylation in diverse UM cell lines.

Phosphorylated fraction of YAP protein in UM lines treated with FR in 10 μ M at the indicated time points. Dots represent the average of 3 independent experiments with s.e.m..

Cytoplasmic localized YAP can be bound by an adaptor protein called 14-3-3. After attachment of the adaptor, degradation by the ubiquitin-proteasome system can occur due to further phosphorylation of the complex. Thus, the amount of total protein might be influenced as well (Zhao et al. 2010). To exclude biased effects because of fluctuation in the total protein amount, we detected both total and phosphorylated YAP protein after 1 hr of treatment with the Gq inhibitor FR and forskolin (**figure 40A/B**).

None of the cell lines showed decreased amount of total protein by Gq inhibition nor Gs activation (**figure 40A**). Additionally, as the quantitative effects of Gq inhibition again were quite small. Significant increase of the phosphorylated protein over 25 % could only be detected in 92.1 and OMM1.3 cells, while Mel285 and Mel202 only showed tendency of elevated fraction of phosphorylated protein that was not significant even after 6 repetitions of the experiment under exact same conditions. Adenylyl cyclase activation and thereby activation of PKA by forskolin was expected to elevate pYAP as it was prior published (Yu et al. 2014). But again, effects of forskolin-induced YAP phosphorylation

Results

were quite weak and could only be shown for Mel285 and 92.1 cells (**figure 40B**). It must be stated that these results are not in any objection with the published article, as 92.1 cell line was used as the only example for an UM cell line with mutated GNAQ to show forskolin mediated effects by Yu et al. (Yu et al. 2014). Very likely AC activation in the other cell lines may not participate in the regulation of the YAP pathway, and a generalization of YAP-pathway involvement cannot be drawn so easily. One can speculate about different expression patterns of the AC itself or its effector proteins in the different cell lines that might explain the varieties in pYAP outcome. Furthermore, YAP is very downstream of Gs or Gq and many other regulators as G12/13 or the Hippo-pathway control its activity (Yu et al. 2012). Thereby the results could be additionally influenced by any compensatory mechanism driven by the other regulators.

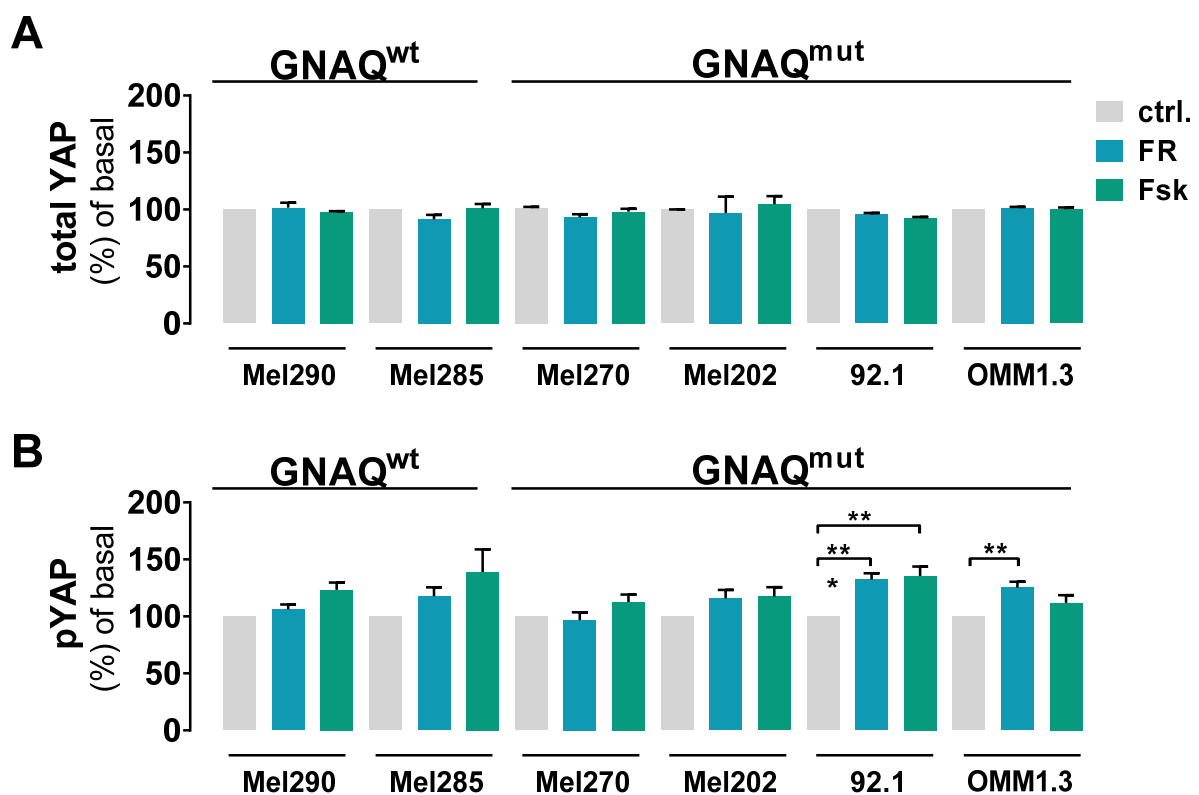


Figure 40: FR induces YAP phosphorylation only in certain UM cells with mutated GNAQ

Total (A) or phosphorylated (B) YAP in UM cell lines after 1 hr of 10 μ M FR or 10 μ M Fsk treatment. Each bar represents the mean of n experiments. Error bar indicate positive s.e.m.s.. Total YAP n=3 of each cell line; phosphor YAP Mel290, Mel285, Mel202 n=6; Mel270 n=7, 92.1 n=7; Omm1.3 n=5. Significant effect to vehicle control was calculated by using the one-sample t-test.

Apart from 92.1 no other cell line showed reliable increased effects on both of these signaling pathways, Gq inhibition and Gs activation. Therefore, we made use of this cell line to indorse, if both pathways would affect YAP phosphorylation simultaneously. Gq and Gs should antagonize effects on YAP phosphorylation. Parallel Gq inhibition and Gs activation consequently should act additively. To proof this concept, we combined Fsk

and FR treatment and determined the outcome head to head with the mono-treatment of both compounds. Indeed, combination of Fsk and FR resulted in approximately 60% enhancement while mono-treatment with either of the compounds elevated basal level about 30% (**figure 41, table 2**).

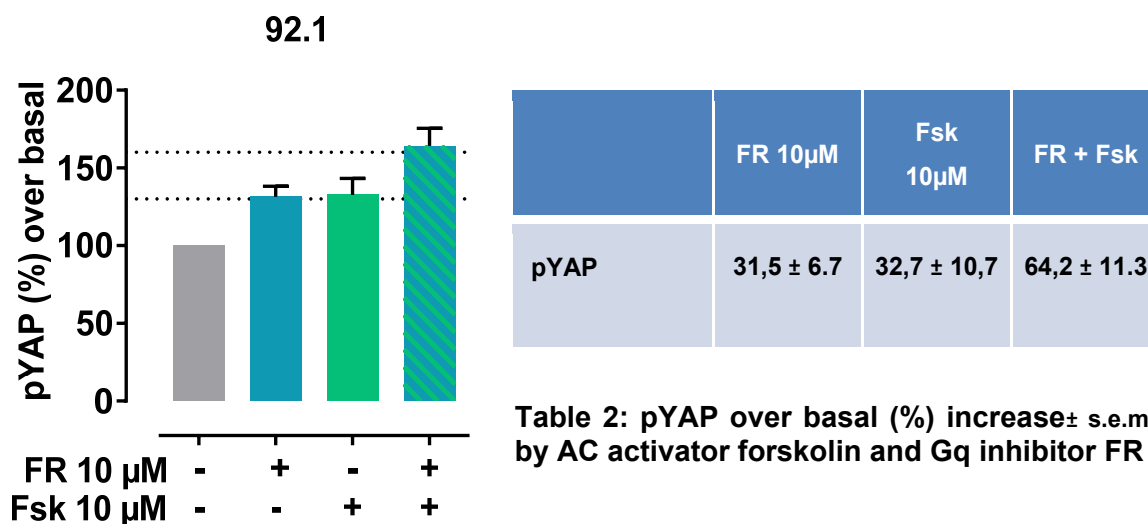


Figure 41: Combined Gq inhibition and Gs activation results in additive YAP phosphorylation in 92.1 cells

(A) Quantification of phosphorylated YAP in 92.1 cells in the density of 75.000 cells/ well in PDL coated 96 well-plates after 1 hr of 10 μ M FR or 10 μ M Fsk or combination treatment. Each bar represents the mean of 5 independent experiments. Error bar indicate positive s.e.m.

4.4.3 Label-free whole cell response of UM cell lines upon FR application

YAP signaling through Gq is suggested to be involved in actin polymerization as UM cells with activating Gq mutation also showed elevated levels of phosphorylated cofilin. Activated cofilin triggers actin polymerization (Feng et al. 2014) and influences cytoskeletal dynamics in this manner. Thus, we wanted to investigate, if we could again take advantage of DMR to detect whole cell response in real time in the different cell lines as response to Gq inhibition.

It has been shown that even for conserved G protein mediated signaling pathways phenotypical cell response might differ between cell lines depending on the cellular background. G protein interaction partners can vary in occurrence of diverse isomers or in stoichiometry in many tissues and therefore also in different cell lines (Schröder et al. 2010). Furthermore, inducing detectable cell shape changes or overall molecular movement within the cell upon signaling deprivation might be harder to achieve as upon signaling activation. Success of signaling disclosure additionally should correlate with the extent of constitutively activity as seen by our prior results. Here HEK293G $\alpha_{q/11}$ -null cells transfected with wt G α_q showed quite high basal activity in IP1 assay (**figure 17**). But this was not high enough as only inhibition of constitutively active G α_q^{Q209L} evoked the negative signaling traces in DMR, while cells transfected with wild type G α_q did not react with detectable mass redistribution upon FR application (**figure 20**).

Results

All UM cell lines responded to 10% FCS, that was used together with forskolin as Gq independent viability control. Interestingly not all cells reacted to the adenylyl cyclase activator. In UM line Mel285 and OMM1.3 cell-response upon forskolin application was silent, while Mel270 and Mel290 only responded with minor signaling. Remarkably, forskolin triggered quite high optical traces in the cell lines Mel202 and 92.1. Correlations between activation of YAP, as downstream of ROCK activation, and morphological changes within the different cell lines are hard to draw. Even though the forskolin signal was strong in YAP phosphorylation and in DMR for 92.1 this was not the case for Mel202. Cellular background seems to be a crucial factor for downstream signaling of activated proteins (**figure 42**).

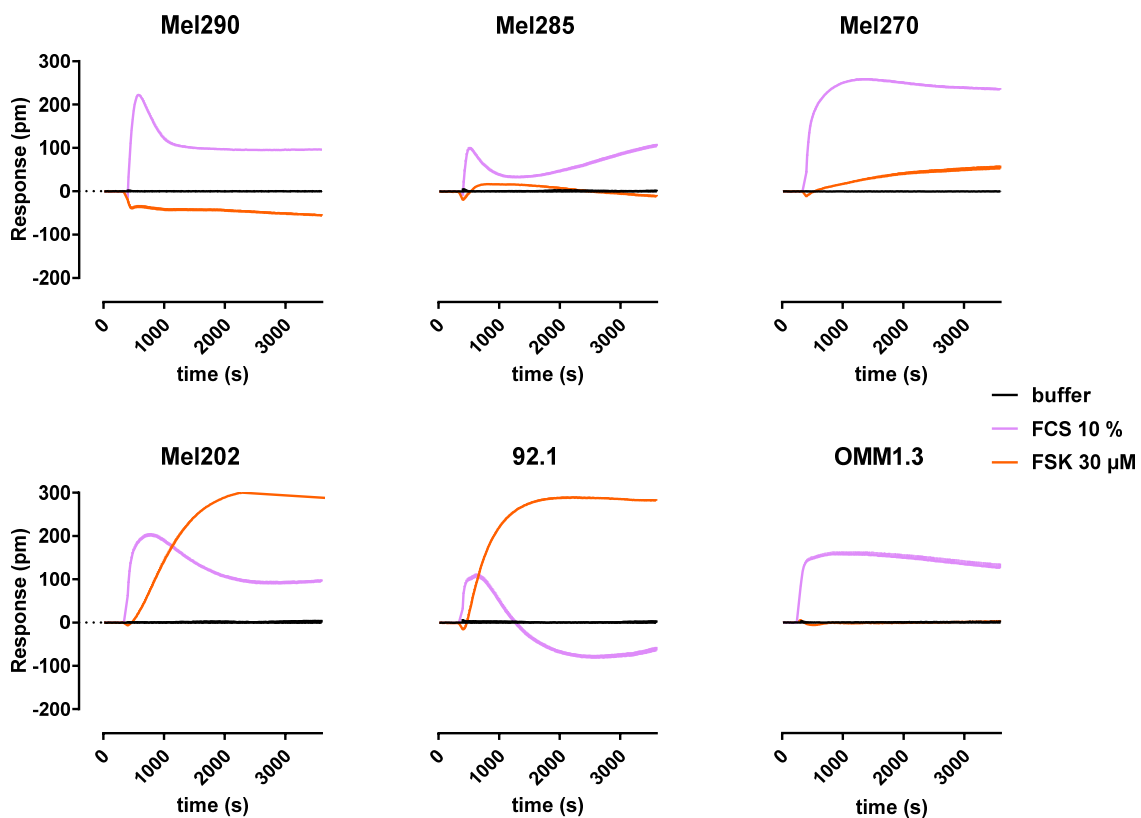


Figure 42: Bio-sensing of cell viability and adenylyl cyclase activation via DMR

DMR profiles of 10% FCS and 30 μM forskolin in UM cell lines. Shown are the representative traces of n independent experiments performed in at least two technical replicates. $n=2$ for OMM1.3 and $n=3$ for all the other cell lines.

DMR furthermore, was not able to expose GTPase-deficient Gq signaling by inverting activity with FR throughout all the UM cell lines. In agreement with the highest Gq tonus in IP1 assay and best response of FR in YAP phosphorylation assay, only 92.1 showed concentration dependent DMR response upon FR addition. Inhibition of Gq signaling in these cells was defined by an initial upwards movement of cellular mass away from the sensor plate creating negative optical traces similar to the traces observed in HEK cells transfected with the $G\alpha_q^{Q209L}$ construct. The early upward oriented movement then was

superimposed with a later signaling event leading to an inversion of the direction (**figure 43**).

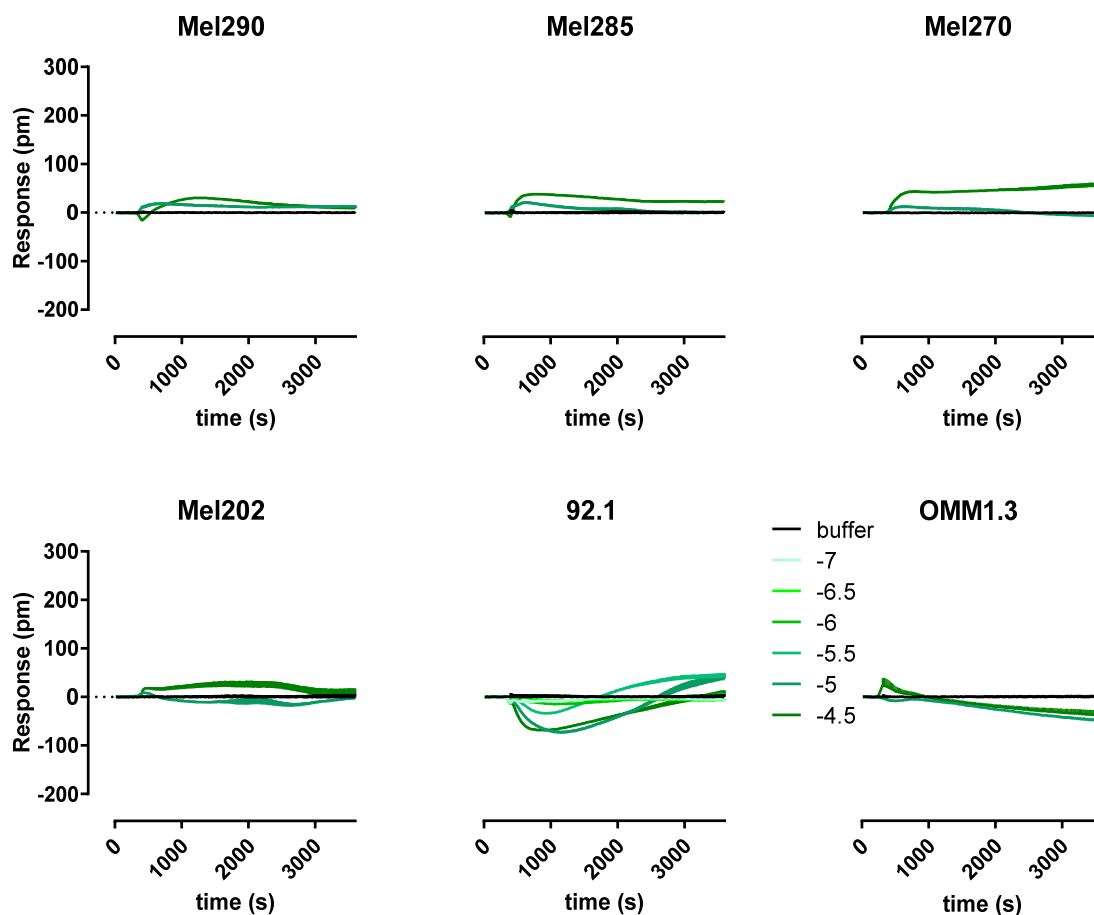


Figure 43: FR-induced DMR profiles in different UM cell lines

DMR profiles of FR in indicated concentrations. Shown are the representative traces of n ($n=2$ for OMM1.3 and $n=3$ for all other cell lines) independent experiments performed in at least two technical replicates.

The preceding negative signals of the 92.1 cell line were used to calculate a dose response curve, where the negative area under the curve for the first 3600s was plotted against enhanced compound concentrations. The pattern of an early negative shift was analog to the observed DMR traces initiated by FR in $G\alpha_q^{Q209L}$ expressing HEK cell system (**figure 44**). Thereby, higher compound amounts perfectly correlated with higher signaling amplitude. But quite high concentrations of FR were needed to induce detectable mass movement within the cell as no clear plateau was reached by using concentrations up to 100 μ M.

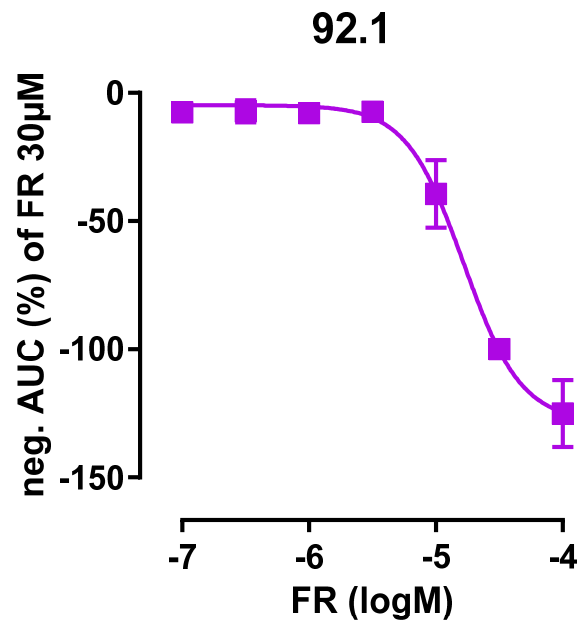


Figure 44: Quantification of FR response in 92.1 cells

Neg. Area under the curve calculated for 1 hr measurement directly after FR application in n=3 independent experiments. Dots represent the mean with s.e.m.

4.4.4. FR inhibits tumor growth of in mice transplanted with UM harboring Gq^{mut}

Throughout this study we were able to demonstrate the inhibition capacity of FR on diverse Gq related pro-survival pathways in uveal melanoma cells expressing the GTPase-deficient mutant Gα_q^{Q209L/P}. However, inhibition of certain pathways driven by an oncogene is not a warrant for tumor suppression as other pathways might take over as a compensatory mechanism upon pathway inhibition. This has been reported in B-Raf mutated UM cells. In a study from 2010, Zhang and co-workers could demonstrate that melanoma cells with mutated B-Raf gained resistance to inhibition by the Raf-inhibitor PLX4720 but were then sensitive towards AKT inhibition (Jiang et al. 2011). Furthermore, a study from 2011 by Steeg and co-workers revealed discrepancies between their in vivo and in vitro observations in regards of drug-generated ERK activation in certain melanoma cells. They suggested that the micro-environment in vivo might be blamed for the different outcomes (Gril et al. 2011). For these reasons, we were eager to verify our in vitro results in an in vivo experiment.

To investigate FR efficiency in vivo, immunodeficient mice underwent transplantation with Mel270 (Q209L) UM cells or A375, a human skin cancer cell line with mutated B-Raf. Tumor treatment for 14 days started when the size of the neo-plasmatic tissue reached 100 mm³. With nearly 90% reduction in ERK signaling, 30% reduction of phosphorylated AKT and over 90% reduction of cell growth in vitro the Mel270 cell line seemed quite promising for these further analyses in vivo. In line with these in vitro observations, tumor size was significantly reduced in the mice already after 10 days of treatment (**figure 45A**). This effect was even more impressive after 14 days of sequential FR application. During these 14 days the size of the tumors was monitored very 3 to 4 days. Tumors in the FR-

group did not gain size throughout the whole treatment-time, whereas the tumors in control group grew progressively. Additionally, histological analysis of sliced neoplastic tissue could remarkably show the growth inhibiting effects of FR on tumor size (**figure 45B**).

In contrast to the UM Mel270 induced tumors, inhibition of Gq did not led to impaired tumor growth in mice injected with CM A375 B-Raf^{V600E} driven cells. Here treatment with FR did not show any advantage compared to vehicle-control application after the same time period. In both treatment groups the tumor started to grow in an exponential manner during the monitored treatment phase (**figure 45C**). This time, the histologically prepared slices of the necrotic tissue showed comparable size and form after the 14 days (**figure 45D**).

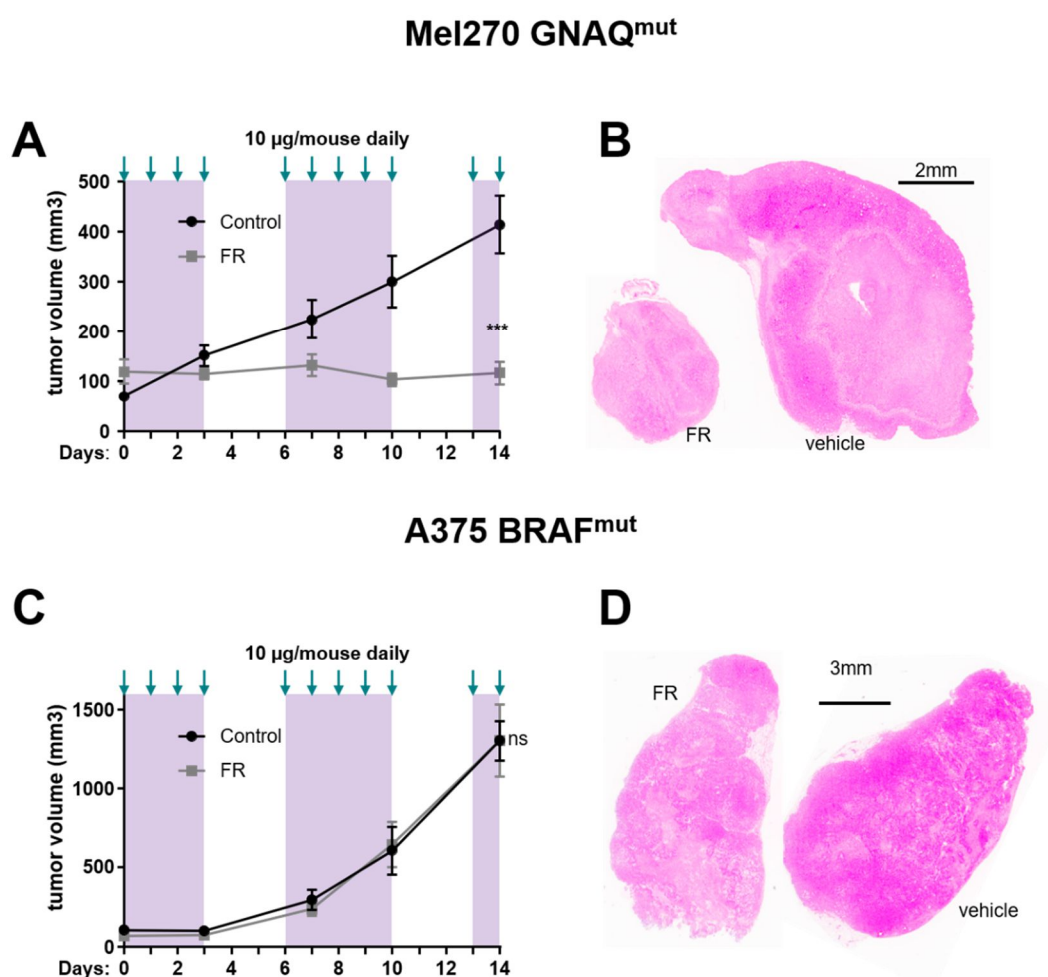


Figure 45: FR inhibits tumor growth in UM with mutated GNAQ

(**A,C**) Effect of FR or vehicle control treatment on tumor growth of UM line Mel270 or skin melanoma A375 in a xenograft mouse model in vivo ($n=5$ animals per control- and FR-treated group for Mel270 and $n=6$ animals in both groups for A375). The tumor size was monitored every 3-4 days during treatment. (**B,D**) Representative histological section of Mel270 and A375 tumor tissue stained with hematoxylin and eosin after the treatment with FR or vehicle. Data points in (**A**) are means of the indicated number of experiments and error bars denote s.e.m. Statistical analysis in was performed with two-way ANOVA. Xenograft experiments were conducted by Xiaodong Feng from Professor Gutkind's lab, San Diego, Californian.

4.5. Comparison of mitogenic-signaling-inhibition potency of the two Gq inhibitors FR and YM

FR900359 is a depsipeptide extracted from *Ardisia crenata*, an ever-green plant coming from East Asia. The non-ribosomal peptide synthase gene cluster produced by symbiotic-bacteria *Candidatus Burkholderia crenata* has recently been decoded (Crüsemann et al. 2018). These bacteria strain is concentrated in the knots of the leaves and has been suggested to produce FR as a defense chemical against insects. The structure of this macrocyclic peptide shows some uncommon characteristics as the cis-configured peptide bond, the two-adjointing ester-bonds as well as some rare N-methylated amino acid building blocks. These features are also found in another structurally very close related depsipeptide YM254890 (Crüsemann et al. 2018), which has been as well characterized as a selective Gq- inhibitor (Nishimura et al. 2010). YM254890 is produced by *Chromobacterium* sp QS3666, a Gram-negative rod with peritrichous flagellae and was first described in 1988/1989 by Fujioka et al (Fujioka et al. 1988).

FR and YM both have been reported to inhibit Gq protein signaling by the same mechanism of action (Schrage et al. 2015; Nishimura et al. 2010) with similar potency (Reher et al. 2018a). Thus, we wanted to know, whether one of the molecules would provide any advantage over the other and therefore, would be more suitable as a base for further drug development. To approach this question, we first looked for general differences like drug vulnerability and binding in HEK293 cells transfected with the target protein, before we moved on and investigated effects in the therapeutically relevant uveal melanoma context.

Both molecules harbor an α,β -unsaturated carbonyl group, which in many cases likes to react with nucleophilic binding partners via Michael-addition and thereby form a covalent binding. But as prior studies have shown for YM as well as for FR the hydrogenated analogs of these molecules still have Gq inhibition potency. This would not be the case, when binding would occur only due to nucleophilic reaction (Schrage et al. 2015; Reher et al. 2018a). Thus, binding mode of the molecules to the interdomain cleft on the $G\alpha_q$ would unlikely be of such covalent nature. However, FR-dependent Gq inhibition has been shown to be resistant to extensive washing in vivo as well as in vitro experiments. Therefore, the binding of FR has been described as pseudo-irreversible (Schrage et al. 2015).

Despite their small structural differences, no major inequalities between mechanistic and functional properties have been described so far for these two resembling molecules. Thus, we reasoned to perform a head-to-head comparison of these two Gq inhibitors.

4.5.1. Drug vulnerability comparison between FR and YM in wash-out experiments

Results from cell-based wash-out experiments can provide information about the drug-target engagement and therefore gives information about drug vulnerability (Tonge 2017). First in line wash-out experiments indeed showed significant but not major alteration regarding stickiness of the molecules. The attempt to remove both Gq-inhibitors from the system completely seemed un-achievable, as initial state could not be restored by washing. But YM was marginally more likely to come off the Gq protein as slightly enhanced IP1 accumulation was detectable for high ligand concentrations after excessive washing of the cell suspension for 6 times with puffer (**figure 46**).

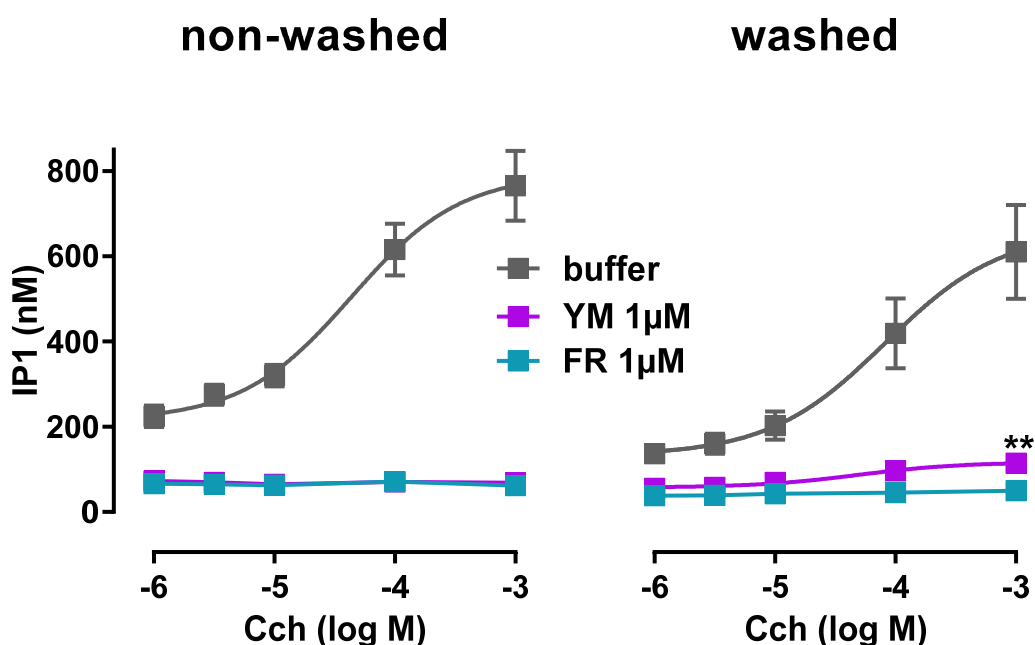


Figure 46: Vulnerability comparison between FR and YM.

IP1 accumulation in HEK293 cells (40 kc/w) after 1 hr of preincubation with FR or YM followed by 30 min stimulation with CCh in indicated concentrations. Cells were either washed or not washed before CCh stimulation. Washing included 6 repetitions of removing buffer and resuspension in buffer inserted with 5 min Incubation time. Dots represent the mean with s.e.m. of $n = 3$ independent experiments. Significance was calculated by unpaired t-test between washed probes of YM and FR incubated cells treated with 1 mM CCh.

By this means, the vulnerability of FR seems to be lower to some extent, as recovery from drug treatment seems to be harder to achieve compared to YM. This result might indicate that binding mode and maybe binding kinetic of these both molecules may not be 100% identical.

4.5.2. Evaluation of FR and YM binding addressed by site-directed mutagenesis

To evaluate alterations between the binding modes of the depsipeptides, we mutated residues critical for YM binding as described in the PNAS paper from 2010, where Nishimura et al. were able to co-crystallize the depsipeptide with the G_{i/q} chimeric-heterotrimer. Amino acids I56, K57 and I190 from the GTPase domain together with V184 and T186 from linker 2 have been shown to form a hydrophobic pocket. This pocket can be utilized by the phenyl-group of YM and create hydrophobic interactions to hold the molecule tight. Substitution of the non-polar isoleucine on position 190 with the polar amino acids arginine led to a dramatic decrease in YM potency (Nishimura et al. 2010).

When we tried to reproduce the results obtained by these loss-of-function mutations, we were quite surprised. These described key mutations, which decreased pIC₅₀ of YM in the depicted SRE assay from the Nishimura paper by more than the factor 700 (I190N), in our hands shifted the YM inhibition curves in IP1 assay only 0.5 log M to the right which equalize approximately a factor of 3. Even more surprising was the fact, that this mutation did not affect FR's inhibition properties in IP1 accumulation assay in any significant way. Similar results were gained for the residues V184 and R60 (**figure 47A**). Arginine on position 60 with its guanidino group was reported to form hydrogen bonds with the macrocycle and so to ensure its V-shape within the binding pocket.

As our outcome differed from these published data, we wanted to exclude an assay biased effect. To clarify discrepancies, we chose carbachol evoked ERK activation as a G_q readout. ERK is known to be very close upstream to SRE activation in the signaling cascade (Gutkind 2000), and therefore amplified effects between these two read-outs should be smaller. Indeed, shifts in inhibition curves in pERK assay were improved compared to the shifts obtained in IP1-assay. But still loss-of-function was not as dramatic as it was described in the PNAS paper. In accordance with Nishimura I190N and R60K ended in loss of YM potency the same extent. Moreover, IC₅₀ shifts were again smaller for FR (**figure 47B**).

Overall, these results emphasize the importance of both likers for binding of the depsipeptides. Observations of FR to be more resistance to mutation-induced potency-decrease could be reconfirmed as alterations of the inhibition curves were only minor compared with the smaller but structurally similar macrocycle YM in IP1 as well as in pERK assay.

To make more valid conclusions, we chose to make further mutations on position I190, as it seemed to be one of the most critical residues for binding of the depsipeptides. This position I190 is only conserved between G α_q , G α_{11} and G α_{14} . The other two members of the G_q family G α_{15} and G α_{16} harbor an arginine on this residue. Notable is that G15 and G16 are not sensitive to neither FR nor YM (Nishimura et al. 2010; Schrage et al. 2015) .

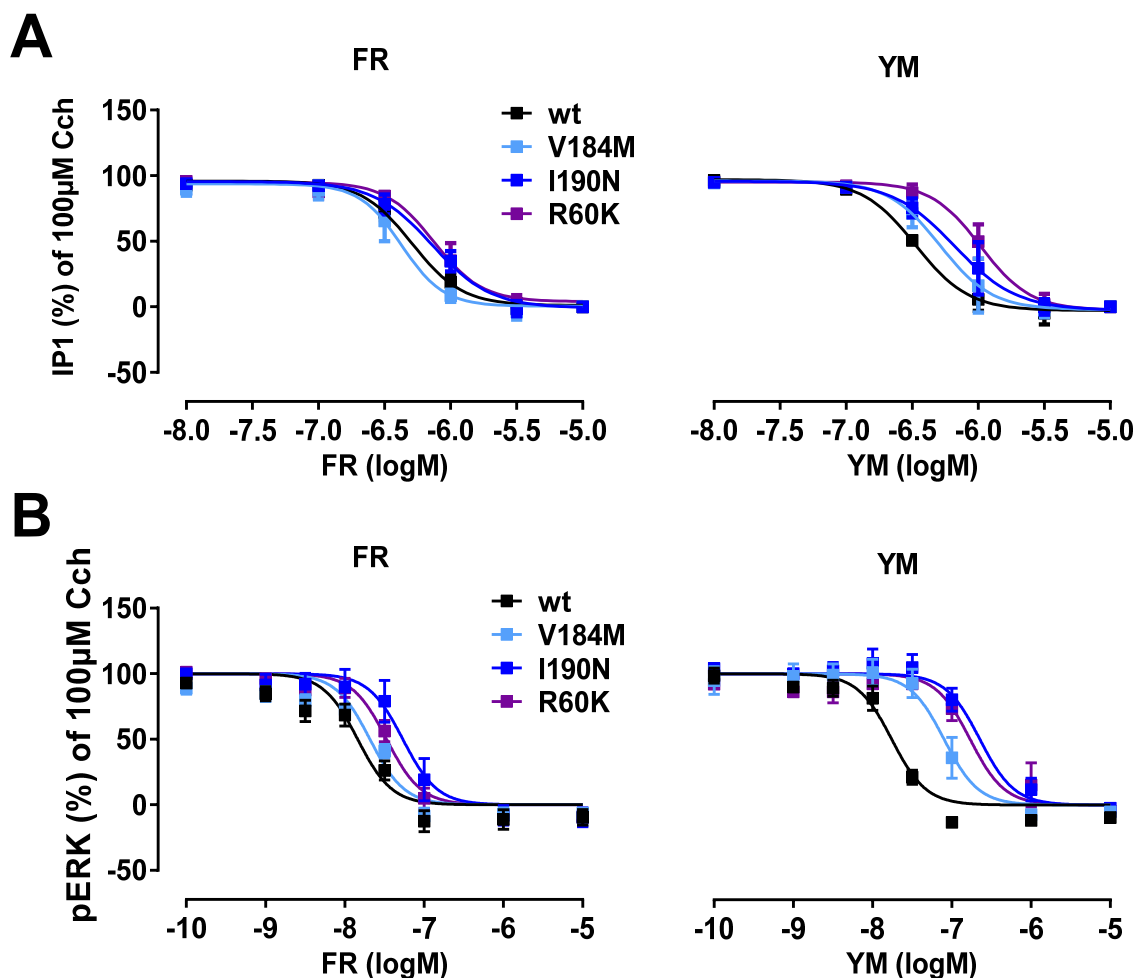


Figure 47: Loss-of-function mutagenesis study for FR and YM.

(A) IP1 accumulation in HEK293G α_{q11} -null cells 48 hrs post transfection with the indicated constructs. 60,000 cells/well were preincubation with FR or YM in the stated concentration and followed by 30 min stimulation with CCh in 100 μ M. (B) ERK phosphorylation of 60,000 cells/well in 96-well plate format. Adherent cells were preincubation with FR or YM in the stated concentration and followed by 3 min CCh stimulation in 100 μ M. (A,B) Dots represent the mean with s.e.m. of n = 3 independent experiments.

Here we replaced isoleucine 190 with two additional amino acids to the already represented arginine. We chose phenylalanine and the sterically very big tryptophan. YM as mentioned, responded to switches between non-polar (I) to polar (N) amino acids more dramatically than FR. However, loss in potency could not only be explained by change in polarity nor by pure satirical properties. Arginine compared to Isoleucine shows higher polarity but additionally its average volume and accessible surface area is also larger (Trinquier and Sanejouand 1998; Miller et al. 1987). However, both macrocycles were more sensitive to substitution trough phenylalanine, that has much more similarities regarding polarity and size to isoleucine than arginine (**table 3**) (Darby and Creighton 1993).

Results

When we replaced the amino acid with the sterically big tryptophan, both molecules seem have a hard time to stick to the protein. Most likely, the hydrophobic binding pocket does not offer enough space for tryptophan to fit in. In this case, the obtained losses in potencies were most severe. Conclusively, the succession of IC₅₀ shifts increased neither synergistically to the size of the amino acid that replaced isoleucine nor to the accessible amino acid surface area. However, by modulation of this position greater loss of inhibition was achieved for the smaller depsipeptide YM (**figure 50A**).

Amino acid	Average volume (Å ³)	Accessible surface area (Å ²)	aa polarity ranking
isoleucine	169	140	1
asparagine	225	196	15
phenylalanine	203	157	2
tryptophan	240	217	6

Table 3: Comparison of amino acid properties. Data collected from Trinquier and Sanejouand 1998 *Protein Engineering, Design and Selection*, Miller et al.1987 *J Mol Biol*.

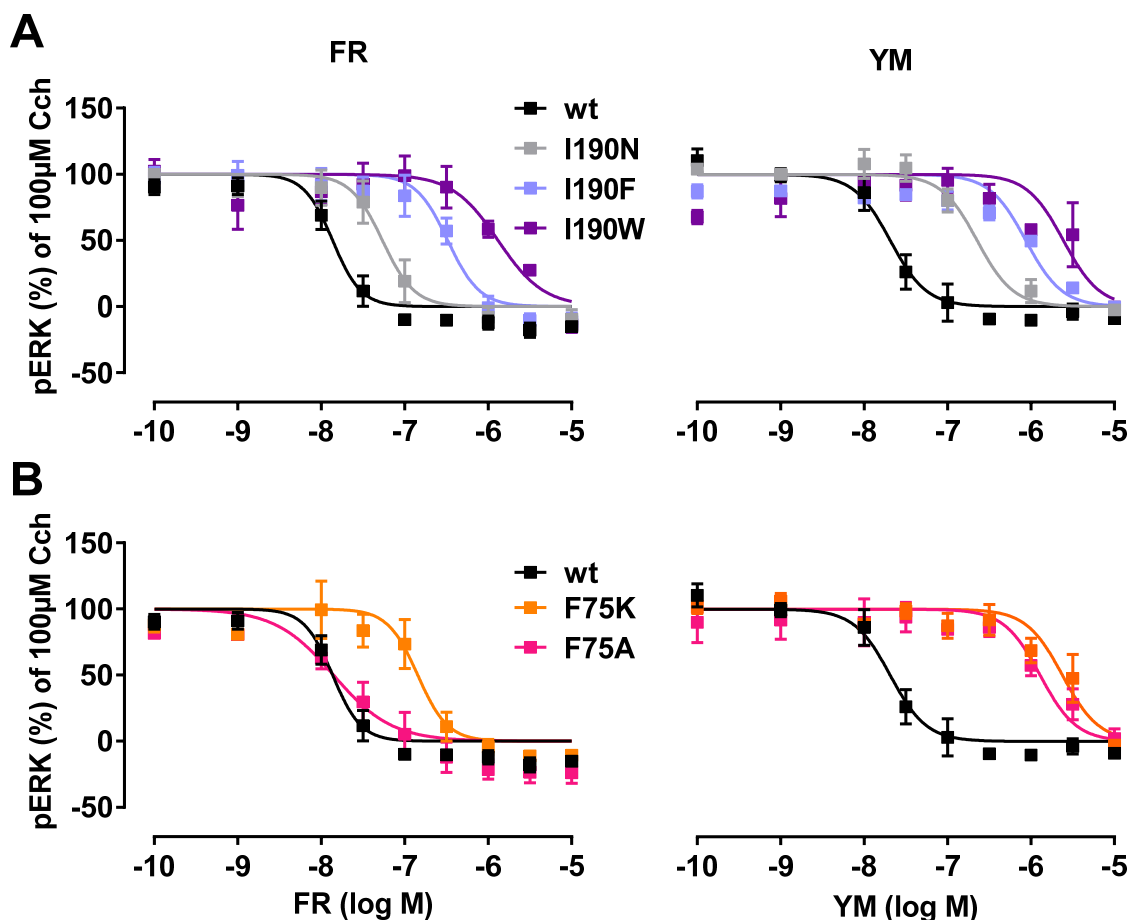


Figure 48: Loss-of-function mutagenesis study for FR and YM.

(A,B) ERK phosphorylation of 40,000 HEK293G α_{q11}^{-null} -cells 48 hrs post transfection with Gq constructs with single amino acid replacement on position I190 (A) or F75 (B) in 96-well plate format. Adherent cells were preincubated either with FR or YM in the stated concentration and followed by 3 min CCh stimulation in 100 μ M before lysis and detection. Dots represents the means of at least n=3 experiments with s.e.m..

A position that is conserved in the whole Gq family is the phenyl on position 75 on the αA helical domain. Nevertheless, Nishimura et al. observed that this residue is also crucial for binding (Nishimura et al. 2010). In the head-to-head comparison between FR and YM we could further confirm the importance of this contact point for both molecules. But again, loss of function was greater for YM as it was for FR. Even more surprising was that by modifying F75 to alanine we only decreased YM's potency whereas potency of FR remained fully.

All in all, we looked for two positions on linker 1 (R60, F75) and for two (I190, V184) on linker 2. For all of the generated G α_q^{mut} constructs, it was easier to detect loss of function for YM (**table 4**). The three additional methyl groups might help FR to anchor tighter to the binding cleft. Only substitution with the big amino acid tryptophan led to similar functional reduction of the two macrocycles.

Results

Gα _q mutant	FR pIC ₅₀ ± s.e.m.	YM pIC ₅₀ ± s.e.m.	FR ΔpIC ₅₀ to wt	YM ΔpIC ₅₀ to wt
Wt	7.86 ± 0.05	7.68 ± 0.07	0	0
R60K	7.47 ± 0.05	6.77 ± 0.09	-0.58	-0.91
V184M	7.68 ± 0.06	7.10 ± 0.07	-0.18	-0.58
I190N	7.27 ± 0.08	6.64 ± 0.10	-0.59	-1.04
I190F	6.48 ± 0.07	6.06 ± 0.08	-1.38	-1.62
I190W	5.88 ± 0.11	5.60 ± 0.11	-1.98	-2.08
F75A	7.85 ± 0.08	5.89 ± 0.08	-0.01	-1.79
F75K	6.84 ± 0.14	5.62 ± 0.07	-1.02	-2.06

Table 4: Comparison of pIC₅₀ values and the ΔpIC₅₀ (log M) shift from wt for FR and YM obtained in pERK assay

4.5.3 FR suppresses cancer hallmarks of uveal melanoma cells with mutated Gq protein with higher potency than YM

Based on this mutagenesis study and the knowledge we gained from the wash-out experiments, we draw the conclusion that both molecules indeed seem to have different binding properties. Next, we wanted to evaluate these differences in a biological relevant matter. Thus, we examine both molecules in parallel in the therapeutically relevant system, the uveal melanoma cell lines.

4.5.3.1 FR superpowers YM in proliferation assay with uveal melanoma cells

To assess the question whether one of the molecules could be superior to the other respectively to the inhibition of cancer relevant out-comes, we first looked for effects on proliferation activity as one of the major cancer hall marks. It was not surprising that Gq inhibition with YM failed to inhibit proliferation in wild type GNAQ/GNA11 UM cell lines Mel290 and Mel285, as we already knew from the FR-data that Gq does not play any proliferative role in these cells. In line with the results observed by Gq inhibition with FR in GNAQ mutant cell lines Mel270, Mel202 and 92.1 also Gq inhibition with YM led to a decreased proliferation activity. Thereby, efficacy regarding cell growth blockade was comparable between the two depsipeptides but potency did differ to some extent. FR was clearly more vigorous in Mel270 and 92.1 cells (**figure 49**).

These results were somehow unexpected as ERK inhibition with FR or YM in the HEK cells system was comparable after 1 hr of incubation for wild type Gq (**table 5**). To elucidate the ostensible discrepancies, we looked for the two factors that were different between these two experiments regarding the assay conditions. On the one hand inhibition of activation of the proliferation driving protein ERK were prior measured on wild

type Gq. GTPase-deficient Gq might have different properties towards binding of YM than it has for FR. On the other hand, time could also be a crucial factor. Proliferation assays were performed after 72 hrs of incubation whereas pERK assays were measured after 1 hr incubation.

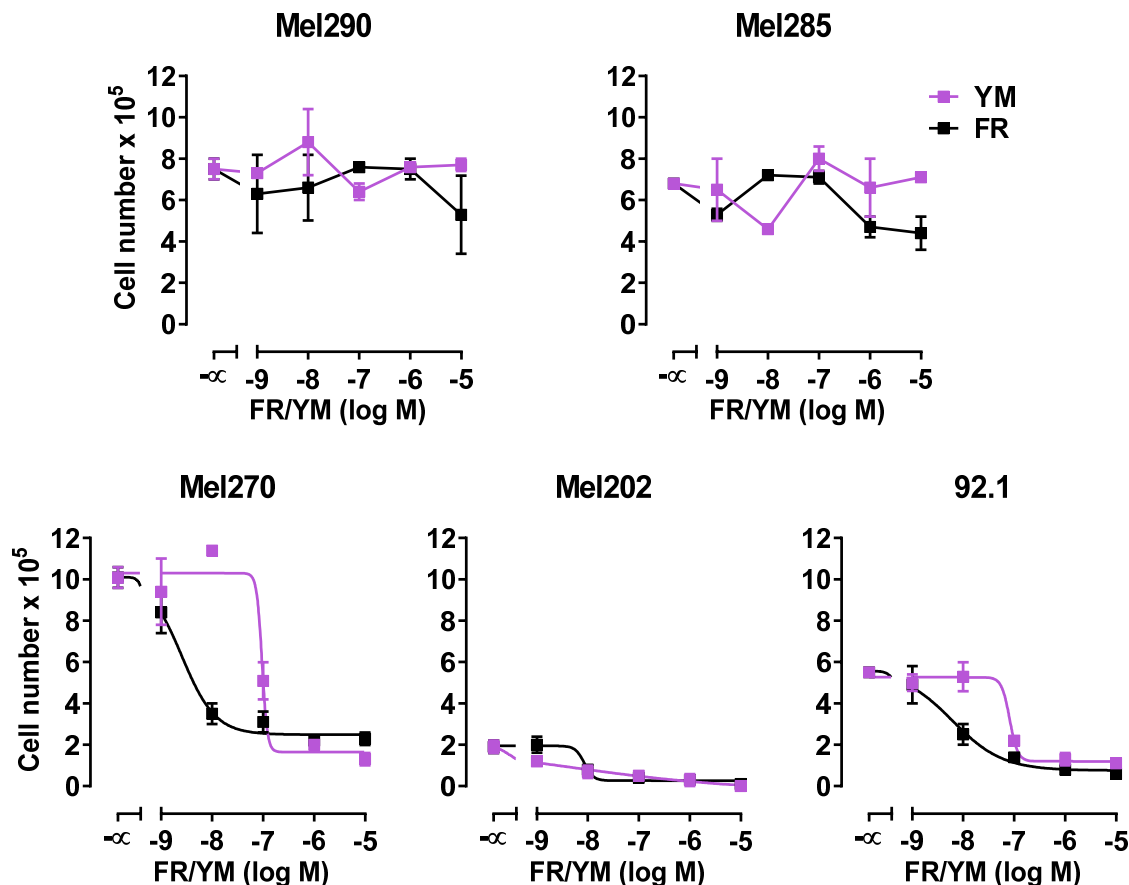


Figure 49: FR and YM in head-to-head comparisons in cell proliferation assay with UM cell lines.

Effect of FR or YM in the indicated concentrations on cell growth of GNAQ/GNA11 wild type and mutant UM lines in culture after 72 hrs of compound exposure. All dots represent the means of $n=2$ independent experiments with s.e.m.

4.5.3.2 Extended application time reveals inequality between macrocycles

To address both variables in one assay, we choose to perform ERK assays on Mel270. This cell line harbors the oncogenic $G\alpha_q^{Q209P}$ protein and was very sensitive regarding inhibition of the MAPK pathway by FR. We redesigned the ERK assay to include variations of incubation time as an additional factor. In our new experiment we measured ERK phosphorylation after 1 hr and 24 hrs of FR or YM application (**figure 50**). Pharmacological inhibition of Gq with either FR or YM resulted in equipotent ERK dephosphorylation after 1 hr of incubation with IC₅₀ values in the nanomolar range.

Results

However, when we looked for inhibition capability after 24 hrs YM had lost around 7-fold of its activity whereas FR potency remained stable (**table 5**).

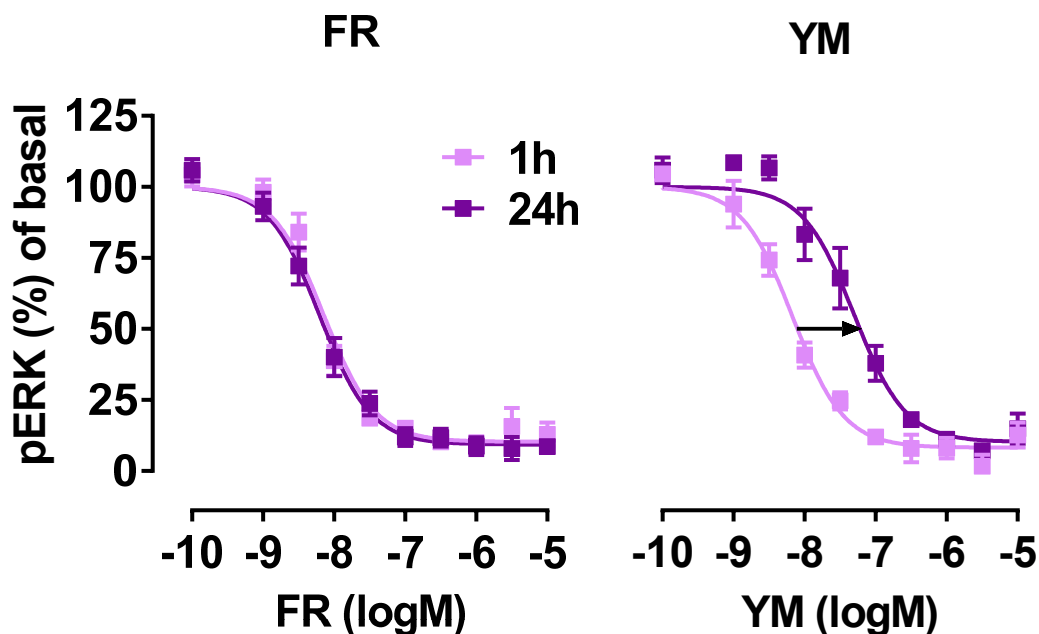


Figure 50: Time-dependent ERK inhibition of FR and YM on Mel270

Quantification of pERK inhibition potency by FR and YM after 1 hr and 24 hrs of incubation under cell culture conditions. All dots represent the means of n=3 independent experiments with s.e.m.

Incubation (h)	FR $pIC_{50} \pm$ s.e.m.	YM $pIC_{50} \pm$ s.e.m.	FR ΔpIC_{50} to 1 hr	YM ΔpIC_{50} to 1 hr
1 hr	8.15 ± 0.06	8.17 ± 0.06	0	0
24 hrs	8.20 ± 0.05	7.30 ± 0.08	0.05	-0.87

Table 5: Comparison of pIC_{50} values and the ΔpIC_{50} shift from 1 hr to 24 hrs for FR and YM obtained in pERK assay in Mel 270 UM cells (figure)

As in the HEK293 cells expressing wild type Gq, also the UM cells expressing GTPase-deficient Gq, did not show different results of ERK inhibition between YM and FR after 1 hr of incubation. But differences in inhibition potency seem to arise by longer incubation.

To further assess incubation time as critical factor, we went on to determine the inhibition capacity of the two Gq-inhibitors on cell proliferation after an even longer period of incubation. For that reason, we decided to look for cell proliferation in Mel270 cells after 4 days and 6 days after FR/YM treatment and evaluated the outcome by bright field microscopy.

After 4 days, cells treated with YM were less dense compared to control, but the cell shape seemed to be unaffected. Proliferation inhibiting effect of YM seems to weaken over time, as cells density was increased on day 6 nearly to the density of vehicle treated cells. Compared to this FR effect on cell growth was more dramatic. On the day 4, only few cells survived the presence of the slightly larger Gq-inhibitor FR. Cells were detached from the plate and normal elongated cell shape was not found under treatment conditions. Furthermore, recovery in the FR-treated wells was not as fast as in the wells treated with YM. At day 6 the cells still were detached from the plates and cell shape was not retained. Anti-proliferative assets of FR were tremendously compared to YM's (**figure 51**).

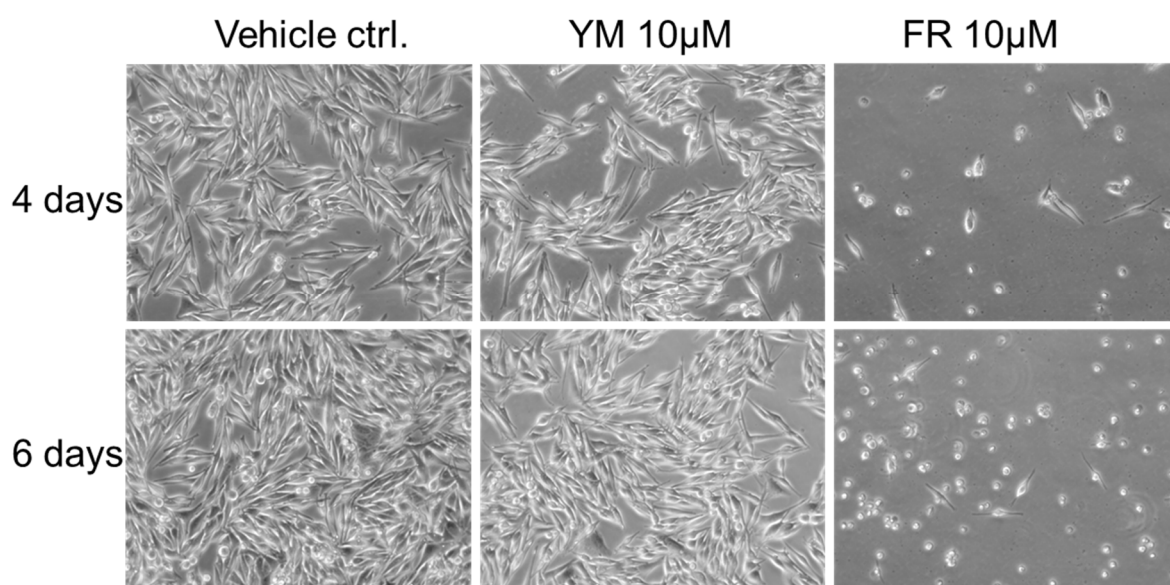


Figure 51: Time-dependent ERK inhibition of FR and YM on Mel270

Representative bright field imaging of n=3 independent experiments of Mel270 cells 4 and 6 days after FR/YM application in 10 µM

Results

Discussion

Tumorigenesis arises from a complex network of pathogenic events, whereby the cell attains properties of self-sufficiency in regards of growth control and proliferation. Cancer cells learn to support themselves with oxygen and initiate angiogenesis to nourish their excessive cell dividing. Leading cause for cell transition to gain these abilities are often the accumulation of genetic alterations of gain-of-function oncogenes and loss-of-function tumor suppressors (Luo et al. 2009).

Deep sequencing has revealed gain-of-function genes GNAQ^{Q209L/P} and GNA11^{Q209L/P} as frequent mutations in uveal melanoma (van Raamsdonk et al. 2009). Gq and G11 proteins are known to promote many pro-survival and pro-metastatic pathways through multiple effector proteins (Feng et al. 2014; Mizuno and Itoh 2009). Furthermore, mutation in one of this genes is believed to be an early event in this type of melanoma formation and suspected to be a crucial initiator for its development (Onken et al. 2008). Hence, targeting the oncogenic Gq and G11 protein should be a reasonable approach to prevent tumorigenesis.

Two macrocyclic depsipeptides produced by bacteria (YM) or by symbiotic bacteria (FR) were described to specifically target this subfamily of G proteins. Under non-pathological circumstances the protein is activated by different GPCRs that are regulated by diverse extracellular stimuli. Receptor activation leads to the exchange of the attached guanine nucleotide from GDP to GTP (Oldham and Hamm 2008).

The two depsipeptides bind into a certain cleft of the protein and prevent the activation by preventing GDP dissociation (Schrage et al. 2015; Nishimura et al. 2010). The gain-of-function mutation of the protein affects the GTPase domain. This domain functions as an autocatalytic switch-off that allows the protein to return from the active GTP- to the inactive GDP-bound form. The hotspot mutation on Q209 to either proline or lysin has been reported to trap the protein in permanent on-set and inhibition by preventing its activation was thought to be less effective (Nishimura et al. 2010; Kimple et al. 2011). Contradictory to this hypothesis, in the framework of this study, we were able to demonstrate that inhibition of oncogenic Gq signaling indeed is a rational approach and can be achieved with the guanine dissociation inhibitor FR.

In a mouse melanoma cell line with mutated G11 protein we could show that FR is able to diminish multiple hallmarks of cancer cells. By using genome edited HEK293 cells we further were able to proof direct interaction of the oncogenic Gq demonstrated in a site-directed mutagenesis approach to target the molecules binding side. Moreover, we were able to understand the mode of FR action on the GTPase-deficient mutant as we could show a GDP-bound fraction of the GTPase-deficient mutant by using label-free dynamic mass redistribution technology. Additionally, we evaluated different uveal melanoma cell lines with either mutated or wild type Gq protein for their sensitivity for FR. Thereby, we established Gq-inhibition as a reasonable strategy to prevent cancer development and could introduce FR as a lead compound suitable for further therapeutic development. In different head-to-head comparisons between the two known Gq inhibitors FR and YM, we could demonstrate the long-term superiority of FR in regard of cell proliferation and mitogenic signaling inhibition. These findings will be discussed here in detail.

5.1. FR as a tool to blunt mitogenic signaling in CM

Malignant cutaneous melanoma is characterized to go through distinct phases to develop its malignant pathogenesis. Unrestricted cell growth is followed by invasive behavior and development of metastasis. The most prominent genetic alteration in CM is an amino acid substitution in the B-Raf protein where valine is exchanged to glutamic acid at position 600 in amino acid secondary structure (Gray-Schopfer et al. 2005). Raf and also the common mutated Ras belong to the p21-GTPase proteins. Like G proteins, they are activated by the exchange of GDP to GTP and are switched off by their GTPase domain (Platz et al. 2008). HcMel12 mouse melanoma cell line is derived from the genetically engineered mouse model of Hgf-Cdk^{R24C} mice. These mice form spontaneous melanomas. Thereby, the malignancy proceeds from melanocytic naevi that form in most cases metastasis (Landsberg et al. 2010). Unlike the most malignant melanoma types that carry mutations in the Raf-Ras-MEK-ERK signaling pathway (Platz et al. 2008) these cells harbor a gain-of-function mutation in GNA11 gene at the hot-spot residue Q209 (Kilian et al. 2016). Reports about GNAQ/11 mutations in cutaneous melanoma are rare (Patel et al. 2016) but they are frequently found in intradermal melanocyte neoplasms as blue naevi (van Raamsdonk et al. 2009).

Here we could show that inhibition of GTPase-deficient G11 with FR initiated HcMel12 cells to differentiate, as we observed morphological cell changes and increase of the differentiation marker gp100. Most likely, differentiation in these cells is under the control of ERK promotion as MEK-i trametinib also enhanced this marker. In line with this observation, we detected elevated levels of phosphorylated ERK protein. Furthermore, we could show that G11 indeed showed constitutive activity by measuring its canonical effector activity. In terms of ERK activation this constitutive activity of G11 protein could be identified as the promoter for this signaling pathway by using our Gq/11 inhibitor. FR inhibited phosphorylation and thereby activation of ERK in a nanomolar concentration range.

As described by literature, IP1 accumulation as direct readout for PLC activation conducted by the G α_{11}^{Q209L} protein was not sensitive towards the inhibitor. However, our experiments showed that FR clearly is not an ERK inhibitor by nature as it blocks this signaling cascade only in case it is under the control of Gq/G11 proteins as the initial drivers. This was concluded as in melanoma cells with additionally B-Raf mutation FR had only minor effect whereas after incubation with the B-Raf inhibitor vemurafenib, almost no phosphorylated ERK was detected.

Vemurafenib is the first selective B-Raf^{V600E} inhibitor and has been successfully used for many years for the treatment of cutaneous melanoma in patients with mutated B-Raf profile. In patients vemurafenib has been shown to be well tolerated and more importantly has been proofed to increase survival by 11.5 month (Czirbesz et al. 2017). As over-activity of Gq apparently participate in activation of the same pathway as B-Raf, it is very reasonable transfer the concept of direct targeting of the oncogene to melanoma cells with gain-of-function GNAQ/11.

5.2. Mechanistic insights into inhibition of the GTPase-deficient mutant

As mutations in GNA11/GNAQ are mutually exclusive, one of these proteins always exists in the non-mutated state in our melanoma cell context. Thus, we wanted to proof interaction of the molecule FR with the GTPase-deficient mutant in a clear Gq/11^{-null} background by using genome edited HEK cells. Hereby, we were able to show FR interaction with both, unmutated and mutated Gq in different assays. Clear proof for the specificity of the results, by this means that the obtained inhibition effects were related to FR interaction with the respectively Gq-analog was achieved, as the vector-transfected cells lacking the target constructs remained unresponsive.

To enlighten the question of the mechanical aspect behind the unexpected inhibition capability of FR on the GTPase-deficient mutant, we attempted two different approaches. First, we validated the existence of a receptor inducible fraction of the GTPase-deficient Gq protein by using DMR. Here, ligand-induced traces of the G α_q^{Q209L} transfected cells clearly indicated a GDP-bound fraction. This could be confirmed by immunoprecipitation of GDP-bound G α_q^{Q209L} . Second, we were able to show direct binding of FR for G α_q^{wt} and G α_q^{Q209L} by loss-of-function mutagenesis studies.

The direct interaction was shown by mutation of the binding site. Hereby, we were able to show loss of FR function by modulating amino acids in the binding pocket on the G α -subunit. The binding surface inherit the two linkers that connect the helical and the GTPase domain (Nishimura et al. 2010). Thereby, linker 2 is one of the flexible regions that are known to undergo conformational changes upon GDP/GTP-exchange (Oldham and Hamm 2008). This binding site is described to be only targetable in the GDP-bound state (Nishimura et al. 2010). Therefore, we suggest that FR functions as a GDI on the GTPase-deficient mutant.

A premise for G α_q^{Q209L} to exist in the GDP-bound state is that its deficient GTPase function might not be as compromised as often reported (Kimple et al. 2011; Patel and Tall 2016). Undeniably, many reports about G α and the catalytic function of its GTPase-deficient analogs exist and are selectively discussed here:

Even though, it has been shown, that G α proteins with analog mutation to the Q61L of Ras protein have a slower GTPase catalytic kinetic, the function of the GTPase domain was shown not completely dysfunctional. The Gs analog G α_s^{Q227L} still remained approximately 1/30 of the wild type GTPase activity (Scheschonka et al. 2000). However, the GTPase properties obtained by Gs and Gi might not be completely transferrable to Gq because wild type hydrolysis of Gq ($k_{cat-GTPase}=0.7 \text{ min}^{-1}$) differs to Gi/Gs ($k_{cat-GTPase}=0.3 \text{ min}^{-1}$) (Berstein et al. 1992). Indeed, the less GTPase-impaired GqR193C was shown to lose $k_{cat-GTPase}$ (140-fold) activity even more than the described loss for G α_s^{Q227L} . In a study to investigate PLC β_1 GAP on Gq, $k_{cat-GTPase}$ of this mutant was reduced 140 fold compared to wild type but GAP activity of PLC β_1 was still functional (Chidiac and Ross 1999).

Additionally to PLC β also regulators of G protein signaling are known to function as GAP on Gq proteins and thereby enhancing their GTPase function (Kimple et al. 2011). GAP activity of e.g. RGS proteins may not be only limited to wild type proteins. Scheschonka

et al. could demonstrate in a study published in 2000 that both RGS2 and RGS3 were able to block CREB reporter gene activity provoked by either $G\alpha_q^{Q209L}/G\alpha_{11}^{Q209L}$ in HEK293 cells and $G\alpha_q^{Q209L}$ -induced IP3 production. Thereby, it remained unclear if inhibition was due to GAP activity or inhibition of protein-protein interaction (Scheschonka et al. 2000).

As we could see by our results, $G\alpha_q^{Q209L}$ is not entirely trapped in the GTP-bound active state. This is further supported by studies showing functional but compromised GTPase function of these proteins. According to these assumptions, FR should be able to bind to the GDP-bound- $G\alpha_q^{Q209L}$ as heterotrimer, because the mutation does not alter the binding pocket. By locking the $G\alpha_q^{Q209L}$ in the GDP-heterotrimeric complex, FR, as a GDI, could accomplish inhibition of the interaction of the protein with its effectors.

5.3. Hypothesis of FR pathway-selectivity

The term 'guanine dissociation inhibitor' (GDI) was first used for a small protein that was found to bind to the Ras-like protein Rab. GDI binding to Rab traps the protein in its inactive state and prevent over all Rab-signaling (Pfeffer et al. 1995). This term was adopted for YM, the first described cell permeable inhibitor that selectively targets $G\alpha_{q/11/14}$ proteins. Like the original termed GDI implicates, YM enables its target protein to be activated by GTP-GDP exchange (Nishimura et al. 2010). Later in 2015 FR that is structurally closely related to YM, was also categorized as a GDI (Schrage et al. 2015).

According to the GDI mechanism of action, FR and YM should be able to switch of all downstream effectors that require former activation by GDP-GTP exchange as schemed in **figure 53** for wild type Gq. This should also account for the GTPase-deficient mutant if FR and YM retained their mode of action as prior suggested. Contradictory, YM failed to inhibit IP1 accumulation in HEK cells transfected with the constitutively active G11-construct $G\alpha_{11}^{Q209L}$ while inhibition of $G\alpha_{11}^{wt}$ was perfectly succeeded (Xiong et al. 2016). Similar observation was gained by this study. IP1 accumulation of Hcme12 cells ($G\alpha_{11}^{Q209L}$) was achieved up to very high amounts of the inhibitor but surprisingly mitogenic signaling was diminished in nanomolar concentrations. This behavior was not restricted to the G11 subfamily as in our hands intrinsic IP1 tonus of HEK cells transfected with the $G\alpha_q^{Q209L}$ construct displayed the same insensitivity towards FR. In this present study we introduced a hypothesis that might explain differential behavior of the canonical Gq/11 effector PLC β towards inhibition by FR.

PLC β is not only an effector, but it also displays an important role as a switch of regulator (Litosch 2013). Thereby, its GAP activity controls the durance of PLC β and $G\alpha_{q/11}$ interaction, whose dynamic-fashion is described as kiss-and-run reaction (Adjobo-Hermans et al. 2013; Harden et al. 2011).

Interestingly, PLC β signaling of the GTPase-deficient mutant $G\alpha_q^{R183C}$ was perfectly inhibited with FR, pointing out that slower GTPase activity cannot solely explain the inability of FR towards PLC signaling driven by $G\alpha_q^{Q209L}$. A notable difference besides the $k_{cat-GTPase}$ between the two Gq analogs R183C and Q209L is their sensitivity towards GAP activity of the PLC. While $G\alpha_q^{R183C}$ -sensitivity towards PLC β -GAP is still functional, GAP activity towards $G\alpha_q^{Q209L}$ is greatly impaired (Chidiac and Ross 1999; Berman et al. 1996).

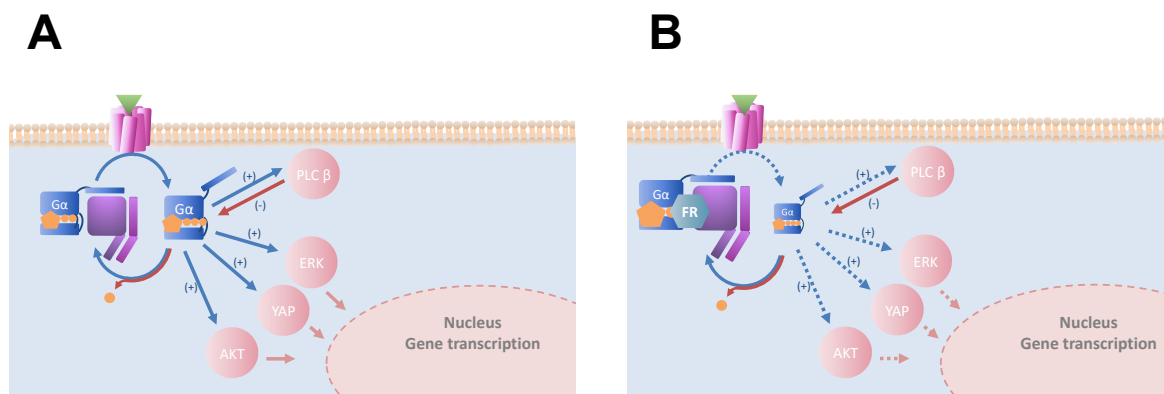


Figure 52: FR as a GDI on wild type Gq

Scheme (A) shows the activation circle of Gq proteins in the attendance of a ligand. Here the G protein circles between an activated and inactivated state. In the monomeric active state, the Gq protein interacts with different effectors. Thereby some effectors like PLC additionally serves as GTPase-accelerating proteins and favors the transition of GTP-bound α -monomer to the inactive GTP-bound heterotrimer. (B) Shows the inhibition of this signaling circle by FR. FR binds to the α -subunit in the heteromeric state and prevents the activation by the receptor.

FRET experiments further demonstrated that although FR inhibits the on-kinetic of PLC β and G α_q^{wt} it did not affect protein-protein-interaction of PLC β with G α_q^{Q209L} . One possible explanation could be reasoned by the mechanism of PLC β -GAP activity that is thought to release the G α -subunit from PLC β . The crystal structure of the PLC β_3 isoform, which was also used to conduct our FRET experiments, together with G α_q , published by Waldo et al. in 2010, emphasized two amino acids in the monomeric G α_q to be important for GAP activity. They could demonstrate that Q209 and R260 of G α_q interact with the EF3 and 4 hands of the PLC β . One of these GAP relevant residues is mutated in the GTPase-deficient mutant. GAP activity of PLC β presumably cannot enfold its proper function when glutamine is substituted with leucine in the G α -subunit (Waldo et al. 2010). In this case PLC β and G α might be clued together and FR is unable to drive its GDI activity. Consequently, all other interactions might be perfectly inhibited while FR is unable to separate the two effectors completely as schemed in **figure 53**. But here we would have to assume that ERK is not downstream of PLC β as often stated (Gutkind 2000).

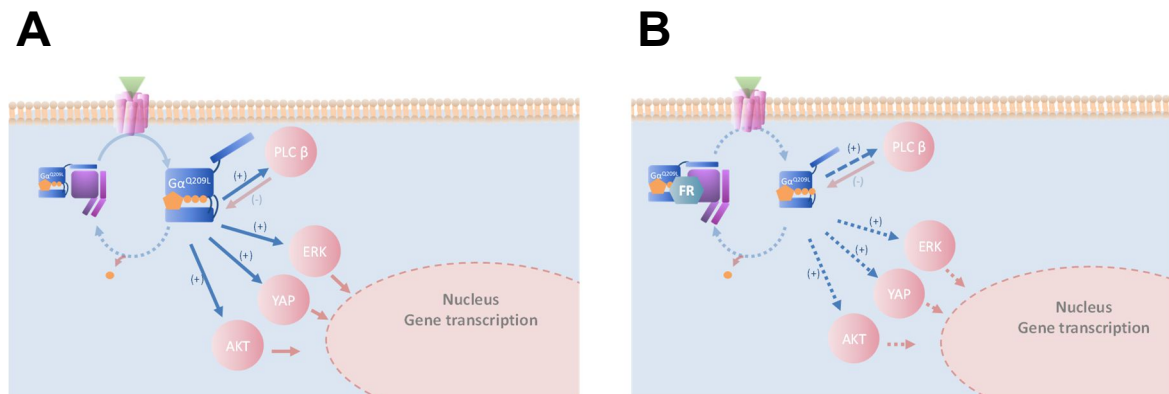


Figure 53: Mechanism of biased inhibition of the GTPase-deficient Gq

Scheme of **(A)** pathway activation of the oncogenic Gq protein: The protein exists in both forms, the active and the inactive form. Due to the GTPase malfunction it becomes independent of the receptor (the receptor is shown as transparent pictogram). In the monomeric active state, the oncogenic Gq protein interacts with different effectors. **(B)** By applying FR to the system, the protein accumulates in the inactive state. However, as PLC is unable to function as a GAP protein, the interaction of the two proteins cannot be disrupted easily. Therefore, the inhibition of other effectors, that are not permanently attached to the active protein, is more effective by FR.

5.4. Targeting the oncogenic protein in a therapeutically relevant system

The mutations affecting the GTPase domain of the Gα_q or Gα₁₁ protein occurs most prominently in the context of uveal melanoma. Therefore, we were eager to test the inhibitor in cell lines originated from the tumor tissue of UM patients and to demonstrate its antiproliferative effects in vitro and in vivo in this highly relevant system.

Interestingly, despite the presents of GTPase-deficient Gq UM cell lines Mel270, Mel202 and OMM1.3 showed quite low intrinsic IP1 tonus, implementing a minor role for PLCβ in these cells. Surprisingly, this low activity was perfectly sensitive towards inhibition with FR. This might hint that inability towards PLCβ inhibition can be overcome dependent on the cellular protein composition. Also, variety in PLCβ-GAP activity between different isoforms might play a role, as UM cells are known to harbor the quite uncommon PLCβ4 that is exclusively found in the eye and in brain tissue (RebeCChi and Pentyla 2000). Only the 92.1 cell line, harboring the oncogenic Gα_q^{Q209L}, had a quite high IP1 tonus but also showed decreased FR sensitivity compared to the other GNAQ^{mut}-cell lines.

However, more importantly, we could show that different mitogenic pathways such as ERK and AKT but also partially YAP could be blunt in UM cell lines with mutated Gq. In contrast, wild type Gq did not display the role of an oncogene in the uveal melanoma cell lines Mel290 and Mel285. Here the pro-survival pathways were unresponsive to FR inhibition.

Different reports exist, which highlight the importance of different pathways for proliferation in uveal melanoma with mutated GNAQ (van Raamsdonk et al. 2009; Yu et al. 2014; Zuidervaart et al. 2005).

By western blot analysis Zuidervaart et al. could determine ERK activity in all UM cell lines (Zuidervaart et al. 2005), which were also used in this present study. Thereby, we were able to confirm their findings, that wild typ GNAQ cell lines Mel290 and Mel285 displayed highest ERK activity. But by using FR we were further able to show, that ERK phosphorylation in these cells was not driven by the GNAQ. Despite of the high ERK tonus, which was sensitive to MEKi by trametinib, proliferation was not entirely ERK dependent, as cells remained approximately 50% of their viability after 72 hrs of MEKi. ERK phosphorylation of GNAQ^{mut} cell lines was sensitive to FR whereby the efficacy and potency did differ throughout cell lines. While ERK activation was almost completely sensitive in OMM1.3, Mel202 and Mel270 cells towards FR, ERK inhibition was not completely driven by GNAQ in 92.1. After FR treatment still 30% of phosphorylated ERK was detectable. Even though ERK was GNAQ dependent and additionally completely sensitive towards MEK-inhibition by trametinib in OMM1.3 cells, the MEK inhibitor underlay the direct targeting of the oncogene in the proliferation assays. This might indicate that more than one Gq- effector participate in proliferation promoting mechanisms.

Although ERK inhibition with the MEK inhibitor trametinib seemed to stop proliferation in most cell lines with mutated GNAQ in this study expect the above mentioned OMM1.3 line, these inhibitors could not proof their benefit in clinical studies. In a randomized phase 2 trial in 2013 beneficial effect of the MEK1&2 inhibitor selumetinib as adjuvant therapy to the chemotherapeutic agents temozolomide or dacarbazine was investigated on 120 patients with metastatic melanoma. In this study selumetinib improved the progression-free survival from 7 to almost 16 weeks but did not enhance the over-all survival rate. Patients with mutations in GNAQ/GNA11 genes seemed to have greater progression-free survival, but this was not valid, as most of the tumors were only scanned for mutations of exon 5 of GNAQ/GNA11, whereby exon 4 in most cases was not analyzed (Carvajal et al. 2014). SUMIT, the follow-up randomized multicenter phase 3 study was assed to clarify the safety and efficacy of this treatment. Patients again treated with either dacarbazine in combination with selumetinib or placebo, but this time progression-free survival was not improved. Interestingly the frequency of GNAQ and GNA11 mutations were extremely high with 94 % of the investigated samples (Carvajal et al. 2018). The poor clinical results are not restricted to selumetinib exclusively as a MEK-i. In a prior phase 1 first-in-human study trametinib was tested in patients with different kinds of melanoma cells regarding its safety, efficacy but also variability in response in correlation with genetic alterations. For the 16 UM patients included in the study, stable disease as best result, was only achieved 4 patients (Falchook et al. 2012).

One reason for limited success might be that in cells with mutated GNAQ/GNA11 gene other pathways might take the proliferating activity over when MEK is inhibited. By using microarray gene expression analysis Ambrosini et al. could identify a pattern of genes that are regulated by MEK in UM cell lines with mutated GNAQ. OMM1.3, 92.1 and Mel270 cells showed significant increase of a gene called c-Jun after treatment with selumetinib. Remarkably this was not the case in melanoma lines with mutated B-Raf. C-Jun is part of the activator protein 1 transcription complex that regulates different signaling events leading e.g. to cell proliferation or apoptosis. As knockdown of this gene in the mentioned UM cells increased anti-proliferative effects of the MEK-i Ambrosini et al. propose that this might be a mechanism for the cells to gain drug resistance. By this means, selumetinib treatment of GNAQ^{mut} cells upregulate a gene that impairs the

Discussion

function of the drug itself. The authors of this study suspect PKC, as another GNAQ downstream effector, to be involved in this negative feedback mechanism (Ambrosini et al. 2012). Supporting this theory, Babchia and co-workers could observe synergistic effects by combining PKCi and MEKi in vitro in UM cells with mutated GNAQ (Chen et al. 2014).

Similar results were obtained by inhibition of the AKT signaling additionally to the ERK signaling. AKT seems to participate in cell proliferation of UM cells, as the combination of the two inhibitors were twice as effective than mono-treatment (Babchia et al. 2010) (Khalili et al. 2012; Ambrosini et al. 2013). While Kahlili et al. did not see any correlation of GNAQ signaling to activate AKT in 92.1 cell line Ambrosini could show reduced fraction of the phosphorylated protein by using GNAQ siRNA in multiple cell lines including the 92.1 cells. By using FR in our study for the different cell lines, we were able to support the observation of Ambrosini et al. and proof GNAQ involvement in this pathway for Mel270, Mel202, OMM1.3 and 92.1. But it must be stated that 92.1 was among the GNAQ^{mut} cell lines the one that was least affected by FR. Only 25% of the pAKT fraction was blunt by Gq inhibition, whereas 60% inhibition was gained in OMM1.3 cells. Again, these results are pointing out that proliferation promoting signaling through GNAQ in UM cells cannot be easily stereotyped by the mutational status of the Gq protein. Activation of the different pro-survival pathways by the oncogenic GNAQ seems to be quite diverse dependent on the cellular background. Hence, it is much more reasonable to directly target the oncogene instead of the downstream effectors that seem to have variations in each cell system.

Beside AKT and ERK signaling another pathway regulated by the oncogenic Gq has become more prominent as cell press released two big articles back to back published in cancer cell in 2014. These two articles were centered around the role of the transcriptional co-activator YAP in uveal melanoma harboring the GTPase-deficient mutant Gq. GNAQ signaling could be identified as perpetrator for YAP activation as knockdown of GNAQ by shRNA/siRNA in 92.1, Mel270 (Yu et al. 2014) and in the metastatic-prone UM cell lines OMM1.3 (Feng et al. 2014) inverted YAP localization or phosphorylation state. Further knockdown approaches to elucidate GNAQ signaling pathway to YAP activation revealed a new pathway involving TRIO, Rho and Rac.

In line with their observation we found higher pYAP (inactive YAP) in cells expressing wild type Gq, but inhibition of Gq in our study with FR only led to significant increase of phosphorylated fractions of the protein in two cell lines, the 92.1 and OMM1.3. This was quite disappointing as the YAP pathway was claimed to take over the key player role over MAPK activation overall in these genotyped cells. But interestingly the cell lines, which were picked for the two articles, were the same showing also response to FR, despite of Mel270. YAP signaling might play a role only in certain cell lines, here again cellular background seems to be a key factor.

To sum up, constitutive active Gq drives different effectors within the uveal melanoma cells activating proliferation and migration. Due to the unavailability of direct Gq-inhibitors so far, many attempts have been drawn to target the downstream effectors alone or in combination (Krantz et al. 2017). As signaling of these downstream proteins may vary dependent on the micro-environment within different cells this approach might fail in some cases. Additionally, other GNAQ pathways might take over the role of the targeted

survival pathway leading to drug-resistance (Ambrosini et al. 2012). In the frame of this study we could show, how FR is able to simultaneously switch off multiple GNAQ driven pro-survival pathways, and therefore we propose this as a new model to treat uveal melanoma patients with mutated Gq.

This allegation was furthermore sustained by a xenograft mouse model, where FR could significantly reduce tumor size of Mel270 cells after 14 days of treatment but was without effect in mice injected with tumor cells with B-Raf mutation.

5.5. macrocyclic Gq-i FR and its analog YM in comparison

FR and YM are two structurally very close related molecules that are reported to have similar inhibition potencies with a slight prevalence for FR (Xiong et al. 2016). In our hands the two molecules showed no difference in potency after one-hour incubation. Superiority of FR was first revealed after extend washing and a longer period of incubation time. These results indicated different drug vulnerability for YM and FR.

In drug discovery IC_{50} values are often used as numeric scale to evaluate lead compounds but this number cannot fully account for the real drug-target engagement that might be important in regards of the drug use (Tonge 2017).

5.6. Limitation of this study and future perspectives

Despite the study could show remarkable results of FR in vitro and in vivo on the constitutively active Gq, several questions remained for further investigations.

In cutaneous melanoma we were able to show biased inhibition of mitogenic ERK signaling over canonical PLC. This was surprising as Gq mediated activation of ERK is believed to be PLC related (Gutkind 2000; Rozengurt 2007). By taking advance of different inhibitors of Gq downstream effectors we could show that ERK activation seems to be regulated by multiple proteins like PKCs and Rho kinases. Results with the PLC-i U73122 were inconclusive as the inactive control molecule was not inactive and thus, leaving the result's specificity as questionable. Therefore, we could not truly clarify if PLC signaling is related to ERK and how exactly ERK activation by Gq is achieved in these cells.

In order to enlighten the mechanism of action we could show that $G\alpha_q^{Q209L}$ exist in the GTP-bound monomeric as well as in the GDP-bound heterotrimeric form. FR has been characterized as a GDI (Schrage et al. 2015). We were able to transfer this mechanism to the GTPase-deficient $G\alpha_q$ as we could show that ligand-induced DMR signal of cells transfected with the $G\alpha_q^{Q209L}$ construct was block with FR perfectly, therefore could conclude that FR inhibits most likely the heterotrimer. But we cannot exclude the possibility that FR additionally binds to the monomeric form of $G\alpha_q^{Q209L}$ and therefore inhibits protein-protein interaction. To clarify this question further, binding studies with FR must be done on GTP versus GDP-bound $G\alpha_q^{Q209L}$.

In addition we were able to show that PLC GAP activity most likely does not function on the GTPase-deficient as it is described to work for the wild type protein (Litosch 2013; Harden et al. 2011; Waldo et al. 2010) and therefore explain FR's inability to inhibit this canonical effector protein. This hypothesis was concluded by the fact, that basal elevated

Discussion

FRET signals between PLC and the $G\alpha_q^{Q209L}$ could not be depressed by FR application. In theory, if GAP activity of PLC functioned on $G\alpha_q^{Q209L}$ it would release $G\alpha_q^{Q209L}$ -GDP from the PLC- $G\alpha_q^{Q209L}$ -GTP interaction complex and the $G\beta\gamma$ heterodimer should then be able to capture the GDP-bound monomer and form a FR accessible GDP-bound heterotrimer. In this case FR should lower the basal FRET signal as it would withdraw the α -subunit from the activation process, but this was not the case in our experiment. But some major questions were left out to be answered. The experiment we performed was done with the PLC β_3 isoform, therefore it would be interesting to see, whether this loss of GAP activity can be transferred to other PLC β isoforms. Waldo et al. could show that Q209 of the $G\alpha_q$ is an important residue in the GTPase-accelerating process of PLC β_3 . More in depth analysis is needed to state if this is also the case for other PLC isoforms.

In context of uveal melanoma, FR could surprisingly blunt PLC signaling driven by the GTPase-deficient $G\alpha_q$. These cells are known to harbor the PLC β_4 isoform (Johansson et al. 2015). An alternative explanation that could be further investigated is that also other factors like GTP and GDP content as well as the total amount of accessible proteins within a certain cellular background might modify the GAP activity of a certain PLC β isoform.

Another interesting observation we made was that in the UM cell lines with constitutively active Gq FR was more potent on ERK and AKT phosphorylation when constitutive activity was caused by the substitution of proline on Q209 versus the substitution by leucine. But we only investigated two cell lines with proline and 2 with leucine substitution. A higher number of different cell lines should be taken in account before further conclusion can be drawn, as we do not know if cell permeability varies throughout the different cell lines. Another option would be to use the clear artificial HEK293 cell background and test the two constructs in the same cell line to exclude bias due to different permeability and cellular background.

Using the uveal melanoma cells as a therapeutically relevant system, we could show the impressive consequence of Gq inhibition on different pro-survival pathways in the cell, cell proliferation and in-vivo tumor growth, but nevertheless this study is limited to proof the concept of direct targeting the oncogenic Gq rather than offering a new therapeutically option. Reasons for why FR as unmodified molecule should not be systemically applied will be discussed next.

FR, as stated, inhibits the signaling transduction of $G\alpha_{q/11/14}$ isoforms (Schrage et al. 2015; Kukkonen 2016). Almost 40% of the GPCRs are couple to Gq/11 proteins and thereby these proteins translate signals from many hormones and neurotransmitters into a cellular response (Sánchez-Fernández et al. 2014). The systemic function of the Gq/11 proteins are indispensable as shown in different knock-out mouse models. Baby mice lacking all 4 alleles of GNAQ and GNA11 did not show any morphological abnormalities, but they were unviable as they could not take up breathing. The mice in this study could only survive with at least one intact GNAQ allele. But these animals develop a hyperplasia of cells of the endocrine system, that produce growth factors and showed the syndrome of dwarfism (Wettschureck et al. 2005). In another knock-out model GNAQ deficient mice show prolonged bleeding time and were unresponsive to platelet aggregation agonist (Offermanns et al. 1997). Additionally many Gq-CPRs as muscarinic,

histaminic or prostaglandin receptors regulate bronchial constriction (Matthey et al. 2017). Therefore, systemic application would not be a suitable approach to treat human.

As systemic application is not advisable one solution might be to modify the molecule chemically in a way that targets only the mutated analog of the protein. Unfortunately prior structure-activity-relationship studies showed that even small changes within the structure of the molecule can lead to huge loss of potency (Xiong et al. 2016; Reher et al. 2018a). Nevertheless, some modifications that show similar potencies might differ in drug-vulnerability as shown in this study for FR and YM. In this study the evaluation of kinetics was only restricted to long term incubation and on wash-out experiments. To find the perfect candidate for further modulations more investigation regarding the kinetic and off-kinetic of the molecule should be done in the future. Also other known FR and YM derivatives, that could be synthesized (Xiong et al. 2016) or can be extracted from *Ardisia* (Reher et al. 2018b), could be implemented in further testing.

Another method to avoid side effects would be to apply FR just locally. In a study to investigate FR as a drug in asthmatic disease in a mouse model Wenzel and co-workers applied the compound as an aerosol directly on to the lung of the mice. By monitoring the heart rate and blood pressure during treatment, no effects were observed in the cardiovascular system as side effect. Further biodistribution measurements, 10 minutes after FR application to the lung were obtained by lung, liver, heart and blood. This measurement revealed that by this local application method FR was 10 times higher present in the lung than in the other tissues (Matthey et al. 2017). As tissue preparations were obtained shortly after FR application it is hard to predict of long-term application would lead to higher accumulation and therefore cause side effects.

Transferring a local application for tumor therapy would require a drug target delivery system. This term means that the drug, in this case FR, would be tagged to a vehicle that recognizes some specific features of the targets, in our case the uveal melanoma cells, and releases the drug at the destination. As the oncogenic $G\alpha_q$ protein is not found in the cell surface but is an intracellular protein the carrier, like in the case of siRNAs should be able to enter the cytoplasm by overcoming the cell membrane barrier (Bae and Park 2011). The development of such an analog of FR might be challenging, but desirable, as the results provided by our study seemed to be very promising.

Discussion

Summary

Malfunctions of GPCRs and G proteins are involved in many diseases including cancer, chronic lung diseases or multiple sclerosis and that is the reason why over 30% of the current drugs on the market have GPCRs as their targets. Modulation of the signaling cascade on the G protein level is more challenging, as there are only few tools known that specifically target this family of proteins. A common understanding is that inhibition on the receptor-level is more specific since only 4 families of G proteins are transducing the signaling of over 800 GPCRs. However, in some cases multiple receptor signaling via one specific G protein is involved in pathology, as it is reported in asthma. Another scenario in which targeting the G protein itself is desirable instead of the receptor is when the G protein starts to signal independent of ligands and receptors. This is the case for the Gq and G11 protein in uveal melanoma.

Uveal melanoma is the most common cancer in the adult eye. The malignancy arises from melanocytes of the uveal tract and patients often suffer under visual field loss or blurry vision. However, the most disastrous consequence of the disease is that over 50% of the patients develop metastasis that are most commonly found in the liver but also in lung or bone. Once the cancer has spread the median survival drops to 13.4 months. Unfortunately, no curing therapy is available so far. Deep-sequencing could expose that over 80% of the uveal melanoma patients carry an activating mutation in the GNAQ or the GNA11 gene that bestow the protein with constitutive activity.

In the presence of a ligand-activated receptor the non-mutated proteins circle between a sedentary heterotrimeric GDP-bound and an active monomeric GTP-bound state. Activation of the protein by a receptor causes the nucleotide exchange from GDP to GTP and leads to dissociation of the protein's α -subunit from the $\beta\gamma$ -heterodimer. An autocatalytic switch-off GTPase domain is present in the α -subunit. By promoting the hydrolysis of the γ -phosphate of the GTP it triggers the nucleotide's transformation back into the di-phosphate and thereby inactivates the protein. The amino acid substitution on the position Q209 to leucine or proline that is commonly detected in uveal melanoma impairs the GTPase activity and traps the protein in its active state.

As a sequel to this discovery, a lot of reports emerged during the last 10 years that elucidated the role of the mutated Gq and G11 proteins as the perpetrator for the on-set of different pro-survival pathways. In that regard many attempts were made to inhibit cell growth and tumor formation by targeting these downstream pathways but none of these efforts could show any clinical success. A more straight-forward approach would be to target the oncogenic protein itself but the only known specific Gq and G11 inhibitors FR and YM were not believed to be suitable to block signaling of the mutated protein because of their mode of action. Former studies demonstrated the mode of action of these macrocyclic depsipeptides as guanine-dissociation inhibitors. By this means these molecules prevent the activation of the protein by blocking GDP dissociation. Therefore, it was long believed that these inhibitors would not counteract the protein with this specific gain-of-function mutation, as the protein is already in the activated state. This conclusion was supported by literature that described the inability of FR and YM to inhibit the canonical effector protein PLC, in case it was activated by the mutated analog of the protein.

Summary

Inconsistent with this hypothesis, Evelyn Gaffal and Thomas Tüting demonstrated that FR indeed suppressed typical hallmarks of cancer cells in a mouse melanoma cell line harboring a somatic gain-of-function mutation in the GNA11 gene. However, mutations of this gene occur in a mutually exclusive manner and therefore one of the proteins would always remain unmutated. This was the leverage point for this study that served to proof and to understand how the Gq inhibitor FR with GDI mode of action blunts mitogenic signaling of the GTPase-deficient $G\alpha_q^{Q209L}$.

Cell-based assays in genome-edited HEK293 cells lacking alleles for GNAQ and GNA11 helped to verify the direct interaction of the molecule with the protein. These cells offered an ideal background to reintroduce the constructs and to clearly distinguish between wild type and GTPase-deficient $G\alpha_q$. Mutagenesis studies furthermore served to verify that the binding region of the molecule is similar between the wild type and mutated protein. Furthermore, whole cell biosensor experiments did not only help to underline interaction of the molecule with its cellular target but also indicated a receptor-activatable fraction of the GTPase-deficient protein, that rationalized FR's inhibitor properties on the active protein, as this fraction indicates existence of a heterotrimeric GDP-bound inactive form. Additionally, we could confirm the existence of the GDP-bound heterotrimeric GTPase-deficient protein by immunoprecipitation together with His-pull-down assays. With the help of FRET experiments we were further able to understand and to build up a hypothesis that might explain the biased inhibition of signaling cascades by blocking the GTPase-deficient $G\alpha_q$. Finally, we rationalized the inhibition of Gq as a potential therapeutic approach to treat uveal melanoma and evaluated the two most prominent Gq inhibitors in regard of their drug vulnerability in this context.

In conclusion the results of this study suggest that molecules like FR are suitable candidates for drug-development. Stratified uveal melanoma patients could benefit from these compounds in the future. Ideally, these compounds should be modified in a way that either specifically target certain tissue or the mutated form of the protein and therefore could extend the survival rates for these patients without major side effects.

Reference

Adjobo-Hermans, Merel J. W.; Crosby, Kevin C.; Putyrski, Mateusz; Bhageloe, Arshia; van Weeren, Laura; Schultz, Carsten et al. (2013): PLC β isoforms differ in their subcellular location and their CT-domain dependent interaction with G α_q . In *Cellular signalling* 25 (1), pp. 255–263.

Ambrosini, Grazia; Musi, Elgilda; Ho, Alan L.; Stanchina, Elisa de; Schwartz, Gary K. (2013): Inhibition of mutant GNAQ signaling in uveal melanoma induces AMPK-dependent autophagic cell death. In *Molecular cancer therapeutics* 12 (5), pp. 768–776. DOI: 10.1158/1535-7163.MCT-12-1020.

Ambrosini, Grazia; Pratilas, Christine A.; Qin, Li-Xuan; Tadi, Madhavi; Surriga, Oliver; Carvajal, Richard D.; Schwartz, Gary K. (2012): Identification of unique MEK-dependent genes in GNAQ mutant uveal melanoma involved in cell growth, tumor cell invasion, and MEK resistance. In *Clinical cancer research : an official journal of the American Association for Cancer Research* 18 (13), pp. 3552–3561. DOI: 10.1158/1078-0432.CCR-11-3086.

American Cancer Society: Cancer Facts & Figures - 2008 2008. Available online at <https://www.cancer.org/research/cancer-facts-statistics/all-cancer-facts-figures/cancer-facts-figures-2008.html>, checked on 11/26/2018.

Ananthanarayanan, Bharath; Stahelin, Robert V.; Digman, Michelle A.; Cho, Wonhwa (2003): Activation mechanisms of conventional protein kinase C isoforms are determined by the ligand affinity and conformational flexibility of their C1 domains. In *The Journal of biological chemistry* 278 (47), pp. 46886–46894. DOI: 10.1074/jbc.M307853200.

Atwood, Brady K.; Lopez, Jacqueline; Wager-Miller, James; Mackie, Ken; Straiker, Alex (2011): Expression of G protein-coupled receptors and related proteins in HEK293, AtT20, BV2, and N18 cell lines as revealed by microarray analysis. In *BMC genomics* 12, p. 14. DOI: 10.1186/1471-2164-12-14.

Babchia, Narjes; Calipel, Armelle; Mouriaux, Frédéric; Faussat, Anne-Marie; Mascarelli, Frédéric (2010): The PI3K/Akt and mTOR/P70S6K signaling pathways in human uveal melanoma cells: interaction with B-Raf/ERK. In *Investigative ophthalmology & visual science* 51 (1), pp. 421–429. DOI: 10.1167/iovs.09-3974.

Bae, You Han; Park, Kinam (2011): Targeted drug delivery to tumors: myths, reality and possibility. In *Journal of controlled release : official journal of the Controlled Release Society* 153 (3), pp. 198–205. DOI: 10.1016/j.jconrel.2011.06.001.

Barbacid, M. (1987): ras genes. In *Annual review of biochemistry* 56, pp. 779–827. DOI: 10.1146/annurev.bi.56.070187.004023.

Berman, David M.; Wilkie, Thomas M.; Gilman, Alfred G. (1996): GAIP and RGS4 Are GTPase-Activating Proteins for the Gi Subfamily of G Protein α Subunits. In *Cell* 86 (3), pp. 445–452. DOI: 10.1016/S0092-8674(00)80117-8.

Berridge, Michael J. (2009): Inositol trisphosphate and calcium signalling mechanisms. In *Biochimica et biophysica acta* 1793 (6), pp. 933–940. DOI: 10.1016/j.bbamcr.2008.10.005.

Reference

Berstein, G.; Blank, J. L.; Jhon, D. Y.; Exton, J. H.; Rhee, S. G.; Ross, E. M. (1992): Phospholipase C-beta 1 is a GTPase-activating protein for Gq/11, its physiologic regulator. In *Cell* 70 (3), pp. 411–418.

Bleasdale, J. E.; Thakur, N. R.; Gremban, R. S.; Bundy, G. L.; Fitzpatrick, F. A.; Smith, R. J.; Bunting, S. (1990): Selective inhibition of receptor-coupled phospholipase C-dependent processes in human platelets and polymorphonuclear neutrophils. In *The Journal of pharmacology and experimental therapeutics* 255 (2), pp. 756–768.

Bommakanti, R. K.; Vinayak, S.; Simonds, W. F. (2000): Dual regulation of Akt/protein kinase B by heterotrimeric G protein subunits. In *The Journal of biological chemistry* 275 (49), pp. 38870–38876. DOI: 10.1074/jbc.M007403200.

Bourne, H. R.; Sanders, D. A.; McCormick, F. (1990): The GTPase superfamily: a conserved switch for diverse cell functions. In *Nature* 348 (6297), pp. 125–132. DOI: 10.1038/348125a0.

Carvajal, Richard D.; Piperno-Neumann, Sophie; Kapiteijn, Ellen; Chapman, Paul B.; Frank, Stephen; Joshua, Anthony M. et al. (2018): Selumetinib in Combination With Dacarbazine in Patients With Metastatic Uveal Melanoma: A Phase III, Multicenter, Randomized Trial (SUMIT). In *Journal of clinical oncology : official journal of the American Society of Clinical Oncology* 36 (12), pp. 1232–1239. DOI: 10.1200/JCO.2017.74.1090.

Carvajal, Richard D.; Schwartz, Gary K.; Tezel, Tongalp; Marr, Brian; Francis, Jasmine H.; Nathan, Paul D. (2016): Metastatic disease from uveal melanoma: treatment options and future prospects. In *The British Journal of Ophthalmology* 101 (1), pp. 38–44. DOI: 10.1136/bjophthalmol-2016-309034.

Carvajal, Richard D.; Sosman, Jeffrey A.; Quevedo, Jorge Fernando; Milhem, Mohammed M.; Joshua, Anthony M.; Kudchadkar, Ragini R. et al. (2014): Effect of selumetinib vs chemotherapy on progression-free survival in uveal melanoma: a randomized clinical trial. In *JAMA* 311 (23), pp. 2397–2405. DOI: 10.1001/jama.2014.6096.

Case, David A.; Cheatham, Thomas E.; Darden, Tom; Gohlke, Holger; Luo, Ray; Merz, Kenneth M. et al. (2005): The Amber biomolecular simulation programs. In *Journal of computational chemistry* 26 (16), pp. 1668–1688. DOI: 10.1002/jcc.20290.

Casimiro, Mathew C.; Crosariol, Marco; Loro, Emanuele; Li, Zhiping; Pestell, Richard G. (2012): Cyclins and cell cycle control in cancer and disease. In *Genes & cancer* 3 (11-12), pp. 649–657. DOI: 10.1177/1947601913479022.

Chang, F.; Lee, J. T.; Navolanic, P. M.; Steelman, L. S.; Shelton, J. G.; Blalock, W. L. et al. (2003): Involvement of PI3K/Akt pathway in cell cycle progression, apoptosis, and neoplastic transformation: a target for cancer chemotherapy. In *Leukemia* 17 (3), pp. 590–603. DOI: 10.1038/sj.leu.2402824.

Charpentier, Thomas H.; Waldo, Gary L.; Lowery-Gionta, Emily G.; Krajewski, Krzysztof; Strahl, Brian D.; Kash, Thomas L. et al. (2016): Potent and Selective Peptide-based Inhibition of the G Protein Gαq. In *The Journal of biological chemistry* 291 (49), pp. 25608–25616. DOI: 10.1074/jbc.M116.740407.

- Chen, X.; Wu, Q.; Tan, L.; Porter, D.; Jager, M. J.; Emery, C.; Bastian, B. C. (2014): Combined PKC and MEK inhibition in uveal melanoma with GNAQ and GNA11 mutations. In *Oncogene* 33 (39), pp. 4724–4734. DOI: 10.1038/onc.2013.418.
- Chidiac, Peter; Ross, Elliott M. (1999): Phospholipase C- β 1 Directly Accelerates GTP Hydrolysis by $G\alpha_q$ and Acceleration Is Inhibited by $G\beta\gamma$ Subunits. In *The Journal of biological chemistry* 274 (28), pp. 19639–19643. DOI: 10.1074/jbc.274.28.19639.
- Cisowski, Jaroslaw; Bergo, Martin O. (2017): What makes oncogenes mutually exclusive? In *Small GTPases* 8 (3), pp. 187–192. DOI: 10.1080/21541248.2016.1212689.
- Colón-González, Francheska; Kazanietz, Marcelo G. (2006): C1 domains exposed: from diacylglycerol binding to protein-protein interactions. In *Biochimica et biophysica acta* 1761 (8), pp. 827–837. DOI: 10.1016/j.bbali.2006.05.001.
- Croce, Carlo M. (2008): Oncogenes and cancer. In *The New England journal of medicine* 358 (5), pp. 502–511. DOI: 10.1056/NEJMra072367.
- Crüseman, Max; Reher, Raphael; Schamari, Isabella; Brachmann, Alexander O.; Ohbayashi, Tsubasa; Kuschak, Markus et al. (2018): Heterologous Expression, Biosynthetic Studies, and Ecological Function of the Selective G_q -Signaling Inhibitor FR900359. In *Angewandte Chemie (International ed. in English)* 57 (3), pp. 836–840. DOI: 10.1002/anie.201707996.
- Czirbesz, Kata; Gorka, Eszter; Balatoni, Tímea; Pánczél, Gitta; Melegh, Krisztina; Kovács, Péter et al. (2017): Efficacy of Vemurafenib Treatment in 43 Metastatic Melanoma Patients with BRAF Mutation. Single-Institute Retrospective Analysis, Early Real-Life Survival Data. In *Pathology oncology research : POR*. DOI: 10.1007/s12253-017-0324-1.
- Dancey, Janet E. (2006): Therapeutic targets: MTOR and related pathways. In *Cancer biology & therapy* 5 (9), pp. 1065–1073.
- Darby, N. J.; Creighton, T. E. (1993): Dissecting the disulphide-coupled folding pathway of bovine pancreatic trypsin inhibitor. Forming the first disulphide bonds in analogues of the reduced protein. In *Journal of molecular biology* 232 (3), pp. 873–896. DOI: 10.1006/jmbi.1993.1437.
- Decatur, Christina L.; Ong, Erin; Garg, Nisha; Anbunathan, Hima; Bowcock, Anne M.; Field, Matthew G.; Harbour, J. William (2016): Driver Mutations in Uveal Melanoma: Associations With Gene Expression Profile and Patient Outcomes. In *JAMA ophthalmology* 134 (7), pp. 728–733. DOI: 10.1001/jamaophthalmol.2016.0903.
- Degorce, François; Card, Amy; Soh, Sharon; Trinquet, Eric; Knapik, Glenn P.; Xie, Bing (2009): HTRF: A technology tailored for drug discovery - a review of theoretical aspects and recent applications. In *Current chemical genomics* 3, pp. 22–32. DOI: 10.2174/1875397300903010022.
- Dong, Jianli; Phelps, Robert G.; Qiao, Rui; Yao, Shen; Benard, Outhiriaradjou; Ronai, Zeev; Aaronson, Stuart A. (2003): BRAF oncogenic mutations correlate with progression rather than initiation of human melanoma. In *Cancer research* 63 (14), pp. 3883–3885.
- Eagle, R. C. (2013): The pathology of ocular cancer. In *Eye (London, England)* 27 (2), pp. 128–136. DOI: 10.1038/eye.2012.237.

Reference

- Etienne-Manneville, Sandrine; Hall, Alan (2002): Rho GTPases in cell biology. In *Nature* 420 (6916), pp. 629–635. DOI: 10.1038/nature01148.
- Falchook, Gerald S.; Lewis, Karl D.; Infante, Jeffrey R.; Gordon, Michael S.; Vogelzang, Nicholas J.; DeMarini, Douglas J. et al. (2012): Activity of the oral MEK inhibitor trametinib in patients with advanced melanoma: a phase 1 dose-escalation trial. In *The Lancet. Oncology* 13 (8), pp. 782–789. DOI: 10.1016/S1470-2045(12)70269-3.
- Feng, Xiaodong; Degese, Maria Sol; Iglesias-Bartolome, Ramiro; Vaque, Jose P.; Molinolo, Alfredo A.; Rodrigues, Murilo et al. (2014): Hippo-independent activation of YAP by the GNAQ uveal melanoma oncogene through a trio-regulated rho GTPase signaling circuitry. In *Cancer cell* 25 (6), pp. 831–845. DOI: 10.1016/j.ccr.2014.04.016.
- Fujioka, Mamoru; Koda, Shigetaka; Morimoto, Yukiyo; Biemann, Klaus (1988): Structure of FR900359, a cyclic depsipeptide from *Ardisia crenata* Sims. In *J. Org. Chem.* 53 (12), pp. 2820–2825. DOI: 10.1021/jo00247a030.
- García-Hoz, Carlota; Sánchez-Fernández, Guzmán; Díaz-Meco, Maria Teresa; Moscat, Jorge; Mayor, Federico; Ribas, Catalina (2010): G alpha(q) acts as an adaptor protein in protein kinase C zeta (PKCzeta)-mediated ERK5 activation by G protein-coupled receptors (GPCR). In *The Journal of biological chemistry* 285 (18), pp. 13480–13489. DOI: 10.1074/jbc.M109.098699.
- García-Recio, Susana; Fuster, Gemma; Fernández-Nogueira, Patricia; Pastor-Arroyo, Eva M.; Park, So Yeon; Mayordomo, Cristina et al. (2013): Substance P autocrine signaling contributes to persistent HER2 activation that drives malignant progression and drug resistance in breast cancer. In *Cancer research* 73 (21), pp. 6424–6434. DOI: 10.1158/0008-5472.CAN-12-4573.
- Gray-Schopfer, Vanessa C.; da Rocha Dias, Silvy; Marais, Richard (2005): The role of B-RAF in melanoma. In *Cancer metastasis reviews* 24 (1), pp. 165–183. DOI: 10.1007/s10555-005-5865-1.
- Griewank, Klaus G.; Yu, Xiaoxing; Khalili, Jahan; Sozen, M. Mert; Stempke-Hale, Katherine; Bernatchez, Chantale et al. (2012): Genetic and Molecular Characterization of Uveal Melanoma Cell Lines. In *Pigment cell & melanoma research* 25 (2), pp. 182–187. DOI: 10.1111/j.1755-148X.2012.00971.x.
- Gril, Brunilde; Palmieri, Diane; Qian, Yong; Anwar, Talha; Ileva, Lilia; Bernardo, Marcelino et al. (2011): The B-Raf status of tumor cells may be a significant determinant of both antitumor and anti-angiogenic effects of pazopanib in xenograft tumor models. In *PLoS ONE* 6 (10), e25625. DOI: 10.1371/journal.pone.0025625.
- Grundmann, Manuel; Merten, Nicole; Malfacini, Davide; Inoue, Asuka; Preis, Philip; Simon, Katharina et al. (2018): Lack of beta-arrestin signaling in the absence of active G proteins. In *Nature communications* 9 (1), p. 341. DOI: 10.1038/s41467-017-02661-3.
- Gschwendt, M.; Kittstein, W.; Johannes, F. J. (1998): Differential effects of suramin on protein kinase C isoenzymes. A novel tool for discriminating protein kinase C activities. In *FEBS Letters* 421 (2), pp. 165–168.

- Gutkind, J. S. (2000): Regulation of mitogen-activated protein kinase signaling networks by G protein-coupled receptors. In *Science's STKE : signal transduction knowledge environment* 2000 (40), re1. DOI: 10.1126/stke.2000.40.re1.
- Hanson, C. Jane; Bootman, Martin D.; Roderick, H. Llewelyn (2004): Cell signalling: IP3 receptors channel calcium into cell death. In *Current biology : CB* 14 (21), R933-5. DOI: 10.1016/j.cub.2004.10.019.
- Harbour, J. William (2012): The genetics of uveal melanoma: an emerging framework for targeted therapy. In *Pigment cell & melanoma research* 25 (2), pp. 171–181. DOI: 10.1111/j.1755-148X.2012.00979.x.
- Harden, T. Kendall; Waldo, Gary L.; Hicks, Stephanie N.; Sondek, John (2011): Mechanism of activation and inactivation of Gq/phospholipase C- β signaling nodes. In *Chemical reviews* 111 (10), pp. 6120–6129. DOI: 10.1021/cr200209p.
- Harlé, A.; Salleron, J.; Perkins, G.; Pilati, C.; Blons, H.; Laurent-Puig, P.; Merlin, J. L. (2015): Expression of pEGFR and pAKT as response-predictive biomarkers for RAS wild-type patients to anti-EGFR monoclonal antibodies in metastatic colorectal cancers. In *British journal of cancer* 113 (4), pp. 680–685. DOI: 10.1038/bjc.2015.250.
- Ho, M. K.; Yung, L. Y.; Chan, J. S.; Chan, J. H.; Wong, C. S.; Wong, Y. H. (2001): G α (14) links a variety of G(i)- and G(s)-coupled receptors to the stimulation of phospholipase C. In *British journal of pharmacology* 132 (7), pp. 1431–1440. DOI: 10.1038/sj.bjp.0703933.
- Hubbard, Katherine B.; Hepler, John R. (2006): Cell signalling diversity of the Gq α family of heterotrimeric G proteins. In *Cellular signalling* 18 (2), pp. 135–150. DOI: 10.1016/j.cellsig.2005.08.004.
- Jaffe, Aron B.; Hall, Alan (2005): Rho GTPases: biochemistry and biology. In *Annual review of cell and developmental biology* 21, pp. 247–269. DOI: 10.1146/annurev.cellbio.21.020604.150721.
- Jiang, Chen Chen; Lai, Fritz; Thorne, Rick F.; Yang, Fan; Liu, Hao; Hersey, Peter; Zhang, Xu Dong (2011): MEK-independent survival of B-RAFV600E melanoma cells selected for resistance to apoptosis induced by the RAF inhibitor PLX4720. In *Clinical cancer research : an official journal of the American Association for Cancer Research* 17 (4), pp. 721–730. DOI: 10.1158/1078-0432.CCR-10-2225.
- Johansson, Peter; Aoude, Lauren G.; Wadt, Karin; Glasson, William J.; Warriar, Sunil K.; Hewitt, Alex W. et al. (2015): Deep sequencing of uveal melanoma identifies a recurrent mutation in PLCB4. In *Oncotarget* 7 (4), pp. 4624–4631. DOI: 10.18632/oncotarget.6614.
- Kadamur, Ganesh; Ross, Elliott M. (2013): Mammalian phospholipase C. In *Annual review of physiology* 75, pp. 127–154. DOI: 10.1146/annurev-physiol-030212-183750.
- Kalinec, G.; Nazarali, A. J.; Hermouet, S.; Xu, N.; Gutkind, J. S. (1992): Mutated alpha subunit of the Gq protein induces malignant transformation in NIH 3T3 cells. In *Molecular and cellular biology* 12 (10), pp. 4687–4693.

Reference

- Khalili, Jahan S.; Yu, Xiaoxing; Wang, Ji; Hayes, Brendan C.; Davies, Michael A.; Lizee, Gregory et al. (2012): Combination small molecule MEK and PI3K inhibition enhances uveal melanoma cell death in a mutant GNAQ- and GNA11-dependent manner. In *Clinical cancer research : an official journal of the American Association for Cancer Research* 18 (16), pp. 4345–4355. DOI: 10.1158/1078-0432.CCR-11-3227.
- Kilian, Marta M.; Loeffler, Karin U.; Pfarrer, Christiane; Holz, Frank G.; Kurts, Christian; Herwig, Martina C. (2016): Intravitreally Injected HcMel12 Melanoma Cells Serve as a Mouse Model of Tumor Biology of Intraocular Melanoma. In *Current eye research* 41 (1), pp. 121–128. DOI: 10.3109/02713683.2015.1004721.
- Kim, Alex; Cohen, Mark S. (2016): The discovery of vemurafenib for the treatment of BRAF-mutated metastatic melanoma. In *Expert opinion on drug discovery* 11 (9), pp. 907–916. DOI: 10.1080/17460441.2016.1201057.
- Kimple, Adam J.; Bosch, Dustin E.; Giguère, Patrick M.; Siderovski, David P. (2011): Regulators of G-protein signaling and their G α substrates: promises and challenges in their use as drug discovery targets. In *Pharmacological reviews* 63 (3), pp. 728–749. DOI: 10.1124/pr.110.003038.
- Kisselev, O. G.; Ermolaeva, M. V.; Gautam, N. (1994): A farnesylated domain in the G protein gamma subunit is a specific determinant of receptor coupling. In *The Journal of biological chemistry* 269 (34), pp. 21399–21402.
- Klein, Ryan R.; Bourdon, David M.; Costales, Chester L.; Wagner, Craig D.; White, Wendy L.; Williams, Jon D. et al. (2011): Direct activation of human phospholipase C by its well known inhibitor u73122. In *The Journal of biological chemistry* 286 (14), pp. 12407–12416. DOI: 10.1074/jbc.M110.191783.
- Kleuss, C.; Raw, A. S.; Lee, E.; Sprang, S. R.; Gilman, A. G. (1994): Mechanism of GTP hydrolysis by G-protein alpha subunits. In *Proceedings of the National Academy of Sciences of the United States of America* 91 (21), pp. 9828–9831.
- Knapen, Lotte M.; Koornstra, Rutger H. T.; Driessen, Johanna H. M.; van Vlijmen, Bas; Croes, Sander; Schalkwijk, Stein et al. (2018): The Impact of Dose and Simultaneous Use of Acid-Reducing Agents on the Effectiveness of Vemurafenib in Metastatic BRAF V600 Mutated Melanoma: a Retrospective Cohort Study. In *Targeted oncology* 13 (3), pp. 363–370. DOI: 10.1007/s11523-018-0564-3.
- Krantz, Benjamin A.; Dave, Nikita; Komatsubara, Kimberly M.; Marr, Brian P.; Carvajal, Richard D. (2017): Uveal melanoma: epidemiology, etiology, and treatment of primary disease. In *Clinical ophthalmology (Auckland, N.Z.)* 11, pp. 279–289. DOI: 10.2147/OPHTH.S89591.
- Kukkonen, Jyrki P. (2016): G-protein inhibition profile of the reported Gq/11 inhibitor UBO-QIC. In *Biochemical and biophysical research communications* 469 (1), pp. 101–107. DOI: 10.1016/j.bbrc.2015.11.078.
- Lambright, D. G.; Noel, J. P.; Hamm, H. E.; Sigler, P. B. (1994): Structural determinants for activation of the alpha-subunit of a heterotrimeric G protein. In *Nature* 369 (6482), pp. 621–628. DOI: 10.1038/369621a0.

- Landis, C. A.; Masters, S. B.; Spada, A.; Pace, A. M.; Bourne, H. R.; Vallar, L. (1989): GTPase inhibiting mutations activate the alpha chain of Gs and stimulate adenylyl cyclase in human pituitary tumours. In *Nature* 340 (6236), pp. 692–696. DOI: 10.1038/340692a0.
- Landsberg, Jennifer; Gaffal, Evelyn; Cron, Mira; Kohlmeyer, Judith; Renn, Marcel; Tüting, Thomas (2010): Autochthonous primary and metastatic melanomas in Hgf-Cdk4 R24C mice evade T-cell-mediated immune surveillance. In *Pigment cell & melanoma research* 23 (5), pp. 649–660. DOI: 10.1111/j.1755-148X.2010.00744.x.
- Lapadula, Dominic; Farias, Eduardo; Randolph, Clinita E.; Purwin, Timothy; McGrath, Dougan; Charpentier, Thomas et al. (2018): Effects of Oncogenic Gαq and Gα11 Inhibition by FR900359 in Uveal Melanoma. In *Molecular cancer research : MCR*. DOI: 10.1158/1541-7786.MCR-18-0574.
- Lee, K. Y.; Ryu, S. H.; Suh, P. G.; Choi, W. C.; Rhee, S. G. (1987): Phospholipase C associated with particulate fractions of bovine brain. In *Proceedings of the National Academy of Sciences of the United States of America* 84 (16), pp. 5540–5544.
- Lee, Mi Young; Mun, Jihye; Lee, Jeong Hyun; Lee, Sunghou; Lee, Byung Ho; Oh, Kwang-Seok (2014): A comparison of assay performance between the calcium mobilization and the dynamic mass redistribution technologies for the human urotensin receptor. In *Assay and drug development technologies* 12 (6), pp. 361–368. DOI: 10.1089/adt.2014.590.
- Lee, Paul H.; Gao, Alice; van Staden, Carlo; Ly, Jenny; Salon, John; Xu, Arron et al. (2008): Evaluation of dynamic mass redistribution technology for pharmacological studies of recombinant and endogenously expressed g protein-coupled receptors. In *Assay and drug development technologies* 6 (1), pp. 83–94. DOI: 10.1089/adt.2007.126.
- Lee, S. B.; Shin, S. H.; Hepler, J. R.; Gilman, A. G.; Rhee, S. G. (1993): Activation of phospholipase C-beta 2 mutants by G protein alpha q and beta gamma subunits. In *The Journal of biological chemistry* 268 (34), pp. 25952–25957.
- Lewit-Bentley, A.; Réty, S. (2000): EF-hand calcium-binding proteins. In *Current opinion in structural biology* 10 (6), pp. 637–643.
- Litosch, Irene (2013): Regulation of phospholipase C-β(1) GTPase-activating protein (GAP) function and relationship to G(q) efficacy. In *IUBMB life* 65 (11), pp. 936–940. DOI: 10.1002/iub.1218.
- Luo, Ji; Solimini, Nicole L.; Elledge, Stephen J. (2009): Principles of cancer therapy: oncogene and non-oncogene addiction. In *Cell* 136 (5), pp. 823–837. DOI: 10.1016/j.cell.2009.02.024.
- Lutz, Susanne; Shankaranarayanan, Aruna; Coco, Cassandra; Ridilla, Marc; Nance, Mark R.; Vettel, Christiane et al. (2007): Structure of Galphaq-p63RhoGEF-RhoA complex reveals a pathway for the activation of RhoA by GPCRs. In *Science (New York, N.Y.)* 318 (5858), pp. 1923–1927. DOI: 10.1126/science.1147554.
- Lyon, Angeline M.; Tesmer, John J. G. (2013): Structural insights into phospholipase C-β function. In *Molecular pharmacology* 84 (4), pp. 488–500. DOI: 10.1124/mol.113.087403.

Reference

- Lyons, J.; Landis, C. A.; Harsh, G.; Vallar, L.; Grünewald, K.; Feichtinger, H. et al. (1990): Two G protein oncogenes in human endocrine tumors. In *Science (New York, N.Y.)* 249 (4969), pp. 655–659.
- Macmillan, D.; McCarron, J. G. (2010): The phospholipase C inhibitor U-73122 inhibits Ca(2+) release from the intracellular sarcoplasmic reticulum Ca(2+) store by inhibiting Ca(2+) pumps in smooth muscle. In *British journal of pharmacology* 160 (6), pp. 1295–1301. DOI: 10.1111/j.1476-5381.2010.00771.x.
- Mahoney, Jacob P.; Sunahara, Roger K. (2016): Mechanistic insights into GPCR-G protein interactions. In *Current opinion in structural biology* 41, pp. 247–254. DOI: 10.1016/j.sbi.2016.11.005.
- Martiny-Baron, G.; Kazanietz, M. G.; Mischak, H.; Blumberg, P. M.; Kochs, G.; Hug, H. et al. (1993): Selective inhibition of protein kinase C isozymes by the indolocarbazole Gö 6976. In *The Journal of biological chemistry* 268 (13), pp. 9194–9197.
- Masoomian, Babak; Shields, Jerry A.; Shields, Carol L. (2018): Overview of BAP1 cancer predisposition syndrome and the relationship to uveal melanoma. In *Journal of Current Ophthalmology* 30 (2), pp. 102–109. DOI: 10.1016/j.joco.2018.02.005.
- Matthey, Michaela; Roberts, Richard; Seidinger, Alexander; Simon, Annika; Schröder, Ralf; Kuschak, Markus et al. (2017): Targeted inhibition of Gq signaling induces airway relaxation in mouse models of asthma. In *Science translational medicine* 9 (407). DOI: 10.1126/scitranslmed.aag2288.
- McArthur, Grant A.; Ribas, Antoni (2013): Targeting oncogenic drivers and the immune system in melanoma. In *Journal of clinical oncology : official journal of the American Society of Clinical Oncology* 31 (4), pp. 499–506. DOI: 10.1200/JCO.2012.45.5568.
- Meng, Zhipeng; Moroishi, Toshiro; Mottier-Pavie, Violaine; Plouffe, Steven W.; Hansen, Carsten G.; Hong, Audrey W. et al. (2015): MAP4K family kinases act in parallel to MST1/2 to activate LATS1/2 in the Hippo pathway. In *Nature communications* 6, p. 8357. DOI: 10.1038/ncomms9357.
- Mierzejewska, Karolina; Siwek, Wojciech; Czapinska, Honorata; Kaus-Drobek, Magdalena; Radlinska, Monika; Skowronek, Krzysztof et al. (2014): Structural basis of the methylation specificity of R.DpnI. In *Nucleic Acids Research* 42 (13), pp. 8745–8754. DOI: 10.1093/nar/gku546.
- Miller, Eric; Yang, Jiayi; DeRan, Michael; Wu, Chunlei; Su, Andrew I.; Bonamy, Ghislain M. C. et al. (2012): Identification of serum-derived sphingosine-1-phosphate as a small molecule regulator of YAP. In *Chemistry & biology* 19 (8), pp. 955–962. DOI: 10.1016/j.chembiol.2012.07.005.
- Miller, S.; Janin, J.; Lesk, A. M.; Chothia, C. (1987): Interior and surface of monomeric proteins. In *Journal of molecular biology* 196 (3), pp. 641–656.
- Milligan, G.; Marshall, F.; Rees, S. (1996): G16 as a universal G protein adapter: implications for agonist screening strategies. In *Trends in pharmacological sciences* 17 (7), pp. 235–237.

- Milligan, Graeme; Kostenis, Evi (2006): Heterotrimeric G-proteins: a short history. In *British journal of pharmacology* 147 Suppl 1, S46-55. DOI: 10.1038/sj.bjp.0706405.
- Mixon, M. B.; Lee, E.; Coleman, D. E.; Berghuis, A. M.; Gilman, A. G.; Sprang, S. R. (1995): Tertiary and Quaternary Structural Changes in G α Induced by GTP Hydrolysis. In *Science (New York, N.Y.)* 270 (5238), pp. 954–960. DOI: 10.1126/science.270.5238.954.
- Miyamae, Akira; Fujioka, Mamoru; Koda, Shigetaka; Morimoto, Yukiyo (1989): Structural studies of FR900359, a novel cyclic depsipeptide from *Ardisia crenata* Sims (Myrsinaceae). In *J. Chem. Soc., Perkin Trans. 1* (5), p. 873. DOI: 10.1039/p19890000873.
- Mizuno, Norikazu; Itoh, Hiroshi (2009): Functions and regulatory mechanisms of Gq-signaling pathways. In *Neuro-Signals* 17 (1), pp. 42–54. DOI: 10.1159/000186689.
- Moore, Amanda R.; Ceraudo, Emilie; Sher, Jessica J.; Guan, Youxin; Shoushtari, Alexander N.; Chang, Matthew T. et al. (2016): Recurrent activating mutations of G-protein-coupled receptor CYSLTR2 in uveal melanoma. In *Nature genetics* 48 (6), pp. 675–680. DOI: 10.1038/ng.3549.
- Mukhopadhyay, S.; Ross, E. M. (1999): Rapid GTP binding and hydrolysis by G(q) promoted by receptor and GTPase-activating proteins. In *Proceedings of the National Academy of Sciences of the United States of America* 96 (17), pp. 9539–9544.
- Nance, Mark R.; Kreutz, Barry; Tesmer, Valerie M.; Sterne-Marr, Rachel; Kozasa, Tohru; Tesmer, John J.G. (2013): Structural and Functional Analysis of the Regulator of G Protein Signaling 2-G α q Complex. In *Structure (London, England : 1993)* 21 (3), pp. 438–448. DOI: 10.1016/j.str.2012.12.016.
- Nishimura, Akiyuki; Kitano, Ken; Takasaki, Jun; Taniguchi, Masatoshi; Mizuno, Norikazu; Tago, Kenji et al. (2010): Structural basis for the specific inhibition of heterotrimeric Gq protein by a small molecule. In *Proceedings of the National Academy of Sciences of the United States of America* 107 (31), pp. 13666–13671. DOI: 10.1073/pnas.1003553107.
- Noel, J. P.; Hamm, H. E.; Sigler, P. B. (1993): The 2.2 Å crystal structure of transducin- α complexed with GTP γ S. In *Nature* 366 (6456), pp. 654–663. DOI: 10.1038/366654a0.
- O'Hayre, Morgan; Vázquez-Prado, José; Kufareva, Irina; Stawiski, Eric W.; Handel, Tracy M.; Seshagiri, Somasekar; Gutkind, J. Silvio (2013): The Emerging Mutational Landscape of G-proteins and G-protein Coupled Receptors in Cancer. In *Nature reviews. Cancer* 13 (6), pp. 412–424. DOI: 10.1038/nrc3521.
- Offermanns, S.; Simon, M. I. (1995): G α 15 and G α 16 couple a wide variety of receptors to phospholipase C. In *The Journal of biological chemistry* 270 (25), pp. 15175–15180.
- Offermanns, S.; Toombs, C. F.; Hu, Y. H.; Simon, M. I. (1997): Defective platelet activation in G α (q)-deficient mice. In *Nature* 389 (6647), pp. 183–186. DOI: 10.1038/38284.
- Oldham, William M.; Hamm, Heidi E. (2008): Heterotrimeric G protein activation by G-protein-coupled receptors. In *Nature reviews. Molecular cell biology* 9 (1), pp. 60–71. DOI: 10.1038/nrm2299.

Reference

- Oldham, William M.; van Eps, Ned; Preinerger, Anita M.; Hubbell, Wayne L.; Hamm, Heidi E. (2006): Mechanism of the receptor-catalyzed activation of heterotrimeric G proteins. In *Nature structural & molecular biology* 13 (9), pp. 772–777. DOI: 10.1038/nsmb1129.
- Onken, Michael D.; Makepeace, Carol M.; Kaltenbronn, Kevin M.; Kanai, Stanley M.; Todd, Tyson D.; Wang, Shiqi et al. (2018): Targeting nucleotide exchange to inhibit constitutively active G protein α subunits in cancer cells. In *Science signaling* 11 (546). DOI: 10.1126/scisignal.aao6852.
- Onken, Michael D.; Worley, Lori A.; Ehlers, Justis P.; Harbour, J. William (2004): Gene expression profiling in uveal melanoma reveals two molecular classes and predicts metastatic death. In *Cancer research* 64 (20), pp. 7205–7209. DOI: 10.1158/0008-5472.CAN-04-1750.
- Onken, Michael D.; Worley, Lori A.; Long, Meghan D.; Duan, Shenghui; Council, M. Laurin; Bowcock, Anne M.; Harbour, J. William (2008): Oncogenic mutations in GNAQ occur early in uveal melanoma. In *Investigative ophthalmology & visual science* 49 (12), pp. 5230–5234. DOI: 10.1167/iovs.08-2145.
- Patel, B. R.; Tall, G. G. (2016): Ric-8A gene deletion or phorbol ester suppresses tumorigenesis in a mouse model of GNAQ(Q209L)-driven melanoma. In *Oncogenesis* 5 (6), e236. DOI: 10.1038/oncsis.2016.45.
- Patel, Sapna P.; Kim, Dae Won; Lacey, Carol L.; Hwu, Patrick (2016): GNA11 Mutation in a Patient With Cutaneous Origin Melanoma: A Case Report. In *Medicine* 95 (4), e2336. DOI: 10.1097/MD.0000000000002336.
- Pfeffer, S. R.; Dirac-Svejstrup, A. B.; Soldati, T. (1995): Rab GDP dissociation inhibitor: putting rab GTPases in the right place. In *The Journal of biological chemistry* 270 (29), pp. 17057–17059.
- Pitcovski, Jacob; Shahar, Ehud; Aizenshtein, Elina; Gorodetsky, Raphael (2017): Melanoma antigens and related immunological markers. In *Critical reviews in oncology/hematology* 115, pp. 36–49. DOI: 10.1016/j.critrevonc.2017.05.001.
- Plasseraud, Kristen M.; Wilkinson, Jeff K.; Oelschlager, Kristen M.; Poteet, Trisha M.; Cook, Robert W.; Stone, John F.; Monzon, Federico A. (2017): Gene expression profiling in uveal melanoma: technical reliability and correlation of molecular class with pathologic characteristics. In *Diagnostic pathology* 12 (1), p. 59. DOI: 10.1186/s13000-017-0650-3.
- Platz, Anton; Egyhazi, Suzanne; Ringborg, Ulrik; Hansson, Johan (2008): Human cutaneous melanoma; a review of NRAS and BRAF mutation frequencies in relation to histogenetic subclass and body site. In *Molecular oncology* 1 (4), pp. 395–405. DOI: 10.1016/j.molonc.2007.12.003.
- Pylayeva-Gupta, Yuliya; Grabocka, Elda; Bar-Sagi, Dafna (2011): RAS oncogenes: weaving a tumorigenic web. In *Nature reviews. Cancer* 11 (11), pp. 761–774. DOI: 10.1038/nrc3106.
- Rebecchi, M. J.; Pentylala, S. N. (2000): Structure, function, and control of phosphoinositide-specific phospholipase C. In *Physiological reviews* 80 (4), pp. 1291–1335. DOI: 10.1152/physrev.2000.80.4.1291.
- Reher, Raphael; Kühl, Toni; Annala, Suvi; Benkel, Tobias; Kaufmann, Desireé; Nubbemeyer, Britta et al. (2018a): Deciphering Specificity Determinants for FR900359-Derived Gq α Inhibitors Based

on Computational and Structure-Activity Studies. In *ChemMedChem* 13 (16), pp. 1634–1643. DOI: 10.1002/cmdc.201800304.

Reher, Raphael; Kuschak, Markus; Heycke, Nina; Annala, Suvi; Kehraus, Stefan; Dai, Hao-Fu et al. (2018b): Applying Molecular Networking for the Detection of Natural Sources and Analogues of the Selective Gq Protein Inhibitor FR900359. In *Journal of natural products* 81 (7), pp. 1628–1635. DOI: 10.1021/acs.jnatprod.8b00222.

Rojas, Rafael J.; Yohe, Marielle E.; Gershburg, Svetlana; Kawano, Takeharu; Kozasa, Tohru; Sondek, John (2007): Galphaq directly activates p63RhoGEF and Trio via a conserved extension of the Dbl homology-associated pleckstrin homology domain. In *The Journal of biological chemistry* 282 (40), pp. 29201–29210. DOI: 10.1074/jbc.M703458200.

Rozengurt, Enrique (2007): Mitogenic signaling pathways induced by G protein-coupled receptors. In *Journal of cellular physiology* 213 (3), pp. 589–602. DOI: 10.1002/jcp.21246.

Rubinstein, Jill C.; Sznol, Mario; Pavlick, Anna C.; Ariyan, Stephan; Cheng, Elaine; Bacchiocchi, Antonella et al. (2010): Incidence of the V600K mutation among melanoma patients with BRAF mutations, and potential therapeutic response to the specific BRAF inhibitor PLX4032. In *Journal of translational medicine* 8, p. 67. DOI: 10.1186/1479-5876-8-67.

Sánchez-Fernández, Guzmán; Cabezudo, Sofía; Caballero, Álvaro; García-Hoz, Carlota; Tall, Gregory G.; Klett, Javier et al. (2016): Protein Kinase C ζ Interacts with a Novel Binding Region of G α q to Act as a Functional Effector*. In *The Journal of biological chemistry* 291 (18), pp. 9513–9525. DOI: 10.1074/jbc.M115.684308.

Sánchez-Fernández, Guzmán; Cabezudo, Sofía; García-Hoz, Carlota; Benincá, Cristiane; Aragay, Anna M.; Mayor, Federico; Ribas, Catalina (2014): G α q signalling: the new and the old. In *Cellular signalling* 26 (5), pp. 833–848. DOI: 10.1016/j.cellsig.2014.01.010.

Scheschonka, A.; Dessauer, C. W.; Sinnarajah, S.; Chidiac, P.; Shi, C. S.; Kehrl, J. H. (2000): RGS3 is a GTPase-activating protein for g(ialpha) and g(qalpha) and a potent inhibitor of signaling by GTPase-deficient forms of g(qalpha) and g(11alpha). In *Molecular pharmacology* 58 (4), pp. 719–728.

Schrage, Ramona; Schmitz, Anna-Lena; Gaffal, Evelyn; Annala, Suvi; Kehraus, Stefan; Wenzel, Daniela et al. (2015): The experimental power of FR900359 to study Gq-regulated biological processes. In *Nature communications* 6, p. 10156. DOI: 10.1038/ncomms10156.

Schröder, Ralf; Janssen, Nicole; Schmidt, Johannes; Kebig, Anna; Merten, Nicole; Hennen, Stephanie et al. (2010): Deconvolution of complex G protein-coupled receptor signaling in live cells using dynamic mass redistribution measurements. In *Nature biotechnology* 28 (9), pp. 943–949. DOI: 10.1038/nbt.1671.

Schröder, Ralf; Schmidt, Johannes; Blättermann, Stefanie; Peters, Lucas; Janssen, Nicole; Grundmann, Manuel et al. (2011): Applying label-free dynamic mass redistribution technology to frame signaling of G protein-coupled receptors noninvasively in living cells. In *Nature protocols* 6 (11), pp. 1748–1760. DOI: 10.1038/nprot.2011.386.

Reference

- Schumacher, Benjamin; Skwarczynska, Malgorzata; Rose, Rolf; Ottmann, Christian (2010): Structure of a 14-3-3 σ -YAP phosphopeptide complex at 1.15 Å resolution. In *Acta crystallographica. Section F, Structural biology and crystallization communications* 66 (Pt 9), pp. 978–984. DOI: 10.1107/S1744309110025479.
- Shapiro, A.; Botha, J. D.; Pastore, A.; Lesk, A. M. (1992): A method for multiple superposition of structures. In *Acta crystallographica. Section A, Foundations of crystallography* 48 (Pt 1), pp. 11–14.
- Sondek, J.; Lambright, D. G.; Noel, J. P.; Hamm, H. E.; Sigler, P. B. (1994): GTPase mechanism of Gproteins from the 1.7-Å crystal structure of transducin α -GDP-AIF-4. In *Nature* 372 (6503), pp. 276–279. DOI: 10.1038/372276a0.
- Strathmann, M.; Simon, M. I. (1990): G protein diversity: a distinct class of α subunits is present in vertebrates and invertebrates. In *Proceedings of the National Academy of Sciences of the United States of America* 87 (23), pp. 9113–9117.
- Takasaki, Jun; Saito, Tetsu; Taniguchi, Masatoshi; Kawasaki, Tomihisa; Moritani, Yumiko; Hayashi, Kazumi; Kobori, Masato (2004): A novel Galphaq/11-selective inhibitor. In *The Journal of biological chemistry* 279 (46), pp. 47438–47445. DOI: 10.1074/jbc.M408846200.
- Taniguchi, Masatoshi; Suzumura, Ken-Ichi; Nagai, Koji; Kawasaki, Tomihisa; Takasaki, Jun; Sekiguchi, Mitsuhiro et al. (2004): YM-254890 analogues, novel cyclic depsipeptides with Galpha(q/11) inhibitory activity from *Chromobacterium* sp. QS3666. In *Bioorganic & medicinal chemistry* 12 (12), pp. 3125–3133. DOI: 10.1016/j.bmc.2004.04.006.
- Tanja Alten, geb. Slodczyk (2017): Bedeutung einer G α q-Protein-Inhibition für die Pathogenese des malignen Melanoms. In *Universität Bonn urn:nbn:de:hbz:5n-45872*. Available online at <http://hss.ulb.uni-bonn.de/2017/4587/4587-index.pdf>, checked on 12/3/2018.
- Taylor, J. M.; Jacob-Mosier, G. G.; Lawton, R. G.; VanDort, M.; Neubig, R. R. (1996): Receptor and membrane interaction sites on G β . A receptor-derived peptide binds to the carboxyl terminus. In *The Journal of biological chemistry* 271 (7), pp. 3336–3339.
- Taylor, S. J.; Chae, H. Z.; Rhee, S. G.; Exton, J. H. (1991): Activation of the β 1 isozyme of phospholipase C by α subunits of the G α class of G proteins. In *Nature* 350 (6318), pp. 516–518. DOI: 10.1038/350516a0.
- The Cancer Genome Atlas Network (2015): Genomic Classification of Cutaneous Melanoma. In *Cell* 161 (7), pp. 1681–1696. DOI: 10.1016/j.cell.2015.05.044.
- Thomas, Anna C.; Zeng, Zhiqiang; Rivière, Jean-Baptiste; O'Shaughnessy, Ryan; Al-Olabi, Lara; St-Onge, Judith et al. (2016): Mosaic Activating Mutations in GNA11 and GNAQ Are Associated with Phakomatosis Pigmentovascularis and Extensive Dermal Melanocytosis. In *The Journal of investigative dermatology* 136 (4), pp. 770–778. DOI: 10.1016/j.jid.2015.11.027.
- Thore, Sophia; Dyachok, Oleg; Gylfe, Erik; Tengholm, Anders (2005): Feedback activation of phospholipase C via intracellular mobilization and store-operated influx of Ca²⁺ in insulin-secreting β -cells. In *Journal of cell science* 118 (Pt 19), pp. 4463–4471. DOI: 10.1242/jcs.02577.

- Tonge, Peter J. (2017): Drug–Target Kinetics in Drug Discovery. In *ACS Chemical Neuroscience* 9 (1), pp. 29–39. DOI: 10.1021/acscemneuro.7b00185.
- Trinquier, G.; Sanejouand, Y. H. (1998): Which effective property of amino acids is best preserved by the genetic code? In *Protein Engineering Design and Selection* 11 (3), pp. 153–169. DOI: 10.1093/protein/11.3.153.
- van Eps, Ned; Preininger, Anita M.; Alexander, Nathan; Kaya, Ali I.; Meier, Scott; Meiler, Jens et al. (2011): Interaction of a G protein with an activated receptor opens the interdomain interface in the alpha subunit. In *Proceedings of the National Academy of Sciences of the United States of America* 108 (23), pp. 9420–9424. DOI: 10.1073/pnas.1105810108.
- van Raamsdonk, Catherine D.; Bezrookove, Vladimir; Green, Gary; Bauer, Jürgen; Gaugler, Lona; O'Brien, Joan M. et al. (2009): Frequent somatic mutations of GNAQ in uveal melanoma and blue naevi. In *Nature* 457 (7229), pp. 599–602. DOI: 10.1038/nature07586.
- van Raamsdonk, Catherine D.; Fitch, Karen R.; Fuchs, Helmut; Angelis, Martin Hrabé de; Barsh, Gregory S. (2004): Effects of G-protein mutations on skin color. In *Nature genetics* 36 (9), pp. 961–968. DOI: 10.1038/ng1412.
- van Raamsdonk, Catherine D.; Griewank, Klaus G.; Crosby, Michelle B.; Garrido, Maria C.; Vemula, Swapna; Wiesner, Thomas et al. (2010): Mutations in GNA11 in uveal melanoma. In *The New England journal of medicine* 363 (23), pp. 2191–2199. DOI: 10.1056/NEJMoa1000584.
- Vaqué, Jose P.; Dorsam, Robert T.; Feng, Xiaodong; Iglesias-Bartolome, Ramiro; Forsthoefel, David J.; Chen, Qianming et al. (2012): A genome-wide RNAi screen reveals a Trio-regulated Rho GTPase circuitry transducing GPCR-initiated mitogenic signals. In *Molecular cell* 49 (1), pp. 94–108. DOI: 10.1016/j.molcel.2012.10.018.
- Vassilev, A.; Kaneko, K. J.; Shu, H.; Zhao, Y.; DePamphilis, M. L. (2001): TEAD/TEF transcription factors utilize the activation domain of YAP65, a Src/Yes-associated protein localized in the cytoplasm. In *Genes & development* 15 (10), pp. 1229–1241. DOI: 10.1101/gad.888601.
- Vicente-Dueñas, Carolina; Romero-Camarero, Isabel; Cobaleda, Cesar; Sánchez-García, Isidro (2013): Function of oncogenes in cancer development: a changing paradigm. In *The EMBO journal* 32 (11), pp. 1502–1513. DOI: 10.1038/emboj.2013.97.
- Waldo, Gary L.; Ricks, Tiffany K.; Hicks, Stephanie N.; Cheever, Matthew L.; Kawano, Takeharu; Tsuboi, Kazuhito et al. (2010): Kinetic scaffolding mediated by a phospholipase C-beta and Gq signaling complex. In *Science (New York, N.Y.)* 330 (6006), pp. 974–980. DOI: 10.1126/science.1193438.
- Walker, Teresa M.; van Ginkel, Paul R.; Gee, Ricardo L.; Ahmadi, Hoda; Subramanian, Lalita; Ksander, Bruce R. et al. (2002): Expression of angiogenic factors Cyr61 and tissue factor in uveal melanoma. In *Archives of ophthalmology (Chicago, Ill. : 1960)* 120 (12), pp. 1719–1725.
- Wall, S. J.; Yasuda, R. P.; Li, M.; Ciesla, W.; Wolfe, B. B. (1992): Differential regulation of subtypes m1-m5 of muscarinic receptors in forebrain by chronic atropine administration. In *The Journal of pharmacology and experimental therapeutics* 262 (2), pp. 584–588.

Reference

- Webb, B. L.; Hirst, S. J.; Giembycz, M. A. (2000): Protein kinase C isoenzymes: a review of their structure, regulation and role in regulating airways smooth muscle tone and mitogenesis. In *British journal of pharmacology* 130 (7), pp. 1433–1452. DOI: 10.1038/sj.bjp.0703452.
- Weinstein, I. Bernard (2002): Cancer. Addiction to oncogenes--the Achilles heel of cancer. In *Science (New York, N.Y.)* 297 (5578), pp. 63–64. DOI: 10.1126/science.1073096.
- Wettschureck, N.; Moers, A.; Wallenwein, B.; Parlow, A. F.; Maser-Gluth, C.; Offermanns, S. (2005): Loss of Gq/11 family G proteins in the nervous system causes pituitary somatotroph hypoplasia and dwarfism in mice. In *Molecular and cellular biology* 25 (5), pp. 1942–1948. DOI: 10.1128/MCB.25.5.1942-1948.2005.
- Wettschureck, Nina; Offermanns, Stefan (2005): Mammalian G proteins and their cell type specific functions. In *Physiological reviews* 85 (4), pp. 1159–1204. DOI: 10.1152/physrev.00003.2005.
- Wilkie, T. M.; Scherle, P. A.; Strathmann, M. P.; Slepak, V. Z.; Simon, M. I. (1991): Characterization of G-protein alpha subunits in the Gq class: expression in murine tissues and in stromal and hematopoietic cell lines. In *Proceedings of the National Academy of Sciences of the United States of America* 88 (22), pp. 10049–10053.
- Xiong, Xiao-Feng; Zhang, Hang; Underwood, Christina R.; Harpsøe, Kasper; Gardella, Thomas J.; Wöldike, Mie F. et al. (2016): Total synthesis and structure-activity relationship studies of a series of selective G protein inhibitors. In *Nature chemistry* 8 (11), pp. 1035–1041. DOI: 10.1038/nchem.2577.
- Yang, Jessica; Manson, Daniel K.; Marr, Brian P.; Carvajal, Richard D. (2018): Treatment of uveal melanoma: where are we now? In *Therapeutic advances in medical oncology* 10, 1758834018757175. DOI: 10.1177/1758834018757175.
- Yin, Helen L.; Janmey, Paul A. (2003): Phosphoinositide regulation of the actin cytoskeleton. In *Annual review of physiology* 65, pp. 761–789. DOI: 10.1146/annurev.physiol.65.092101.142517.
- Ying, Han; Biroc, Sandra L.; Li, Wei-Wei; Aliche, Bruno; Xuan, Jian-Ai; Pagila, Rene et al. (2006): The Rho kinase inhibitor fasudil inhibits tumor progression in human and rat tumor models. In *Molecular cancer therapeutics* 5 (9), pp. 2158–2164. DOI: 10.1158/1535-7163.MCT-05-0440.
- Yu, Fa-Xing; Luo, Jing; Mo, Jung-Soon; Liu, Guangbo; Kim, Young Chul; Meng, Zhipeng et al. (2014): Mutant Gq/11 promote uveal melanoma tumorigenesis by activating YAP. In *Cancer cell* 25 (6), pp. 822–830. DOI: 10.1016/j.ccr.2014.04.017.
- Yu, Fa-Xing; Zhao, Bin; Panupinthu, Nattapon; Jewell, Jenna L.; Lian, Ian; Wang, Lloyd H. et al. (2012): Regulation of the Hippo-YAP pathway by G-protein-coupled receptor signaling. In *Cell* 150 (4), pp. 780–791. DOI: 10.1016/j.cell.2012.06.037.
- Zhang, Hang; Nielsen, Alexander L.; Boesgaard, Michael W.; Harpsøe, Kasper; Daly, Norelle L.; Xiong, Xiao-Feng et al. (2018): Structure-activity relationship and conformational studies of the natural product cyclic depsipeptides YM-254890 and FR900359. In *European journal of medicinal chemistry* 156, pp. 847–860. DOI: 10.1016/j.ejmech.2018.07.023.

- Zhang, Ru; Xie, Xin (2012): Tools for GPCR drug discovery. In *Acta Pharmacologica Sinica* 33 (3), pp. 372–384. DOI: 10.1038/aps.2011.173.
- Zhao, Bin; Li, Li; Lu, Qing; Wang, Lloyd H.; Liu, Chen-Ying; Lei, Qunying; Guan, Kun-Liang (2011a): Angiomotin is a novel Hippo pathway component that inhibits YAP oncoprotein. In *Genes & development* 25 (1), pp. 51–63. DOI: 10.1101/gad.2000111.
- Zhao, Bin; Li, Li; Tumaneng, Karen; Wang, Cun-Yu; Guan, Kun-Liang (2010): A coordinated phosphorylation by Lats and CK1 regulates YAP stability through SCF(beta-TRCP). In *Genes & development* 24 (1), pp. 72–85. DOI: 10.1101/gad.1843810.
- Zhao, Bin; Tumaneng, Karen; Guan, Kun-Liang (2011b): The Hippo pathway in organ size control, tissue regeneration and stem cell self-renewal. In *Nature cell biology* 13 (8), pp. 877–883. DOI: 10.1038/ncb2303.
- Zhao, Bin; Wei, Xiaomu; Li, Weiquan; Udan, Ryan S.; Yang, Qian; Kim, Joungmok et al. (2007): Inactivation of YAP oncoprotein by the Hippo pathway is involved in cell contact inhibition and tissue growth control. In *Genes & development* 21 (21), pp. 2747–2761. DOI: 10.1101/gad.1602907.
- Zheng, Lei; Baumann, Ulrich; Reymond, Jean-Louis (2004): An efficient one-step site-directed and site-saturation mutagenesis protocol. In *Nucleic Acids Research* 32 (14), e115. DOI: 10.1093/nar/gnh110.
- Zhou, Yuhang; Huang, Tingting; Cheng, Alfred S. L.; Yu, Jun; Kang, Wei; To, Ka Fai (2016): The TEAD Family and Its Oncogenic Role in Promoting Tumorigenesis. In *International journal of molecular sciences* 17 (1). DOI: 10.3390/ijms17010138.
- Zuidervaart, W.; van Nieuwpoort, F.; Stark, M.; Dijkman, R.; Packer, L.; Borgstein, A-M et al. (2005): Activation of the MAPK pathway is a common event in uveal melanomas although it rarely occurs through mutation of BRAF or RAS. In *British journal of cancer* 92 (11), pp. 2032–2038. DOI: 10.1038/sj.bjc.6602598.

List of Figures

Figure 1: Uveal melanoma arising from the choroid;	2
Figure 2: Homology between the Gq-family members.	4
Figure 3: Receptor-mediated G protein activation.	5
Figure 4: GTPase function as autocatalytic off-switch.	6
Figure 5: Gq activates PLC catalytic activity to hydrolyze PIP ₂ .	8
Figure 6: PLC acts as a GAP for Gq proteins.	10
Figure 7: Overview of GNAQ/11 driven pro-survival pathways.	11
Figure 8: GNAQ signaling to induce YAP activity..	14
Figure 9: Comparison of YM-254890 and FR900359 structures.	16
Figure 10 Scheme of FR function as a GDI on Gq preventing its activation	17
Figure 11: Gq inhibitor FR lack capability for complete inhibition of Gα _q ^{Q209L} induced IP1 accumulation.	51
Figure 12: FR suppresses downstream pro-survival but not canonical PLC signaling pathway of oncogenic Gα ₁₁ ^{Q209L} in mouse melanoma cell line HCmel12.	53
Figure 13: Inhibition of basal ERK phosphorylation in HCmel12 cells by targeting various Gq-downstream effectors.	54
Figure 14: FR fail to abolish ERK in melanoma cells with additional B-Raf mutation.	56
Figure 15: FR inhibits canonical and mutagenic signaling driven by wild type Gq/11.	57
Figure 16: Transiently expressed Gα _q wt and mutated Gα _q ^{Q209L} increase PLC activity in HEK 293 cells.	58
Figure 17: FR effect on canonical PLC activation versus mitogenic ERK phosphorylation HEK cells expressing wild type and Q209L construct.	59
Figure 18: AKT phosphorylation regulated by Gq signaling in HEK293 cells.	60
Figure 19: YAP phosphorylation regulated by Gq signaling in HEK293 cells.	61
Figure 20: DMR bio-sensing of intrinsic Gq inhibition by FR	63
Figure 21: Quantification of DMR bio-sensing of intrinsic Gq inhibition by FR	64
Figure 22: DMR bio-sensing of intrinsic Gq inhibition by FR	65
Figure 23: Detection of GDP and GTP bound Gα _q	66
Figure 24: FR binding on wild type and GTPase-deficient Gα _q	67
Figure 25: Schematic description of PLC-Gq interaction and GAP activity	68
Figure 26: FR inhibition of PLC-β downstream signaling initiated by GTPase impaired Gq R183C	69
Figure 27: PLCβ3 interaction with wild type Gα _q and GTPase-deficient Gα _q ^{Q209L} interaction in presents and absents of FR.	71

Figure 28: PLCβ3 interaction with wild type Gα_q and GTPase-deficient Gα_q^{Q209L} interaction in presents and absents of FR.	72
Figure 29: Intrinsic Gq activity in Uveal Melanoma cells expressing either wild type Gq or GTPase-deficient mutant.	73
Figure 30: Intrinsic Gq activity in Uveal Melanoma cells expressing either wild type Gq or GTPase-deficient mutant.	74
Figure 31: FR blunts [AlF$_4$]-mediated IP1 accumulation in Mel 290 cells.	75
Figure 32: FR inhibits ERK signaling in Uveal Melanoma cells carrying GTPase-deficient Gq mutant.	77
Figure 33: FR inhibits proliferation in GTPase but not wild type Gq uveal melanoma cell lines.	79
Figure 34: Inhibition of ERK signaling prevents cell growth in GNAQ^{mut} UM cells lines	80
Figure 35: AKT pathway activity in uveal melanoma cells	81
Figure 36: Time dependent inhibition of AKT phosphorylation in UM cells	82
Figure 37: FR inhibits partially AKT phosphorylation in UM cells with mutated GNAQ	83
Figure 38: FR inhibits partially AKT phosphorylation in UM cells with mutated GNAQ	84
Figure 39: Time dependent FR effect on YAP phosphorylation in diverse in UM cell lines.	85
Figure 40: FR induces YAP phosphorylation only in certain UM cells with mutated GNAQ	86
Figure 41: Combined Gq inhibition and Gs activation results in additive YAP phosphorylation in 92.1 cells	87
Figure 42: Bio-sensing of cell viability and adenylyl cyclase activation via DMR	88
Figure 43: FR induced DMR profiles in different UM cell lines	89
Figure 44: Quantification of FR response in 92.1 cells	90
Figure 45: FR inhibits tumor growth in UM with mutated GNAQ	91
Figure 46: Vulnerability comparison between FR and YM.	93
Figure 47: Loss-of-function mutagenesis study for FR and YM.	95
Figure 48: Loss-of-function mutagenesis study for FR and YM.	97
Figure 49: FR and YM in head-to-head comparisons in cell proliferation assay with UM cell lines.	99
Figure 50: Time-dependent ERK inhibition of FR and YM on Mel270	100
Figure 51: Time-dependent ERK inhibition of FR and YM on Mel270	101
Figure 52: FR as a GDI on wild type Gq	107
Figure 53: Mechanism of biased inhibition of the GTPase-deficient Gq	108

List of Figures

Figure M1: Sequence of PLB4	47
Figure M2: PLCB4 PCR product	48

Abbreviations list

AJCC	American Joint Committee on Cancer
AKT	protein kinase B
AMOT	Angiomotin
AUC	area under the curve
BAP1	BRCA1 associated protein-1
B-Raf	B-Raf serine/threonine-protein kinase
C3	propionic acid
cAMP	cyclic adenosine monophosphate
CCh	carbachol
Cdk	cyclin-dependent kinases
CM	cutaneous melanoma
C-Met	tyrosine kinase c-Met
CRISPR	Clustered Regularly Interspaced Short Palindromic Repeats
CTGF	connective tissue growth factor
CYR61	Cysteine-rich angiogenic inducer 61
CysLTR2	cysteinyl leukotriene receptor 2
DAG	diacyl-glycerin
dH2O	demineralized water
DMR	dynamic mass redistribution

Abbreviations list

Dsk	Dark skin phenotype
EGF	Epidermal growth factor
EIF1AX	Eukaryotic translation initiation factor 1A
ERK	extracellular-signal regulated kinase
FCS	fetal calf serum
FFA2	free fatty acid receptor 2
FRET	fluorescence resonance energy transfer
FSK	forskolin
GAP	GTPase-activating proteins
GDP	guanine diphosphate
GDI	Guanine-dissociation inhibitor
GEP	gene expression profile
Gq-i	Gq protein inhibitor
GNA11	Gene encoding G α 11-subunit
GNAQ	Gene encoding G α q-subunit
gp100	glycoprotein 100
GPCR	G protein-coupled receptor
GTP	guanine triphosphate
HA	Human influenza hemagglutinin
HEK	human embryonal kidney

HTRF	homogeneous time resolved fluorescence
IC50	concentration of half maximum inhibition
IP	immunoprecipitation
IP1	inositol monophosphate
IP3	inositol trisphosphate
$k_{\text{cat-GTP}}$	kinetic of GTPase
LATS1/2	Large tumor suppressor kinase 1/2
log M	logarithm of molar concentration at base 10
M	mol per liter
M3	muscarinic receptor M3
MAPK	mitogen-activated protein kinase
MDA	melanocyte differentiation antigens
MEK-i	Mitogen-activated protein kinase kinase-inhibitor
MST1/2	<i>macrophage-stimulating 1/2 gene</i>
nm	nanometer
nM	nanomolar
PCR	polymerase chain reaction
PD	Pull-down
PI3K-i	phosphoinositid-3-Kinasen-inhibitor
PIP ₂	phosphatidylinositol-4,5-phosphate

Abbreviations list

PKC	protein kinase C
PLC	phospholipase C
RGS	Regulators of G protein signaling
RhoA	Ras homolog gene A
ROCK	Rho-associated protein kinase
rpm	rounds per minute
s.e.m.	standard error of the mean
S1P	sphingosine 1-phosphate
SF3B1	Splicing factor 3B subunit 1
shRNA	short hairpin RNA
siRNA	Small interfering RNA
TEAD	protein with TEA domain
TKR	tyrosine-kinase receptors
TRIO	Triple functional domain protein
UM	uveal melanoma
wt	wild type
YAP	yes-associated protein
μ l	microliter
μ M	micromolar

Publications

Research Articles:

Annala S, Feng X, Shridhar N, Eryilmaz F, Patt J, Yang JH, Pfeil E, Cervantes-Villagrana R, Inoue A, Häberlein F, Slodczyk T, Reher R, Kehraus S, Monteleone S, Schrage R, Heycke N, Rick U, Engel S, Pfeifer A, Kolb P, König G, Bünemann M, Tüting T, Vázquez-Prado J, Gutkind S, Gaffal E, Kostenis E. (2019) Direct targeting of G_q and G_{α11} oncoproteins in cancer cells *Science Signaling* (in press)

Malfacini D, Patt J, **Annala S**, Harpsøe K, Eryilmaz F, Reher R, Crüsemann M, Hanke W, Zhang H, Tietze D, Gloriam DE, Bräuner-Osborne H, Strømgaard K, König GM, Inoue A, Gomeza J, Kostenis E. (2019) Rational design of a heterotrimeric G protein α subunit with artificial inhibitor sensitivity. *J Biol Chem*. doi:10.1074/jbc.RA118.007250.

Reher R, Kuschak M, Heycke N, **Annala S**, Kehraus S, Dai HF, Müller CE, Kostenis E, König GM, Crüsemann M. (2018) Applying Molecular Networking for the Detection of Natural Sources and Analogues of the Selective G_q Protein Inhibitor FR900359. *J Nat Prod*. 81(7):1628-1635. doi: 10.1021/acs.jnatprod.8b00222.

Reher R, Kühl T, **Annala S**, Benkel T, Kaufmann D, Nubbemeyer B, Odhiambo JP, Heimer P, Bäuml CA, Kehraus S, Crüsemann M, Kostenis E, Tietze D, König GM, Imhof D. (2018) Deciphering Specificity Determinants for FR900359-Derived G_q α Inhibitors Based on Computational and Structure-Activity Studies. *ChemMedChem*. 13(16):1634-1643. doi: 10.1002/cmdc.201800304.

Matthey M, Roberts R, Seidinger A, Simon A, Schröder R, Kuschak M, **Annala S**, König GM, Müller CE, Hall IP, Kostenis E, Fleischmann BK, Wenzel D. (2017) Targeted inhibition of G_q signaling induces airway relaxation in mouse models of asthma. *Sci Transl Med*. 2017 Sep 13;9(407). doi: 10.1126/scitranslmed.aag2288.

Schrage R, Schmitz AL, Gaffal E, **Annala S**, Kehraus S, Wenzel D, Büllsbach KM, Bald T, Inoue A, Shinjo Y, Galandrin S, Shridhar N, Hesse M, Grundmann M, Merten N, Charpentier TH, Martz M, Butcher AJ, Slodczyk T, Armando S, Effern M, Namkung Y, Jenkins L, Horn V, Stößel A, Dargatz H, Tietze D, Imhof D, Galés C, Drewke C, Müller CE, Hölzel M, Milligan G, Tobin AB, Gomeza J, Dohlman HG, Sondak J, Harden TK, Bouvier M, Laporte SA, Aoki J, Fleischmann BK, Mohr K, König GM, Tüting T, Kostenis E. (2015) The experimental power of FR900359 to study G_q-regulated biological processes. *Nat Commun*. 14;6:10156. doi: 10.1038/ncomms10156.

Publications

Keller K, Maass M, Dizayee S, Leiss V, **Annala S**, Köth J, Seemann WK, Müller-Ehmsen J, Mohr K, Nürnberg B, Engelhardt S, Herzig S, Birnbaumer L, Matthes J. (2015) Lack of G α i2 leads to dilative cardiomyopathy and increased mortality in β 1-adrenoceptor overexpressing mice. *Cardiovasc Res.* 108(3):348-56. doi: 10.1093/cvr/cvv235.

Posters:

Suvi Annala, Asuka Inoue, Manuel Grundmann, Nicole Merten, Stefan Kehraus, Laura Jenkins, Katrin Büllsbach, Graeme Milligan, Jesús Gomeza, Gabriele M. König & Evi Kostenis (2016) FR900359: a cyclic depsipeptide to explore the role of G α q proteins in biological systems. Cutting Edge Concepts in Molecular Pharmacology: GPCRs, G-proteins, TRP channels (Berlin, DE, March 3.-5.)

Alessandra Ewertz, **Suvi Annala**, Evi Kostenis, Florian Rothweiler, Jindrich Cinatl, Martin Michaelis, Gabriele M. König, Ulrich Jaehde, Ganna V. Kalayda (2016) Effects of the G α q-inhibitor FR900359 on sensitive and cisplatin-resistant lung carcinoma cells. CESAR Annual Meeting 2016: Early Drug Development and Biomarkers (Munich, DE, September 8.-10.)

Jim Küppers, **Suvi Annala**, Tobias Benkel, Markus Kuschak, Aliaa Abdelrahman, Christa E. Müller, Evi Kostenis, Michael Gütschow (2017) Heterocyclized dipeptide derivatives as inhibitors for heterotrimeric G proteins. 53rd Gordon Research Conference: Heterocyclic Compounds (Newport, USA, June 18.-23.)

Acknowledgement

Zunächst gilt mein Dank meiner Doktormutter, Frau Prof. Dr. Evi Kostenis, die es mir ermöglicht hat die Herausforderung einer Doktorarbeit in Ihrem Arbeitskreis anzunehmen. Sie war nicht nur wissenschaftlich zu jeder Zeit eine mehr als kompetente Hilfe, sondern hat sich auch großartig für unsere Publikationen eingesetzt.

Des Weiteren bedanke ich mich bei meiner 2. Gutachterin Frau Priv.-Doz. Dr. Evelyn Gaffal, für die experimentelle Unterstützung in unserem gemeinsamen Projekt aber auch für die Organisation der Aderhautmelanomzellen, die ein wichtiger Bestandteil dieser Studie sind.

Bedanken möchte ich mich auch bei Frau Prof. Dr. Tanja Schneider und Herrn Prof. Dr. Benjamin Odermatt für die Übernahme der fachnahen und fachfremden Begutachtung dieser Arbeit im Rahmen der Promotionskommission.

Für experimentelle Unterstützung möchte ich mich zudem bei Dr. Xiadong Feng, Dr. Naveen Shridhar, Rodolfo Daniel Cervantes-Villagrana, Prof. Dr. Asuka Inoue, Dr. Tanja Slodczyk, Dr. Stefania Monteleone, Dr. Ramona Schrage, Sandra Engel, Prof. Dr. Peter Kolb, Prof. Dr. Moritz Bünemann, Prof. Dr. Thomas Tüting, Prof. Dr. José Vázquez-Prado und Prof. Dr. Silvio Gutkind bedanken. Für die Bereitstellung des Gq-Inhibitors FR900359 bedanke ich mich bei Frau Prof. Dr. Gabriele König, Dr. Stefan Kehraus und Dr. Raphael Reher.

Ein besonderer Dank geht auch an meine lieben Mitarbeiter aus dem Arbeitskreis Kostenis, die für mich nicht nur unterstützende Kollegen waren, sondern auch Freunde geworden sind: Funda Erylimaz, Nina Heycke, Eva Pfeil, Julian Patt, Ulricke Rick, Nina Katharina Schmitt, Felix Häberlein und die Restlichen Mitglieder der AG.

Auch möchte ich mich bei meinen ehemaligen Bürokollegen Katrin Krebs und Manuel Grundmann für viele anregende Büro- und Mensagespräche bedanken.

Am Ende möchte ich vor allem auch bei meiner Mutter und meiner lieben Schwester Sari Elina bedanken, von denen ich gelernt habe auch bei Rückschlägen nicht zu kapitulieren, sondern einen Weg nach vorne zu suchen.